A Novel Connection between CtIP and the BRCA1/BARD1 Tumour Suppressor Complex Emerges through Functional RNAi Screening

---

Dissertation

zur Erlangung der naturwissenschaftlichen Doktorwürde

(Dr. sc. nat.)

vorgelegt der

Mathematisch-naturwissenschaftlichen Fakultät

der

Universität Zürich

von

Hella Anna Bolck

aus

Deutschland

Promotionskomitee

Prof. Dr. Alessandro A. Sartori (Vorsitz und Leitung der Dissertation)

Prof. Dr. Anne Müller

Prof. Dr. Orlando Schärer

Dr. Thomas Marti

Zürich, 2016

Contents

Summary

The human CtIP protein promotes error-free repair of DNA double-strand breaks (DSBs) by the homologous recombination (HR) pathway. Furthermore, CtIP has emerged as a multivalent adaptor with important implications in a variety of genome stability maintenance pathways such as cell cycle checkpoint control, DNA replication and transcriptional regulation. Therefore, it is not surprising that haploid insufficiency of *CtIP* predisposes mice to multiple types of tumours and *CtIP* mutations have been linked to several human cancers. Intriguingly however, many aspects of how CtIP is involved in counteracting tumourigenesis and cancer progression are still poorly understood to date.

In my PhD thesis, I sought to gain insights into the molecular network of factors and pathways collaborating with CtIP in the surveillance of genome integrity by multiplexed image-based RNAi screening. Specifically, I developed a high content screening assay to interrogate a large number of human genes for synthetic genetic interactions with CtIP in presence or absence of the chemotherapeutic drug camptothecin (CPT). From the screen data analysis, BARD1, the obligate interaction partner of the well-known BRCA1 tumour suppressor, emerged as a candidate for constituting a synthetic sick gene pair with CtIP. Indeed, I could demonstrate that simultaneous disruption of BARD1 and CtIP decreased cell viability to a greater extent than depletion of BARD1 or CtIP alone. More-

over, I showed that BARD1 and CtIP physically interact even in absence of an intact BRCA1/BARD1 heterodimer, indicating that BARD1 and CtIP might have a functional connection beyond the BRCA1/BARD1 complex. Finally, I determined that concurrent loss-of-function of CtIP and BARD1 leads to a severe increase of endogenous DNA lesions arising in the context of DNA replication and ultimately to chromosomal breakage. Taken together, I propose that CtIP and BARD1 cooperate to promote faithful replication thereby contributing to genome stability and counteracting cancer development.

Zusammenfassung

Krebs entsteht, wenn sich die Funktion bestimmter Sequenzen (Gene) des Erbguts (DNA) durch Mutationen so verändert, dass sich Zellen infolgedessen unkontrolliert teilen. Um zu verhindern, dass DNA-Schäden zu Mutationen führen, verfügen menschliche Zellen über eine Vielzahl an Reparatursystemen. Das humane CtIP Protein ist dabei vor allem für die Reparatur von DNA-Doppelstrangbrüchen essentiell. Neben dieser Funktion ist CtIP auch an der Regulation einer Reihe weiterer zellulärer Prozesse beteiligt, die Einfluss auf die Stabilität des Genoms haben, darunter an der Kontrolle des Zellzyklus sowie der DNA-Replikation und -Transkription. Es ist daher nicht erstaunlich, dass die Lebenserwartung von Mäusen mit einer heterozygoten Deletion des CtIP-Gens durch die Bildung zahlreicher Tumore stark reduziert ist. Mutationen innerhalb des CtIP-Gens sind außerdem in Verdacht mit einer Reihe von Krebsarten im Zusammenhang zu stehen. Wie CtIP auf molekularer Ebene der Tumorentstehung entgegenwirkt, ist bisher allerdings noch weitgehend unbekannt.

Das Ziel meiner Doktorarbeit war es daher, das molekulare Netzwerk, in welchem CtIP interagiert um die Krebsentstehung zu verhindern, genauer zu untersuchen. Aus diesem Grund habe ich ein RNA-Interferenz Screening Verfahren entwickelt, mithilfe dessen ich eine große Anzahl von sogenannten genetischen Interaktionen mit CtIP ermitteln kon-

nten. Diese Analyse habe ich zum einen in unbehandelten Zellen, zum anderen aber auch nach Behandlung mit dem Chemotherapeutikum Camptothecin (CPT) durchgeführt. Aus der Datenanalyse des Screens ging hervor, dass CtIP und BARD1, der Interaktionspartner des bekannten BRCA1 Tumorsuppressor Proteins, möglicherweise durch eine negative genetische Interaktion charakterisiert sind. Tatsächlich konnte ich im Folgenden zeigen, dass der gleichzeitige Verlust von CtIP und BARD1 das Überleben der Zellen stärker beeinträchtigt als der einzelne Verlust von CtIP oder BARD1. Ich konnte weiterhin demonstrieren, dass das CtIP und das BARD1-Protein miteinander interagieren können, ohne dass es dazu des gemeinsamen Interaktionspartners BRCA1 bedarf. Dies deutet darauf hin, dass CtIP und BARD1 eine funktionelle Rolle erfüllen könnten, die über die Funktionen des BRCA1/BARD1 Heterodimers hinausgeht. Schlussendlich konnte ich darlegen, dass der gleichzeitige Verlust von CtIP und BARD1 einen schwerwiegenden Anstieg von endogenen DNA Schäden bedingt, die durch Fehler während der Replikation entstehen. Diese führen letztlich zu Brüchen innerhalb der Chromosomen und Schäden am Genom. Zusammengefasst komme ich in meiner Doktorarbeit zu dem Schluss, dass CtIP und BARD1 kooperieren um eine fehlerfreie Replikation der DNA zu unterstützen, und dass dieser Mechanismus entscheidend dazu beitragen könnte der Krebsentstehung entgegenzuwirken.

Introduction

1.1 Genome instability, a driving force for cancer development

The body of an adult human being is made up of approximately 4 x 10^{13} cells whose size, number and type ultimately define not only appearance but also the structure and functions of this organism [1]. Stored inside the nucleus of almost every cell resides a helical molecule called deoxyribonucleic acid (DNA). This carries the genetic information necessary to build and maintain an organism by governing cell division and survival. It is of utmost importance that these processes are tightly controlled because their deregulation can give rise to cancer, a disease that is characterized by excessive cell proliferation. Early on it became clear that changes to the DNA, called mutations, are the underlying cause for most types of cancer. Today it is a widely accepted concept that unrestrained proliferation and the adaptability associated with cancer development are achieved by a multistep process involving numerous mutations and clonal expansion [2–4]. In addition, it was found that almost all human cancers have an unstable genome, which is considered to play a key role for the accumulation of genetic changes in the form of mutations

and rearrangements and the transformation of a normal into a malignant cell [5]. Furthermore, through the study of human genetic disorders it was discovered that germline mutations in genes that are involved in the maintenance of genomic integrity and DNA repair predispose their carriers to tumour development [5–7]. This has led to the notion that the acquisition of genomic instability (defined as a mutator phenotype) is a hallmark of cancer [8, 9].

1.2 The DNA damage response (DDR) counteracts genome instability

The genome is constantly exposed to endogenous and exogenous DNA damage that may cause mutations leading to carcinogenesis. DNA lesions can be induced by ionizing radiation as encountered for example during radiography (x-rays), by ultraviolet light from the sun or by certain chemical agents such as heterocyclic amines in overcooked meat or chemotherapeutical drugs. Remarkably, spontaneous DNA damage, mostly caused by DNA replication errors, hydrolytic cytosine deamination and oxidative DNA base damage, occurs at a rate of up to 10^5 lesions per cell per day [10–12] (Figure 1).

In order to counteract these insults and preserve genome stability, cells are equipped with a coordinated signal-transduction network, which is collectively known as the DNA damage response (DDR). A series of events constitute the DDR, such as detection of the DNA damage by sensors, accumulation of repair factors by mediators and repair of the lesion by effectors [12] (Figure 1.1). The DDR also includes signalling mechanisms mediating cell cycle arrest and regulation of DNA replication to prevent cells from prolif-

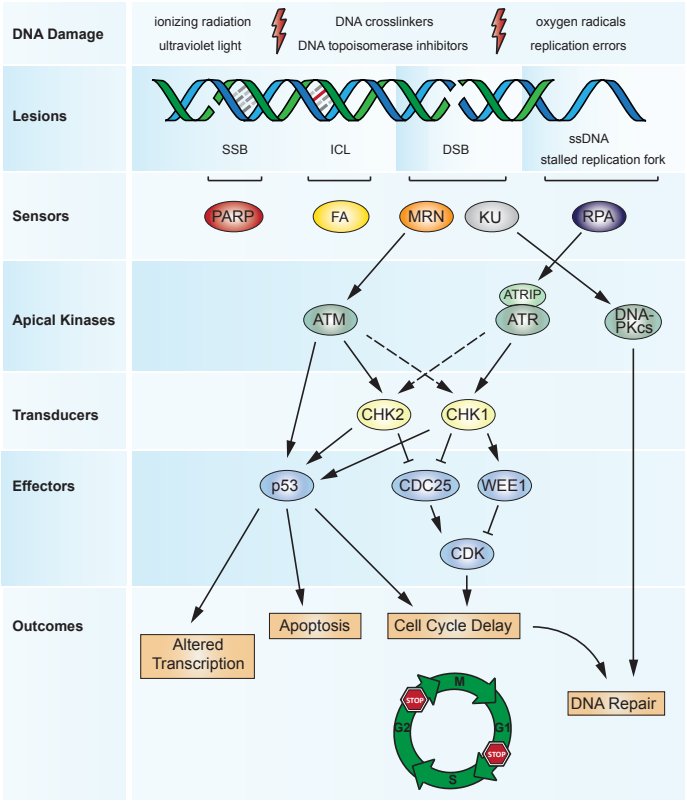

Figure 1.1: The DNA damage response (DDR). Exogenous and endogenous DNA damaging agents generate various types of lesions including DNA single- and double-strand breaks (SSBs and DSBs). The multifunctional MRN complex detects DSBs, while FA-proteins are required for the DNA interstrand crosslink (ICL)-induced checkpoint response. PARP predominantly acts as a SSB sensor protein. RPA binds to regions of ssDNA that are exposed at stalled replication forks or after DSB resection. MRN and RPA mediate the recruitment of ATM and ATR-ATRIP, respectively, and the subsequent activation of the corresponding pathways, coordinating cell-cycle checkpoints, DNA repair and apoptotic responses to DNA damage. The Ku70/Ku80 heterodimer (KU) competes with MRN for binding to DSBs. KU recruits DNA-PKcs, which is a major component of the canonical NHEJ machinery during DSB repair. MRN on the other hand initiates HR. Once activated, the DNA damage signalling cascade extends through multiple phosphorylation events primarily via the cell-cycle checkpoint kinases CHK1 and CHK2. Their signals converge on downstream effectors such as the tumour suppressor protein p53, the CDC25 protein phosphatase and the WEE1 tyrosine kinase. As a result, CDK activity is inhibited, delaying cell cycle progression from G_1 to S (the G_1/S checkpoint) or from G_2 to M phase (the G_2/M checkpoint). The DNA damage response (DDR) thus orchestrates a variety of cellular outcomes: the transcriptional programme of the damaged cell is altered and the cell cycle is transiently arrested, thereby facilitating repair of the DNA lesions. In situations where DNA damage is too severe and cannot be repaired, the DDR triggers apoptosis or senescence. ADP = adenosine diphosphate; ATM = ataxia telangiectasia mutated protein; ATR = ATM- and Rad3-related; ATRIP = ATR-interacting protein; CDK = cyclin-dependent kinase; DNA-PK = DNA-dependent protein kinase; DNA-PKcs = DNA-PK catalytic subunit; FA = Fanconi anaemia complementation group proteins; HR = homologous recombination; ICL = interstrand crosslink; MRN = MRE11-RAD50-NBS1 complex; NEHJ = nonhomologous end joining; PARP = poly(ADP)-ribose polymerase; RPA = replication protein A; ssDNA = single-stranded DNA. Adapted from [13].

erating as long as DNA integrity is compromised. Should DNA repair not be attainable leading to a catastrophic level of genomic instability, the DDR can impact on downstream cell fate decisions, such as programmed cell death or senescence. Upon DNA damage induction, three members of the phosphatidylinosit-ol-3-kinase (PI3K) related kinases (PIKKs), namely ATM (ataxia telangiectasia mutated), ATR (ATM- and Rad3-related) and DNA-PKcs (DNA-dependent protein kinase catalytic subunit), are recruited to damaged chromatin and trigger the DDR [14]. Downstream of ATM and ATR, phosphorylation events are initiated to activate multiple transducer and effector proteins, most notably p53 and the downstream checkpoint kinases CHK1 and CHK2, which in turn phosphorylate WEE1 kinase and CDC25 phosphatases. Consequently, through regulating the activity of cyclin-dependent kinases (CDKs) and an adjusting of the transcriptional program, cell cycle arrest is achieved allowing time for repair, thereby preventing replication or cell division in the presence of damaged DNA (Figure 1.1).

Depending on the nature of the lesion, specific pathways are available for DNA repair. The base excision repair (BER) pathway removes minor changes to DNA such as oxidised or alkylated bases, small base adducts and single-strand breaks (SSBs) via incision of the damaged base [10, 15]. A key player in this process is the poly(ADP-ribose) polymerase (PARP). Upon detection of SSBs, PARP covalently attaches poly(ADP-ribose) chains to itself and to acceptor proteins in the vicinity of the lesion, thereby facilitating the repair of SSBs (Figure 1.1). The nucleotide excision repair (NER) pathway addresses more complex, DNA helix-distorting base lesions, such as pyrimidine dimers that can arise from exposure to UV light, by excision of the damaged oligonucleotide [16]. Errors encountered during DNA replication such as mis-incorporated nucleotides or insertions and deletions

are recognized and removed by the mismatch repair (MMR) pathway [17]. Replication-blocking lesions of various kinds may be bypassed by either DNA template switching or translesion synthesis (TLS). A special class of DNA polymerases with less stringent base-pairing properties performs the latter mechanism by temporarily taking over from the obstructed replicative polymerase to circumvent damage-induced replication blocks [18]. DNA double-strand breaks (DSBs) represent the most dangerous type of lesions since a single unrepaired DSB can be sufficient to kill a cell, whereas mis-repaired DSBs potentially result in chromosomal re-arrangements, that can directly promote carcinogenesis. Therefore, cells have evolved four mechanistically distinct DSB repair pathways: homologous recombination (HR), non-homologous end-joining (NHEJ), alternative NHEJ and single-strand annealing (SSA). NHEJ and HR denote the two major DSB repair pathways (see below), with NHEJ operating throughout the cell cycle and HR being most active during S-phase [19, 20]. Finally, repair of DNA interstrand cross-links (ICL), which represent highly cytotoxic lesion inhibiting both DNA replication and transcription, is achieved by a complex mechanism coordinated by the Fanconi Anemia (FA) pathway. It involves the cooperation of several repair pathways including NER, TLS and HR [21] (Figure 1.1). Failure of the DDR is often causative for genetic alterations from single point mutations to gross chromosomal rearrangements thereby giving rise to genome instability. It is widely accepted that defects in DDR promote cancer development. In fact, tumour genome profiling by deep sequencing has demonstrated that DDR genes are frequently mutated in all cancer types [22]. However, DDR defects can also provide an inherent weakness of cancer cells that can be harnessed for treatment (“Achilles heel of cancer”). Genotoxic radio- and chemotherapy that cause DNA damage exceeding the repair capacity of the DDR

has been the mainstay of cancer treatment for many decades [22–24]. Moreover, exploiting specific vulnerabilities of DDR pathways in cancer cells directly holds great promise for targeted cancer therapy and is currently under vigorous investigation [13, 25].

1.3 Homologous recombination (HR) is required for genome stability and tumour avoidance

The most serious threat to genome integrity and cell survival is posed by simultaneous breakage of both complementary DNA strands creating a DSB. DSBs are generated upon exposure to ionizing radiation (IR) or a number of chemotherapeutic drugs such as topoisomerase poisons (e.g. camptothecin, CPT) and arise as a consequence of collapsed replication forks [26, 27]. Moreover, DSBs are produced as intermediates during meiosis, V(D)J- and class switch recombination, important physiological processes allowing for slight genetic variability and adaptation [28, 29]. Due to the deleterious consequences a DSB may entail, all organisms are equipped with two major DSB repair pathways: NHEJ and HR. NHEJ is initiated by quick association of the Ku heterodimer to DSBs which triggers religation of the broken DNA ends without the need of extensive processing (Figure 1.2). Even though, NHEJ can in principle function throughout the cell cycle, it predominates in G_1. Importantly, repair by the NHEJ pathway is prone to errors [19]. During S-phase, when an undamaged sister chromatid becomes available as a template, DSBs are therefore preferentially repaired by the HR pathway.

HR is initiated by recognition of a DSB by the MRE11-RAD50-NBS1 (MRN) complex and subsequent DNA-end resection, a process that generates tails of 3' single stranded DNA

(ssDNA) and thereby commits repair irreversibly to HR [30, 31] (Figure 1.2).

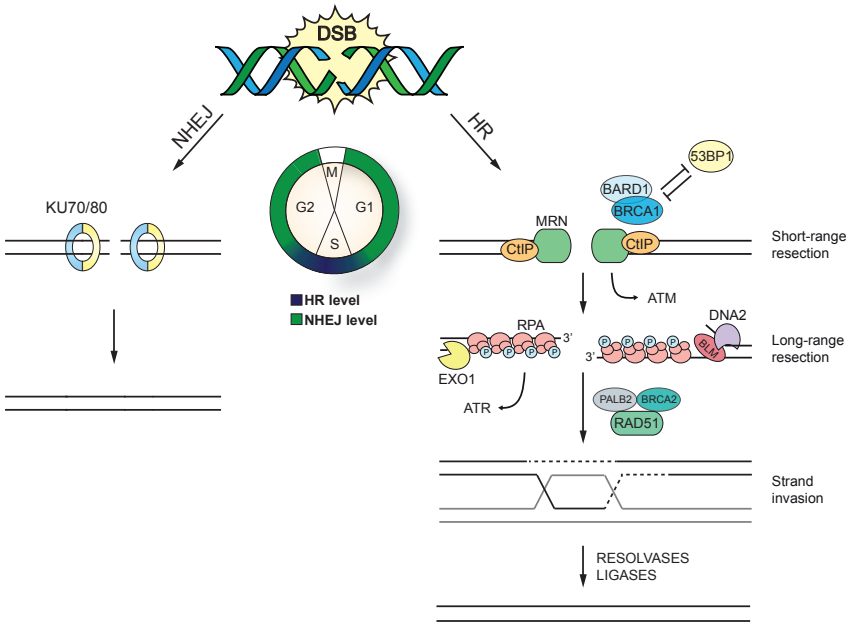

Figure 1.2: DNA double-strand break (DSB repair). DSBs are predominantly repaired by two distinct pathways: NHEJ or HR. NHEJ operates throughout the cell cycle, but mainly during the G_1 and G_2 phases, whereas HR peaks in S phase. Rapid association of the Ku70/80 heterodimer to DSBs promotes NHEJ. Alternatively, MRN, which is initially recruited to DSBs in competition with Ku70/80, initiates HR together with CtIP by performing short-range DNA-end resection to generate short 3' ssDNA overhangs. BRCA1/BARD1 antagonises 53BP1 to facilitate DSB resection. Next, long-range resection is catalysed either by EXO1 or BLM in conjunction with DNA2. Importantly, ssDNA stretches are immediately coated by RPA and the formation of RPA-coated ssDNA stimulates the activation of ATR. Displacement of RPA by RAD51 is mediated by BRCA2 and PALB2, resulting in the formation of RAD51 nucleoprotein filaments. Subsequent strand invasion into the homologous DNA template and capturing of the second DNA end leads to the formation of a double Holliday junction, which is processed by resolvases. Finally, the DNA is sealed by ligases to accomplish error-free repair of the DSB. 53BP = p53 binding protein; BRCA1 = Breast cancer type 1 susceptibility protein; BARD1 = BRCA1-associated ring domain 1; CtBP = C-terminal binding protein; CtIP = CtBP-interacting protein; PALB1/2 = partner and localiser of BRCA1/2. Adapted from [13].

Due to its significance for DSB repair pathway choice, DNA-end resection has been the subject of vigorous investigation over the recent years. As a result, a two-step end resection mechanism has been proposed for mammalian cells: Upon recognition of the DSB, the MRN nuclease complex tethers the broken ends and in conjunction with the

CtBP-interacting protein (CtIP) performs an initial “end-trimming” of 50-100 nucleotides from the DSB ends [32]. This is followed by a more processive long-range resection step carried out by either exonuclease 1 (EXO1) or the BLM helicase together with DNA2 creating long ssDNA stretches of up to several thousand nucleotides [33, 34] (Figure 1.2). Genetic studies in S. cerevisiae have long implicated the Mre11-Rad50-Xrs2 (MRX) complex, homologue to the human MRN, in the initial processing of DSBs. The MRE11 nuclease subunit exhibits both a DNA endonuclease and a 3’-5’ exonuclease activity, thus possessing the opposite polarity to generate 3’ ssDNA tails at DSB ends [35]. Recently however, emerging genetic and biochemical evidence has indicated a slightly different mode for the first step of DNA-end resection in yeast: MRX in conjunction with Sae2, the yeast homologue of human CtIP, introduces an internal incision about 300 bp proximal to DSB thereby creating an entry point for bidirectional resection catalysed by the Mre11 exonuclease in 3’–5’ direction, EXO1 in 5’–3’ direction and possibly also by DNA2 [36, 37]. Besides its crucial role in DNA-end resection, MRN promotes the recruitment of ATM to DSBs via its NBS1 subunit and subsequent ATM activation involving auto-phosphorylation on serine 1981 [38]. ATM in turn phosphorylates a variety of DDR factors, including histone H2AX at serine 139 (γH2AX) and CHK2 at threonine 68 to mediate DNA damage checkpoint signalling and DSB repair [14]. Following resection, ssDNA stretches are immediately coated by replication protein A (RPA) [39] (Figure 1.2). RPA is an evolutionarily conserved, heterotrimeric complex consisting of RPA1, RPA2 and RPA3 [40]. Importantly, RPA-coated ssDNA recruits the ATR kinase, which phosphorylates RPA2 at serine 33 [32, 41]. This primes RPA2 for further phosphorylation on residues closer to the N-terminus including serine 4 and serine 8. RPA-Ser4/Ser8 phos-

phorylation hence marks the mature, hyper-phosphorylated and chromatin-bound form of RPA2 that serves as an important signalling platform orchestrating the DDR and cell cycle checkpoint response [19, 41]. Following DNA-end processing and RPA recruitment, the BRCA2-PALB2 complex promotes RAD51 nucleation onto ssDNA, thereby replacing RPA [42]. The RAD51 nucleoprotein filament then invades the homologous, intact DNA template forming a displacement loop. The second end of the broken chromosome is captured and anneals to the complementary strand of the donor DNA molecule, resulting in the formation of two Holliday junctions (HJs). After DNA synthesis and ligation of both strands, the double HJ is either dissolved or is dismantled by the catalytic action of resolvases in order to complete repair [13, 43] (Figure 1.2). HR requires a homologous DNA sequence, which becomes available only through DNA replication. Thus, repair by HR can only occur during S/G_2 phases of the cell cycle but is error-free since it copies the missing genetic information from the undamaged sister chromatid [20]. It is therefore important to note, that for example, more than 50% of breast and ovarian cancers harbour mutations in genes involved in HR signifying the importance of this repair pathway for tumour avoidance [22].

1.4 Faithful DNA replication is pivotal for genome stability

Accurate duplication of the genome is a fundamental biological process critical for the integrity of the genome and the suppression of cancer-causing mutations. To ensure that genome duplication occurs exactly once during S-phase of the cell cycle, its initiation is tightly controlled by temporarily separating it into two steps. First, in a pro-

cess called origin licensing, the replicative DNA helicase minichromosome maintenance complex (MCM) is loaded at replication origins. This happens exclusively during late mitosis and G_1 phase and requires the origin recognition complex (ORC) and the activities of the CDC6 (cell division cycle 6) ATPase and CDT1 (chromatin licensing and DNA replication factor 1) [44, 45]. Only during the subsequent G_1-S transition, the MCM helicase is activated (origin firing) and additional factors are recruited to from the CMG (Cdc45–MCM–GINS) complex, a prerequisite for replication start [46]. Once formed, CMG unwinds the origin allowing replisome assembly and genome replication (Figure 1.3). A central role in this process is held by cyclin-dependent kinases (CDKs) as they not only trigger origin firing but also inhibit licensing of newly replicated DNA until the next cycle, which is critical to prevent DNA re-replication [47, 48]. In eukaryotes, DNA replication is initiated at multiple origins from which replication forks travel outwards in both directions. Once DNA replication begins, cells fire replication origins not all at once but in a regulated fashion, dividing them into early- and late-replicating origins. In fact, most licensed origins do not fire at all in an unperturbed S-phase but stay dormant to be triggered as a backup in case some replication forks become obstructed [49].

Numerous obstacles of both exogenous and endogenous sources constantly challenge the fidelity of DNA replication potentially resulting in a phenomenon collectively termed 'replication stress', a crucial driving force of genome instability and a feature of pre-cancerous and cancerous cells [27, 50] (Figure 1.3). Generally, replication stress is defined as slowing or stalling in replication fork progression [50]. It can be caused by unrepaired DNA lesions, which form physical barriers to replication fork progression or by a number of other obstructions such as mis-incorporated ribonucleotides [51] or certain

DNA sequences that are intrinsically challenging to replicate because of their secondary structures, such as telomeres, trinucleotide repeats or G-quadruplexes [27, 52]. Replication fork progression may also be slowed down if the availability of essential factors like nucleotides or replication machinery components is limited [53, 54]. In fact, chemotherapeutic agents such as hydroxyurea (HU) function by depleting the intracellular nucleotide pool thus interfering with replication fork progression particularly in highly proliferating cancer cells [55]. Problems to maintain replication speed may also arise if replication and transcription complexes, which both act on DNA, collide [56]. Moreover, inappropriate replication initiation can also trigger replication stress. Excess firing of origins may deplete nucleotide pools and slow replication fork speed, whereas reduced replication initiation can lead to under-replicated regions and susceptibility to chromosome breakage [57, 58]. A particular low density of replication initiation is observed at common fragile sites (CFSs), which represent late-replicating regions of the genome that are especially vulnerable to replication stress [59, 60]. Finally overexpression or constitutive activation of oncogenes such as H-Ras, c-Myc or cyclin E is an emerging source of replication stress. Even though the exact mechanism of their contribution to replication stress has not been fully understood, it has been proposed that oncogenes promote increased origin firing, thus exhausting the nucleotide pools and possibly causing an increased incidence of collisions with the transcription machinery [50, 61–63].

Because of the serious implications of replication stress, cells have evolved a complex network responding to replication stress (Figure 1.3). Upon replication fork stalling, the replicative helicase is uncoupled from the DNA polymerase resulting in the formation of long stretches of single-stranded DNA (ssDNA) that are rapidly coated by the ssDNA-

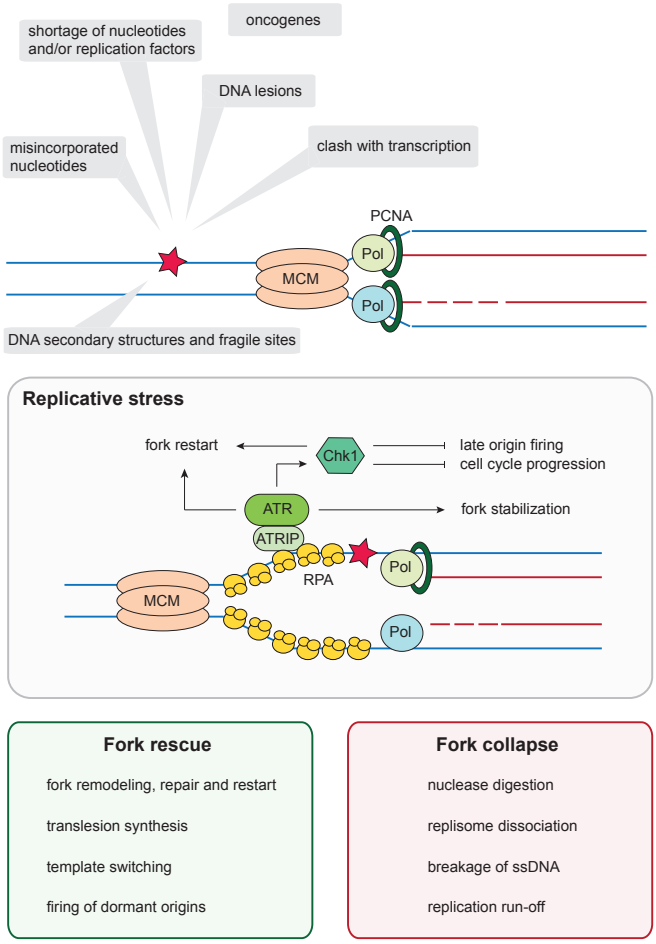

Figure 1.3: Mechanisms of replication fork stalling and the replication stress response. Parental DNA is unwound by the MCM complex and replicated by polymerases bound to the processivity factor PCNA. When replication stalls at a DNA lesion (red star), DNA synthesis can resume downstream, generating a primer–template junction that can be recognized by ATR and ATRIP. ATR then initiates a signalling cascade primarily mediated by the effector kinase CHK1. This response promotes fork stabilization and restart, while preventing progression through the cell cycle until replication is completed. Replication forks stalled at DNA lesions that are stabilized by the ATR pathway can resume replication. If stalled forks are not stabilized, or if they persist for extended periods of time, replication forks will collapse, thereby preventing replication restart. The mechanism by which a replication fork collapses is still ambiguous, and several possibilities are presented here. MCM = Mini-chromosome maintenance; PCNA = proliferating cell nuclear antigen. Adapted from [27].

binding protein RPA [64]. This in turn acts as a signal to activate the central component of the replication stress response, the ATR kinase [65, 66]. ATR gets recruited to RPA-bound ssDNA by the ATR-interacting protein (ATRIP) or via the recruitment of its

allosteric activator TopBP1 by the concerted action of Rad17 and the Rad9–Hus1–Rad1 (9-1-1) complex [19, 67]. ATR induces gradual phosphorylation of several target proteins, such as H2AX (serine 139) and RPA2 (serine 33) triggering the DDR [68]. The key consequences of its activation are mediated by phosphorylation of its downstream effector CHK1 on serine 345 among others, which orchestrates the cellular response to replication stress by stabilizing stalled replication forks (local effect), inhibiting the firing of alternative origins and preventing cell cycle progression (global effects). These events provide time for the resolution of the replication barrier and allow the cell to restart the replication fork once the stress has been removed [54, 69] (Figure 1.3). Of note, accumulating evidence suggests that regulated remodelling of replication forks into four-way junctions, known as fork reversal, can promote fork stability and repair during perturbed replication [70].In this context, more and more evidence emerged implying that stalled replication forks may have undergone structural changes and thus depend on DNA helicases for reactivation. Several non-replicative helicases, including BLM, WRN and SMARCAL1 have been described to promote fork restart [71–73]. If stalled forks cannot be recovered, alternative mechanisms to rescue global replication involve firing of dormant origins, repriming of replication or activating the DNA damage tolerance pathways such as TLS or template switching [18, 74, 75] (Figure 1.3).

If forks are not stabilized or persist for extended periods of time they will ultimately collapse leading to the generation of DSBs (Figure 1.3). This process is particularly accelerated if the ATR-CHK1 pathway is abrogated [67]. The resulting DSBs lead to the activation of the DNA damage kinases ATM and DNA-PK and their respective downstream targets [19]. How stalled forks are processed into DSBs remains equivocal. It is

possible that cells attempt to resolve otherwise irresolvable stalled fork structures using nucleases like MUS81-EME1 or DNA2 to deliberately generate a DSB in order to facilitate HR-mediated repair and restart [76, 77]. However, nucleolytic cleavage of stalled replication forks into DSBs may also be a symptom of aberrant activation of nucleases in the absence of appropriate mechanism for fork protection as it was shown for MRE11 [78] and DNA2 [79]. Secondly, persistent ssDNA found particularly at stalled replication forks represent a vulnerable structure prone to passive breakage as well as endonucleolytic cleavage [80]. Besides long stretches of ssDNA, nicks and gaps as naturally occurring intermediates of several DNA repair and related pathways are intricately susceptible to replication stress-induced DNA lesions as they could be passively converted into DSBs upon encounters with the replication machinery [19, 27] (Figure 1.3).

1.5 Consequences of deregulated replication

Obstacles encountered during replication activate the ATR-CHK1-pathway thus triggering the S and G_2/M cell cycle checkpoints [81]. However, not all replication problems sufficiently activate these cell cycle surveillance pathways and hence localized alterations of fork progression can escape from checkpoint control [82]. Therefore, incompletely replicated loci or unresolved replication intermediates might not be addressed before the onset of mitosis and thus can be carried over to the next cell cycle. 53BP1 protein recognizes such sites of unrepaired DNA damage forming nuclear bodies upon subsequent entry into G_1 in an attempt to shield them against erosion and mark them for repair during the next cell cycle [83, 84]. Potential consequences of cells entering mitosis with

incompletely replicated or damaged chromosomes include chromatid breaks, anaphase bridges or chromosome mis-segregation. Indeed, recent data suggest that 53BP1 nuclear bodies indicate sites of unresolved or broken anaphase bridges [85]. Lagging chromosomes that arise from mitotic errors can promote the formation of micronuclei and excessive DNA damage in the daughter cells [86]. Thus, undetected replication stress jeopardizes the completion of chromosome duplication and successful mitotic commitment potentially causing chromosome aberrations and consequently chromosome instability. Taken together, this underlines the importance of faithful replication as a barrier against tumourigenesis [57, 87]. Indeed, current models of cancer development would argue that the onset of replication stress represents an early event promoting subsequent mutations that confer growth advantages to pre-cancerous cells. It was demonstrated that DNA damage response markers accumulate in human cancer cells even in the absence of exogenous genotoxic treatment at early stages of cancer development [88, 89]. DNA damage could conceivably arise as a result of enhanced replication stress due to uncontrolled induction of oncogenes among other reasons, increasing the level of DNA breakage, mutation and rearrangements. This may fuel mutations targeting DDR pathways, thereby facilitating persistent genomic instability and hence promoting the progression from a precancerous condition to malignancy [9, 90].

1.6 HR proteins function to restart stalled and collapsed replication forks

Faithful genome duplication requires the precise coordination of DNA replication and repair. Intriguingly, a growing body of evidence suggests that proteins involved in the repair of DSBs by the HR pathway also perform key functions in preventing and addressing replication stress-induced lesions [91–95]. Recent reports have provided evidence that RAD51 for example promotes restart of stalled replication forks in a process that does not trigger HR [94]. Furthermore, the MRE11 and DNA2 nuclease were implicated in replication fork recovery [76, 96]. Upon collapse of stalled replication forks and formation of one-ended DSBs, the HR pathway becomes essential to carry out DSB resection, strand invasion, and reassembly of a new replication fork at RAD51-generated D-loop intermediates [19]. Likewise, CtIP and the BRCA1/BARD1 complex have recently been implicated in supporting faithful DNA replication.

The human CtIP protein

The human CtIP protein was initially identified as an interaction partner of the CtBP transcriptional co-repressor complex that plays important roles in development and cancer [97]. Moreover, CtIP was found to be associated with two other bona fide tumour suppressor proteins, BRCA1 and retinoblastoma (pRB), from which it was alternatively termed the retinoblastoma binding protein 8 (RBBP8) [98, 99] (Figure 1.4A). Despite these early reports about its role in gene regulation, CtIP has become extensively recognized for its

function in initiating the repair of DSBs by HR by carrying out DNA-end-resection in conjunction with the MRN complex to generate short 3'- ssDNA tails [32]. Its crucial role in DSB repair as well as the fact that CtIP interacts with a number of proteins related to carcinogenesis have led to the notion that CtIP might be a tumour suppressor itself. Support for the hypothesis came from findings that homozygous deletion of *CtIP* in mice leads to early embryonic lethality while heterozygous animals are viable, but develop multiple tumours, particularly large lymphomas [100]. In colorectal and endometrial cancers, *CtIP* frameshift mutations were reported as a result of microsatellite instability [101, 102] and epigenetic inactivation of *CtIP* correlates with breast cancer and is associated with resistance to the drug tamoxifen [103, 104] further confirming a significant link between CtIP and cancer.

At the molecular level, human CtIP is a 125 kDa nuclear protein of 897 amino acids, which is significantly conserved among mammals [97]. The C-terminus of CtIP is evolutionarily highly conserved and shares significant sequence homology with Saccharomyces cerevisiae Sae2, an orthologue protein required for both meiotic and mitotic DSB repair in yeast [32, 107] (Figure 1.4A). Cells expressing a mutant lacking the C-terminal part of CtIP are deficient in DNA-end resection further emphasizing the importance of this domain for proper DSB repair function [32]. Remarkably, rare hypomorphic mutations in the CtIP gene resulting in expression of a C-terminal truncated protein have been identified to cause severe microcephaly, growth retardation and skeletal abnormalities as well as impaired DSB resection and ATR activation in patients with Seckel and Jawad syndromes [108, 109]. The N-terminal domain of CtIP forms a coiled-coil motif that is essential for oligomerization [110–113] (Figure 1.4A). Furthermore, it was found that CtIP tetramer-

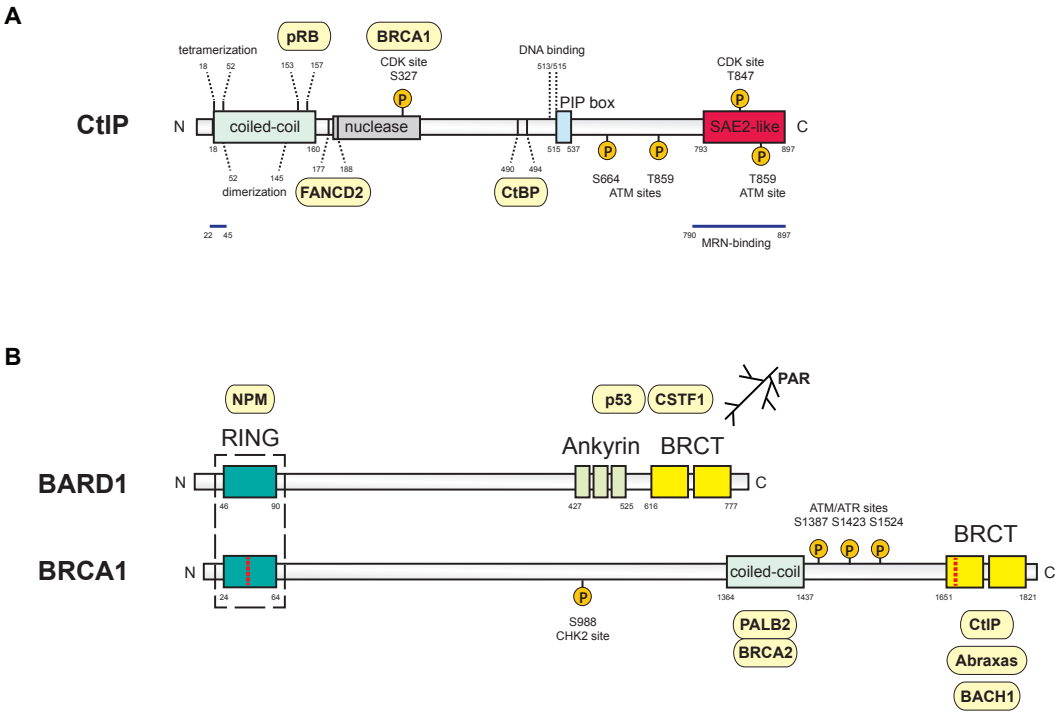

Figure 1.4: Schematic overviews of CtIP and BRCA1/BARD1 proteins. (**A**) CtIP protein architecture. The N-terminus of CtIP contains themultimerization regions within a coiled-coil domain and a consensus motif for pRb-binding (LECEE). The middle region consists of a FANCD2-binding motif, the nuclease domain that includes residues from approximately 180 to 350, the DNA- and CtBP-binding sites and a PIP-box mediating interaction with PCNA. CDK phosphorylation at S327 mediates BRCA1 interaction and ATM phosphorylates S664, S745 and T859 in response to DNA damage. The C-terminal part of CtIP is evolutionary most conserved and contains the CDK phosphorylation site T847 essential for DNA-end resection. MRN-binding regions are located in both N- and C- terminal regions of CtIP. Adapted from [105]. (**B**) The BARD1 protein architecture is compared to that of BRCA1. The N-terminal regions of both proteins contain a conserved RING finger domain required for heterodimer formation (dashed box) and E3 ubiquitin ligase activity. At the C-terminus, BRCA1 and BARD1 each possess two conserved BRCT domains for phosphor-epitope binding. BARD1 additionally harbours three ankyrin repeats that facilitate protein–protein interaction. The BARD1 N-terminus interacts with NPM/B23, a chaperon protein involved in centrosome duplication and cell proliferation. The region between the ANK and BRCT domains was shown to bind to either CSTF1 or the tumour suppressor p53 in a competitive manner thus regulating cell cycle progression and apoptosis. No phospho-proteins interacting specifically with the BARD1-BRCT domain have been discovered to date but a recent report reveals that they may bind to negatively charged PARylated substrates. The BRCT repeats at the BRCA1 C-terminus recognize phosphorylated S(p)XF motifs on the direct binding partners CtIP, CCDC98/Abraxas or BACH1. The central region of BRCA1 contains phosphorylation substrate residues for the ATM and ATR kinases (S1387A, S1423A and S1524A) and Chk2 (S988A) and a coiled-coil domain that associates with PALB2/BRCA2 during HR. Hotspots for common clinical mutations in BRCA1 are highlighted (red dashed line). Adapted from [106]. BACH1 = BTB and CNC homolog 1; BRCT = BRCA1 carboxy-terminal (domain); CCDC98 (Abraxas) = coiled-coil domain containing protein 98; CSTF1 = cleavage stimulation factor subunit 1 50kDa; CtBP = C-terminal binding protein; FANCD2 = Fanconi anemia complementation group protein D2; NPM = Nucleophosmin/B23; PAR = poly(ADP-ribose); PIP box = PCNA-interacting peptide box; pRB = Retinoblastoma protein; RING = Really interesting new gene.

ization is required for effective accumulation at DSBs and its function in HR [112, 113]. Nevertheless, it remains possible that CtIP can also function in its dimeric form in some aspects of DNA repair [111, 112]. Both, CtIP N- and C-terminal regions are involved in mediating the interaction between CtIP and the MRN complex [114]. Additionally, this interaction is strongly regulated by CtIP phosophorylation. Twelve potential CDK phosphorylation sites can be found in CtIP and phosphorylation of at least five of them facilitates the interaction with the FHA and BRCT phospho-peptide binding domains of Nbs1 and furthermore primes CtIP for modification by the ATM kinase [114]. Upon DNA damage, ATM phosphorylates CtIP on at least three residues (serine 664 and 745 and threonine 859) thereby enabling HR [114] (Figure 1.4A). Remarkably, it has been found that mutation of a critical CDK site at threonine 847 (T847) renders CtIP incapable of performing its functions to support HR [32, 114, 115]. Yet, the precise mechanism of how T847 phosphorylation activates CtIP is still unclear as CtIP-T847A mutants remain nuclease proficient in vitro, and are capable of binding to Nbs1 [114, 116]. Along that line, an endonuclease activity has been recently assigned to CtIP residing in the middle part of the protein (Figure 1.4A). However, this activity seems to be dispensable for DNA-end resection of “clean” DSB ends, but important for the processing of ends containing secondary structures such as DNA hairpins or protein–DNA adducts stemming from lesions induced by topoisomerase poisons and ionizing radiation or at inverted repeats or CFS [116–118]. In this model, the essential role for the CtIP protein in DSB repair would likely involve a non-catalytic role through CtIP-dependent recruitment of other DNA damage repair factors underlining the fact some known modifications affect a general CtIP-dependent resection function independent of its nuclease activity [116].

Since the discovery of the role of CtIP in HR-directed repair of DSBs, it has emerged as a key concept that CtIP-dependent resection of the DNA ends plays a key role in activation of ATR and CHK1 kinases to induce the cell cycle checkpoint [32, 67]. Recently however, a study by Koushoult et al. established that CtIP was dispensable for initial ATR–CHK1 activation after DNA damage but DNA-end resection was critically required for sustained ATR–CHK1 checkpoint signalling and for maintaining both the intra-S and G_2/M checkpoints in the face of persisting DNA damage [119].

The role of CtIP in genome stability maintenance beyond its role in HR and cell cycle checkpoints is furthermore emphasized by recent findings implicating it in additional pathways addressing different kinds of DNA lesions. CtIP was shown to remove DNA interstrand crosslinks through interaction with the FA-protein FANCD2 [120] (Figure 1.4A) as well as DNA intermediates that form secondary structures or replication blocks [117]. Importantly, it has been suggested that CtIP belongs to the key HR proteins mediating faithful DNA replication as it was shown to be associated with unperturbed replication forks and act on stalled as well as on collapsed forks [95, 121]. CtIP is thought to ensure replication fork progression and to prevent the formation of under-replicated regions especially in the context of common fragile sites [117, 121]. It is also important to note, that even before these roles of CtIP were uncovered, a minimal region of the CtIP protein (residues 515 to 537) was described comprising a consensus PCNA-interacting motif (PIP-box) that mediates the assembly of CtIP into replication foci during S-phase [122] (Figure 1.4A). Although the function of this PIP-box remained enigmatic, it was proposed that PCNA facilitates CtIP localization to sites of on-going replication. This concept gained new impetus when an iPond-SILAC-MS screen identified CtIP in the vicinity of active replication

forks [95].

The BRCA1/BARD1 tumour suppressor complex

The breast cancer early onset gene 1 (*BRCA1*) is involved in a network of several DNA repair protein complexes performing fundamental roles in genome stability maintenance and the suppression of cancer [123]. The landmark discoveries describing that germline mutations in the *BRCA1* gene confer a lifetime risk of up to 90% for developing breast cancer and the strong evidence implying that *BRCA1* may also be mutated in many sporadic cancers [124–126] (Figure 1.4B) has sparked intensive investigations about the physiological roles of this factor in tumour suppression. Key studies following the initial molecular cloning of *BRCA1* strongly implied that the protein possesses central functions in the DDR and thus in preserving chromosomal integrity [127]. It was found that homozygous disruption of *BRCA1* in the mouse germline causes early embryonic lethality and impedes cell proliferation [128, 129]. Cells defective for BRCA1 exhibit elevated levels of chromosome aberrations, such as DNA breaks and chromatid exchanges, enhanced sensitivity to DNA-damaging agents and defects in cell-cycle checkpoint function [130–135]. Consistently, BRCA1 relocates to nuclear foci upon DNA damage induction [135–137] and cells lacking functional BRCA1 are highly impaired in performing HR at endonuclease-induced DSBs [138]. Taken together, these findings firmly established BRCA1 as a custodian of chromosome integrity with an important role in homology-directed DNA repair. A comprehensive understanding of how BRCA1 contributes to the aforementioned functions on the molecular level is however still incomplete and many important questions remain unresolved. Further progress in defining how BRCA1 promotes HR was made by

demonstrating that loss of 53BP1 (TP53BP1, tumour suppressor p53 binding protein 1) rescues the lethality, tumourigenesis, and genome instability of BRCA1-deficient mice [139–141]. It was shown that 53BP1 inhibits DNA-end resection in BRCA1 deficient cells and promotes error-prone NHEJ in S-phase. BRCA1, on the other hand, facilitates the removal of 53BP1 in S phase to allow resection of DSBs generating the initial substrate of RAD51-dependent HR [30, 140]. Thus, it was proposed that BRCA1 as well as 53BP1 possess the ability to associate with DSBs, but BRCA1 channels repair into HR, whereas 53BP1 favours NHEJ by antagonizing DNA-end resection. Cells lacking BRCA1 therefore fail to prevent NHEJ in S phase, and chromosomal aberrations arise from inappropriate joining of replication-associated DSBs [142].

In vivo, BRCA1 forms an obligate heterodimer with the structurally related BRCA1-associated ring domain 1 (BARD1) and it has been suggested that BRCA1 requires the interaction with BARD1 to maintain chromosome integrity and HR function [143–145] (Figure 1.4B). It has been described that both proteins exhibit close homology within their conserved amino-terminal RING finger domains and between the C-terminal tandem BRCA1 carboxy-terminal (BRCT) domains [143]. Moreover, BARD1 harbors three ankyrin (ANK) repeats located upstream of the BRCT domains with an essential function in chromosome stability and HR [144]. The interaction between BRCA1 and BARD1 is mediated by the flanking regions of the RING finger motif of the two molecules and confers E3 ubiquitin ligase activity to the RING domains of the heterodimer [146, 147]. Consequently, BRCA1/BARD1 directs its auto-ubiquitylation as well as ligation of K6-linked ubiquitin structures occurring during S-phase and in response to replication stress and DNA damage [148]. For instance, it was reported that CtIP is a substrate for K6-ubiquitin

chains catalysed by BRCA1/BARD1 triggering the association of CtIP with chromatin following DNA damage [149]. Furthermore, the BRCA1/BARD1 E3 ligase has functions in the regulation of transcription in response to DNA damage by ubiquitination of phosphorylated RNA Pol II and by mono-ubiquitination of H2A/H2AX to modulate chromatin structure [150, 151]. Besides, the BRCA1/BARD1 E3 ligase activity has been implicated in cell cycle control, particularly in mitotic progression, as it was shown to regulate several targets involved in centrosome amplification and spindle formation such as the nucleolar protein nucleophosmin (NPM), γ-Tubulin and Aurora B [152–154]. Importantly, the E3 ubiquitin ligase activity of BRCA1/BARD1 is thought to contribute to genome stability by facilitating HR [144, 145] but the precise mechanism remains elusive [123].

Further light was shed on the significance of the BRCA1/BARD1 interaction by a recent study indicating that BRCA1/BARD1 is assembled at the site of DNA damage in a biphasic pattern. Thus, BRCA1 recruitment involves a novel interaction between its partner protein BARD1 and poly(ADP-ribose) chains at the DSB, which mediates the rapid recruitment of the heterodimer [155] (Figure 1.4B). Similarly, the BARD1-BRCT domain has been shown to specifically recognize histone H3 dimethylated at lysine 9 through its interaction with HP1 proteins thus anchoring BRCA1/BARD1 at sited of DNA damage [156]. Genetically, the significance of the BRCA1/BARD1 interaction is underscored by the necessity of BARD1 for the majority of BRCA1 in vivo functions. Specifically, it was described that *BARD1* deficiency fully recapitulates *BRCA1* nullizygosity, with BARD1 knockouts displaying embryonic lethality, genomic instability, and cancer susceptibility [157, 158]. However, given the critical interaction, it is surprising that *BRCA1* is frequently mutated whereas *BARD1* mutations in both hereditary and sporadic breast can-

cer are relatively rare [159–162]. New insights into the tumourigenic potential of BARD1 loss-of-function came from studies revealing that BARD1 spliced isoforms are often more abundant than the full-length product in cervical, breast, ovarian and endometrial cancer cell lines [163] thus implying that aberrant BARD1 splicing may confer oncogenic properties. Further evidence for this mechanism came from findings that in cancer cells BARD1 spliced isoforms frequently harbour opposing functions compared to the full-length protein [154, 163, 164]. It remains unclear why BARD1 loss-of-function in cancer proceeds predominantly through alternative splicing as opposed to mutation. BARD1 deletion may be too deleterious for cancerous cells to overcome and alternative splicing could provide a mechanism in which activity is finely modulated, rather than abolished [161]. Alternatively, essential functions of BARD1 extending beyond its BRCA1-related roles may contribute to its cellular indispensability. In fact, several BRCA1-independent roles of BARD1 have been suggested. BARD1 was for example found to bind and stabilize p53 thus inducing apoptosis in a manner that is antagonized by BRCA1 [165, 166]. Furthermore, BARD1 is considered to play a role in the inhibition of mRNA maturation upon DNA damage by binding to the mRNA poly-adenylation factor CSTF1 (cleavage stimulation factor, subunit 1), a mechanism likely involved in cell cycle regulation [167, 168].

Besides the interaction with its key binding partner BARD1 through their N-terminal RING domains, BRCA1 forms complexes with numerous other factors and hence it is reasonable to propose that the tumour suppressive roles of BRCA1 are manifested through its interactions (Figure 1.4B). With regard to the DNA repair function, the tumour suppressor properties of BRCA1 are predominantly mediated by the BRCT domain, that binds phosphorylated serine motifs [169]. Remarkably, already in early studies, an interaction

between CtIP and the BRCA1-BRCT motif was uncovered [98, 170] and it was shown that this is mediated by CDK phosphorylation of CtIP at serine 327 (S327) during G_2 phase of the cell cycle [171]. Later, evidence emerged that BRCA1 interacts with CtIP and MRN in the S/G_2 phases to favour DNA-end resection and thus HR [32, 172, 173]. Indeed, it was found that DNA-end resection and HR are impaired in BRCA1-deficient cells [138, 174] and that chicken DT40 cells expressing human CtIP defective in interacting with BRCA1 (S327A) is incapable to perform HR [173]. However, subsequent studies have come to challenge the significance of the CtIP-BRCA1 interaction by presenting several lines of evidence implying that complex formation with BRCA1 is not essential for CtIP-mediated DNA end-resection and HR [175–177], and possibly only fine-tunes resection speed [178]. However, if BRCA1 is dispensable for DNA-end resection, the question remained how it promotes HR. It has been suggested that the CtIP–BRCA1 complex formation in mammalian cells involves the removal of the 53BP1 effector protein RIF1 from DSB regions, which otherwise blocks DNA-end resection [179]. Thus the principle role of BRCA1 in DSB repair may involve its function in antagonizing 53BP1 in S-phase thus facilitating CtIP-mediated DNA-end resection and subsequent HR [177].

Further insights in the tumour suppressive activities of BRCA1 have emerged from studies which have uncovered a role of BRCA1 activity at the replication fork as being central to its DNA repair function. Previous studies already indicated that upon replication stalling, BRCA1 rapidly relocalizes to replication foci containing PCNA [180]. Recently, it was found that BRCA1 participates in replication fork protection as it was demonstrated that BRCA1 prevents degradation of nascent strands at stalled replication forks [92]. BRCA1 also regulates multiple aspects of replication to promote DNA ICL repair. It was

shown for instance, that BRCA1 is required to unload the CMG helicase complex from chromatin after replication forks collide with an ICL [181]. Moreover, BRCA1 is involved in the recruitment of FANCD2 and subsequent processing of ICLs independently of its HR activity [182]. By adapting the bacterial replication terminator Tus/Ter complex to induce site-specific replication fork stalling in mouse cells, it became apparent that BRCA1 is required for HR at stalled replication forks and that in this incidence HR is regulated differently than at endonuclease-mediated chromosomal DSBs [183]. Furthermore, BRCA1 was shown to control the step-wise recruitment of MRE11, FANCD2 and finally CtIP to stalled replication forks, followed by their concerted actions to promote fork recovery [121] thus raising the question of whether the CtIP–BRCA1 interaction may function to alleviate blocked replication forks [118]. Consistent with those novel roles ascribed to BRCA1, it was described that primary mammary epithelial cells from patients with heterozygous BRCA1 mutations experience higher loads of replication stress while other BRCA1 functions remained unaltered indicating that the proficiency in responding to replication fork stalling might be the limiting factor in BRCA1 genome integrity control [184].

1.7 Synthetic genetic interactions provide a rational to harness specific DNA repair defects of cancer cells for targeted therapies

To protect the genome, cells have evolved a diverse set of pathways designed to sense, signal, and repair multiple types of DNA damage. Recently the interconnectedness of DDR mechanisms has become more and more appreciated as it was discovered that

partial redundancy of different DDR pathways can coordinate with one another and act compensatory in the absence of the optimal response [19, 185, 186]. Moreover, it has been considerably recognized that genetic interactions (GIs), which describe the extent to which the phenotype of a first gene mutation is modified by the presence of a second one, can provide detailed information regarding functional relationships between genes and the structure of their underlying biological pathways. Thus, determining GI profiles within a cells presents an exciting possibility to understand the buffering relationships between DNA repair mechanisms in more detail [186–188]. Formally, GIs can be defined as the deviation from the expectation that the combined effect on the fitness of an organism of two mutations will be the product of their individual effects [189]. In this context, two classes of GIs have been described: negative or alternatively termed aggravating or synthetic sick/lethal (SSL) GIs, whereby the resulting phenotype is more severe than is expected from the phenotypes associated with the single mutants (Figure 1.5) or positive (alleviating) GIs, where the combined phenotype is less severe than anticipated [190, 191].

However, in the last decade the analysis of GIs has not only proven to constitute a critical tool for systems biology to decipher molecular pathways. Particularly SSL interactions have been intensively investigated in order to identify drugs that will cause lethality to cancer cells that harbour inherent defects without harming normal cells (Figure 1.5). More precisely, during their pathogenesis, many cancer cells acquire mutations in DSB repair genes and become dependent on a compensatory mechanism in order to survive. Thus, for example compromised abilities to repair DNA damage confers a weakness that can be therapeutically exploited on the basis of the concept of synthetic lethality, whereby phar-

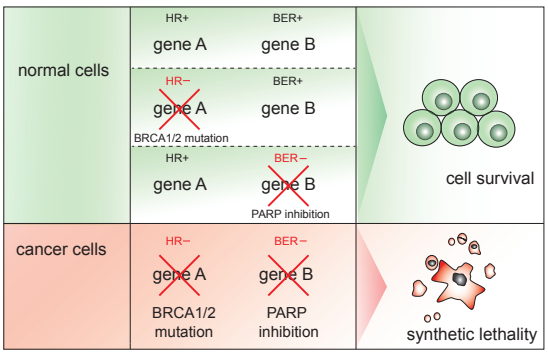

Figure 1.5: Synthetic lethality can be harnessed for cancer therapy. Synthetic lethality is defined as a combination of mutations or perturbations in two or more genes that leads to cell death, whereas inactivation of any one of the genes alone does not. Perturbation of genes can occur through genetic mutation or silencing, depletion by RNAi or chemical inhibition and is depicted by a red cross. Please refer to the main text for details about the example given for synthetic lethality between *BRCA1/2* mutation and PARP inhibition. ADP = adenosine diphosphate; BER = base excision repair; DDR = DNA damage response; DNA = deoxyribonucleic acid; RNAi = RNA interference; SMI = small molecule inhibitor.

macological inhibition of the "back-up" pathway induces greater toxicity in DNA repair-deficient cancer cells as compared with normal cells [13, 23, 24, 192] (Figure 1.5). The first "proof-of-principle" study verifying synthetic lethality as a suitable approach for targeted cancer therapy was published in 2005, after it had been demonstrated that HR-defective BRCA1- or BRCA2-deficient cell lines display dramatically increased sensitivity to inhibition of the SSB repair enzyme PARP [193, 194]. The current understanding suggests that inhibition of PARP leads to the accumulation of SSBs which are converted into DSBs upon encountering DNA replication forks during S-phase when HR is most active [185]. Consequently, in the absence of functional HR, such as in cancer cells lacking BRCA1 or BRCA2, PARP inhibition results in the accumulation of DSBs and, ultimately, in apoptosis or mitotic catastrophe (Figure 1.5). Importantly, normal cells survive the treatment owing to functional HR, providing the kind of selectivity that is considered the

ultimate goal of cancer therapy. Following the initial description of the mechanism, clinical development of potent small molecule PARP inhibitors (PARPis) rapidly advanced, and the first Phase II results in 2009 showed that monotherapy with the PARPi olaparib (AZD-2281; AstraZeneca) achieved encouraging response rates of 41% and 33% in patients with *BRCA1*- or *BRCA2*-mutated advanced breast and ovarian cancers, respectively [195, 196]. As the concept of personalised medicine emerged, tumour-specific defects represent a promising therapeutic target to be exploited for the selective elimination of cancer cells. Particularly recent advances in ribonucleic acid interference (RNAi) technologies and the development of sophisticated screening platforms for SSL interactions holds great potential to achieve a better understanding of cellular functions and their underlying genetic networks, thus more and more genetic interactions may be uncovered as potential targets for synthetic lethality in cancer therapy [188, 191, 197]. Recently, a number of candidate synthetic lethal interactions targeting for instance p53-mutant tumour cells have been proposed [198, 199], including inhibition of the DNA damage kinases ATR and CHK1 [200, 201]. Likewise, oncogenic *K-Ras* mutations have been found to be synthetically lethal with ATR inhibition [202]. In this context, the recently discovered small molecule inhibitors of the HR proteins RPA and RAD51 represent promising candidates to harness defective DDR pathways in cancer cells in the near future [203, 204].

Aims

The cellular response to DNA damage is essential to safeguard genome integrity and to prevent malignant transformation. Human CtIP (RBBP8) was originally discovered as an interacting partner of the three tumour suppressor proteins; CtBP, BRCA1 and retinoblastoma (pRB) that are significantly involved in controlling cell cycle progression and proliferation. Nowadays, CtIP is most considerably recognized for its key role in the repair of DNA double-strand breaks (DSBs) by the homologous recombination (HR) pathway. As critical functions of CtIP in other DNA repair pathways as well as in cell cycle checkpoint control and DNA replication are emerging, CtIP is more and more considered to be a core factor for genome stability maintenance. Accordingly, haploid insufficiency of *CtIP* has been shown to predispose mice to multiple types of tumours and *CtIP* mutations have been linked to several human cancers. Many aspects of CtIP functions in counteracting genome instability and cancer development are however still poorly understood.

In my PhD thesis work, I took an unbiased approach to examine CtIP genetic interactions in unperturbed human cells and in response to DNA damage in order to explore the molecular network of CtIP involved in the maintenance of genome stability.

Aim 1: Develop a platform to determine genetic interaction profiles of CtIP in human cells.

Large-scale mapping of genetic interactions provides a powerful tool to dissect the functional organisation of cellular networks that govern processes such as genome stability maintenance and tumour suppression. Therefore, the major aim of my PhD project was to develop a platform to systematically survey genetic interactions of CtIP in human cells in the absence or presence of DNA damage by employing high-content RNA interference (RNAi)-based screening. In the first part of my thesis, I describe the approach we employed to uncover genetic interactions with CtIP in detail.

Aim 2: Elucidate the molecular mechanism underlying the SSL interaction between CtIP and BARD1.

From the analysis of the RNAi screen, the BRCA1-associated RING domain protein 1 (BARD1) emerged as a strong candidate for synthetic sick/lethal (SSL) interactions with CtIP. Following up on my screen results, I focussed on investigating the molecular mechanism underlying the SSL relationship between CtIP and BARD1. At the same time, I sought to shed new light on the significance of the CtIP-BRCA1/BARD1 interaction and its role in genome integrity maintenance. Thus, in the second part of my thesis, my central aim was to elucidate how CtIP and BARD1 promote faithful DNA replication, thereby contributing to genome stability and cell survival.

Taken together, the findings from the two sections described above have constituted a scientific manuscript that will be submitted for publication in a peer-reviewed journal shortly.

Aim 3: Investigate CtIP functions in DNA interstrand crosslink repair.

Recently, CtIP has been implicated the cellular response to DNA interstrand crosslinks (ICLs). Distinct DNA repair activities are required for the resolution of ICLs, including recognition of the lesion and signalling by FANCD2, nucleolytic incision of the crosslink, and repair of the DSB intermediate through HR. During this process, FANCD2 interacts with CtIP, thereby tethering CtIP to the site of the ICL in order to ensure proper coordination of DNA-end resection and subsequent HR. Importantly, FANCD2 mono-ubiquitination was found to be critical for the accumulation of CtIP at ICL-damaged chromatin, presumably by facilitating the FANCD2-CtIP interaction. Thus, my aim in this project was to address the question whether CtIP can bind to ubiquitin. The data I have contributed were included in a publication by Murina et al. in the peer-reviewed journal *Cell Reports* in 2014. The scientific manuscript and an indication of my contribution are included in the Appendix.

Material and Methods

Cells

U2OS, HEK293T, and HEK293 cells were grown in Dulbecco's modified Eagle's medium (DMEM) supplemented with 10% fetal calf serum (FCS), 100 U/ml penicillin, and 100 mg/ml streptomycin.

The generation of a stable MRC5 cell line with inducible shRNA-expression was described previously [120]. MRC5^{shCtIP} and MRC5^{shLacZ} cells were grown in DMEM supplemented with 10% Tet system approved FCS, 100 U/ml penicillin, 100 mg/ml streptomycin, Blasticidin (5 mg/ml), and Zeocin (250 mg/ml). To induce shRNA expression, cells were treated with 1 µg/ml doxycycline (Dox) as indicated.

The Flp-In T-REx system (Invitrogen, Life Technologies) was used to generate cell lines stably expressing siRNA-resistant GFP-BARD1. A pEGFP-C1 plasmid comprising human BARD1 was kindly provided by Prof. Xiaochun Yun (University of Michigan). The sequence was altered to be resistant to siBARD1 #1 by site-directed mutagenesis using Expand Long Template PCR System (Roche). The resulting BARD1 sequence was subcloned to obtain siRNA-resistant GFP-BARD1-containing pcDNA5/FRT/TO vectors carrying different point mutations. U2OS/Flp-In cells stably expressing GFP-BARD1

constructs were generated as described previously [205]. Single clones resistant to 250 µg/ml hygromycin B and 12.5 µg/ml blasticidin S were selected and screened for inducible GFP-BARD1 expression by both immunofluorescence microscopy and immunoblotting. To induce expression of GFP-BARD1, cells were treated with 1 µg/ml doxycycline (Dox) as indicated.

U2OS^{Cas9WT} and U2OS$^{Cas9\Delta CtIP}$ cell lines were generated as described previously [206]. In brief, U2OS-Flp-In cells inducibly expressing Cas9-FLAG (U2OS^{Cas9}) were transfected with a plasmid (DU46129, U6_gRNA) encoding a short guide RNA (sgRNA) targeting CtIP or the empty vector as control. 8 h after transfection, Cas9-FLAG expression was induced with Dox (1 µg/ml). Two days later, cells were replated at high dilutions to obtain single-cell derived colonies. These were expanded and screened for sgRNA incision by PCR and restriction digest as well as for loss of CtIP by immunoblotting. Since this procedure yielded only a clonal population of cells showing a reduction of CtIP protein levels of approximately 30%, these cells were subjected to another round of sgRNA transfection, Cas9 expression and clonal selection finally establishing the cell lines used here. Ultimately, the targeted genomic region was amplified by PCR using the following primers (forward 5'-AGCAAGTAGAAGTGTGGAGCA-3'; reverse 5'-ACAAAGCCACTACAGTCTCAAC-3') and analysed for the presence of insertion and deletion mutations by deep sequencing.

Combinatorial RNAi image-based screening and data analysis.

MRC5^{shCtIP} cells were treated with 1 µg/ml Dox or left untreated (control) for 48 h prior to reverse transfection with a custom Silencer® Select siRNA library (Ambion) targeting

207 human genes. The library comprised of three independent siRNA oligonucleotides per target arrayed alongside controls in 384-well plates (Greiner bio-one). All liquid handling was completed using an EL406 microplate washer and dispenser (BioTek). RNAi screens were performed in three biological replicates, each consisting of two technical replicates. In brief, 0.8 pmol siRNA (Ambion Silencer® Select) dissolved in 5 µl nuclease-free water were pre-spotted in each well of an assay plate. To this 25 µl DMEM (without supplements) containing 0.05 µl Lipofectamin RNAiMax (Invitrogen) was added. The mix was incubated for 1 h at RT before dispensing 180 cells resuspended in 50 µl DMEM supplemented with 10% FCS, 100 U/ml penicillin, and 100 mg/ml streptomycin leading to a final concentration of 10 nM siRNA per well. For MRC5^{shCtIP} cells that had been exposed to Dox before, the cell culture media was kept supplemented with 0.1 µg/ml Dox throughout the screen. Upon reverse transfection, cells were incubated for 6 days followed by formaldehyde fixation and Hoechst staining (bisBenzimide H 33342; Sigma-Aldrich). The cells were imaged on two coupled ImageXpress micro (IXM) HCS microscopes (Molecular Devices) acquiring 9 images per well with a Nikon CFI S Fluor 10X objective. Finally, quantitative image analysis was carried out using CellProfiler (Broad Institute [207]) and Matlab (The MathWorks) to assess the number of nuclei per well.

As numbers of nuclei per well represent discrete data, square root transformation was applied and within-plate normalization was performed to median values of negative control conditions (percentage of control), i.e. mock transfected cells or cells treated with non-targeting siRNAs. The strictly standardized mean difference (SSMD) was used to measure the magnitude of difference in cell viability between the cytotoxic positive control (siRNA against kinesin family member 11) and the negative controls as a means for

quality control [208]. Target genes whose depletion induced cytotoxicity reducing cell numbers to more than 20% of the overall median cell number were excluded from further analysis. To identify negative synthetic genetic interactions with CtIP, a multiplicative model was applied and an interaction score, termed the (ϵ)-score, was computed. Based on the assumption that the combined effect of two individual perturbations (V_{ab}) will be the product of their individual effects (V_a and V_b), the ϵ score determined the difference between the observed phenotype and the effect that would be expected if the two genes do not interact [189]. Theses ϵ scores were used as a basis of hit ranking applying the Redundant siRNA Activity (RSA) algorithm. First, siRNAs were ranked according to their ϵ score after which the RSA method was used to assign P-values to each target gene indicating the statistical significance of all siRNAs targeting a single gene being distributed significantly higher in the ranking than would be expected by chance, calculated based on an iterative hypergeometric distribution formula [209]. A P-value cut-off of $p<0.05$ was chosen to determine a set of candidate hits. Those were further analysed for known associations with the CtIP protein and grouped according to their molecular functions using the STRING database and DAVID functional annotation clustering [210, 211].

Transfection

Plasmids were transfected either by using the standard calcium phosphate method or by FuGENE 6 (Roche) according to manufacturer's instructions. The FLAG-tagged expression construct for human BARD1 was a kind gift of Prof. Xiaochun Yun (University of Michigan). All point mutations were introduced by site-directed mutagenesis using Expand Long Template PCR System (Roche) and confirmed by sequencing.

siRNA oligos were transfected at a final concentration of 10 nM using Lipofectamine RNAiMAX (Invitrogen). For co-depletion experiments, the respective siRNAs were transfected at a final concentration of 10 nM + 10 nM of each oligonucleotide and the total amount of oligonucleotides was kept equal by transfecting a non-targeting siRNA (Ctrl) in the single depletion samples. All siRNAs used in this study were purchased from Ambion (Silencer® Select siRNAs). The following oligonucleotides (sequences in 5' to 3' direction or Ambion siRNA ID are given) were used: Ctrl (Ambion Negative Control #2), CtIP (GCUAAAACAGGAACGAAUC) [32], CtIP #2 (s11849), BARD1 #1 (s1885), BARD1 #2 (s1886), BARD1 #3 (s1887), BARD1 #4 (CTGAATATTATACCAGATGAA), BRCA1 #2 (s458), BRCA1 #4 (GGAACCUGUCUCCACAAAG). If not indicated, siBARD1 denotes the use of siBARD1 #1 and siBRCA1 denotes siBRCA1 #2.

Antibodies

A complete list of all primary used in this study can be found in table 3.1. Secondary HRP-conjugated anti-mouse and anti-rabbit antibodies were form GE-Healthcare. AlexaFluor-488, -594 and -647-conjugated secondary antibodies were from Invitrogen.

Drugs and cell culture supplements.

Hydroxyurea (HU, Sigma-Aldrich), aphidicolin (Aph, a kind gift of Prof. Massimo Lopes) and camptothecin (CPT, Sigma-Aldrich) were used as indicated in Figure legends. ATR inhibitor (VE-821) was provided by Vertex Pharmaceuticals (Abingdon, UK). dNTP analogs BrdU, CldU, IdU (Sigma-Aldrich), and EdU (Life Technologies) were used as indicated. For native BrdU labeling, cells were grown with BrdU (30 µM) for 24 h.

Antibody target	Species	Supplier/Reference	Application[a]
53BP1	rabbit	ab-21083 (abcam)	IF
pATM S1981	rabbit	ab-81292 (abcam)	IB
ATM	mouse	GTX70103 (GeneTex)	IB
BARD1	rabbit	Gift from R. Baer	IB and IF
BRCA1 (D-9)	mouse	sc-6954 (Santa Cruz)	IB
BrdU	mouse	RPN202 (GE Healthcare)	IF
pCHK1 S345	rabbit	2341(Cell Signaling)	IB
CHK1 (G-4)	mouse	sc-8408 (Santa Cruz)	IB
CtIP (D-4)	mouse	sc-271339 (Santa Cruz)	IB
DNA2	rabbit	Gift from P. Cejka	IB
EXO1	rabbit	A302-640A (Bethyl)	IB
FLAG	mouse	F3165 (Sigma)	IB
GAPDH	mouse	MAB374 (millipore)	IB
γH2AX (20E3)	rabbit	9718 (Cell Signaling)	IF and FACS
MRE11 (12D7)	mouse	GTX70212 (GeneTex)	IB
ORC2	rabbit	559266 (BD PharMingen)	IB
pRPA S4/S8	rabbit	A300-245A (Bethyl)	IB and IF
RPA2 (Ab-3)	mouse	NA19L (Calbiochem)	IB and FACS
pHistone3 S10	rabbit	06-570 (millipore)	FACS
α-Tubulin	mouse	T-9026 (Sigma Aldrich)	IB
TetR	rabbit	631110 (Clontech)	IB

[a] IB: Immunoblot, IF: Immunofluorescence, IP: Immunoprecipitation

Table 3.1: Primary antibodies

Immunoblotting and Immunoprecipitation.

If not specified otherwise, cell extracts were prepared in Laemmli buffer (4% SDS, 20% glycerol, 120 mM Tris-HCl pH 6.8). Proteins were resolved by SDS–PAGE and transferred to nitrocellulose. Immunoblots were performed by using the appropriate antibodies and proteins visualized using the ECL detection system (Western BrightTM, Advansta) imaging on a FusionSolo (Witec AG).

When indicated, a Triton X-100-insoluble (chromatin-enriched) fraction was isolated as described in Peña-Diaz et al. [212]. Briefly, cells were rinsed twice in cold PBS and incubated for 5 min on ice in pre-extraction buffer (25 mM HEPES (pH 7.4), 50 mM NaCl,

1 mM EDTA, 3 mM $MgCl_2$, 300 mM sucrose, 0.5% Triton X-100, and protease inhibitors). After buffer removal and rinsing in PBS, adherent cellular material was harvested by scraping it into Laemmli buffer. The chromatin-enriched fraction was then heat denatured, sonicated, and analysed by immunoblotting.

Flag-BARD1 wild-type or L44P mutant transiently expressed in HEK293T cells were lysed in RIPA buffer (50 mM Tris-HCl (pH 7.5), 1% NP-40, 0.25% Sodium-deoxycholate, 150 mM NaCl, 1 mM EDTA, 0.1% SDS, protease inhibitors (1 mM benzamidine and 0.1 mM PMSF)), subjected to benzonase treatment (10 U Benzonase® (Roche)) for 30 min at 4 ℃, cleared by centrifugation (14000 rpm) and immunoprecipitated using the M2-agarose anti-FLAG resin (Sigma-Aldrich) overnight at 4 ℃. Immunocomplexes were stringently washed four times with RIPA buffer followed by one wash with TEN100 buffer (0.1 mM EDTA, 20 mM Tris-HCl, pH 7.4, 100 mM NaCl), boiled in SDS-sample buffer and analysed by SDS-PAGE followed by immunoblotting.

Immunofluorescence Microscopy

U2OS cells grown on coverslips were either fixed directly in 4% formaldehyde in PBS (w/v) and permeabilized or pre-extracted for 5-10 min on ice before fixation in formaldehyde for 15 min as described previously [32]. After incubation with the indicated primary antibodies and appropriate AlexaFluor-488, -594 and -647-conjugated secondary antibodies (1:1'000) (Life Technologies), coverslips were mounted with Vectrashield® (Vector Laboratories) containing DAPI and sealed. Images were acquired on a Leica DMI 6000 fluorescence microscope. Laser microirradiation was performed as described previously [213].

Images were analysed using a customized CellProfiler [207] pipeline to identify nuclei (DAPI channel) and the number of 53BP1 bodies. For complementation experiments, nuclei were identified and classified according to intensities measured in the green channel (expression of GFP-tagged fusion proteins). The number of 53BP1 bodies in these was determined.

Colony formation assay

MRC5^{shCtIP} cells were transfected with the indicated siRNA using Lipofectamine RNAiMax (Invitrogen). On the next day, cells were re-plated into two sets of 6-well plates at low cell dilutions (triplicates). 48 h post transfection one set of 6-well plates was exposed to 1µg/ml Dox to induce shCtIP while the other one was kept untreated as a control. Cells were cultured for 10 days to allow formation of colonies. Subsequently, these were fixed in methanol and stained in crystal violet/ethanol (0.5/20%) solution. Colonies reaching a minimum of 50 cells were counted and the number of colonies without Dox was set to be 100% for each siRNA transfection in order to determine the effect of CtIP co-depletion.

CellTiter-Blue® Cell Viability assay.

For drug hypersensitivity assays, cells transfected with siRNA where indicated were seeded in triplicates at a density of 500 or 1000 cells/well in 96 well plate 24 h post-transfection or after administration of 1 µg/ml Dox (MRC5shRNA). Cells were exposed to the indicated doses of drugs at 24 h after plating and grown for 4 days at 37° C. To measure cell viability, CellTiter-Blue® reagent (Promega) was added on the last day, cells were incubated at 37 ℃ for 4-24 h, and then fluorescence was measured at 560/590 nm.

For screen validation, 500 or 1000 U2OS cells were reverse transfected with 10 nM + 10 nM of the indicated siRNAs in a 96-well plate in triplicates. Cell proliferation was allowed for 6 days before addition of CellTiter-Blue® reagent (Promega).

Metaphase spreads

HEK293 cells were transfected with the indicated siRNAs for 48 h, subsequently treated with HU for 4 h and allowed to recover for 48 h. Metaphase spreads were prepared as described in Murina et al. [120]. In brief, cells were treated with colcemid (Gibco) for 3 h prior to harvesting by trypsinization. The cell pellet was resuspended in 5 ml of a 0.075 M hypotonic potassium chloride (KCL, PanReac AppliChem) solution and incubated for 30 min. at 37 ℃ for swelling. For fixation, cells were incubated in 5% acetic acid (PanReac AppliChem) in ddH2O for 3 min. followed by two rounds of fixation by ethanol (EtOH, Merck) and acetic acid in a 3:1 ratio for 10 min.. Fixed cells were resuspended in fixative to the appropriate cell density, spread on glass slides (Menzel-Gläser, ThermoFisher) and stained with Giemsa (GIBCO). Phase contrast images were acquired using an Olympus IX83 inverted at 100x magnification.

DNA fiber analysis.

DNA fiber analysis was carried out as described previously [78]. In brief, asynchronous U2OS cells were labeled with 33 µM CldU for 30 min followed by exposure to 2 mM HU for 2 h and chased with 340 µM IdU for 40 min before collection and resuspension in PBS. Cells were lysed (lysis buffer: 200 mM Tris-HCl (pH 7.4), 50 mM EDTA, 0.5% SDS) and DNA fibers were stretched onto glass slides and fixed in Methanol:Acetic acid (3:1,

Merck). After rehydration in PBS, these were denatured with 2.5 M HCl for 1 h, washed with PBS and blocked with 2% BSA in PBS containing 0.1% Tween 20 for 30 min. The newly replicated CldU and IdU tracks were stained by standard immunofluorescence using anti-BrdU antibodies (primarys: α-IdU, α-BrdU from BD Biosciences; α-CldU, α-BrdU from Abcam and secondarys: α-mouse Alexa Fluor 488 from Invitrogen and α-rat Cy3 from Immuno Research). Coverslips were mounted using Antifade Gold (Invitrogen). Images were acquired on a Leica DMI 6000 fluorescence microscope and analysed using Fiji software [214]. Statistics were calculated in Graph Pad Prism (GraphPad Software Inc.).

Flow Cytometry Analysis

Where indicated, cells were transfected with siRNA as described above and the knockdown was allowed to persist for 48 h. Analysis of cell cycle, RPA, γH2AX and pS10-H3 was carried out as previously described [215]. Shortly, cells were treated as described in the Figure legends, harvested by trypsinization and fixed using 4% formaldehyde/PBS. For RPA staining, cells were pre-extracted in 0.3% Triton X-100/PBS on ice for 10 min prior to fixation. For assessment of pS10-H3, cells were permeabelized after fixation. EdU incorporation was analysed using the Click-iT EdU technology (ThermoFisher) according to manufacturer's instructions. For RPA/γH2AX and pS10-H3 analyses, cells were incubated in 0.5% saponin/1% BSA/PBS containing the primary antibodies for 2 h at RT, followed by incubation with a secondary antibody and staining of the DNA with DAPI (DNA content). Fluorescence was measured on a LSR II Fortessa (BD Bioscience) and analysed with FlowJo X (Tree Star).

To assess apoptosis, U2OS were transfected with siRNA as described above and re-plated into gelatin-coated (0.1% in PBS) 6-well tissue culture plates. On the indicated days cells were harvested by trypsinization. Cells were collected in polysterene FACS tubes and washed with annexin binding buffer (10 mM HEPES/NaOH, 140 mM NaCl, 2.5 mM $CaCl_2$ (pH 7.4)). After washing, cells were stained in 50 µl annexin binding buffer including 5 µl annexin V-FITC (eBioscience) and propidium iodide (1ug/ml; ThermoFisher) for 20 min at RT. Cells were then washed with annexin binding buffer before analysis by flow cytometry with a LSRII Fortessa (BD Bioscience) and analysed with FlowJo X (Tree Star).

Statistical analysis

Statistical differences were determined by unpaired t test except for fork asymmetry, which was analysed by Mann-Whitney U test and quantification of 53BP1 nuclear bodies, which was analysed by Kolmogorov-Smirnov test. In all cases: ns – not significant ($P > 0.05$); * – $P \leq 0.05$; ** – $P \leq 0.01$; *** – $P \leq 0.001$; **** – $P \leq 0.0001$.

HR reporter assay

U2OS-TLR cells were transfected with siRNA as described above. After 6 h, cells were transfected with the *I-SceI*-expression plasmid and the exogenous donor template containing the missing part of *eGFP*. 72 h after siRNA transfection, cells were collected by trypsinization, and analysed by flow cytometry using a LSRII Fortessa (BD Bioscience) as described previously [112]. Data analysis was performed using FlowJo X (Tree Star) to assess the percentages of eGFP-positive cells depicting the efficiency of homologous

recombination.

Pulsed field gel electrophoresis (PFGE)

U2OS cells were transfected with siRNA as described above and pulse labelling of the replication forks with [^{14}C]thymidine was performed before and during HU treatment. Cells were harvested and PFGE was performed as described in [216].

Results

4.1 Multiplexed RNAi and drug-sensitivity screen to investigate synthetic genetic interactions of CtIP in the presence or absence of DNA damage.

In order to expand our understanding of *CtIP* gene functions and their impact on the cellular homeostasis in response to DNA damage, we performed multiplexed high-throughput RNA interference (RNAi) screens with isogenic cell lines differing only in their CtIP expression status in the presence or absence of the DNA damaging agent camptothecin (CPT). To assess synthetic genetic interactions in these cells by combinatorial RNAi, we manually curated an arrayed siRNA library targeting 207 human genes. About 40% of those target genes are implicated in the DNA repair processes and cell cycle checkpoint control. Among them, we selected key players from a wide range of DDR pathways, which might function in either distinct or partly compensatory pathways with respect to HR. Furthermore, we included target genes involved in other cellular pathways like DNA replication and transcription, as well as protein modifiers such as kinases, phosphatases and ubiquitin ligases (Figure 4.1A).

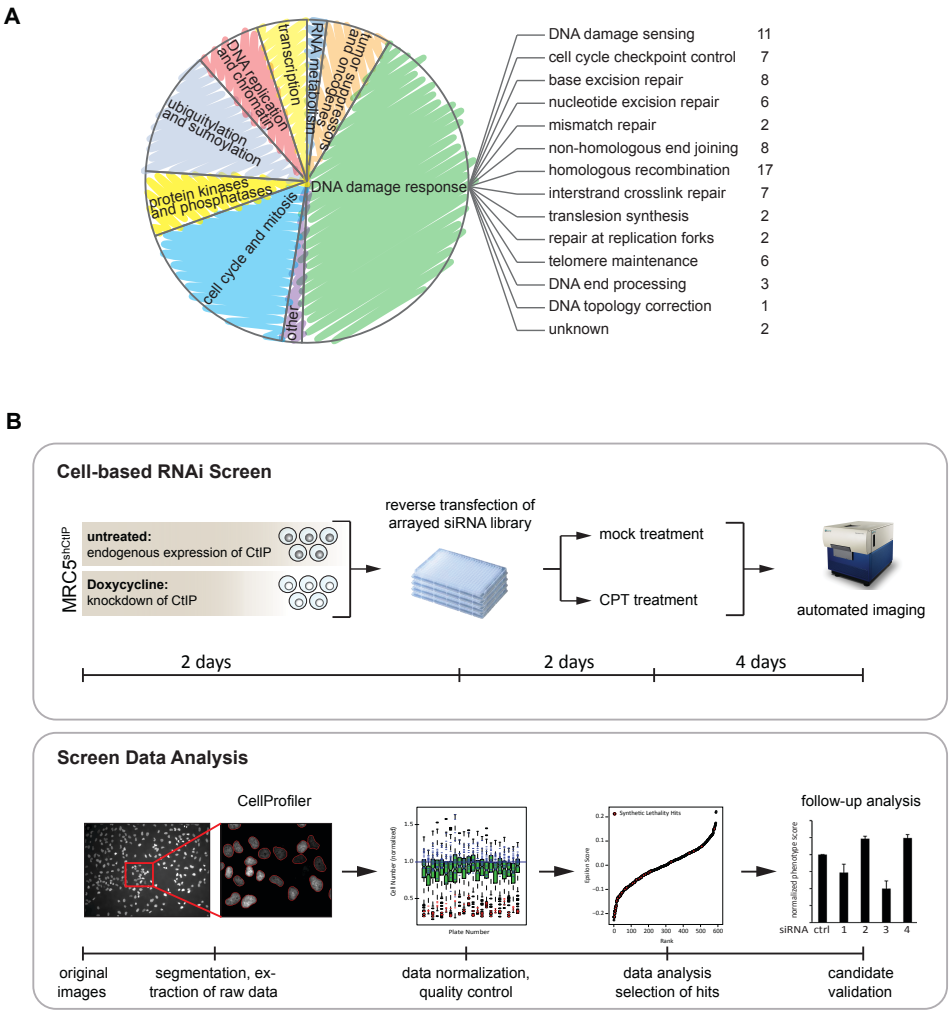

Figure 4.1: Multiplexed RNAi and drug-sensitivity screen to investigate synthetic genetic interactions of CtIP in the presence or absence of DNA damage. (**A**) Classification of genes targeted by oligonucleotides of the custom-designed siRNA library. (**B**) Schematic overview of experimental setup and data analysis of the RNAi screen.

To minimize the potential risk of seed sequence-driven off-target effects [217], we employed a Silencer® Select siRNA library (Ambion) consisting of three siRNAs targeting distinct regions of each gene, singly arrayed in 384-well plates alongside controls. As Silencer® Select siRNA oligonucleotides are designed to enhance target specificity and potency by harbouring chemical modifications, we used them at a minimum effective

amount of 8 pmol siRNA per well further reducing the risk of off-target effects [218]. To monitor various biological and technical parameters of the screening procedure, we dedicated 24 wells per assay plate to internal controls. This included three different non-targeting siRNAs (siNegCtrl #1, siNegCtrl #2, siLuciferase) as well as mock-transfected cells. An siRNA targeting CtIP was used as a positive control for CPT hypersensitivity [32]. To assess the efficiency of siRNA transfection, a cytotoxic positive control was included, which silences kinesin family member 11 (siKif11), a gene critical for cell viability [219]. To perform the combinatorial RNAi screen, we used MRC5^{shCtIP} cells, in which we conditionally downregulated CtIP for 48 h prior to reverse transfection of the arrayed siRNA library (Figure 4.1B). Two days post siRNA transfection, cells were either mock-treated or incubated with 10 nM CPT to induce DNA damage. Six days after siRNA transfection, cells were fixed and the nuclei were stained with Hoechst. Consequently, microscopic images of each well were acquired and image analysis was performed using CellProfiler [207], an open-source software tool for quantitative analysis of biological images, to extract the number of cells per well as a read-out for cell viability (Figure 4.1B). RNAi screens were conducted in biological triplicates, each replicate screen consisting of technical duplicates.

Our experimental set up led to four different conditions in which genetic perturbations were conducted: 1) Cells with normal CtIP expression that had not been exposed to DNA damage (–Dox, untreated), 2) Cells with normal CtIP expression exposed to DNA damage (–Dox, CPT), 3) Cells depleted of CtIP that had not been exposed to DNA damage (+Dox, untreated) and 4) Cells depleted of CtIP exposed to DNA damage (+Dox, CPT). In total, our screening approaches generated about 15000 data points for subsequent

analysis. After image segmentation and feature extraction, we first visualized our data output in order to monitor the overall screen performance. Raw data was displayed as plate-well series plot, a scatter plot that summarizes the data points across the plates from all replicates of the screen. This representation indicated the absence of cross-plate systematic errors such as spatial effects or batch-to-batch variations (Figure 4.2A). Moreover, within-plate experimental artefacts (edge effects or drift) were examined by plotting the median cell numbers of each row or column across all screening plates (Figure 4.2B). A small, but expected, decrease of median cell numbers in column eight and fourteen depicted the presence of two wells containing siKif11 in that column. Overall, no potential systematic problems or plate effects caused by the experimental procedure itself were evident from raw data display.

For the screen data analysis, we first square-root transformed the raw data to render its distribution closely symmetric and approximately normal making it more suitable for statistical analysis. This was followed by normalization of each data point to the median of negative controls per plate (percentage of control, POC) to adjust for variation between plates. For quality control, we subsequently monitored the correlation of normalized cell numbers between the three biological replicates. Pearson correlation coefficients ranging between 0.69 and 0.81 revealed good data reproducibility (Figure 4.2C). The strictly standardized mean difference (SSMD) was used to measure the magnitude of difference in cell viability between the cytotoxic positive control (siKif11) and the negative reference (Ctrl) as a second mean for quality control. Adopting the criterion for a very strong positive control, SSMD values of approximately 3.0 for each assay plate, suggested good differentiation between positive and negative controls and indicated high quality data

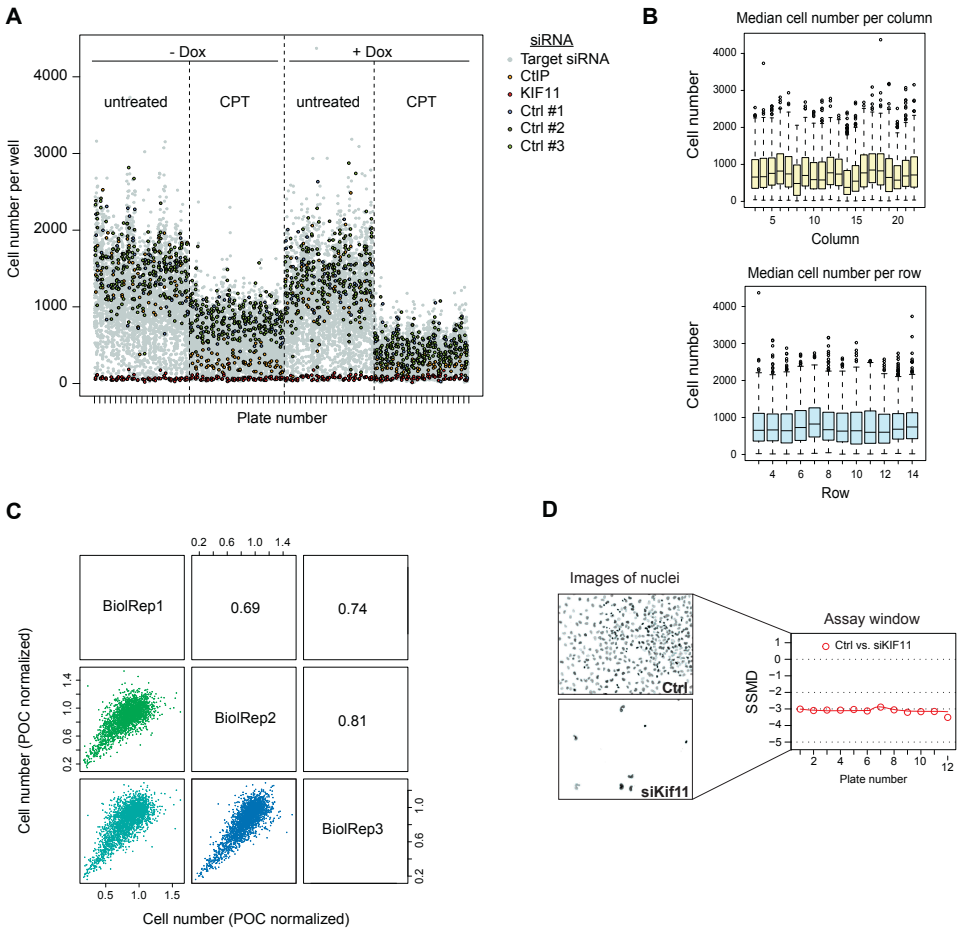

Figure 4.2: Visualizing data outputs of the screen for quality control and data analysis. (**A**) Plate-well series plot to display the raw cell numbers measured in each well from all replicates of the screen. (**B**) Median values of raw cell numbers per row or column across all plates from the screen reveal the absence of row or column artefacts like edge effect or drift. (**C**) Replicate correlation plots to visualize overall reproducibility. The x- and y-axis represent two biological replicates and each data point represents data obtained from one well. Pearson correlation coefficients between the three biological replicates are displayed. (**D**) Representative images of Hoechst-stained nuclei from cells transfected with a non-targeting siRNA (Ctrl) or the cytotoxic siKif11, respectively. To measure the magnitude of difference between these two populations as a indication for efficient siRNA transfection, the strictly standardized means difference (SSMD) was computed for each assay plate. Results for one replicate screen are shown. By adopting the criterion for a very strong positive control, SSMD values indicate good data quality

(Figure 4.2D) [208]. This confirmed what had been anticipated in the plate-well series plot, where the values for siKif11-transfected cells clustered at the low end of cell number values for each plate (Figure 4.2A). Moreover, this plot indicated the expected CPT hyper-

sensitivity of cells expressing reduced CtIP levels [32]. Transient transfection of an siRNA targeting CtIP (data points depicted in orange in data sets -Dox) as well as Dox-mediated induction of shCtIP on the batch level resulted in a reduction of cell viability upon exposure to CPT (compare –Dox +CPT and +Dox +CPT). Taken together, our quality assessment indicated that our control measures met our expectations and therefore no screening data needed to be excluded from the analysis due to poor data quality. To eliminate bias resulting from the ratio between small numbers, we next removed siRNA mediating high cytotoxicity from further analysis. We thus excluded 29 target genes whose depletion reduced cell viability to less than 20% of the overall median cell number per well.

To identify negative synthetic genetic interactions with CtIP in the absence of DNA damage, we applied a multiplicative model and computed an interaction score, termed the epsilon (ϵ) score. Based on the assumption that the combined effect of two individual perturbations will be the product of their individual effects, the ϵ score determined the difference between the observed phenotype and the effect that would be expected if the two genes do not interact [189]. Theses ϵ scores were then used to compute a hit ranking based on the Redundant siRNA Activity (RSA) algorithm. First, siRNAs were ranked according to their ϵ scores. Consequently, the RSA method was used to assign p-values to each target gene. The RSA p-values were calculated based on an iterative hypergeometric distribution formula developed by König et al.[209]. They indicated the statistical significance of all siRNAs targeting a single gene being distributed significantly higher in the ranking than would be expected by chance. A p-value cut-off of $p<0.05$ was chosen to determine a set of high-confidence candidate hits depicting putative SSL interactions with CtIP loss of function (Figure 4.3A). SSL genetic interactions with CtIP occurring in

the absence of CPT treatment were further analysed for known associations with the CtIP protein and grouped according to their molecular functions using the STRING database and DAVID functional annotation clustering [210, 211]. Not surprisingly, our candidate hits clustered in three different cellular pathways: DNA repair, cell cycle control and transcription (Figure 4.3B).

Another class of synthetic interactions is represented by the so-called 'synthetic rescue', whereby the combined phenotype of two gene disruptions is less severe than anticipated from the single perturbations as it enhances cell proliferation. Such positive genetic interactions could potentially also be identified from our screening data. To this end, we reinterpreted the ϵ scores in order to determine which target gene depletion conferred a growth advantage to cells lacking CtIP. Interestingly, the top scoring candidates identified as synthetic rescue gene pairs with CtIP were the PIKK member and histone acetyl transferase scaffold protein TRRAP (TRansformation/tRanscription domain-Associated Protein) [220] and the DNA replication processivity factor PCNA (Proliferating cell nuclear antigen) [221]. However, these results need to be interpreted with caution as the well dimensions in a 384-well plate limits cell proliferation considerably and might therefore restrict the discovery of growth-enhancing phenotypes.

As a second aim of our screen, we sought to identify proteins, which would confer hypersensitivity to the DNA damaging agent CPT upon depletion in a CtIP-proficient background. For this analysis, we calculated the fold-change in cell viability between untreated cells and those that had been exposed to CPT for each siRNA [222]. Subsequently, we used the RSA algorithm for a target gene ranking according to the increase in CPT hypersensitivity. As expected, cells depleted of known DDR genes such as *CtIP* (alternative

A

Candidate Hits SSL

Gene	Gene ID	Rank	RSA p-value
LMO4	8543	1	0.0019
MRE11A	4361	2	0.0055
ESCO1	114799	3	0.0078
CDC25A	993	4	0.0116
DDB2	1643	5	0.0126
E2F6	1876	6	0.0149
TP53	7157	7	0.0152
BARD1	580	8	0.0175
E2F3	1871	9	0.0193
SLX4	84464	10	0.0245
CDC6	990	11	0.0290
KAT5	10524	12	0.0374
CHFR	5573	13	0.0386
EXO1	9156	14	0.0392
RAD54L	8438	15	0.0440
LIG1	3978	16	0.0451
RAD18	56852	17	0.0460
POLQ	10721	18	0.0486
CTBP2	1488	19	0.0509
LIG3	3980	20	0.0521
BRCA1	672	21	0.0550

C

Candidate Hits CPT hypersensitivity

Gene	Gene ID	Rank	RSA p-value
RBBP8	5932	1	1.64E-6
BARD1	580	2	1.07E-5
BRCA1	672	3	8.59E-5
SMC5	23137	4	0.0001
RAD51	5888	5	0.0003
SMC6	79677	6	0.0004
SMC3	9126	7	0.0008
ESCO1	114799	8	0.0016
UIMC1	51720	9	0.0040
BRCA2	675	10	0.0046
NFKBIL2	4796	11	0.0059
ATR	545	12	0.0102
CtIP (Ctrl)	5932	13	0.0119
CDC27	996	14	0.0126
RAD54L	8438	15	0.0129
MUS81	80198	16	0.0199
EXO1	9156	17	0.0200
RIF1	55183	18	0.0208
C1orf135	79000	19	0.0224
DNA2	1763	20	0.0228
STK11	6794	21	0.0232
ZNF350	59348	22	0.0305
SIAH1	6477	23	0.0352
RPA3	6119	24	0.0397
RAD18	56852	25	0.0403
RPA2	6118	26	0.0474

B

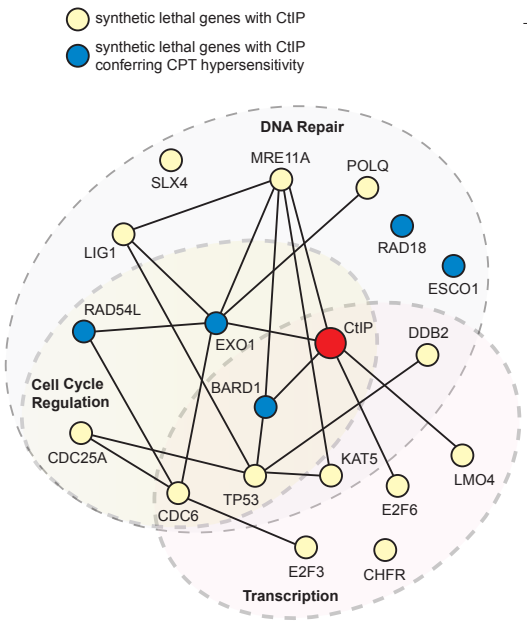

Figure 4.3: RNAi screen hit lists. (**A**) Candidate synthetic lethal genes with CtIP determined by a multiplicative model and Redundant siRNA activity (RSA) using a p-value cut-off of $p<0.05$. Additionally, CTBP2, LIG3 and BRCA1 are displayed. (**B**) Candidate hits for synthetic lethality with CtIP were functionally analysed in the context of experimental protein networks obtained from the STRING database (straight lines depict protein associations) and mapped to their associated biological process using DAVID functional annotation clustering. Target genes promoting resistance to CPT are highlighted. (**C**) Candidate genes displaying hypersensitivity to CPT upon disruption were determined by analysis of the fold-change in cell viability between untreated and CPT-treated cells for each siRNA. RSA was employed to generate a hitlist based on a p-value cut-off of $p<0.05$.

name *RBBP8*), *BRCA1*, *BARD1*, *RAD51*, *ATR* and *RPA2* were hypersensitive to CPT (Figure 4.3C). Remarkably, CtIP, BRCA1 and BARD1 were identified as top scoring candidates emphasising the importance of these DDR factors in the cellular response to DSBs. Of note, a large number of the factors identified were in concordance with proteins already identified to mediate resistance to CPT, including *NFKBIL2*, *SMC3*, *EXO1*, *RAD18* and *SMC6* [213, 223–226]. Since we failed to uncover genes that had not previously been linked with the DDR, we decided not to follow up on any of these hits. Nevertheless, these findings served as a validation for the success of our screening and data analysis strategies. SSL hits that also conferred CPT hypersensitivity upon disruption are indicated in Figure 4.3B.

A third possible application of our screen would have been the investigation of so called 'differential genetic interactions' [186]. These describe how functional interconnections between pathways are altered in response to DNA damage by comparing the genetic interactome with and without perturbation by a DNA-damaging agent. However, as expected, CtIP-depleted MRC5^{shCtIP} cells were highly sensitive to CPT *per se*, thus the number of cells assayed per double perturbation decreased dramatically in this condition. Acquiring data from a sufficient number of cells is a critical parameter for the sensitivity of the detection of genetic interactions [197]. Hence, the data we acquired in the +Dox +CPT condition was not suitable for the identification of differential genetic interactions. Adjustments in experimental design would be necessary in order to mitigate this problem. Thus, we refrained from further analysis of our existing data sets.

Taken together, our focused screen uncovered a set of potential SSL interactions with

the *CtIP* gene. Moreover, we identified a number of proteins that mediated resistance to CPT-induced DNA damage. In my doctoral thesis, I have subsequently focused on the validation and functional characterization of SSL interactions with CtIP in the absence of DNA damage. Among the high-confidence candidates, we selected four genes (*ESCO1, DDB, BARD1, and SLX4*) for further retesting and validation of the genetic interaction with CtIP by complementary assays (data not shown). During this extensive and time-consuming period, we obtained the most promising and reproducible results for the SSL interaction between CtIP and BARD1. Therefore, we decided to further investigate the functional interconnection between these two proteins. In the second part of my PhD thesis I hence sought to determine how CtIP and BARD1 collaboratively contribute to cell survival.

Manuscript

CtIP and BRCA1/BARD1 cooperate to promote faithful DNA replication

Hella A. Bolck[1], Sara Przetocka[1], Roger Meier[2], Christina Walker[1], Kay Hänggi[1], Christine von Aesch[1], Reihanheh Zarrizi[3], Peter Horvath[4], Simon F. Nørrelykke[2], Michael Stebler[2], Adrian Thalmann[1], Antonio Porro[1], Claus Storgaard Sørensen[3] and Alessandro A. Sartori[1]

[1]Institute of Molecular Cancer Research, University of Zürich, Switzerland. [2]Scientific Center for Optical and Electron Microscopy (ScopeM), ETH Zürich, Switzerland. [3]Biotech Research and Innovation Centre, University of Copenhagen, Denmark. [4]Synthetic and System Biology Unit, Hungarian Academia of Sciences, Biological Research Center (BRC), Szeged, Hungary

Manuscript for publication in a peer-reviewed journal.

The next part of the "Results" is adapted from a manuscript that will be submitted for publication. Consequently, there are some minor repetitions to the previous section about the RNAi screen. However, since the publication of my project will be one major aim of my PhD, I would like to present this important part in its entirety and kindly ask you to accept small duplications.

I devised the original ideas for this study together with Alessandro A. Sartori and performed the RNAi screen and most of the experiments. Roger Meier, Peter Horvath and Michael Stebler contributed to RNAi screening and data analysis. Sara Przetocka, Christina Walker, Kay Hänggi, Christine von Aesch, Reihanheh Zarrizi, Adrian Thalmann and Antonio Porro helped to perform experiments. Simon F. Nørrelykke contributed to image analysis and Claus Sørensen to experimental designs and data analysis. I analysed the data and wrote the manuscript with critical input from Alessandro A. Sartori.

4.2 RNAi screening reveals a negative synthetic genetic interaction between CtIP and BARD1

In order to investigate functional relationships of the *CtIP* gene, we analysed synthetic genetic interactions of CtIP by RNA interference (RNAi)-based screening, which was described in detail in the previous section. Subsequently, we primarily focussed on aggravating, or, alternatively termed, synthetic sick/lethal genetic interactions (SSL). SSL interactions occur if two otherwise viable single gene disruptions lead to lethality or severely impaired cell growth (synthetic sickness) when combined [190]. In order to carry out systematic perturbation screens, we generated and characterised MRC5^{shCtIP} human fetal lung fibroblast cells in which we can conditionally downregulate CtIP protein levels through the expressing of a short hairpin RNA (shRNA) against CtIP under the control of a doxycycline (Dox)-inducible promoter (Figure 4.4A) [120]. Importantly, the extent of CtIP disruption after Dox-induction and siRNA transfection are comparable and both result in CPT hypersensitivity, a well established phenotype of CtIP-deficiency (Figure 4.4A and Supplementary Figure 4.4A) [32]. Using MRC5^{shCtIP} cells, we conducted a multiplexed image-based RNAi screen interrogating 207 human genes for synthetic growth defects with CtIP (Figure 4.4B). Our image and data analysis pipeline revealed eighteen SSL candidate genes scoring below our cut-off (RSA p-value < 0.05) to potentially exhibit a negative genetic interaction with CtIP (Figure 4.4C). Among the strongest candidates, we found the BRCA1-associated RING domain protein 1 (BARD1) (Figure 4.4D). Remarkably, in our screen data analysis, BRCA1, the obligate interaction partner of BARD1, scored just above the p-value cut-off suggesting that co-depletion of BARD1 and CtIP might cause a more severe growth defect than the co-depletion of BARD1 and CtIP (Figure 4.4D).

Subsequently, we confirmed the negative synthetic genetic interaction between CtIP and either BARD1 or BRCA1 in MRC5^{shCtIP} cells by colony formation assays using identical as well as different siRNAs as in the screen (Figure 4.4E). Consistent with our screening data, co-depletion of CtIP and BARD1 significantly decreased cell viability compared to depletion of CtIP alone, whereas co-depletion of CtIP and BRCA1 only partially replicated

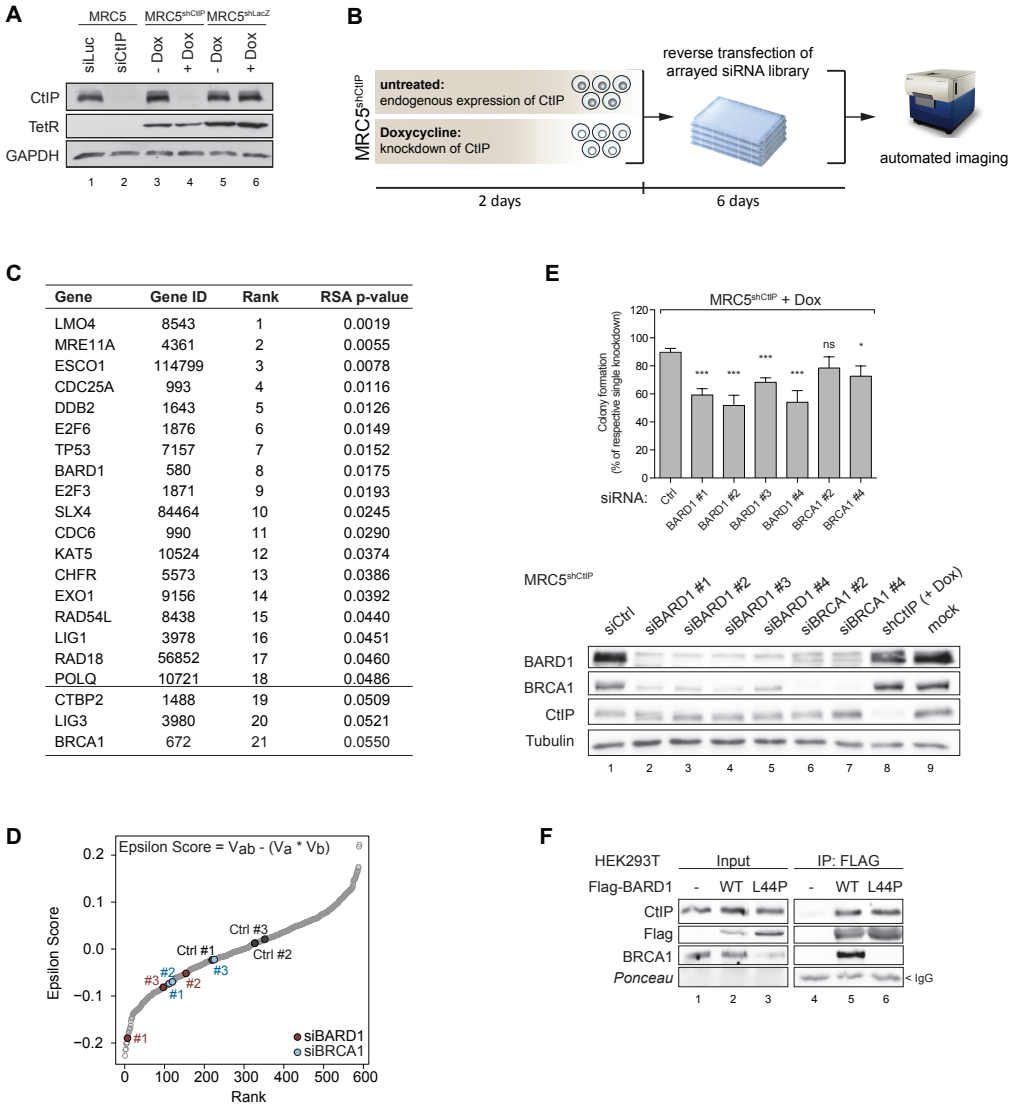

Figure 4.4: Identification of a synthetic sick genetic interaction between CtIP and BARD1 by RNAi image-based screening. (**A**) SV40-transformed MRC5 cells were transfected with the indicated siRNAs for 48 h. MRC5 cells stably expressing doxycycline (Dox)-inducible shRNA against CtIP (MRC5^{shCtIP}) or LacZ (MRC5^{shLacZ}, control) were cultivated in the absence or presence of Dox (1 µg/ml) for 48 h. Whole cell lysates were prepared and subjected to immunoblotting to indicate the extent of CtIP depletion. (**B**) Schematic outline of the RNAi screen to investigate synthetic genetic interactions of CtIP. (**C**) Candidate genes for SSL interactions with CtIP were ranked by redundant siRNA activity (RSA) analysis. A RSA p-value cut-off of $p < 0.05$ was defined to determine a hit list. (**D**) Genetic interactions were defined in terms of deviation (Epsilon Score) from the expectation that the combined effect on cell viability (V) of two gene disruptions (A and B) will be the product of their individual effects (given by the formula). Epsilon Scores for all individual siRNAs are displayed. Epsilon Scores for non-targeting siRNAs (siCtrl) and siRNAs against BARD1 and BRCA1 are highlighted. (**E**) MRC5^{shCtIP} cells were transfected with the indicated siRNAs and subjected to colony formation assay. Bars represent the reduction of cell viability upon CtIP co-depletion by Dox-inducible shRNA compared to siRNA-mediated knockdown of BARD1 or BRCA1 alone. Data represent the mean ± s.e.m. ($n \geq 3$). Whole-cell extracts of the corresponding samples were analysed by western blotting. (**E**) HEK293T cells were transfected with Flag-BARD1 expression constructs for 48 h. Whole-cell extracts were analyzed by western blotting before (input) and after immunoprecipitation (IP) using anti-Flag antibody coupled to agarose beads.

this phenotype. These findings were further corroborated by combinatorial siRNA depletion studies in U2OS cells (Supplementary Figure 4.4B). In line with previous findings, we also observed a notable interdependency of BRCA1 and BARD1 protein stability in cells depleted for either protein respectively [143, 157].

The most accepted mechanistic explanation of negative synthetic genetic interactions comprises two genes functioning in parallel, mutually compensatory pathways, known as between-pathway SSL. Physical interaction, on the other hand, is often interpreted to denote gene products functioning within the same pathway or protein complex [227, 228]. However, recent findings revealed that multiple negative interactions occur between factors implicated in the same molecular pathway or even within one complex [191, 229]. Since protein-protein interactions between BARD1 and BRCA1 and between BRCA1 and CtIP are well established, this prompted us to carry out co-immunoprecipitations using Flag-tagged BARD1 expression constructs. As expected, CtIP efficiently co-precipitated with Flag-BARD1 wild type (WT) indicating that CtIP and BRCA1/BARD1 exist in a trimeric complex (Figure 4.4F). Interestingly, we observed that a significant fraction of CtIP retains the ability to form a complex with BARD1-L44P, a mutation that disrupts the BRCA1-BARD1 dimer [230]. Thus, we concluded that BARD1 and CtIP interact, at least in part, independently of their common interaction partner BRCA1.

Taken together, our results unveiled the presence of a negative genetic interaction between BARD1 and CtIP, two DDR factors residing within the same multi-protein complex. We failed to detect a comparable SSL interaction between CtIP and BRCA1 implying that BARD1 and CtIP might have a functional connection beyond the BRCA1/BARD1 heterodimer.

4.3 Prolonged downregulation of CtIP and BARD1 triggers a cell stress response associated with hallmarks of endogenous DNA damage.

To investigate the underlying mechanisms for the synthetic sick relationship between CtIP and BARD1, we depleted the respective proteins alone or in combination in U2OS cells.

After four days, downregulation of BARD1, but not CtIP, resulted in a marked increase of apoptosis (Figure 4.5A and B). Intriguingly, co-depletion of both proteins further elevated the fraction of apoptotic cells compared to knockdown of BARD1 alone. Conversely, downregulation of CtIP and BARD1 for only two days was not sufficient to induce apoptosis above basal levels (Supplementary Figure 4.5A). Co-depletion of BRCA1 and CtIP resulted in a similar trend of increased apoptosis; albeit to a lesser extent as the combined disruption of BARD1 and CtIP (Figure 4.5B) reminiscent of the results of the RNAi screen (Figure 4.4). Additionally, we also observed that prolonged abrogation of CtIP or BARD1 expression delayed cell proliferation and compromised replication as indicated by a reduction of S-phase cells and slower incorporation of nucleotides (Supplementary Figure 4.5B). Comparable to the increase of apoptosis, the delay in S-phase became apparent only several cell divisions after depletion of the respective proteins. We therefore hypothesize that cells deficient for CtIP and BARD1 encounter problems during each round of DNA replication.

To address whether cells depleted of CtIP and/or BARD1/BRCA1 accumulate DNA lesions, we analysed the levels of the histone variant H2AX phosphorylated on serine 139 (γH2AX) by flow cytometry at two days after siRNA transfection (Figure 4.5C). Even though apoptosis was not effectively induced at this early time point, we found a marked increase of γH2AX-positive nuclei in CtIP/BARD1-deficient cells (Figure 4.5C). This was accompanied by an increase of cells arrested in G_2/M phase, which became evident already upon single depletion of the respective proteins, but was further elevated after simultaneous disruption of BARD1 and CtIP. Conversely, co-depletion of CtIP and BRCA1 was not able to fully emulate these phenotypes (Figure 4.5C). Therefore, we concluded that the concurrent loss of CtIP and BARD1 leads to DNA damage predominantly manifesting in G_2/M cells, ultimately slowing down cell proliferation and inducing cell death. We next investigated the role of CtIP, BARD1 and BRCA1 in the G_2/M cell cycle checkpoint using phosphorylated serine 10 at histone 3 (pS10-H3) as a mitotic marker. We found that CtIP-depleted cells could enter mitosis without impediments (Figure 4.5D). Surprisingly, mitotic cells were decreased about two-fold upon BARD1 but not BRCA1 disruption suggesting a previously uncharacterized role for BARD1 in the G_2/M cell cycle transition.

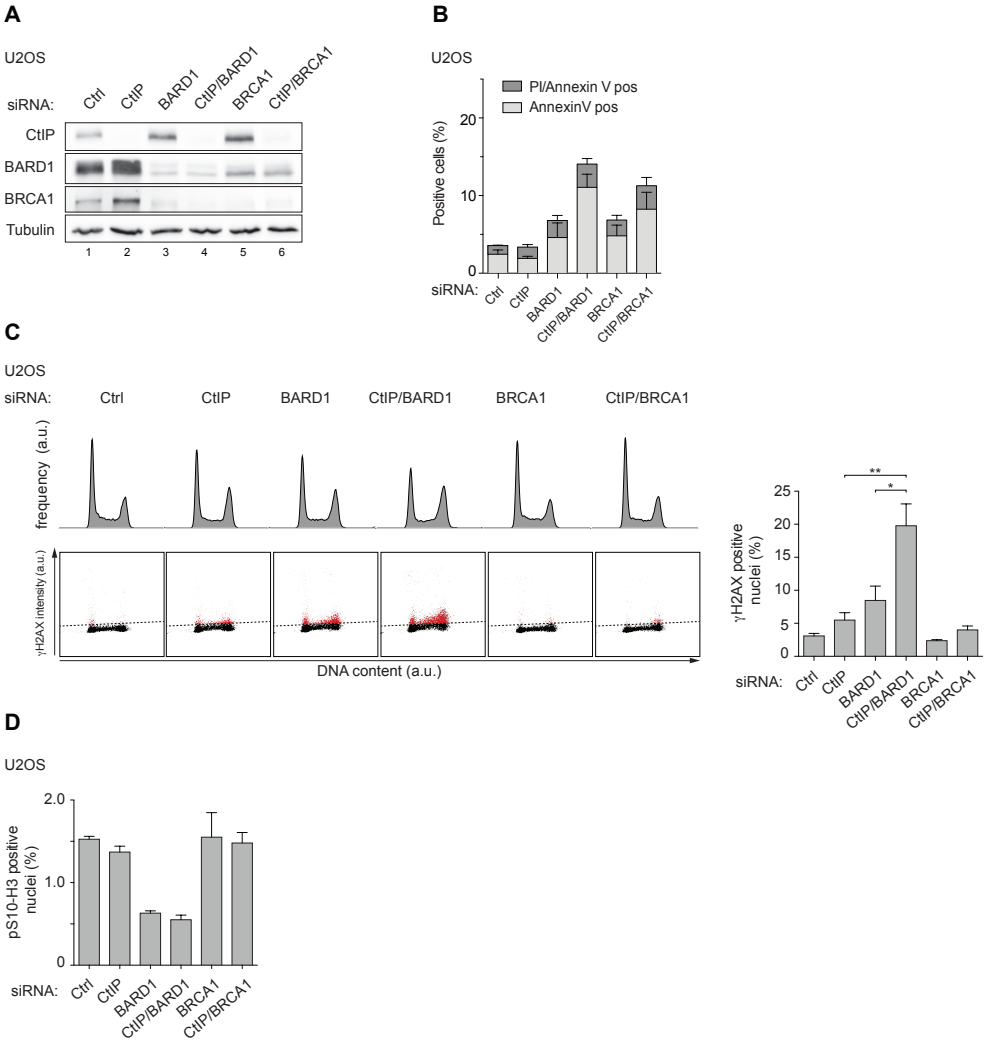

Figure 4.5: Simultaneous disruption of BARD1 and CtIP provokes apoptosis and is associated with accumulation of γH2AX. (**A**) U2OS cells were transfected with the indicated siRNA, and the knockdown was allowed to persist for 48 h. Whole-cell extracts were analysed by western blotting with the indicated antibodies. (**B**) Cells were transfected with the indicated siRNA as in (A) and were harvested at four days post transfection. Induction of apoptosis was determined by flow cytometric analysis. Annexin V^{FITC}-positive staining indicates early apoptotic cells, whereas Annexin V-positive/PI-positive staining indicates late apoptotic cells. (**C**) and (**D**) U2OS cells were treated as in (A). 48 h after siRNA transfection, cells were harvested and were fixed, permeabilized and immunostained with anti-γH2AX or anti-phospho-histone H3 along with DAPI before analysis by flow cytometry. Quantification gates were established in samples transfected with siCtrl. (**C**) Representative cell cycle distributions and representative dot plots depicting the intensity of the γH2AX signal (y axis) against the DNA content (x axis) for each knockdown condition are shown. Percentages indicate mean $\pm$ s.e.m. of γH2AX-positive cells ($n \geq 3$). (**D**) Percentages indicate mean $\pm$ s.e.m. of phospho-histone H3-positive cells (n = 2). a. u. = arbitrary units.

This finding implies that cellular stress experienced by cells lacking BARD1 during S/G_2 phase is sufficient to trigger cell cycle arrest and possibly apoptosis as a secondary event in a subset of cells.
Combined, these results suggest a scenario in which endogenous DNA lesions accumulate during each cell cycle in cells co-depleted of CtIP and BARD1. This results in BARD1-dependent partial G_2/M arrest, impaired proliferation and apoptotic cell death upon sustained disruption of both factors.

4.4 Loss-of-function of CtIP and BARD1 causes signs of elevated replication stress.

It has been recently proposed that unresolved replication intermediates can get converted into DNA lesions upon entry of a cell into mitosis. 53BP1 protein was shown to recognizes such sites of unrepaired DNA damage forming nuclear bodies (NBs) upon subsequent entry into G_1 to shield them against erosion [83, 84]. To address, whether BARD1 and CtIP counteract replication stress-induced DNA damage, we determined the prevalence of 53BP1 NBs in cells depleted of CtIP and/or BARD1 or BRCA1 by immunofluorescence microscopy (Figure 4.6A and Supplementary Figure 4.6A)). Remarkably, downregulation of CtIP or BARD1 respectively increased the average number of 53BP1 NBs per nucleus significantly. Concurrent disruption of CtIP and BARD1 further amplified the number of nuclei with supernumerary 53BP1 NBs. In line with previous reports, we find that the average increase of 53BP1 NBs in CtIP/BARD1-depleted cells was caused by a marked shift towards few nuclei with a much higher prevalence of 53BP1 NBs, which is illustrated by their elevated incidence in the 90th percentile of cells analysed [83]. Knockdown of BRCA1 induced a similar phenotype like knockdown of BARD1 implying a role for the BRCA1/BARD1 heterodimer in counteracting accumulation of 53BP1 NBs (Supplementary Figure 4.6A). From these results we inferred that depletion of CtIP and/or BARD1 is sufficient to elicit endogenous chromosomal stress that manifests as 53BP1 nuclear bodies in a subset of cells. Likely, 53BP1 NBs, once formed, can persist in case HR-mediated repair fails to address these DNA lesions during subsequent G_2/S phases. Alternatively,

53BP1 might accumulate upon induction of DSBs for example at a collapsed replication fork during S phase.
Importantly, 53BP1 NBs could be fully restored to basal levels by the stable expression of siRNA-resistant GFP-BARD1 wildtype (WT) ruling out off-target effects of the siRNA-mediated knockdown (Figure 4.6B and Supplementary Figure Figure 4.6B). Expression of the GFP-BARD1 L44P mutant [230] on the other hand, was not able to reduce 53BP1 NBs to normal levels corroborating previous findings that the BRCA1/BARD1 complex is necessary to counteract the impediments leading to formation of 53BP1 NBs.

To further substantiate our findings beyond relying solely on RNAi-mediated protein depletion, we attempted generating stable U2OS CtIP knockout cells using the CRISPR/Cas9 technology as described by Munoz et al. [206]. However, CtIP demonstrated to be essential for long-term cell survival, hence we were unable to produce a full knockout. Nevertheless, we succeeded in targeting several of the CtIP alleles present in U2OS cells to generate a cell line with markedly reduced CtIP expression ($U2OS^{Cas9\Delta CtIP}$) (Supplementary Figure 4.6C). Consistently, we observed increased formation of 53BP1 NBs in $U2OS^{Cas9\Delta CtIP}$ cells upon treatment with low doses of the DNA polymerases inhibitor aphidicolin (Aph) that selectively impair progression of replication forks through physiological barriers [231] (Supplementary Figure 4.6C). Besides 53BP1 NBs, micronuclei (MN) formation is considered another marker of chromosome breakage stemming from replication stress-induced DNA lesions [79]. Accordingly, we detected a two-fold increase in the number of micronuclei upon disruption of CtIP and BARD1 (Figure 4.6C). Collectively, these data strongly implies crucial roles of CtIP and BARD1 in counteracting endogenous replication stress.
Next, we sought to directly analyse replication fork progression in cells devoid of CtIP and/or BARD1 that are experiencing mild replication stress induced by hydroxyurea (HU) treatment. By conducting a dual-labelling DNA fiber assay, we compared the tract lengths of sister replication forks. Sister forks depict two replisomes that have originated from the same origin of replication but travel in opposite directions. If replication progresses without perturbations, sister forks are characterized by similar replication rates resulting in symmetrical patterns of CldU/IdU incorporation [232]. However, our analysis revealed

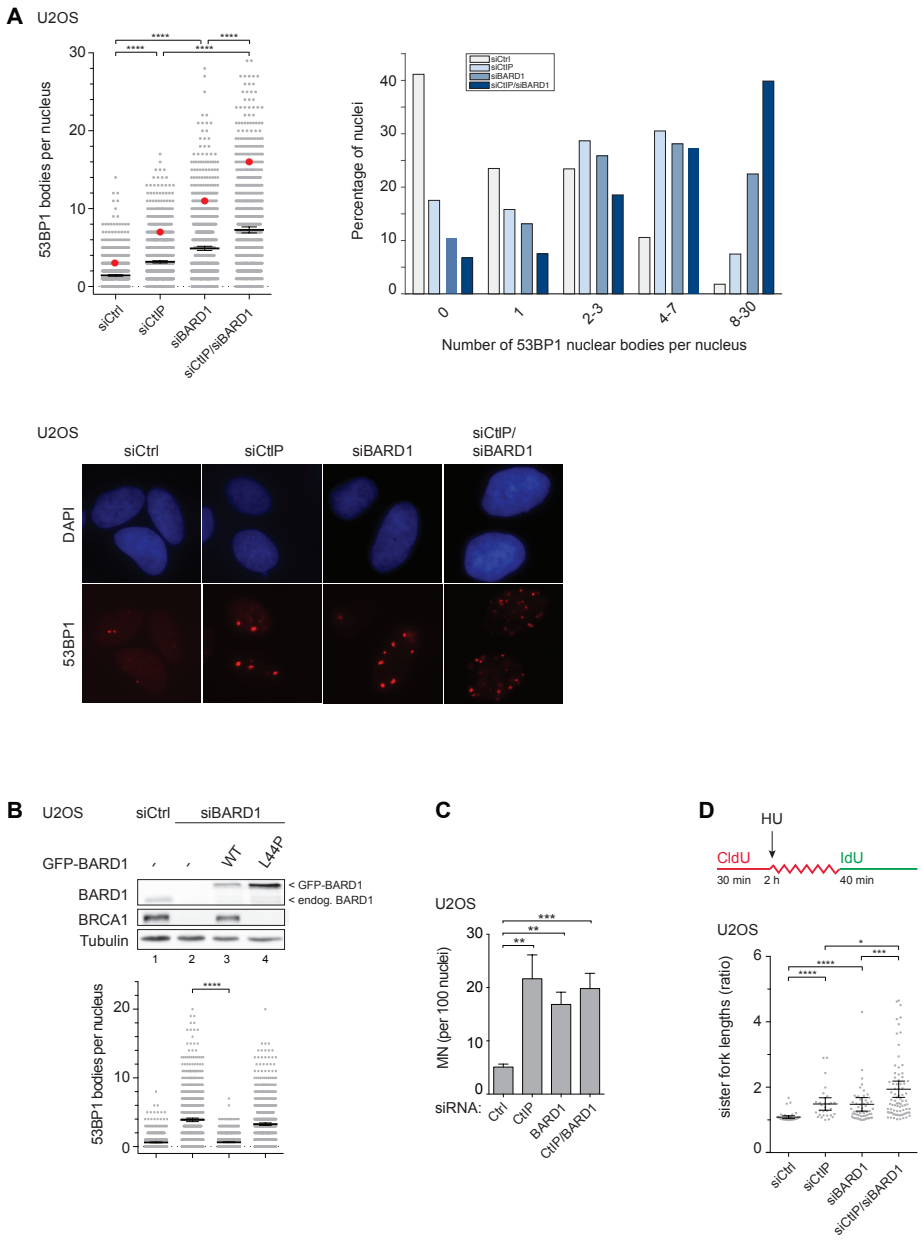

Figure 4.6: CtIP- and BARD1-deficiency induces 53BP1 nuclear bodies and replication fork stalling. (**A**) U2OS cells were transfected with the indicated siRNA. After 48 h of knockdown, cells were fixed and immunofluorescence was performed with anti-53BP1 antibody (red) along with DAPI staining. Upper left panel: Box plots represent quantification of 53BP1 nuclear bodies per nucleus. Black bars denote mean $\pm$ 95 % confidence interval, red circles denote the 90th percentile assessed in at least 900 nuclei (n $\geq$ 3). Right panel: Frequency distributions indicate the percentage of cells displaying a certain range of 53BP1 nuclear bodies for each knockdown condition. Bottom panel: Representative images are shown. Whole-cell extracts of the corresponding samples analysed by western blotting are shown in Supplementary Figure 4.6A.

Figure 4.6: (**B**) Parental U2OS cells and U2OS cells stably expressing siRNA-resistant GFP-tagged wildtype (WT) or mutant (L44P) human BARD1 were transfected with siCtIP for 48 h, and immunofluorescence was performed with anti-53BP1 antibodies. Box plots represent quantification of 53BP1 nuclear bodies from at least 600 nuclei (n = 3). Black bars denote mean ± 95 % confidence interval. Whole-cell extracts of corresponding samples were analysed by immunoblotting. Representative images are shown in Supplementary Figure 4.6B. (**C**) The number of micronuclei (MN) in cells treated as in (A) was quantified by immunofluorescence microscopy in DAPI-stained cells. Data represent the mean ± s.e.m. (n = 5). (**D**) DNA fiber analysis of U2OS cells treated as in (A). Cells were pulsed with CldU, exposed to 2 mM HU for 2 h, and pulsed with IdU. Box plots indicate the ratios of left/right fork lengths of bidirectional replication forks traveling from a single origin. The lines denote mean ratios ± 95 % confidence interval (n = 2). Representative images are shown in Supplementary Figure 4.6D.

marked fork asymmetry in HU-treated cells lacking CtIP or BARD1 that was increased in a additive manner upon co-depletion of both factors (Figure 4.6D and Supplementary Figure 4.6D). These results indicate that individual forks are more susceptible to persistent stalling in CtIP/BARD1-deficient cells. Thus, we not only provide evidence that simultaneous loss of CtIP and BARD1 leads to a synergistic increase of endogenous DNA damage but also to prolonged fork stalling suggesting that CtIP and BARD1 play important but non-overlapping roles to ensure faithful DNA replication.

4.5 DNA double-strand breaks (DSBs) arising in the absence of CtIP and BARD1 cannot be resolved and causes chromosomal aberrations.

Upon infliction of DNA lesions, the DDR signalling network is elicited to coordinate the DNA damage response. A key feature of the DDR is the activation of the apical kinases ATM (ataxia telangiectasia mutated) and ATR (ATM-and Rad3-related). According to current understanding, formation of DSBs leads to the initial recruitment and activation of ATM mediating the phosphorylation of its downstream target CHK2, among others. ATR, on the other hand, is activated by RPA binding to regions of single-stranded DNA (ssDNA) that are exposed at stalled replication forks or after DSB resection inducing a signalling cascade that involves the effector kinase CHK1 [13, 19]. To assess in more detail what kind of DNA lesions are induced in the absence of CtIP and BARD1, we monitored DNA damage signalling by ATM- and ATR-pathway activation (Figure 4.7A).

Control cells that had been treated with HU to induce replication stress demonstrate the characteristic activation of the ATR-CHK1 pathway upon fork stalling. However, CHK1 phosphorylation was largely unaltered upon CtIP, BARD1 or BRCA1 depletion and co-depletions in the absence of exogenous treatments. Conversely, the ATM-dependent arm of the DDR was initiated readily when CtIP or BARD1 were disrupted, displaying an additive increase upon ablation of both proteins (Figure 4.7A). Knockdown of BRCA1 alone or concurrently with CtIP did not cause ATM auto-phosphorylation of the same magnitude as CtIP/BARD1 depletion. From this data we hypothesized that persisting DNA lesions occurring upon CtIP/BARD1 disruption might partially represent replication-associated DNA DSBs. Therefore, we wanted to address the possibility that DSBs might arise concurrently with DNA replication, for example as a consequence of replication fork collapse. We treated [^{14}C]thymidine-pulse labelled cells with HU and performed pulsed field gel electrophoresis (PFGE) to analyse the DNA fragments generated during replication (Figure 4.7B). Interestingly, knockdown of CtIP, BARD1 or both barely induced damage at sites of newly replicating DNA. Chemical inhibition of Wee1 on the other hand caused a clear elevation of DNA breaks in newly replicated areas thereby confirming previous findings [216]. From our analysis we thus inferred, that in cells lacking CtIP and BARD1, formation of DSBs happens most likely not concomitantly to DNA replication and is therefore not the result of enhanced collapse of stalled replication forks.

Since persisting DSBs can potentially cause chromosomal rearrangements, we next analysed metaphase spreads from cells lacking CtIP and/or BARD1, which had been exposed to mild HU-treatment followed by a release from the replication stress to allow cell cycle progression (Figure 4.7C). Intriguingly, depletion of either CtIP or BARD1 alone elevated the prevalence of chromosomal aberrations per metaphase significantly while co-depletion of both proteins led to a further increase of chromosomal abnormalities. Most notably, we predominantly observed chromosomal fragments and deletions that can be the result of chromosome or chromatid breakage [233]. To complement our data, we investigated whether CtIP/BARD1 downregulation was associated with changes in the sensitivity of cells to HU-induced replication stress (Supplementary Figure 4.7A). In line with previous reports, we show that ATR inhibition impairs cell survival in cells

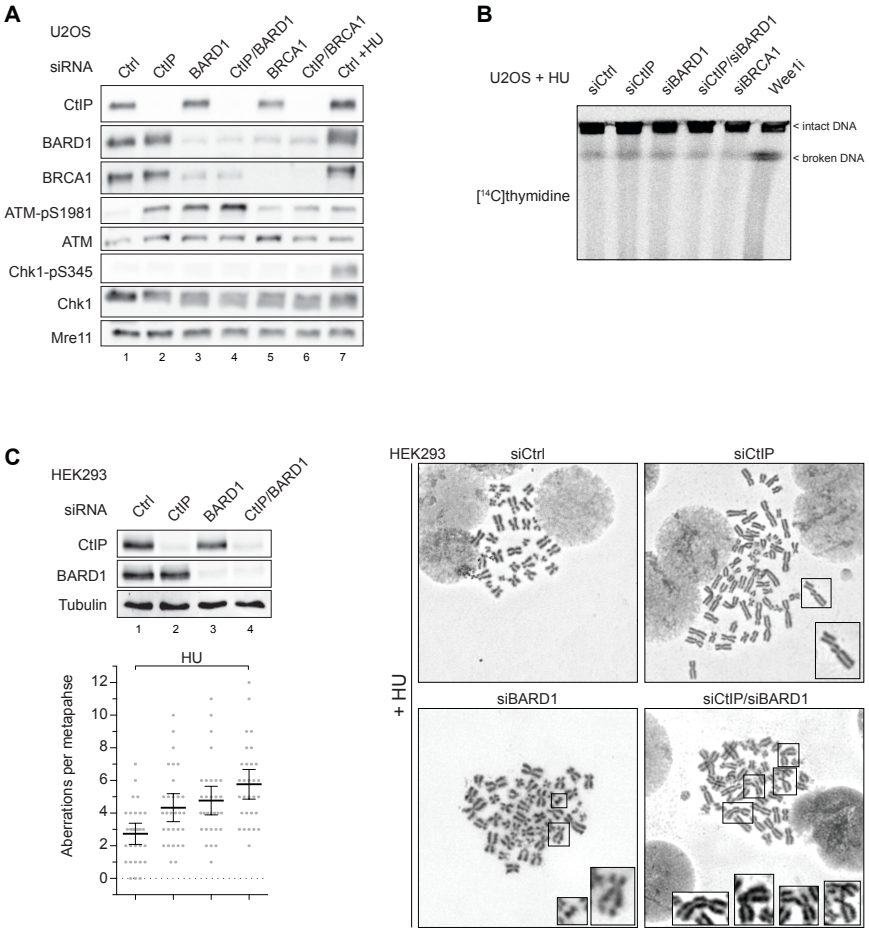

Figure 4.7: Cells experience elevated levels of DSB formation and chromosomal aberrations in the absence of CtIP and BARD1. (**A**) U2OS cells were transfected with the indicated siRNA for 48 h. One sample transfected with a non-targeting siRNA (siCtrl) was treated with 2 mM HU for 2 h prior to harvest. Whole-cell extracts were analysed by immunoblotting with the indicated antibodies. (**B**) U2OS cells treated as in (A) and U2OS cells treated with a chemical inhibitor of Wee1 (Wee1i) were pulse-labelled with methyl-[^{14}C]thymidine 48 h after siRNA transfection and concomitantly treated with 2 mM HU for 4 h. Cells were harvested and DNA fragments were separated by pulsed field gel electrophoresis (PFGE). (**C**) HEK293 cells were transfected with the indicated siRNAs for 48 h, treated with 2 mM HU for 4 h, and released from HU for 48 h. Prior to harvest, cells were arrested in metaphase with 0.1 µg/ml colcemid for 3 h. Metaphase spreads were prepared according to standard protocols and stained with Giemsa stain. Representative images are shown and specific chromosomal aberrations are magnified as insets (right panel). Lower left panel: Aberrations from 30 metaphase spreads were analysed. Box plots indicate aberrations per metaphase, black lines denote the mean $\pm$ 95 % confidence interval (n = 3). Whole-cell lysates of the same samples were subjected to immunoblotting (upper left panel)

upon HU-treatment [54, 234]. Knockdown of BARD1 conferred slight hypersensitivity to chronic exposure to HU-induced replication stress compared to control cells. However, cells were not sensitized to HU-treatment by downregulation of CtIP indicating that its loss-of-function is compliant with cell survival despite inducing considerable levels of DNA lesions and chromosomal aberrations (Figures 4.5B, 4.6A and 4.7C).

CtIP as well as BARD1 play essential roles in HR-mediated DSB repair [32, 145]. In line with previous reports, we found that CtIP depletion strongly interfered with HR at I-SceI-induced DSBs measured in an HR reporter assay (Supplementary Figure 4.7B) [205, 235]. Likewise, HR was almost completely blocked by depletion of BARD1 or co-depletion of BARD1 and CtIP. Since defective HR should result in hypersensitivity towards DSB-inducing agents, we additionally assessed cell survival upon chronic exposure to CPT. Elevated sensitivity towards this drug was evident in CtIP- as well as in BARD1-depleted cells, while co-depleted cells showed epistatic sensitivity towards CPT (Supplementary Figure 4.7C) Consequently, these results support a critical role for both, CtIP and BARD1 in facilitating DSB repair by HR. Since it was shown that BRCA1 can recruit CtIP to chromatin and into nuclear DNA repair foci following DSB formation [149], we also tested whether the HR deficiency was due to impaired CtIP recruitment subsequent to knockdown of BARD1 or BRCA1. However, in cells that had not been exposed to genotoxic stress, neither BARD1 nor BRCA1 downregulation affected the recruitment of CtIP to chromatin considerably (Supplementary Figure 4.7D). Correspondingly, CtIP could readily accumulate at sites of laser-induced DNA damage in the absence of BARD1 (Supplementary Figure 4.7E), contradicting the notion that CtIP recruitment is compromised by BARD1 disruption in this setting. Collectively our findings imply that the simultaneous absence of BARD1 and CtIP causes DSB formation and can result in chromosomal aberrations. In addition, we determine that CtIP/BARD1-deficient cells are dysfunctional in HR, which would be the preferable pathway to address DSBs. Moreover, our data suggests that DNA lesions induced by loss of CtIP alone do not impair cell survival upon mild induction of replications stress.

4.6 CtIP prevents excessive ssDNA formation in response to fork stalling

To substantiate the concept that CtIP plays a major role in supporting correct DNA replication, we sought to examine the molecular consequences of replication stress in cells devoid of CtIP. To this end, we assessed DNA damage signalling in cells lacking CtIP expression following acute exposure to HU or to the topoisomerase I-inhibitor CPT. A common feature of stalled forks, but also of resected DSBs, is the presence of single-stranded DNA (ssDNA) and the subsequent recruitment of RPA followed by hyper-phosphorylation of the RPA2 subunit on several residues, among them serine 4 and serine 8 [32, 65, 119, 236]. Intriguingly, upon mild HU treatment, we found RPA2 hyper-phosphorylation to be increased in CtIP-depleted cells when compared to control cells (Figure 4.8A). CHK1 phosphorylation on serine 345 was however largely unaffected by the knockdown of CtIP. In contrast, and consistent with the literature, when DSBs were induced by treating cells with CPT, RPA2 and CHK1 phosphorylations were decreased upon depletion of CtIP confirming that the absence of CtIP impairs DNA-end resection of CPT-induced DSBs [32]. By using a flow cytometry-based method to detect RPA retention on damaged chromatin [237], we further corroborated our previous finding, observing that the percentage of HU-induced RPA-positive cells was increased upon CtIP disruption (Figure 4.8B). Correspondingly, the percentage of HU-induced γH2AX-positive cells was slightly but reproducibly elevated in this assay. To more directly evaluate whether RPA2 hyper-phosphorylation corresponded to the formation of ssDNA we immuno-stained bromodeoxyuridine (BrdU)-labeled cells with an anti-BrdU antibody. Consistently, the BrdU signal was strikingly increased in response to HU following the knockdown of CtIP (Figure 4.8C). Remarkably, U2OS$^{\text{Cas9}\Delta\text{CtIP}}$ cells expressing only residual levels of CtIP displayed a similar increase of RPA-coated ssDNA upon exposure to HU (Supplementary Figures 4.8A and B). Consistent with our previous findings in HeLa cells transfected with siRNA targeting CtIP, U2OS$^{\text{Cas9}\Delta\text{CtIP}}$ cells exhibited no hypersensitivity towards HU-induced replication stress in terms of cell survival (Supplementary Figure 4.8C). However, in marked contrast to cells transfected with siRNA against CtIP, we neither detected a substantial

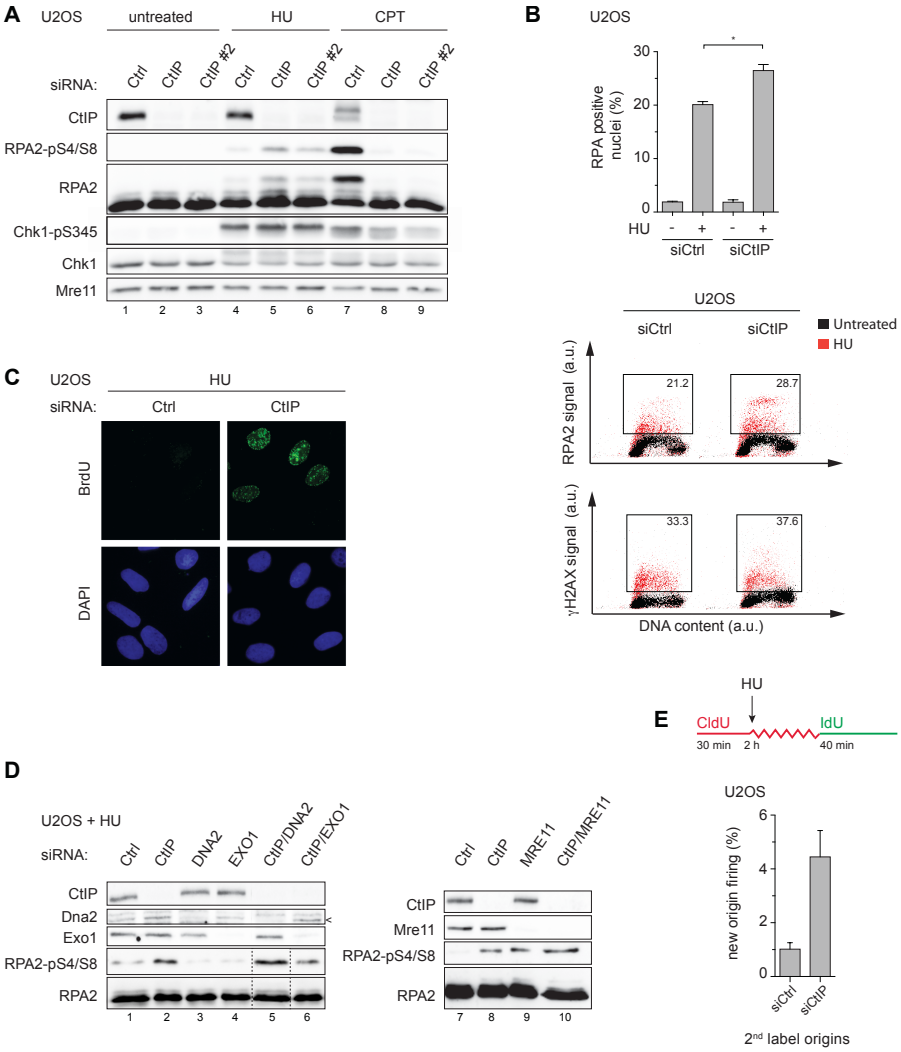

Figure 4.8: CtIP counteracts the formation of excess RPA-coated ssDNA in response to replication stress. (**A**) U2OS cells were transfected with the indicated siRNA for 48 h and were left untreated or were incubated with either HU (2 mM) for 2 h or CPT (1 µM) for 1 h prior to harvest. Whole-cell extracts were analysed by western blotting with the indicated antibodies. (**B**) Cells treated as in (A) were harvested, permeabilized, fixed, immunostained with anti-RPA2 and anti-γH2AX antibodies and analysed by FACS. Bottom panel: Dot plots represent the intensity of the signals for RPA2 or γH2AX staining (y axis) against the DNA content (x axis). Quantification gates were established in untreated samples transfected with siCtrl. The square marks the gate and shown are the percentages of HU treated-cells contained in them. Upper panel: Percentages indicate mean ± s.e.m. of RPA2-positive cells (n = 3). a. u. = arbitrary units. (**C**) Cells treated as in (A) were immunostained for BrdU to visualize single-stranded DNA under non-denaturing conditions. (**D**) U2OS cells were transfected with the indicated siRNAs for 48 h and were treated with HU (2 mM) for 2 h prior to harvest. Whole-cell extracts were analysed by western blotting with the indicated antibodies. (**E**) DNA fiber analysis of U2OS cells as in Figure 4.6D. DNA fibers were enumerated and the percentage of new origins (IdU-labeled only) was quantified. Box plots indicate mean ± s.e.m. (n = 2).

reduction in the levels of phosphorylated RPA2 nor significant hypersensitivity upon CPT-treatment in U2OS$^{Cas9\Delta CtIP}$ cells (Supplementary Figures 4.8A, B and C). These findings suggest that even though low levels of CtIP are sufficient to maintain DNA-end resection at CPT-induced DSBs, they are inadequate to perform CtIP functions during the response to replication stress. Collectively, these data reveal that DNA damage in cells lacking CtIP challenged by replication stress is characterized by increased ssDNA formation, a common intermediate at replication-associated DNA lesions. However, the question remained how CtIP counteracts the generation of surplus levels of ssDNA in the face of replication stress. Excessive fork degradation by promiscuous nucleases such as MRE11 and DNA2 that perform uncontrolled resection of stalled replication forks has recently been described [78, 238]. Since several HR proteins, like Rad51 and BRCA1/2, have been implicated in preventing uncontrolled nucleolytic resection of stalled forks [92, 94], it was conceivable that CtIP might restrain the activity of a nuclease that, upon loss of CtIP functions, unleashes its potent activity to excessively resect DNA in the vicinity of stalled replication forks. However, neither co-depletion of MRE11, DNA2 nor EXO1 repressed the HU-induced increase of phosphorylated RPA2 in cells lacking CtIP (Figure 4.8D). Thus, we concluded that CtIP is not implicated in protecting stalled replication forks from nucleolytic degradation. However, by conducting a DNA fiber assay, we determined that CtIP-depleted cells showed a considerable increase in new origin firing in response to HU-treatment (Figure 4.8E). This might indicate that the increase of ssDNA formation in CtIP-deficient cells that are experiencing replication stress is likely caused by activating of alternative origin firing.

In summary, we showed that CtIP functions to prevent the excessive generation of ssDNA, a toxic intermediate induced by replication stress. We furthermore found that the negative effects of CtIP disruption on DNA replication are enhanced by simultaneous loss of the BRCA1/BARD1 complex. We describe the identification of a SSL genetic interaction between CtIP and BARD1 that is however not fully recapitulated by CtIP and BRCA1. As an underlying cause for the synthetic sick phenotype, we propose the profound inability to efficiently prevent and resolve replication stress in the absence of CtIP and BARD1. From our analysis we concluded, that ablation of both proteins led to a severe increase

of endogenous DNA lesions arising in the context of replication and ultimately to the generation of DNA DSBs. Moreover, without BARD1 and CtIP, the HR pathway, addressing these lesions, was drastically impaired and consequently chromosomal aberrations arose. Since an elevated incidence of chromosomal abnormalities would likely induce programmed cell death, we inferred that this mechanism might contribute to the synthetic sick phenotype of CtIP and BARD1 depletion.

Supplementary Figures

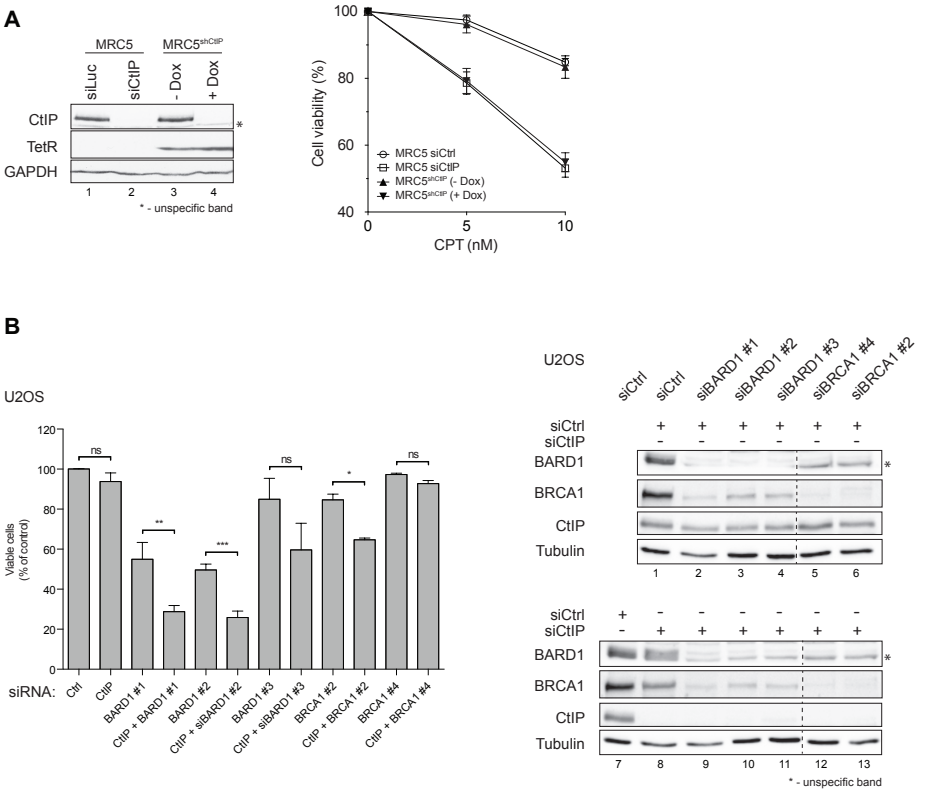

Supplementary Figure 4.4. (**A**) MRC5 cells were transfected with the indicated siRNAs for 48 h. MRC5^{shCtIP} cells were cultivated in the absence or presence of Dox (1 µg/ml) for 48 h. Cells were then treated with the indicated doses of CPT. Cell survival was determined after 4 days using the CellTiter-Blue® cell viability assay. Data represents the mean ± s.e.m. (n = 5). Whole-cell extracts of the corresponding samples were analysed by western blotting. (**B**) U2OS cells were reverse transfected with combinations of the indicated siRNAs in 96-well plates. The knockdown was allowed to persist for 6 days upon which survival was determined using the CellTiter-Blue® cell viability assay (Promega). Data are presented as mean ± s.e.m. (n $\geq$ 2). Whole-cell extracts of the corresponding samples were analysed by western blotting.

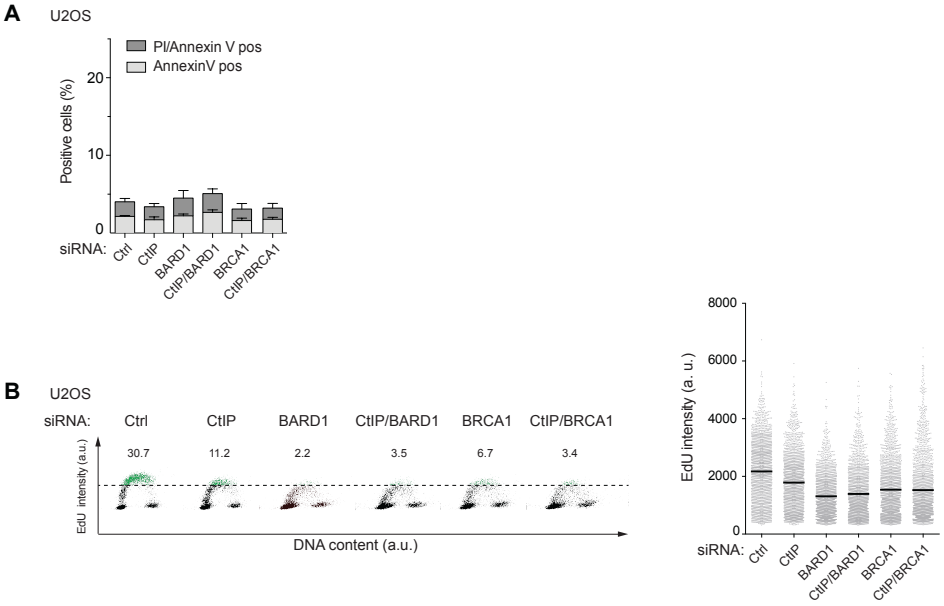

Supplementary Figure 4.5. (**A**) U2OS cells were transfected with siRNA as in Figure 4.5A, and the knockdown was allowed to persist for 48 h. Cells were then harvested and the induction of apoptosis was determined by flow cytometric analysis. Annexin V^{FITC}-positive staining indicates early apoptotic cells whereas Annexin V-positive/PI-positive staining indicates late apoptotic cells. (**B**) U2OS cells were transfected with the indicated siRNAs for five days, pulse-labelled with EdU and analysed by FACS. Left panel: Dot plots represent the intensity of the signals for EdU (y axis) against the DNA content (x axis). Quantification gates were established in samples transfected with siCtrl. Dashed line denotes the threshold for EdU incorporation and percentage of cells with EdU intensities above the threshold are indicated. Right panel: Representation of EdU intensities from 10 000 EdU-positive cells (n = 2). Black bar indicates mean value. a. u. = arbitrary units.

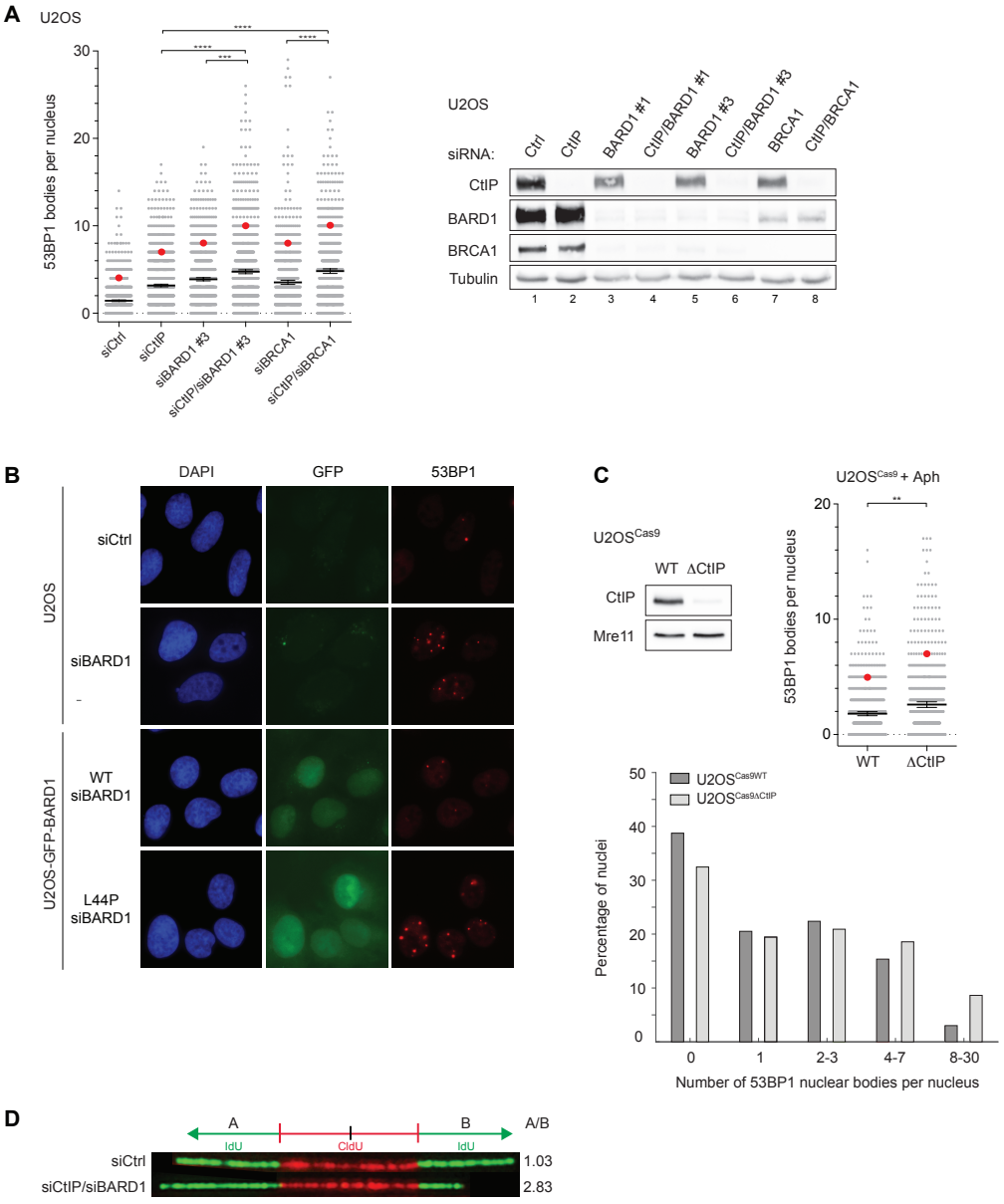

Supplementary Figure 4.6. (**A**) U2OS cells were transfected with the indicated siRNA as in Figure 4.6A. After 48 h of knockdown, cells were fixed, and immunofluorescence was performed with anti-53BP1 along with DAPI staining. Box plots represent quantification of 53BP1 nuclear bodies per nucleus. Black bars denote mean ± 95 % confidence interval, red circles the 90th percentile assessed in at least 900 nuclei (n ≥ 3). Right panel: Whole-cell extracts of the corresponding samples from this figure and Figure 4.6A were analysed by western blotting. (**B**) Representative images from cells described in Figure 4.6B. (**C**) U2OS^{Cas9WT} and U2OS$^{Cas9\Delta CtIP}$ cells were treated with 0.2 µM aphidicolin (Aph) for 24 h, fixed and immunostained for 53BP1. Box plots represent quantification of 53BP1 nuclear bodies per nucleus. Black bars denote mean ± 95 % confidence interval, red circles the 90th percentile assessed in at least 600 nuclei (n = 2). Bottom panel: Frequency distribution of 53BP1 nuclear bodies for each cell line. Upper left panel: Whole-cell extracts of the corresponding cell lines were analysed by western blotting. (**D**) Representative images from DNA fibers described in Figure 4.6D.

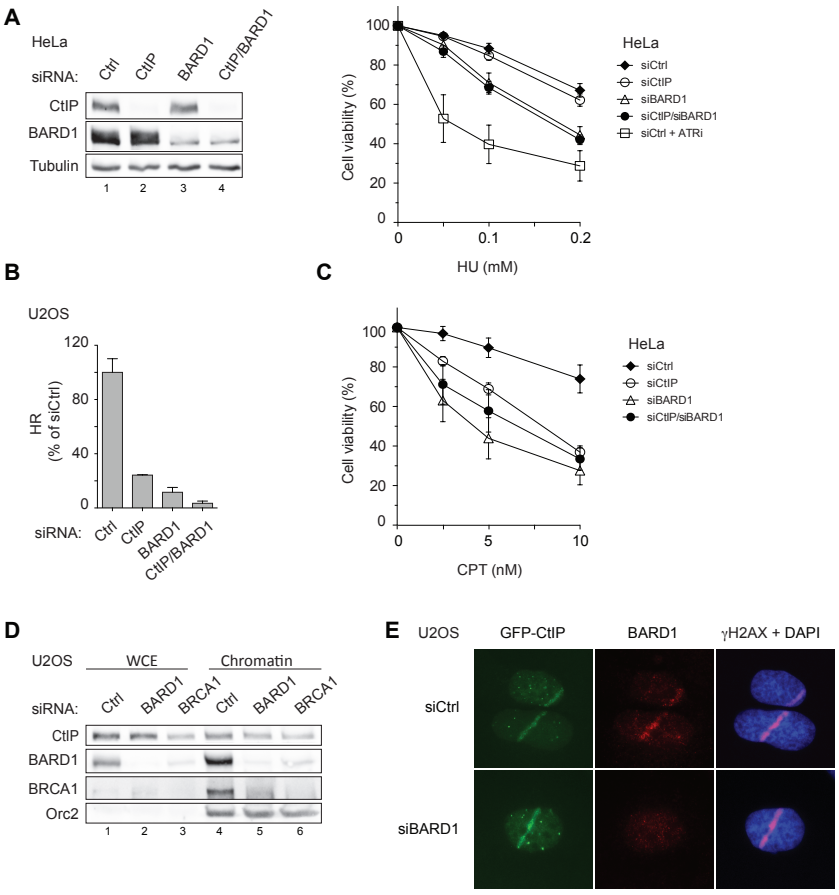

Supplementary Figure 4.7. (**A**) HeLa cells were transfected with the indicated siRNA. 48 h post-transfection, cells were pre-treated for 15 min with 10 µM ATRi (where indicated) and then treated with the indicated doses of HU. Survival was determined after 4 days using the CellTiter-Blue® cell viability assay. Data are presented as mean ± s.e.m. ($n \geq 3$). Whole-cell extracts of the corresponding samples were analysed by western blotting. (**B**) U2OS cell lines containing a classical DNA repair GFP-based reporter for HR were transfected with the indicated siRNAs and six hours later transfected with the *I-SceI* expression plasmid and the exogenous *GFP* donor template. Cells were harvested 72 h after siRNA transfection and GFP-positive cells indicating HR repair activity were assessed by flow cytometry. Data are presented as mean ± s.e.m. (n = 2). (**C**) Same cells as in (A) were treated with the indicated doses of CPT. Survival was determined after 4 days using the CellTiter-Blue® cell viability assay. Data are presented as mean ± s.e.m. (n = 4). (**D**) U2OS cells were transfected with the indicated siRNA. After 48 h of knockdown, total cell extracts (WCE) and chromatin-enriched fractions (Chromatin) were prepared and analysed by immunoblotting using the indicated antibodies. (**E**) U2OS cells stably expressing GFP-tagged CtIP were grown on coverslips and transfected with BARD1 siRNA for 48 h. For the last 24 h cells were cultivated in the presence BrdU (10 µM) prior to laser micro-irradiation. 15 min post irradiation, cells were fixed, immunostained for BARD1 and γH2AX and analysed by fluorescence microscopy.

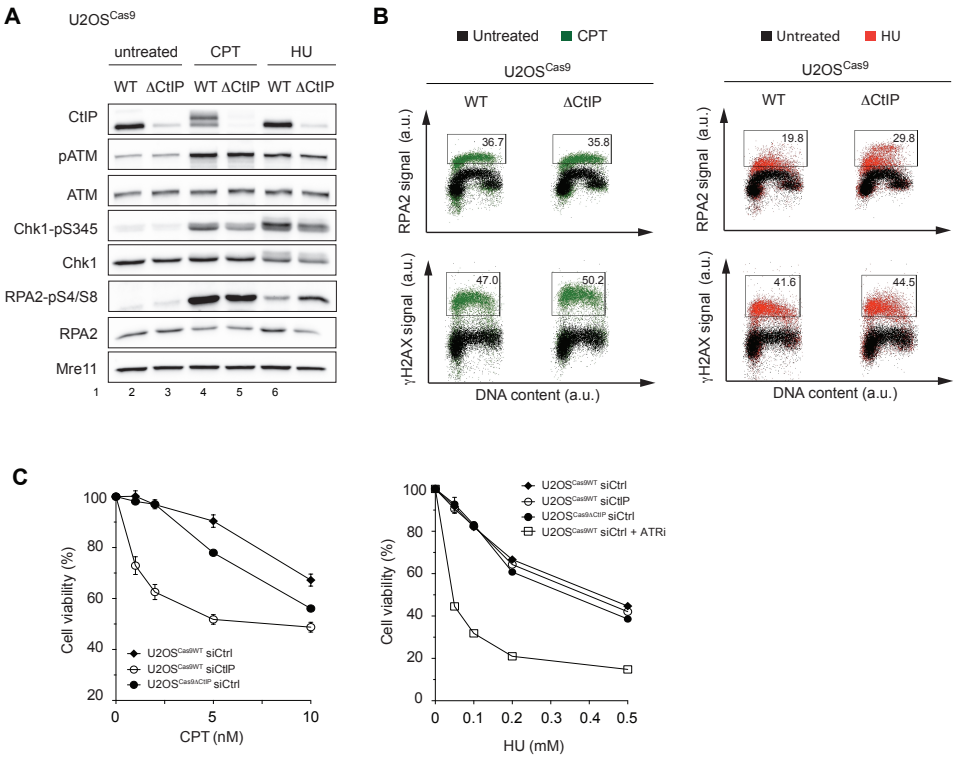

Supplementary Figure 4.8. (**A**) U2OS^{Cas9WT} or U2OS$^{Cas9\Delta CtIP}$ cells were either mock-treated, treated with CPT (1 µM) for 1 h or with HU (2 mM) for 2 h prior to harvest. Whole-cell extracts were analysed by western blotting. (**B**) Cells treated as in (A) were harvested, permeabilized, fixed, immunostained with anti-RPA2 or anti-γH2AX antibodies and analysed by FACS. Dot plots represent the intensity of the signals for RPA2 or γH2AX staining (y axis) against the DNA content (x axis). Quantification gates were established in untreated samples of U2OS^{Cas9WT}. The square marks the gate and shows the percentage of drug-treated cells contained in it. a. u. = arbitrary units. (**C**) U2OS^{Cas9WT} or U2OS$^{Cas9\Delta CtIP}$ cells were transfected with the indicated siRNA. 48 h post-transfection, cells were pre-treated for 15 min with 10 µM ATRi (where indicated) and then treated with the indicated doses of HU or CPT. Survival was determined after 4 days using the CellTiter-Blue® cell viability assay. Data are presented as mean $\pm$ s.e.m. (n $\geq$ 3).

Discussion

The DDR is essential to safeguard genome integrity and to prevent malignant transformation. Human CtIP is most considerably recognized for its key role in the repair of DNA DSBs by the HR pathway yet more recently, it has emerged as an important player in genome stability maintenance beyond its role in DSB processing. In order to explore the molecular network of CtIP and to provide insights into the organization of biological pathways which CtIP participates in, I investigated synthetic genetic interactions with CtIP. Through multiplexed RNAi-based screening in the absence or presence of the DNA-damaging agent CPT, I assessed genetic interactions with CtIP on the one hand and genes conferring CPT hypersensitivity on the other hand. Analysis of the latter confirmed a number of factors that had already been shown to mediate resistance towards CPT. Unfortunately, we failed to uncover genes that had not previously been linked with the DDR in this part of the screen and therefore refrained from further investigation.

However, our screen analysis revealed a number of interesting candidate genes for synthetic sick/synthetic lethal (SSL) interactions with CtIP. One of our SSL candidate hits was for example DNA polymerase θ (encoded by the *POLQ* gene), a protein implicated in the error-prone microhomology-mediated end-joining (MMEJ) pathway of DSB repair. Intriguingly, the absence of DNA polymerase θ was shown to enhance cell death in HR-deficient cells in a publication that was issued after we had completed our screen [239], thus confirming one of the SSL interactions we identified. In addition, our RNAi screen uncovered a novel SSL genetic interaction between CtIP and BARD1. As part of my PhD thesis, I demonstrate the importance for this interconnection during DNA replication and the replication stress response. Remarkably, the negative genetic interaction between CtIP and BARD1 affects two components residing in a single protein complex. It

has been previously reported that DDR pathways represent a hotspot for within-pathway SSL interactions and that negative genetic interactions frequently connect components of the same essential protein complex [228, 229]. Indeed, CtIP as well as BARD1 have described to be essential for cell survival and their knockout in mice caused embryonic lethality at day E4 and E7.5, respectively [100, 240]. Consistently, human cell lines lacking CtIP or BARD1 have not been established to date. Subsequently, we sought to elucidate the molecular mechanism underlying the SSL relationship between CtIP and BARD1. From our analysis we propose that CtIP and BARD1 are involved in different aspects of preventing and addressing endogenous DNA lesions arising in the context of DNA replication stress.

CtIP has previously been proposed to associate with unperturbed replication forks to ensure replication fork progression and to prevent the formation of under-replicated regions especially in the context of common fragile sites [95, 117, 121, 122]. CtIP was furthermore shown to act upon replication fork stalling by suppressing new origin firing and promoting fork restart [121]. Here we find, that siRNA-mediated silencing of CtIP expression causes accumulation of RPA-coated ssDNA in cells experiencing mild replication stress induced by acute HU treatment. Importantly, ssDNA formation is a common intermediate at replication-associated lesions [79, 216]. It may be caused by helicase and polymerase uncoupling, by unscheduled origin firing or by uncontrolled fork resection by promiscuous nucleases [54, 64, 78, 92]. RPA-coating shields stalled replication forks against fatal breakage at regions of unprotected ssDNA and it was perceived that excessive ssDNA generation may lead to exhaustion of cellular pools of RPA thus promoting irreversible fork collapse [54]. However, here we show that RPA2 hyper-phosphorylation was rather modest following HU treatment compared to its potent induction in response to the DSB-inducing agent CPT. Thus, we assume that the amount of ssDNA generated after acute exposure to mild doses of HU, though markedly increased upon CtIP depletion, is not sufficient to exhaust the cellular RPA pool. In addition, we found that the ATR-CHK1 pathway is functional in CtIP-deficient cells following replication stress. We furthermore sought to determine the molecular mechanism responsible for the surplus formation of RPA-coated ssDNA in CtIP-deficient cells treated with HU. Upon fork stalling, limited nucleolytic re-

section allows RAD51-dependent HR to facilitate repair and restart of the blocked fork [94]. However, promiscuous nucleases, such as MRE11 and DNA2 and possibly also EXO1, have been described to perform uncontrolled resection of stalled replication forks in the absence of proper control mechanisms [92, 238]. From our analysis, we could not provide compelling evidence indicating that the increase in ssDNA in cells devoid of CtIP was mediated by any of the three nucleases implicated in DNA resection, MRE11, DNA2 or EXO1. Consistently, Yeo et al. [121] suggested that CtIP is dispensable for protecting stalled replication forks from nucleolytic degradation. In line with this study, we observed a substantial increase of new origin firing in the absence of CtIP representing an alternative explanation for the increased generation of ssDNA in CtIP-deficient cells encountering HU-induced replication stress. Interestingly, CtIP deficiency was not associated with hypersensitivity to HU treatment. Hence, we concluded that RPA shielding stabilizes and protects the ssDNA intermediates formed as a consequence of perturbed DNA replication in cells lacking CtIP. We furthermore inferred that interference with replication fork progression may render CtIP-deficient cells susceptible to accumulating low amounts of DNA lesions but their prevalence is not sufficient to impair cell survival. Consistently, downregulation of CtIP in the absence of any exogenous treatments provoked mild replication-associated DNA damage determined by a slight increase of γH2AX, an elevated incidence of 53BP1 nuclear bodies and chromosomal aberrations. Conversely, CtIP disruption was insufficient to affect G_2/M checkpoint activation or apoptosis induction significantly. Therefore, we assume that cells lacking CtIP can survive in the presence of mild replication stress associated with few DNA lesions.

BARD1, on the other hand, had not been studied yet in the context of DNA replication or in the response to replication stress. However, evidence for the presence of BARD1 at the replication fork was recently presented in a study by Dungrawala et al. which identified BARD1 alongside its heterodimeric partner BRCA1 at HU-stalled forks by using an iPond-SILAC-approach coupled with mass spectrometry [95]. For the first time, here, we investigated the functional consequences of BARD1 disruption on DNA replication. Intriguingly, we observed an unexpected cell cycle response indicating that BARD1 is required for G_2/M transition in otherwise unperturbed cells. Moreover, siRNA-mediated de-

pletion of BARD1 alone activated the DDR involving elevated levels of γH2AX and 53BP1 nuclear bodies, and the generation of chromosomal aberrations. Furthermore, cells lacking BARD1 displayed modest but significant hypersensitivity towards HU, indicating that BARD1 counteracts replication-associated DNA damage. Thus, we propose that not only BRCA1 but also its obligate binding partner BARD1 possesses important functions in safeguarding genome integrity by promoting faithful DNA replication. It is, however, important to note, that siRNA-mediated knockdown of BARD1 destabilized BRCA1 considerably. Thus, we cannot rule out that the phenotypes described here are in fact mediated at least in part by a function associated with BRCA1/BARD1 heterodimerization. To dissect the details of individual contributions of either BARD1 or BRCA1 on promoting faithful DNA replication would be very challenging and was therefore beyond the scope of this work.

Remarkably, we found that co-depletion of BARD1 and CtIP did not only cause a synthetic sick growth defect but was also accompanied by a synergistic increase of endogenous DDR activation at early time points. Even though the induction of apoptotic cell death as well as of H2AX phosphorylation was already notable upon downregulation of BARD1 alone, both phenotypes were significantly augmented upon simultaneous disruption of CtIP. As the increase in γH2AX occurred predominantly in the G_2/M population of cells co-depleted for CtIP and BARD1 and was accompanied by an accumulation of cells arresting in the G_2/M phase of the cell cycle, we reasoned that cells lacking CtIP and BARD1 might have problems to accurately complete replication during S phase. In support of this notion, CtIP/BARD1-deficient cells displayed an additive increase in sister fork asymmetry during recovery from exposure to HU, implying that CtIP and BARD1 might cooperate to counteract replication fork stalling. To further investigate the hypothesis that CtIP and BARD1 promote faithful DNA replication, we monitored the prevalence of 53BP1 nuclear bodies, which have recently been shown to form in regions of under-replicated DNA and are primarily observed in cells that have experienced replication stress in the previous S phase [83, 84]. Intriguingly, upon co-depletion of CtIP/BARD1 we observed a striking synergistic increase in 53BP1 nuclear bodies potentially marking chromosomal loci with unresolved replication stress. Even though the type of DNA lesion accountable

for 53BP1 accumulation on chromatin following replication stress has not been determined to date, it is worth noting that DSBs were suggested to contribute to their genesis [83]. In support of this hypothesis, we demonstrated that simultaneous downregulation of CtIP and BARD1 induced the activation of ATM in an additive manner. Thus, we postulated that 53BP1 nuclear bodies stemming originally from replication impediments could partly denote sites of DNA DSBs. Interestingly, in this context 53BP1 has been shown to associate in nuclear foci at DSBs upon induction of severe DNA damage [142]. Thus, 53BP1 bodies might also indicate sites of DNA rupture and persisting DSBs. This notion was further strengthened by the finding that CtIP and BARD1 deficiency caused an additive increase in chromosomal aberrations, particularly chromatid breaks, fragments and a few chromosome fusions [233], which can form upon mitotic chromosome breakage or if DSBs are not faithfully repaired [19, 241]. Taken together, we concluded that CtIP and BARD1 cooperate to counteract the formation of DSBs stemming from aberrantly resolved replication-associated DNA lesions.

Nevertheless, it remained possible that a higher frequency of fork collapse might be the source for the elevated incidence of DSBs in cells lacking CtIP and/or BARD1. We specifically addressed this question and found that depletion of neither CtIP nor BARD1 alone or in combination caused the formation of DSBs in newly replicated DNA following HU-treatment. Thus, DSBs are likely generated by other mechanisms than fork collapse. Notably, a previous study suggested that constitutive activation of the ATM-CHK2 pathway can occur in a DSB-independent manner in cells displaying elevated rates of endogenous replication fork stalling due to the absence of the BLM helicase [242]. However, we reasoned that DSB induction should be a prerequisite for the chromosomal aberrations observed upon CtIP/BARD1 co-depletion. Interestingly, recent data specified that 53BP1 nuclear bodies predominantly indicate sites of unresolved or broken anaphase bridges [85] supporting the notion that DSBs might rather arise from persisting, toxic replication intermediates. Following this rationale, we determined that DSBs, once formed, could not be addressed by the HR pathway due to its impairment in the absence of BARD1 and CtIP. We thus inferred that error-free, HR-mediated dissolution of 53BP1 nuclear bodies during subsequent S and G_2 phases of the cell cycle was compromised in cells lacking

CtIP and BARD1 and as a consequence, deleterious DNA lesions such as DSBs might therefore persist.
In this context it is important to note, that 53BP1 might shield damaged chromatin from deleterious consequences of un- or mis-repaired DNA breaks in a mechanism analogous to the one proposed by Toledo et al. [54]. In case DNA lesions accumulate and sequester all available 53BP1, every new round of replication would potentially generate additional regions of under-replicated DNA and might ensue further DNA breakage. Moreover, it is tempting to speculate that in cells devoid of CtIP and BARD1, DNA breaks could become an inappropriate substrate for error-prone repair mechanisms like NHEJ due to the impairment of HR. In fact, it is well established that association of 53BP1 with DSBs promotes NHEJ [30, 243]. Hence, the resulting incidence of chromosomal breaks and rearrangements could hardly be compatible with cell survival and might serve as an explanation for the synthetic sick phenotype observed between CtIP and BARD1. Moreover, unresolved replication intermediates can occasionally manifest in anaphase bridges, chromosome breakage and mis-segregation giving rise to cell division defects such as micronuclei [241, 244]. Consistently, we also noticed a considerable increase of micronuclei formation upon either CtIP or BARD1 disruption and upon co-depletion of both factors.

Collectively, in my PhD thesis I propose that CtIP and BARD1 functions are interconnected through a synthetic sick genetic interaction. In the absence of BARD1 and CtIP, disproportionate levels of endogenous DNA lesions arise in the context of replication and cannot be appropriately addressed due to simultaneous dysfunction of the HR pathway. Our data is consistent with the hypothesis that endogenous DNA damage can conceivably arise as a result of enhanced replication stress increasing the level of DNA breakage and chromosomal aberrations [87]. Importantly, if DNA damage exceeds the repair capacity, programmed cell death would be initiated. In rare cases however, such aberrations may escape from cell surveillance pathways and contribute to mutagenesis and malignant transformation.

The evidence presented here underlines the essential role of HR for counteracting endogenous DNA damage in order to protect cells against spontaneous chromosome in-

stability. A critical function in mediating HR has been ascribed to the BRCA1/BARD1 heterodimer [138, 144]. Subsequently, it was established that CtIP interacts with BRCA1 and initially this interactions was implicated in facilitating DNA-end resection [172, 173]. However, recent findings have challenged the significance of the CtIP-BRCA1 interaction as it was demonstrated that complex formation with BRCA1 is dispensable for CtIP-mediated DNA end-resection and HR [175–177]. Furthermore, several studies have uncovered novel roles in preserving the integrity of DNA replication forks particularly for BRCA1 [92, 181, 183], whereas the significance of its obligate interaction partner BARD1 in these processes was often overlooked. Here, we reveal that CtIP genetically and physically interacts with BARD1 to cooperate in promoting faithful DNA replication. Thus, we uncovered a previously uncharacterized role of the CtIP–BARD1/BRCA1 protein network for combating replication stress, genome instability and hence the development of cancer.

Moreover, important implications for the tumour suppressive role of CtIP emerge from our study. It was already proposed by Bartek et al. in 2007, that dosage insufficiencies of DNA repair genes might only be unmasked once a cell is challenged with an increased load of DNA damage such as replicative stress induced by pre-cancerous lesions [245]. Further support for this important concept emerged when it was discovered that primary mammary epithelial cells from patients with heterozygous BRCA1 mutations experience higher loads of replication stress while other BRCA1 functions, such as promoting HR, remained unaltered [184]. Hence, the authors of this study concluded that the proficiency to respond to replication fork stalling might be the limiting factor in BRCA1 genome integrity control. Similar results were obtained in cells lacking the BLM helicase and it was found that the deficiency of BLM likely generates enhanced replication stress similar to the situation in pre-cancerous tissues [242]. By using the CRISPR/Cas9 technology, here, we demonstrate that expression of diminished levels of CtIP also contributes to a phenotype of mild but persistent replication stress that may dampen cell surveillance mechanisms but can ultimately cause increased chromosomal aberrations. Hence, consequences of reduced CtIP expression might potentially provoke genomic instability and tumour susceptibility. Our novel findings therefore underscore the importance of CtIP as one of the HR proteins with a crucial role in combating situations of elevated endogenous replication

stress thus elucidating further details of the significance of CtIP for tumour suppression.

Bibliography

[1] Eva Bianconi, Allison Piovesan, Federica Facchin, Alina Beraudi, Raffaella Casadei, Flavia Frabetti, Lorenza Vitale, Maria Chiara Pelleri, Simone Tassani, Francesco Piva, Soledad Perez-Amodio, Pierluigi Strippoli, and Silvia Canaider. An estimation of the number of cells in the human body. *Annals of human biology*, 40(6):463–471, November 2013.

[2] P C Nowell. The clonal evolution of tumor cell populations. *Science (New York, N.Y.)*, 194(4260): 23–28, October 1976.

[3] Christine L Chaffer and Robert A Weinberg. How does multistep tumorigenesis really proceed? *Cancer discovery*, 5(1):22–24, January 2015.

[4] Penny A Jeggo, Laurence H Pearl, and Antony M Carr. DNA repair, genome stability and cancer: a historical perspective. *Nature reviews. Cancer*, 16(1):35–42, January 2016.

[5] Simona Negrini, Vassilis G Gorgoulis, and Thanos D Halazonetis. Genomic instability–an evolving hallmark of cancer. *Nature reviews. Molecular cell biology*, 11(3):220–228, March 2010.

[6] R Fishel, M K Lescoe, M R Rao, N G Copeland, N A Jenkins, J Garber, M Kane, and R Kolodner. The human mutator gene homolog MSH2 and its association with hereditary nonpolyposis colon cancer. *Cell*, 75(5):1027–1038, December 1993.

[7] K W Kinzler and B Vogelstein. Cancer-susceptibility genes. Gatekeepers and caretakers. *Nature*, 386 (6627):761–763, April 1997.

[8] L A Loeb. Mutator phenotype may be required for multistage carcinogenesis. *Cancer Research*, 51 (12):3075–3079, June 1991.

[9] Douglas Hanahan and Robert A Weinberg. Hallmarks of cancer: the next generation. *Cell*, 144(5): 646–674, March 2011.

[10] Deborah E Barnes and Tomas Lindahl. Repair and genetic consequences of endogenous DNA base damage in mammalian cells. *Annual review of genetics*, 38:445–476, 2004.

[11] Jan H J Hoeijmakers. DNA damage, aging, and cancer. *The New England journal of medicine*, 361 (15):1475–1485, October 2009.

[12] Stephen P Jackson and Jiri Bartek. The DNA-damage response in human biology and disease. *Nature*, 461(7267):1071–1078, October 2009.

[13] Daniela Hühn, Hella A Bolck, and Alessandro A Sartori. Targeting DNA double-strand break signalling and repair: recent advances in cancer therapy. *Swiss medical weekly*, 143:w13837, 2013.

[14] Jacob Falck, Julia Coates, and Stephen P Jackson. Conserved modes of recruitment of ATM, ATR and DNA-PKcs to sites of DNA damage. *Nature*, 434(7033):605–611, March 2005.

[15] Hans E Krokan and Magnar Bjørås. Base excision repair. *Cold Spring Harbor perspectives in biology*, 5(4):a012583, April 2013.

[16] Orlando D Schärer. Nucleotide excision repair in eukaryotes. *Cold Spring Harbor perspectives in biology*, 5(10):a012609, October 2013.

[17] Josef Jiricny. The multifaceted mismatch-repair system. *Nature reviews. Molecular cell biology*, 7(5): 335–346, May 2006.

[18] Philip A Knobel and Thomas M Marti. Translesion DNA synthesis in the context of cancer research. *Cancer cell international*, 11:39, 2011.

[19] Alberto Ciccia and Stephen J Elledge. The DNA damage response: making it safe to play with knives. *Molecular cell*, 40(2):179–204, October 2010.

[20] Ketki K Karanam, Ran R Kafri, Alexander A Loewer, and Galit G Lahav. Quantitative Live Cell Imaging Reveals a Gradual Shift between DNA Repair Mechanisms and a Maximal Use of HR in Mid S Phase. *Molecular cell*, 47(2):320–329, July 2012.

[21] Hyungjin Kim and Alan D D'Andrea. Regulation of DNA cross-link repair by the Fanconi anemia/BRCA pathway. *Genes & development*, 26(13):1393–1408, July 2012.

[22] Laurence H Pearl, Amanda C Schierz, Simon E Ward, Bissan Al-Lazikani, and Frances M G Pearl. Therapeutic opportunities within the DNA damage response. *Nature reviews. Cancer*, 15(3):166–180, March 2015.

[23] Christopher J Lord and Alan Ashworth. The DNA damage response and cancer therapy. *Nature*, 481 (7381):287–294, January 2012.

[24] Nicola J Curtin. DNA repair dysregulation from cancer driver to therapeutic target. *Nature reviews. Cancer*, 12(12):801–817, December 2012.

[25] Mark J O'Connor. Targeting the DNA Damage Response in Cancer. *Molecular cell*, 60(4):547–560, November 2015.

[26] J H Hoeijmakers. DNA repair mechanisms. *Maturitas*, 38(1):17–22– discussion 22–3, February 2001.

[27] Michelle K Zeman and Karlene A Cimprich. Causes and consequences of replication stress. *Nature cell biology*, 16(1):2–9, January 2014.

[28] S Keeney and M J Neale. Initiation of meiotic recombination by formation of DNA double-strand breaks: mechanism and regulation. *Biochemical Society transactions*, 34(Pt 4):523–525, August 2006.

[29] Fabrícia Lima Fontes, Daniele Maria Lopes Pinheiro, Ana Helena Sales de Oliveira, Rayssa Karla de Medeiros Oliveira, Tirzah Braz Petta Lajus, and Lucymara Fassarella Agnez-Lima. Role of DNA repair in host immune response and inflammation. *Mutation research. Reviews in mutation research*, 763:246–257, January 2015.

[30] J Ross Chapman, Martin R G Taylor, and Simon J Boulton. Playing the end game: DNA double-strand break repair pathway choice. *Molecular cell*, 47(4):497–510, August 2012.

[31] Elizabeth M Kass and Maria Jasin. Collaboration and competition between DNA double-strand break repair pathways. *FEBS letters*, 584(17):3703–3708, September 2010.

[32] Alessandro A Sartori, Claudia Lukas, Julia Coates, Martin Mistrik, Shuang Fu, Jiri Bartek, Richard Baer, Jiri Lukas, and Stephen P Jackson. Human CtIP promotes DNA end resection. *Nature*, 450 (7169):509–514, November 2007.

[33] Lorraine S Symington and Jean Gautier. Double-strand break end resection and repair pathway choice. *Annual review of genetics*, 45:247–271, 2011.

[34] Yi Zhou, Pierre Caron, Gaëlle Legube, and Tanya T Paull. Quantitation of DNA double-strand break resection intermediates in human cells. *Nucleic acids research*, 42(3):e19, February 2014.

[35] Matthew L Nicolette, Kihoon Lee, Zhi Guo, Mridula Rani, Julia M Chow, Sang Eun Lee, and Tanya T Paull. Mre11-Rad50-Xrs2 and Sae2 promote 5' strand resection of DNA double-strand breaks. *Nature Structural & Molecular Biology*, 17(12):1478–1485, December 2010.

[36] Valerie Garcia, Sarah E L Phelps, Stephen Gray, and Matthew J Neale. Bidirectional resection of DNA double-strand breaks by Mre11 and Exo1. *Nature*, 479(7372):241–244, November 2011.

[37] Elda Cannavo and Petr Cejka. Sae2 promotes dsDNA endonuclease activity within Mre11-Rad50-Xrs2 to resect DNA breaks. *Nature*, 514(7520):122–125, October 2014.

[38] Tanya T Paull. Mechanisms of ATM Activation. *Annual review of biochemistry*, 84:711–738, 2015.

[39] Ellen Fanning, Vitaly Klimovich, and Andrew R Nager. A dynamic model for replication protein A (RPA) function in DNA processing pathways. *Nucleic acids research*, 34(15):4126–4137, 2006.

[40] M S Wold and T Kelly. Purification and characterization of replication protein A, a cellular protein required for in vitro replication of simian virus 40 DNA. *Proceedings of the National Academy of Sciences of the United States of America*, 85(8):2523–2527, April 1988.

[41] Shengqin Liu, Stephen O Opiyo, Karoline Manthey, Jason G Glanzer, Amanda K Ashley, Courtney Amerin, Kyle Troksa, Meena Shrivastav, Jac A Nickoloff, and Greg G Oakley. Distinct roles for DNA-PK, ATM and ATR in RPA phosphorylation and checkpoint activation in response to replication stress. *Nucleic acids research*, 40(21):10780–10794, November 2012.

[42] Madalena Tarsounas, Derek Davies, and Stephen C West. BRCA2-dependent and independent formation of RAD51 nuclear foci. *Oncogene*, 22(8):1115–1123, February 2003.

[43] Mary Ellen Moynahan and Maria Jasin. Mitotic homologous recombination maintains genomic stability and suppresses tumorigenesis. *Nature reviews. Molecular cell biology*, 11(3):196–207, March 2010.

[44] Dirk Remus, Fabienne Beuron, Gökhan Tolun, Jack D Griffith, Edward P Morris, and John F X Diffley. Concerted loading of Mcm2-7 double hexamers around DNA during DNA replication origin licensing. *Cell*, 139(4):719–730, November 2009.

[45] Dominik Boos, Jordi Frigola, and John F X Diffley. Activation of the replicative DNA helicase: breaking up is hard to do. *Current opinion in cell biology*, 24(3):423–430, June 2012.

[46] Ivar Ilves, Tatjana Petojevic, James J Pesavento, and Michael R Botchan. Activation of the MCM2-7 helicase by association with Cdc45 and GINS proteins. *Molecular cell*, 37(2):247–258, January 2010.

[47] M Shirayama, A Tóth, M Gálová, and K Nasmyth. APC(Cdc20) promotes exit from mitosis by destroying the anaphase inhibitor Pds1 and cyclin Clb5. *Nature*, 402(6758):203–207, November 1999.

[48] Anne-Sophie Boyer, David Walter, and Claus Storgaard Sørensen. DNA replication and cancer: From dysfunctional replication origin activities to therapeutic opportunities. *Seminars in cancer biology*, January 2016.

[49] Hisao Masai, Seiji Matsumoto, Zhiying You, Naoko Yoshizawa-Sugata, and Masako Oda. Eukaryotic chromosome DNA replication: where, when, and how? *Annual review of biochemistry*, 79:89–130, 2010.

[50] Abdelghani Mazouzi, Georgia Velimezi, and Joanna I Loizou. DNA replication stress: Causes, resolution and disease. *Experimental cell research*, 329(1):85–93, November 2014.

[51] Jacob Z Dalgaard. Causes and consequences of ribonucleotide incorporation into nuclear DNA. *Trends in genetics : TIG*, 28(12):592–597, December 2012.

[52] Matthew L Bochman, Katrin Paeschke, and Virginia A Zakian. DNA secondary structures: stability and function of G-quadruplex structures. *Nature reviews. Genetics*, 13(11):770–780, November 2012.

[53] Jérôme Poli, Olga Tsaponina, Laure Crabbé, Andrea Keszthelyi, Véronique Pantesco, Andrei Chabes, Armelle Lengronne, and Philippe Pasero. dNTP pools determine fork progression and origin usage under replication stress. *The EMBO journal*, 31(4):883–894, February 2012.

[54] Luis Ignacio Toledo, Matthias Altmeyer, Maj-Britt Rask, Claudia Lukas, Dorthe Helena Larsen, Lou Klitgaard Povlsen, Simon Bekker-Jensen, Niels Mailand, Jiri Bartek, and Jiri Lukas. ATR prohibits replication catastrophe by preventing global exhaustion of RPA. *Cell*, 155(5):1088–1103, November 2013.

[55] A Collins and D J Oates. Hydroxyurea: effects on deoxyribonucleotide pool sizes correlated with effects on DNA repair in mammalian cells. *European journal of biochemistry / FEBS*, 169(2):299–305, December 1987.

[56] Anne Helmrich, Monica Ballarino, Evgeny Nudler, and Laszlo Tora. Transcription-replication encounters, consequences and genomic instability. *Nature Structural & Molecular Biology*, 20(4):412–418, April 2013.

[57] Hocine W Mankouri, Diana Huttner, and Ian D Hickson. How unfinished business from S-phase affects mitosis and beyond. *The EMBO journal*, 32(20):2661–2671, October 2013.

[58] Indiana Magdalou, Bernard S Lopez, Philippe Pasero, and Sarah A E Lambert. The causes of replication stress and their consequences on genome stability and cell fate. *Seminars in cell & developmental biology*, 30:154–164, June 2014.

[59] Efrat Ozeri-Galai, Ronald Lebofsky, Ayelet Rahat, Assaf C Bester, Aaron Bensimon, and Batsheva Kerem. Failure of origin activation in response to fork stalling leads to chromosomal instability at fragile sites. *Molecular cell*, 43(1):122–131, July 2011.

[60] Valeria Naim, Therese Wilhelm, Michelle Debatisse, and Filippo Rosselli. ERCC1 and MUS81-EME1 promote sister chromatid separation by processing late replication intermediates at common fragile sites during mitosis. *Nature cell biology*, 15(8):1008–1015, August 2013.

[61] Thanos D Halazonetis, Vassilis G Gorgoulis, and Jiri Bartek. An oncogene-induced DNA damage model for cancer development. *Science (New York, N.Y.)*, 319(5868):1352–1355, March 2008.

[62] Seetha V Srinivasan, David Dominguez-Sola, Lily C Wang, Olivier Hyrien, and Jean Gautier. Cdc45 is a critical effector of myc-dependent DNA replication stress. *Cell reports*, 3(5):1629–1639, May 2013.

[63] R M Jones, O Mortusewicz, I Afzal, M Lorvellec, P García, T Helleday, and E Petermann. Increased replication initiation and conflicts with transcription underlie Cyclin E-induced replication stress. *Oncogene*, 32(32):3744–3753, August 2013.

[64] Tony S Byun, Marcin Pacek, Muh-ching Yee, Johannes C Walter, and Karlene A Cimprich. Functional uncoupling of MCM helicase and DNA polymerase activities activates the ATR-dependent checkpoint. *Genes & development*, 19(9):1040–1052, May 2005.

[65] Lee Zou and Stephen J Elledge. Sensing DNA damage through ATRIP recognition of RPA-ssDNA complexes. *Science (New York, N.Y.)*, 300(5625):1542–1548, June 2003.

[66] Christina A MacDougall, Tony S Byun, Christopher Van, Muh-ching Yee, and Karlene A Cimprich. The structural determinants of checkpoint activation. *Genes & development*, 21(8):898–903, April 2007.

[67] Karlene A Cimprich and David Cortez. ATR: an essential regulator of genome integrity. *Nature reviews. Molecular cell biology*, 9(8):616–627, August 2008.

[68] Luis I Toledo, Matilde Murga, and Oscar Fernandez-Capetillo. Targeting ATR and Chk1 kinases for cancer treatment: A new model for new (and old) drugs. *Molecular Oncology*, 5(4):368–373, August 2011.

[69] Andres J Lopez-Contreras and Oscar Fernandez-Capetillo. The ATR barrier to replication-born DNA damage. *DNA repair*, 9(12):1249–1255, December 2010.

[70] Kai J Neelsen and Massimo Lopes. Replication fork reversal in eukaryotes: from dead end to dynamic response. *Nature reviews. Molecular cell biology*, 16(4):207–220, April 2015.

[71] Csanád Z Bachrati and Ian D Hickson. RecQ helicases: guardian angels of the DNA replication fork. *Chromosoma*, 117(3):219–233, June 2008.

[72] Alberto Ciccia, Andrea L Bredemeyer, Mathew E Sowa, Marie-Emilie Terret, Prasad V Jallepalli, J Wade Harper, and Stephen J Elledge. The SIOD disorder protein SMARCAL1 is an RPA-interacting protein involved in replication fork restart. *Genes & development*, 23(20):2415–2425, October 2009.

[73] P Pichierri, A Franchitto, P Mosesso, and F Palitti. Werner's syndrome protein is required for correct recovery after replication arrest and DNA damage induced in S-phase of cell cycle. *Molecular biology of the cell*, 12(8):2412–2421, August 2001.

[74] Silvana Mourón, Sara Rodriguez-Acebes, María I Martínez-Jiménez, Sara García-Gómez, Sandra Chocrón, Luis Blanco, and Juan Mendez. Repriming of DNA synthesis at stalled replication forks by human PrimPol. *Nature Structural & Molecular Biology*, 20(12):1383–1389, December 2013.

[75] Kristina Trenz, Alessia Errico, and Vincenzo Costanzo. Plx1 is required for chromosomal DNA replication under stressful conditions. *The EMBO journal*, 27(6):876–885, March 2008.

[76] Saravanabhavan Thangavel, Matteo Berti, Maryna Levikova, Cosimo Pinto, Shivasankari Gomathinayagam, Marko Vujanovic, Ralph Zellweger, Hayley Moore, Eu Han Lee, Eric A Hendrickson, Petr Cejka, Sheila Stewart, Massimo Lopes, and Alessandro Vindigni. DNA2 drives processing and restart of reversed replication forks in human cells. *Journal of Cell Biology*, 208(5):545–562, March 2015.

[77] Alberto Ciccia, Neil McDonald, and Stephen C West. Structural and functional relationships of the XPF/MUS81 family of proteins. *Annual review of biochemistry*, 77:259–287, 2008.

[78] Katharina Schlacher, Nicole Christ, Nicolas Siaud, Akinori Egashira, Hong Wu, and Maria Jasin. Double-strand break repair-independent role for BRCA2 in blocking stalled replication fork degradation by MRE11. *Cell*, 145(4):529–542, May 2011.

[79] Martin R Higgs, John J Reynolds, Alicja Winczura, Andrew N Blackford, Valérie Borel, Edward S Miller, Anastasia Zlatanou, Jadwiga Nieminuszczy, Ellis L Ryan, Nicholas J Davies, Tatjana Stankovic, Simon J Boulton, Wojciech Niedzwiedz, and Grant S Stewart. BOD1L Is Required to Suppress Deleterious Resection of Stressed Replication Forks. *Molecular cell*, July 2015.

[80] José M Sogo, Massimo Lopes, and Marco Foiani. Fork reversal and ssDNA accumulation at stalled replication forks owing to checkpoint defects. *Science (New York, N.Y.)*, 297(5581):599–602, July 2002.

[81] Jiri Bartek, Claudia Lukas, and Jiri Lukas. Checking on DNA damage in S phase. *Nature reviews. Molecular cell biology*, 5(10):792–804, October 2004.

[82] Saed Mohebi, Ken'Ichi Mizuno, Adam Watson, Antony M Carr, and Johanne M Murray. Checkpoints are blind to replication restart and recombination intermediates that result in gross chromosomal rearrangements. *Nature communications*, 6:6357, 2015.

[83] Claudia Lukas, Velibor Savic, Simon Bekker-Jensen, Carsten Doil, Beate Neumann, Ronni Sølvhøj Pedersen, Merete Grøfte, Kok Lung Chan, Ian David Hickson, Jiri Bartek, and Jiri Lukas. 53BP1 nuclear bodies form around DNA lesions generated by mitotic transmission of chromosomes under replication stress. *Nature cell biology*, 13(3):243–253, March 2011.

[84] J A Harrigan, R Belotserkovskaya, J Coates, D S Dimitrova, S E Polo, C R Bradshaw, P Fraser, and S P Jackson. Replication stress induces 53BP1-containing OPT domains in G1 cells. *Journal of Cell Biology*, 193(1):97–108, April 2011.

[85] Songmin Ying, Sheroy Minocherhomji, Kok Lung Chan, Timea Palmai-Pallag, Wai Kit Chu, Theresa Wass, Hocine W Mankouri, Ying Liu, and Ian D Hickson. MUS81 promotes common fragile site expression. *Nature cell biology*, 15(8):1001–1007, August 2013.

[86] Karen Crasta, Neil J Ganem, Regina Dagher, Alexandra B Lantermann, Elena V Ivanova, Yunfeng Pan, Luigi Nezi, Alexei Protopopov, Dipanjan Chowdhury, and David Pellman. DNA breaks and chromosome pulverization from errors in mitosis. *Nature*, 482(7383):53–58, February 2012.

[87] Hélène Gaillard, Tatiana García-Muse, and Andrés Aguilera. Replication stress and cancer. *Nature reviews. Cancer*, 15(5):276–289, May 2015.

[88] Vassilis G Gorgoulis, Leandros-Vassilios F Vassiliou, Panagiotis Karakaidos, Panayotis Zacharatos, Athanassios Kotsinas, Triantafillos Liloglou, Monica Venere, Richard A Ditullio, Nikolaos G Kastrinakis, Brynn Levy, Dimitris Kletsas, Akihiro Yoneta, Meenhard Herlyn, Christos Kittas, and Thanos D Halazonetis. Activation of the DNA damage checkpoint and genomic instability in human precancerous lesions. *Nature*, 434(7035):907–913, April 2005.

[89] Jirina Bartkova, Zuzana Horejsí, Karen Koed, Alwin Krämer, Frederic Tort, Karsten Zieger, Per Guldberg, Maxwell Sehested, Jahn M Nesland, Claudia Lukas, Torben Ørntoft, Jiri Lukas, and Jiri Bartek. DNA damage response as a candidate anti-cancer barrier in early human tumorigenesis. *Nature*, 434 (7035):864–870, April 2005.

[90] Matthias Dobbelstein and Claus Storgaard Sørensen. Exploiting replicative stress to treat cancer. *Nature reviews. Drug discovery*, 14(6):405–423, June 2015.

[91] Therese Wilhelm, Indiana Magdalou, Aurélia Barascu, Hervé Técher, Michelle Debatisse, and Bernard S Lopez. Spontaneous slow replication fork progression elicits mitosis alterations in homologous recombination-deficient mammalian cells. *Proceedings of the National Academy of Sciences of the United States of America*, 111(2):763–768, January 2014.

[92] Katharina Schlacher, Hong Wu, and Maria Jasin. A distinct replication fork protection pathway connects Fanconi anemia tumor suppressors to RAD51-BRCA1/2. *Cancer cell*, 22(1):106–116, July 2012.

[93] Bianca M Sirbu, W Hayes McDonald, Huzefa Dungrawala, Akosua Badu-Nkansah, Gina M Kavanaugh, Yaoyi Chen, David L Tabb, and David Cortez. Identification of proteins at active, stalled, and collapsed replication forks using isolation of proteins on nascent DNA (iPOND) coupled with mass spectrometry. *The Journal of biological chemistry*, 288(44):31458–31467, November 2013.

[94] Eva Petermann, Manuel Luís Orta, Natalia Issaeva, Niklas Schultz, and Thomas Helleday. Hydroxyurea-stalled replication forks become progressively inactivated and require two different RAD51-mediated pathways for restart and repair. *Molecular cell*, 37(4):492–502, February 2010.

[95] Huzefa Dungrawala, Kristie L Rose, Kamakoti P Bhat, Kareem N Mohni, Gloria G Glick, Frank B Couch, and David Cortez. The Replication Checkpoint Prevents Two Types of Fork Collapse without Regulating Replisome Stability. *Molecular cell*, 59(6):998–1010, September 2015.

[96] Helen E Bryant, Eva Petermann, Niklas Schultz, Ann-Sofie Jemth, Olga Loseva, Natalia Issaeva, Fredrik Johansson, Serena Fernandez, Peter McGlynn, and Thomas Helleday. PARP is activated at stalled forks to mediate Mre11-dependent replication restart and recombination. *The EMBO journal*, 28(17):2601–2615, September 2009.

[97] U Schaeper, T Subramanian, L Lim, J M Boyd, and G Chinnadurai. Interaction between a cellular protein that binds to the C-terminal region of adenovirus E1A (CtBP) and a novel cellular protein is disrupted by E1A through a conserved PLDLS motif. *The Journal of biological chemistry*, 273(15): 8549–8552, April 1998.

[98] A K Wong, P A Ormonde, R Pero, Y Chen, L Lian, G Salada, S Berry, Q Lawrence, P Dayananth, P Ha, S V Tavtigian, D H Teng, and P L Bartel. Characterization of a carboxy-terminal BRCA1 interacting protein. *Oncogene*, 17(18):2279–2285, November 1998.

[99] C Fusco, A Reymond, and A S Zervos. Molecular cloning and characterization of a novel retinoblastoma-binding protein. *Genomics*, 51(3):351–358, August 1998.

[100] Phang-Lang Chen, Feng Liu, Suna Cai, Xiaoqin Lin, Aihua Li, Yumay Chen, Bingnan Gu, Eva Y-H P Lee, and Wen-Hwa Lee. Inactivation of CtIP leads to early embryonic lethality mediated by G1 restraint and to tumorigenesis by haploid insufficiency. *Molecular and cellular biology*, 25(9):3535–3542, May 2005.

[101] S Vilkki, V Launonen, A Karhu, P Sistonen, I Västrik, and L A Aaltonen. Screening for microsatellite instability target genes in colorectal cancers. *Journal of medical genetics*, 39(11):785–789, November 2002.

[102] Terry J Gaymes, Azim M Mohamedali, Miranda Patterson, Nazia Matto, Alexander Smith, Austin Kulasekararaj, Rajani Chelliah, Nicola Curtin, Farzin Farzaneh, Sydney Shall, and Ghulam J Mufti. Microsatellite instability induced mutations in DNA repair genes CtIP and MRE11 confer hypersensitivity to poly (ADP-ribose) polymerase inhibitors in myeloid malignancies. *Haematologica*, 98(9):1397–1406, September 2013.

[103] Isabel Soria-Bretones, Carmen Sáez, Manuel Ruíz-Borrego, Miguel A Japón, and Pablo Huertas. Prognostic value of CtIP/RBBP8 expression in breast cancer. *Cancer medicine*, 2(6):774–783, December 2013.

[104] Minhao Wu, David Ramos Soler, Martin C Abba, Maria I Nunez, Richard Baer, Christos Hatzis, Antonio Llombart-Cussac, Antonio Llombart-Bosch, and C Marcelo Aldaz. CtIP silencing as a novel mechanism of tamoxifen resistance in breast cancer. *Molecular cancer research : MCR*, 5(12):1285–1295, December 2007.

[105] Nodar Makharashvili and Tanya T Paull. CtIP: A DNA damage response protein at the intersection of DNA metabolism. *DNA repair*, May 2015.

[106] Irmgard Irminger-Finger, Magda Ratajska, and Maxim Pilyugin. New concepts on BARD1: Regulator of BRCA pathways and beyond. *The international journal of biochemistry & cell biology*, 72:1–17, December 2015.

[107] Eleni P Mimitou and Lorraine S Symington. DNA end resection–unraveling the tail. *DNA repair*, 10(3): 344–348, March 2011.

[108] Per Qvist, Pablo Huertas, Sonia Jimeno, Mette Nyegaard, Muhammad J Hassan, Stephen P Jackson, and Anders D Børglum. CtIP Mutations Cause Seckel and Jawad Syndromes. *PLoS Genetics*, 7(10): e1002310, October 2011.

[109] Zehra Agha, Zafar Iqbal, Maleeha Azam, Maimoona Siddique, Marjolein H Willemsen, Tjitske Kleefstra, Christiane Zweier, Nicole de Leeuw, Raheel Qamar, and Hans van Bokhoven. A complex microcephaly syndrome in a Pakistani family associated with a novel missense mutation in RBBP8 and a heterozygous deletion in NRXN1. *Gene*, 538(1):30–35, March 2014.

[110] Manu J Dubin, Philippa H Stokes, Eleanor Y M Sum, R Scott Williams, Valentina A Valova, Phillip J Robinson, Geoffrey J Lindeman, J N Mark Glover, Jane E Visvader, and Jacqueline M Matthews. Dimerization of CtIP, a BRCA1- and CtBP-interacting protein, is mediated by an N-terminal coiled-coil motif. *The Journal of biological chemistry*, 279(26):26932–26938, June 2004.

[111] Hailong Wang, Zhengping Shao, Linda Z Shi, Patty Yi-Hwa Hwang, Lan N Truong, Michael W Berns, David J Chen, and Xiaohua Wu. CtIP protein dimerization is critical for its recruitment to chromosomal DNA double-stranded breaks. *The Journal of biological chemistry*, 287(25):21471–21480, June 2012.

[112] Owen R Davies, Josep V Forment, Meidai Sun, Rimma Belotserkovskaya, Julia Coates, Yaron Galanty, Mukerrem Demir, Christopher R Morton, Neil J Rzechorzek, Stephen P Jackson, and Luca Pellegrini. CtIP tetramer assembly is required for DNA-end resection and repair. *Nature Structural & Molecular Biology*, 22(2):150–157, February 2015.

[113] Sara N Andres, C Denise Appel, James W Westmoreland, Jessica S Williams, Yvonne Nguyen, Patrick D Robertson, Michael A Resnick, and R Scott Williams. Tetrameric Ctp1 coordinates DNA binding and DNA bridging in DNA double-strand-break repair. *Nature Structural & Molecular Biology*, 22(2):158–166, February 2015.

[114] Hailong Wang, Linda Z Shi, Catherine C L Wong, Xuemei Han, Patty Yi-Hwa Hwang, Lan N Truong, Qingyuan Zhu, Zhengping Shao, David J Chen, Michael W Berns, John R Yates, Longchuan Chen, and Xiaohua Wu. The interaction of CtIP and Nbs1 connects CDK and ATM to regulate HR-mediated double-strand break repair. *PLoS Genetics*, 9(2):e1003277, 2013.

[115] Pablo Huertas, Felipe Cortés-Ledesma, Alessandro A Sartori, Andrés Aguilera, and Stephen P Jackson. CDK targets Sae2 to control DNA-end resection and homologous recombination. *Nature*, 455 (7213):689–692, October 2008.

[116] Nodar Makharashvili, Anthony T Tubbs, Soo-Hyun Yang, Hailong Wang, Olivia Barton, Yi Zhou, Rajashree A Deshpande, Ji-Hoon Lee, Markus Löbrich, Barry P Sleckman, Xiaohua Wu, and Tanya T Paull. Catalytic and noncatalytic roles of the CtIP endonuclease in double-strand break end resection. *Molecular cell*, 54(6):1022–1033, June 2014.

[117] Hailong Wang, Yongjiang Li, Lan N Truong, Linda Z Shi, Patty Yi-Hwa Hwang, Jing He, Johnny Do, Michael Jeffrey Cho, Hongzhi Li, Alejandro Negrete, Joseph Shiloach, Michael W Berns, Binghui Shen, Longchuan Chen, and Xiaohua Wu. CtIP Maintains Stability at Common Fragile Sites and Inverted Repeats by End Resection-Independent Endonuclease Activity. *Molecular cell*, 54(6):1012–1021, June 2014.

[118] Tomas Aparicio, Richard Baer, Max Gottesman, and Jean Gautier. MRN, CtIP, and BRCA1 mediate repair of topoisomerase II-DNA adducts. *Journal of Cell Biology*, 212(4):399–408, February 2016.

[119] Arne Nedergaard Kousholt, Kasper Fugger, Saskia Hoffmann, Brian D Larsen, Tobias Menzel, Alessandro A Sartori, and Claus Storgaard Sørensen. CtIP-dependent DNA resection is required for DNA damage checkpoint maintenance but not initiation. *Journal of Cell Biology*, 197(7):869–876, June 2012.

[120] Olga Murina, Christine von Aesch, Ufuk Karakus, Lorenza P Ferretti, Hella A Bolck, Kay Hänggi, and Alessandro A Sartori. FANCD2 and CtIP Cooperate to Repair DNA Interstrand Crosslinks. *Cell reports*, April 2014.

[121] Jung Eun Yeo, Eu Han Lee, Eric Hendrickson, and Alexandra Sobeck. CtIP mediates replication fork recovery in a FANCD2-regulated manner. *Human molecular genetics*, March 2014.

[122] Bingnan Gu and Phang-Lang Chen. Expression of PCNA-binding domain of CtIP, a motif required for CtIP localization at DNA replication foci, causes DNA damage and activation of DNA damage checkpoint. *Cell cycle (Georgetown, Tex.)*, 8(9):1409–1420, May 2009.

[123] Qinqin Jiang and Roger A Greenberg. Deciphering the BRCA1 Tumor Suppressor Network. *The Journal of biological chemistry*, June 2015.

[124] N Rahman and M R Stratton. The genetics of breast cancer susceptibility. *Annual review of genetics*, 32:95–121, 1998.

[125] Mary-Claire King, Joan H Marks, Jessica B Mandell, and New York Breast Cancer Study Group. Breast and ovarian cancer risks due to inherited mutations in BRCA1 and BRCA2. *Science (New York, N.Y.)*, 302(5645):643–646, October 2003.

[126] Synnöve Staff, Jorma Isola, and Minna Tanner. Haplo-insufficiency of BRCA1 in sporadic breast cancer. *Cancer Research*, 63(16):4978–4983, August 2003.

[127] Y Miki, J Swensen, D Shattuck-Eidens, P A Futreal, K Harshman, S Tavtigian, Q Liu, C Cochran, L M Bennett, and W Ding. A strong candidate for the breast and ovarian cancer susceptibility gene BRCA1. *Science (New York, N.Y.)*, 266(5182):66–71, October 1994.

[128] C Y Liu, A Flesken-Nikitin, S Li, Y Zeng, and W H Lee. Inactivation of the mouse Brca1 gene leads to failure in the morphogenesis of the egg cylinder in early postimplantation development. *Genes & development*, 10(14):1835–1843, July 1996.

[129] R Hakem, J L de la Pompa, C Sirard, R Mo, M Woo, A Hakem, A Wakeham, J Potter, A Reitmair, F Billia, E Firpo, C C Hui, J Roberts, J Rossant, and T W Mak. The tumor suppressor gene Brca1 is required for embryonic cellular proliferation in the mouse. *Cell*, 85(7):1009–1023, June 1996.

[130] S X Shen, Z Weaver, X Xu, C Li, M Weinstein, L Chen, X Y Guan, T Ried, and C X Deng. A targeted disruption of the murine Brca1 gene causes gamma-irradiation hypersensitivity and genetic instability. *Oncogene*, 17(24):3115–3124, December 1998.

[131] R Scully, S Ganesan, K Vlasakova, J Chen, M Socolovsky, and D M Livingston. Genetic analysis of BRCA1 function in a defined tumor cell line. *Molecular cell*, 4(6):1093–1099, December 1999.

[132] M E Moynahan, T Y Cui, and M Jasin. Homology-directed dna repair, mitomycin-c resistance, and chromosome stability is restored with correction of a Brca1 mutation. *Cancer Research*, 61(12):4842–4850, June 2001.

[133] B Xu, Kim St, and M B Kastan. Involvement of Brca1 in S-phase and G(2)-phase checkpoints after ionizing irradiation. *Molecular and cellular biology*, 21(10):3445–3450, May 2001.

[134] X Xu, Z Weaver, S P Linke, C Li, J Gotay, X W Wang, C C Harris, T Ried, and C X Deng. Centrosome amplification and a defective G2-M cell cycle checkpoint induce genetic instability in BRCA1 exon 11 isoform-deficient cells. *Molecular cell*, 3(3):389–395, March 1999.

[135] A Bhattacharyya, U S Ear, B H Koller, R R Weichselbaum, and D K Bishop. The breast cancer susceptibility gene BRCA1 is required for subnuclear assembly of Rad51 and survival following treatment with the DNA cross-linking agent cisplatin. *The Journal of biological chemistry*, 275(31):23899–23903, August 2000.

[136] R Scully, J Chen, A Plug, Y Xiao, D Weaver, J Feunteun, T Ashley, and D M Livingston. Association of BRCA1 with Rad51 in mitotic and meiotic cells. *Cell*, 88(2):265–275, January 1997.

[137] R Scully, J Chen, R L Ochs, K Keegan, M Hoekstra, J Feunteun, and D M Livingston. Dynamic changes of BRCA1 subnuclear location and phosphorylation state are initiated by DNA damage. *Cell*, 90(3):425–435, August 1997.

[138] M E Moynahan, J W Chiu, B H Koller, and M Jasin. Brca1 controls homology-directed DNA repair. *Molecular cell*, 4(4):511–518, October 1999.

[139] Liu Cao, Xioaling Xu, Samuel F Bunting, Jie Liu, Rui-Hong Wang, Longyue L Cao, J Julie Wu, Tie-Nan Peng, Junjie Chen, André Nussenzweig, Chu-Xia Deng, and Toren Finkel. A selective requirement for 53BP1 in the biological response to genomic instability induced by Brca1 deficiency. *Molecular cell*, 35(4):534–541, August 2009.

[140] Samuel F Bunting, Elsa Callen, Nancy Wong, Hua-Tang Chen, Federica Polato, Amanda Gunn, Anne Bothmer, Niklas Feldhahn, Oscar Fernandez-Capetillo, Liu Cao, Xiaoling Xu, Chu-Xia Deng, Toren Finkel, Michel Nussenzweig, Jeremy M Stark, and André Nussenzweig. 53BP1 inhibits homologous recombination in Brca1-deficient cells by blocking resection of DNA breaks. *Cell*, 141(2):243–254, April 2010.

[141] Peter Bouwman, Amal Aly, Jose M Escandell, Mark Pieterse, Jirina Bartkova, Hanneke van der Gulden, Sanne Hiddingh, Maria Thanasoula, Atul Kulkarni, Qifeng Yang, Bruce G Haffty, Johanna Tommiska, Carl Blomqvist, Ronny Drapkin, David J Adams, Heli Nevanlinna, Jiri Bartek, Madalena Tarsounas, Shridar Ganesan, and Jos Jonkers. 53BP1 loss rescues BRCA1 deficiency and is associated with triple-negative and BRCA-mutated breast cancers. *Nature Structural & Molecular Biology*, 17(6):688–695, June 2010.

[142] Stephanie Panier and Simon J Boulton. Double-strand break repair: 53BP1 comes into focus. *Nature reviews. Molecular cell biology*, 15(1):7–18, January 2014.

[143] L C Wu, Z W Wang, J T Tsan, M A Spillman, A Phung, X L Xu, M C Yang, L Y Hwang, A M Bowcock, and R Baer. Identification of a RING protein that can interact in vivo with the BRCA1 gene product. *Nature genetics*, 14(4):430–440, December 1996.

[144] Marsha Laufer, Subhadra V Nandula, Ami P Modi, Shuang Wang, Maria Jasin, Vundavalli V V S Murty, Thomas Ludwig, and Richard Baer. Structural requirements for the BARD1 tumor suppressor in chromosomal stability and homology-directed DNA repair. *The Journal of biological chemistry*, 282 (47):34325–34333, November 2007.

[145] Ulrica K Westermark, Marsha Reyngold, Adam B Olshen, Richard Baer, Maria Jasin, and Mary Ellen Moynahan. BARD1 participates with BRCA1 in homology-directed repair of chromosome breaks. *Molecular and cellular biology*, 23(21):7926–7936, November 2003.

[146] J E Meza, P S Brzovic, M C King, and R E Klevit. Mapping the functional domains of BRCA1. Interaction of the ring finger domains of BRCA1 and BARD1. *The Journal of biological chemistry*, 274 (9):5659–5665, February 1999.

[147] R Hashizume, M Fukuda, I Maeda, H Nishikawa, D Oyake, Y Yabuki, H Ogata, and T Ohta. The RING heterodimer BRCA1-BARD1 is a ubiquitin ligase inactivated by a breast cancer-derived mutation. *The Journal of biological chemistry*, 276(18):14537–14540, May 2001.

[148] Joanna R Morris and Ellen Solomon. BRCA1 : BARD1 induces the formation of conjugated ubiquitin structures, dependent on K6 of ubiquitin, in cells during DNA replication and repair. *Human molecular genetics*, 13(8):807–817, April 2004.

[149] Xiaochun Yu, Shuang Fu, Maoyi Lai, Richard Baer, and Junjie Chen. BRCA1 ubiquitinates its phosphorylation-dependent binding partner CtIP. *Genes & development*, 20(13):1721–1726, July 2006.

[150] Lea M Starita, Andrew A Horwitz, Michael-Christopher Keogh, Chikashi Ishioka, Jeffrey D Parvin, and Natsuko Chiba. BRCA1/BARD1 ubiquitinate phosphorylated RNA polymerase II. *The Journal of biological chemistry*, 280(26):24498–24505, July 2005.

[151] Angus Chen, Frida E Kleiman, James L Manley, Toru Ouchi, and Zhen-Qiang Pan. Autoubiquitination of the BRCA1*BARD1 RING ubiquitin ligase. *The Journal of biological chemistry*, 277(24):22085–22092, June 2002.

[152] Ko Sato, Ryosuke Hayami, Wenwen Wu, Toru Nishikawa, Hiroyuki Nishikawa, Yoshiko Okuda, Haruki Ogata, Mamoru Fukuda, and Tomohiko Ohta. Nucleophosmin/B23 is a candidate substrate for the BRCA1-BARD1 ubiquitin ligase. *The Journal of biological chemistry*, 279(30):30919–30922, July 2004.

[153] Lea M Starita, Yuka Machida, Satish Sankaran, Joshua E Elias, Karen Griffin, Brian P Schlegel, Steven P Gygi, and Jeffrey D Parvin. BRCA1-dependent ubiquitination of gamma-tubulin regulates centrosome number. *Molecular and cellular biology*, 24(19):8457–8466, October 2004.

[154] Stephan Ryser, Eva Dizin, Charles Edward Jefford, Bénédicte Delaval, Sarantis Gagos, Agni Christodoulidou, Karl-Heinz Krause, Daniel Birnbaum, and Irmgard Irminger-Finger. Distinct roles of BARD1 isoforms in mitosis: full-length BARD1 mediates Aurora B degradation, cancer-associated BARD1beta scaffolds Aurora B and BRCA2. *Cancer Research*, 69(3):1125–1134, February 2009.

[155] Mo Li and Xiaochun Yu. Function of BRCA1 in the DNA damage response is mediated by ADP-ribosylation. *Cancer cell*, 23(5):693–704, May 2013.

[156] Wenwen Wu, Hiroyuki Nishikawa, Takayo Fukuda, Vinayak Vittal, Masahide Asano, Yasuo Miyoshi, Rachel E Klevit, and Tomohiko Ohta. Interaction of BARD1 and HP1 Is Required for BRCA1 Retention at Sites of DNA Damage. *Cancer Research*, 75(7):1311–1321, April 2015.

[157] V Joukov, J Chen, E A Fox, J B Green, and D M Livingston. Functional communication between endogenous BRCA1 and its partner, BARD1, during Xenopus laevis development. *Proceedings of the National Academy of Sciences of the United States of America*, 98(21):12078–12083, October 2001.

[158] Reena Shakya, Matthias Szabolcs, Ellen McCarthy, Elson Ospina, Katia Basso, Subhadra Nandula, Vundavalli Murty, Richard Baer, and Thomas Ludwig. The basal-like mammary carcinomas induced by Brca1 or Bard1 inactivation implicate the BRCA1/BARD1 heterodimer in tumor suppression. *Proceedings of the National Academy of Sciences of the United States of America*, 105(19):7040–7045, May 2008.

[159] Chiara Ghimenti, Elisa Sensi, Silvano Presciuttini, Isa Maura Brunetti, PierFranco Conte, Generoso Bevilacqua, and Maria A Caligo. Germline mutations of the BRCA1-associated ring domain (BARD1) gene in breast and breast/ovarian families negative for BRCA1 and BRCA2 alterations. *Genes, chromosomes & cancer*, 33(3):235–242, March 2002.

[160] T H Thai, F Du, J T Tsan, Y Jin, A Phung, M A Spillman, H F Massa, C Y Muller, R Ashfaq, J M Mathis, D S Miller, B J Trask, R Baer, and A M Bowcock. Mutations in the BRCA1-associated RING domain (BARD1) gene in primary breast, ovarian and uterine cancers. *Human molecular genetics*, 7 (2):195–202, February 1998.

[161] J Chen and W A Weiss. Alternative splicing in cancer: implications for biology and therapy. *Oncogene*, January 2014.

[162] S De Brakeleer, J De Grève, R Loris, and N Janin. Cancer predisposing missense and protein truncating BARD1 mutations in non-BRCA1 or BRCA2 breast cancer families - De Brakeleer - 2010 - Human Mutation - Wiley Online Library. *. . . mutation*, 2010.

[163] Lin Li, Stephan Ryser, Eva Dizin, Dietmar Pils, Michael Krainer, Charles Edward Jefford, Francesco Bertoni, Robert Zeillinger, and Irmgard Irminger-Finger. Oncogenic BARD1 isoforms expressed in gynecological cancers. *Cancer Research*, 67(24):11876–11885, December 2007.

[164] Judith C Sporn, Torsten Hothorn, and Barbara Jung. BARD1 expression predicts outcome in colon cancer. *Clinical cancer research : an official journal of the American Association for Cancer Research*, 17(16):5451–5462, August 2011.

[165] I Irminger-Finger, W C Leung, J Li, M Dubois-Dauphin, J Harb, A Feki, C E Jefford, J V Soriano, M Jaconi, R Montesano, and K H Krause. Identification of BARD1 as mediator between proapoptotic stress and p53-dependent apoptosis. *Molecular cell*, 8(6):1255–1266, December 2001.

[166] Anis Feki, Charles Edward Jefford, Philip Berardi, Jian-Yu Wu, Laetitia Cartier, Karl-Heinz Krause, and Irmgard Irminger-Finger. BARD1 induces apoptosis by catalysing phosphorylation of p53 by DNA-damage response kinase. *Oncogene*, 24(23):3726–3736, May 2005.

[167] F E Kleiman and J L Manley. Functional interaction of BRCA1-associated BARD1 with polyadenylation factor CstF-50. *Science (New York, N.Y.)*, 285(5433):1576–1579, September 1999.

[168] F E Kleiman and J L Manley. The BARD1-CstF-50 interaction links mRNA 3' end formation to DNA damage and tumor suppression. *Cell*, 104(5):743–753, March 2001.

[169] Reena Shakya, Latarsha J Reid, Colleen R Reczek, Francesca Cole, Dieter Egli, Chyuan-Sheng Lin, Dirk G deRooij, Steffen Hirsch, Kandasamy Ravi, James B Hicks, Matthias Szabolcs, Maria Jasin, Richard Baer, and Thomas Ludwig. BRCA1 tumor suppression depends on BRCT phosphoprotein binding, but not its E3 ligase activity. *Science (New York, N.Y.)*, 334(6055):525–528, October 2011.

[170] X Yu, L C Wu, A M Bowcock, A Aronheim, and R Baer. The C-terminal (BRCT) domains of BRCA1 interact in vivo with CtIP, a protein implicated in the CtBP pathway of transcriptional repression. *The Journal of biological chemistry*, 273(39):25388–25392, September 1998.

[171] Xiaochun Yu and Junjie Chen. DNA damage-induced cell cycle checkpoint control requires CtIP, a phosphorylation-dependent binding partner of BRCA1 C-terminal domains. *Molecular and cellular biology*, 24(21):9478–9486, November 2004.

[172] Longchuan Chen, Christian J Nievera, Alan Yueh-Luen Lee, and Xiaohua Wu. Cell cycle-dependent complex formation of BRCA1.CtIP.MRN is important for DNA double-strand break repair. *The Journal of biological chemistry*, 283(12):7713–7720, March 2008.

[173] Maximina H Yun and Kevin Hiom. CtIP-BRCA1 modulates the choice of DNA double-strand-break repair pathway throughout the cell cycle. *Nature*, 459(7245):460–463, May 2009.

[174] J N Snouwaert, L C Gowen, A M Latour, A R Mohn, A Xiao, L DiBiase, and B H Koller. BRCA1 deficient embryonic stem cells display a decreased homologous recombination frequency and an increased frequency of non-homologous recombination that is corrected by expression of a brca1 transgene. *Oncogene*, 18(55):7900–7907, December 1999.

[175] Kyoko Nakamura, Toshiaki Kogame, Hiroyuki Oshiumi, Akira Shinohara, Yoshiki Sumitomo, Keli Agama, Yves Pommier, Kimiko M Tsutsui, Ken Tsutsui, Edgar Hartsuiker, Tomoo Ogi, Shunichi Takeda, and Yoshihito Taniguchi. Collaborative action of Brca1 and CtIP in elimination of covalent modifications from double-strand breaks to facilitate subsequent break repair. *PLoS Genetics*, 6(1): e1000828, January 2010.

[176] Colleen R Reczek, Matthias Szabolcs, Jeremy M Stark, Thomas Ludwig, and Richard Baer. The interaction between CtIP and BRCA1 is not essential for resection-mediated DNA repair or tumor suppression. *Journal of Cell Biology*, 201(5):693–707, May 2013.

[177] Federica Polato, Elsa Callen, Nancy Wong, Robert Faryabi, Samuel Bunting, Hua-Tang Chen, Marina Kozak, Michael J Kruhlak, Colleen R Reczek, Wen-Hwa Lee, Thomas Ludwig, Richard Baer, Lionel Feigenbaum, Stephen Jackson, and André Nussenzweig. CtIP-mediated resection is essential for viability and can operate independently of BRCA1. *The Journal of experimental medicine*, May 2014.

[178] Andrés Cruz-García, Ana López-Saavedra, and Pablo Huertas. BRCA1 accelerates CtIP-mediated DNA-end resection. *Cell reports*, 9(2):451–459, October 2014.

[179] Cristina Escribano-Díaz, Alexandre Orthwein, Amélie Fradet-Turcotte, Mengtan Xing, Jordan T F Young, Ján Tkáč, Michael A Cook, Adam P Rosebrock, Meagan Munro, Marella D Canny, Dongyi Xu, and Daniel Durocher. A cell cycle-dependent regulatory circuit composed of 53BP1-RIF1 and BRCA1-CtIP controls DNA repair pathway choice. *Molecular cell*, 49(5):872–883, March 2013.

[180] J Chen, D P Silver, D Walpita, S B Cantor, A F Gazdar, G Tomlinson, F J Couch, B L Weber, T Ashley, D M Livingston, and R Scully. Stable interaction between the products of the BRCA1 and BRCA2 tumor suppressor genes in mitotic and meiotic cells. *Molecular cell*, 2(3):317–328, September 1998.

[181] David T Long, Vladimir Joukov, Magda Budzowska, and Johannes C Walter. BRCA1 promotes unloading of the CMG helicase from a stalled DNA replication fork. *Molecular cell*, 56(1):174–185, October 2014.

[182] Samuel F Bunting, Elsa Callen, Marina L Kozak, Jung Min Kim, Nancy Wong, Andres J Lopez-Contreras, Thomas Ludwig, Richard Baer, Robert B Faryabi, Amy Malhowski, Hua-Tang Chen, Oscar Fernandez-Capetillo, Alan D'Andrea, and André Nussenzweig. BRCA1 functions independently of homologous recombination in DNA interstrand crosslink repair. *Molecular cell*, 46(2):125–135, April 2012.

[183] Nicholas A Willis, Gurushankar Chandramouly, Bin Huang, Amy Kwok, Cindy Follonier, Chuxia Deng, and Ralph Scully. BRCA1 controls homologous recombination at Tus/Ter-stalled mammalian replication forks. *Nature*, 510(7506):556–559, June 2014.

[184] Shailja Pathania, Sangeeta Bade, Morwenna Le Guillou, Karly Burke, Rachel Reed, Christian Bowman-Colin, Ying Su, David T Ting, Kornelia Polyak, Andrea L Richardson, Jean Feunteun, Judy E Garber, and David M Livingston. BRCA1 haploinsufficiency for replication stress suppression in primary cells. *Nature communications*, 5:5496, 2014.

[185] Nuala McCabe, Nicholas C Turner, Christopher J Lord, Katarzyna Kluzek, Aneta Bialkowska, Sally Swift, Sabrina Giavara, Mark J O'Connor, Andrew N Tutt, Małgorzata Z Zdzienicka, Graeme C M Smith, and Alan Ashworth. Deficiency in the repair of DNA damage by homologous recombination and sensitivity to poly(ADP-ribose) polymerase inhibition. *Cancer Research*, 66(16):8109–8115, August 2006.

[186] Sourav Bandyopadhyay, Monika Mehta, Dwight Kuo, Min-Kyung Sung, Ryan Chuang, Eric J Jaehnig, Bernd Bodenmiller, Katherine Licon, Wilbert Copeland, Michael Shales, Dorothea Fiedler, Janusz Dutkowski, Aude Guénolé, Haico van Attikum, Kevan M Shokat, Richard D Kolodner, Won-Ki Huh, Ruedi Aebersold, Michael-Christopher Keogh, Nevan J Krogan, and Trey Ideker. Rewiring of genetic networks in response to DNA damage. *Science (New York, N.Y.)*, 330(6009):1385–1389, December 2010.

[187] Aude Guénolé, Rohith Srivas, Kees Vreeken, Ze Zhong Wang, Shuyi Wang, Nevan J Krogan, Trey Ideker, and Haico van Attikum. Dissection of DNA damage responses using multiconditional genetic interaction maps. *Molecular cell*, 49(2):346–358, January 2013.

[188] Michael C Bassik, Martin Kampmann, Robert Jan Lebbink, Shuyi Wang, Marco Y Hein, Ina Poser, Jimena Weibezahn, Max A Horlbeck, Siyuan Chen, Matthias Mann, Anthony A Hyman, Emily M Leproust, Michael T McManus, and Jonathan S Weissman. A systematic mammalian genetic interaction map reveals pathways underlying ricin susceptibility. *Cell*, 152(4):909–922, February 2013.

[189] Sean R Collins, Maya Schuldiner, Nevan J Krogan, and Jonathan S Weissman. A strategy for extracting and analyzing large-scale quantitative epistatic interaction data. *Genome biology*, 7(7):R63, 2006.

[190] William G Kaelin. The Concept of Synthetic Lethality in the Context of Anticancer Therapy. *Nature reviews. Cancer*, 5(9):689–698, August 2005.

[191] Assen Roguev, Dale Talbot, Gian Luca Negri, Michael Shales, Gerard Cagney, Sourav Bandyopadhyay, Barbara Panning, and Nevan J Krogan. Quantitative genetic-interaction mapping in mammalian cells. *Nature methods*, 10(5):432–437, February 2013.

[192] Christopher J Lord, Andrew N J Tutt, and Alan Ashworth. Synthetic lethality and cancer therapy: lessons learned from the development of PARP inhibitors. *Annual review of medicine*, 66:455–470, 2015.

[193] Hannah Farmer, Nuala McCabe, Christopher J Lord, Andrew N J Tutt, Damian A Johnson, Tobias B Richardson, Manuela Santarosa, Krystyna J Dillon, Ian Hickson, Charlotte Knights, Niall M B Martin, Stephen P Jackson, Graeme C M Smith, and Alan Ashworth. Targeting the DNA repair defect in BRCA mutant cells as a therapeutic strategy. *Nature*, 434(7035):917–921, April 2005.

[194] Helen E Bryant, Niklas Schultz, Huw D Thomas, Kayan M Parker, Dan Flower, Elena Lopez, Suzanne Kyle, Mark Meuth, Nicola J Curtin, and Thomas Helleday. Specific killing of BRCA2-deficient tumours with inhibitors of poly(ADP-ribose) polymerase. *Nature*, 434(7035):913–917, April 2005.

[195] Andrew Tutt, Mark Robson, Judy E Garber, Susan M Domchek, M William Audeh, Jeffrey N Weitzel, Michael Friedlander, Banu Arun, Niklas Loman, Rita K Schmutzler, Andrew Wardley, Gillian Mitchell, Helena Earl, Mark Wickens, and James Carmichael. Oral poly(ADP-ribose) polymerase inhibitor olaparib in patients with BRCA1 or BRCA2 mutations and advanced breast cancer: a proof-of-concept trial. *The Lancet*, 376(9737):235–244, July 2010.

[196] M William Audeh, James Carmichael, Richard T Penson, Michael Friedlander, Bethan Powell, Katherine M Bell-McGuinn, Clare Scott, Jeffrey N Weitzel, Ana Oaknin, Niklas Loman, Karen Lu, Rita K Schmutzler, Ursula Matulonis, Mark Wickens, and Andrew Tutt. Oral poly(ADP-ribose) polymerase inhibitor olaparib in patients with BRCA1 or BRCA2 mutations and recurrent ovarian cancer: a proof-of-concept trial. *The Lancet*, 376(9737):245–251, July 2010.

[197] Christina Laufer, Bernd Fischer, Maximilian Billmann, Wolfgang Huber, and Michael Boutros. Mapping genetic interactions in human cancer cells with RNAi and multiparametric phenotyping. *Nature methods*, April 2013.

[198] Sandra Morandell, H Christian Reinhardt, Ian G Cannell, Jacob S Kim, Daniela M Ruf, Tanya Mitra, Anthony D Couvillon, Tyler Jacks, and Michael B Yaffe. A reversible gene-targeting strategy identifies synthetic lethal interactions between MK2 and p53 in the DNA damage response in vivo. *Cell reports*, 5(4):868–877, November 2013.

[199] Brooke M Emerling, Jonathan B Hurov, George Poulogiannis, Kazumi S Tsukazawa, Rayman Choo-Wing, Gerburg M Wulf, Eric L Bell, Hye-Seok Shim, Katja A Lamia, Lucia E Rameh, Gary Bellinger, Atsuo T Sasaki, John M Asara, Xin Yuan, Andrea Bullock, Gina M Denicola, Jiaxi Song, Victoria Brown, Sabina Signoretti, and Lewis C Cantley. Depletion of a putatively druggable class of phosphatidylinositol kinases inhibits growth of p53-null tumors. *Cell*, 155(4):844–857, November 2013.

[200] Philip M Reaper, Matthew R Griffiths, Joanna M Long, Jean-Damien Charrier, Somhairle MacCormick, Peter A Charlton, Julian M C Golec, and John R Pollard. Selective killing of ATM- or p53-deficient cancer cells through inhibition of ATR. *Nature chemical biology*, 7(7):428–430, July 2011.

[201] S Origanti, S-r Cai, A Z Munir, L S White, and H Piwnica-Worms. Synthetic lethality of Chk1 inhibition combined with p53 and/or p21 loss during a DNA damage response in normal and tumor cells. *Oncogene*, 32(5):577–588, January 2013.

[202] Elda Grabocka, Yuliya Pylayeva-Gupta, Mathew J K Jones, Veronica Lubkov, Eyoel Yemanaberhan, Laura Taylor, Hao Hsuan Jeng, and Dafna Bar-Sagi. Wild-type H- and N-Ras promote mutant K-Ras-driven tumorigenesis by modulating the DNA damage response. *Cancer cell*, 25(2):243–256, February 2014.

[203] Tracy M Neher, Diane Bodenmiller, Richard W Fitch, Shadia I Jalal, and John J Turchi. Novel irreversible small molecule inhibitors of replication protein A display single-agent activity and synergize with cisplatin. *Molecular cancer therapeutics*, 10(10):1796–1806, October 2011.

[204] Brian Budke, Jay H Kalin, Michal Pawlowski, Anna S Zelivianskaia, Megan Wu, Alan P Kozikowski, and Philip P Connell. An optimized RAD51 inhibitor that disrupts homologous recombination without requiring Michael acceptor reactivity. *Journal of medicinal chemistry*, 56(1):254–263, January 2013.

[205] Lorenzo Lafranchi, Harmen R de Boer, Elisabeth G E de Vries, Shao-En Ong, Alessandro A Sartori, and Marcel A T M van Vugt. APC/C(Cdh1) controls CtIP stability during the cell cycle and in response to DNA damage. *The EMBO journal*, 33(23):2860–2879, December 2014.

[206] Ivan M Munoz, Piotr Szyniarowski, Rachel Toth, John Rouse, and Christophe Lachaud. Improved genome editing in human cell lines using the CRISPR method. *PloS one*, 9(10):e109752, 2014.

[207] Anne E Carpenter, Thouis R Jones, Michael R Lamprecht, Colin Clarke, In Han Kang, Ola Friman, David A Guertin, Joo Han Chang, Robert A Lindquist, Jason Moffat, Polina Golland, and David M Sabatini. CellProfiler: image analysis software for identifying and quantifying cell phenotypes. *Genome biology*, 7(10):R100, 2006.

[208] Xiaohua Douglas Zhang. A pair of new statistical parameters for quality control in RNA interference high-throughput screening assays. *Genomics*, 89(4):552–561, April 2007.

[209] Renate König, Chih-yuan Chiang, Buu P Tu, S Frank Yan, Paul D DeJesus, Angelica Romero, Tobias Bergauer, Anthony Orth, Ute Krueger, Yingyao Zhou, and Sumit K Chanda. A probability-based approach for the analysis of large-scale RNAi screens. *Nature methods*, 4(10):847–849, October 2007.

[210] Andrea Franceschini, Damian Szklarczyk, Sune Frankild, Michael Kuhn, Milan Simonovic, Alexander Roth, Jianyi Lin, Pablo Minguez, Peer Bork, Christian von Mering, and Lars J Jensen. STRING v9.1: protein-protein interaction networks, with increased coverage and integration. *Nucleic acids research*, 41(Database issue):D808–15, January 2013.

[211] Da Wei Huang, Brad T Sherman, and Richard A Lempicki. Systematic and integrative analysis of large gene lists using DAVID bioinformatics resources. *Nature protocols*, 4(1):44–57, 2009.

[212] Javier Peña-Diaz, Stephanie Bregenhorn, Medini Ghodgaonkar, Cindy Follonier, Mariela Artola-Borán, Dennis Castor, Massimo Lopes, Alessandro A Sartori, and Josef Jiricny. Noncanonical mismatch repair as a source of genomic instability in human cells. *Molecular cell*, 47(5):669–680, September 2012.

[213] Wassim Eid, Martin Steger, Mahmoud El-Shemerly, Lorenza P Ferretti, Javier Peña-Diaz, Christiane König, Emanuele Valtorta, Alessandro A Sartori, and Stefano Ferrari. DNA end resection by CtIP and exonuclease 1 prevents genomic instability. *EMBO reports*, 11(12):962–968, December 2010.

[214] Johannes Schindelin, Ignacio Arganda-Carreras, Erwin Frise, Verena Kaynig, Mark Longair, Tobias Pietzsch, Stephan Preibisch, Curtis Rueden, Stephan Saalfeld, Benjamin Schmid, Jean-Yves Tinevez, Daniel James White, Volker Hartenstein, Kevin Eliceiri, Pavel Tomancak, and Albert Cardona. Fiji: an open-source platform for biological-image analysis. *Nature methods*, 9(7):676–682, July 2012.

[215] Josep V Forment and Stephen P Jackson. A flow cytometry-based method to simplify the analysis and quantification of protein association to chromatin in mammalian cells. *Nature protocols*, 10(9): 1297–1307, September 2015.

[216] Halfdan Beck, Viola Nähse, Marie Sofie Yoo Larsen, Petra Groth, Trevor Clancy, Michael Lees, Mette Jørgensen, Thomas Helleday, Randi G Syljuåsen, and Claus Storgaard Sørensen. Regulators of cyclin-dependent kinases are crucial for maintaining genome integrity in S phase. *Journal of Cell Biology*, 188(5):629–638, March 2010.

[217] Shane Marine, Amit Bahl, Marc Ferrer, and Eugen Buehler. Common seed analysis to identify off-target effects in siRNA screens. *Journal of biomolecular screening*, 17(3):370–378, March 2012.

[218] Daniel R Caffrey, Juan Zhao, Zhili Song, Michael E Schaffer, Steven A Haney, Romesh R Subramanian, Albert B Seymour, and Jason D Hughes. siRNA off-target effects can be reduced at concentrations that match their individual potency. *PloS one*, 6(7):e21503, 2011.

[219] Roger Meier, Andrea Franceschini, Peter Horvath, Marilou Tetard, Roberta Mancini, Christian von Mering, Ari Helenius, and Pierre-Yves Lozach. Genome-wide small interfering RNA screens reveal VAMP3 as a novel host factor required for Uukuniemi virus late penetration. *Journal of virology*, 88 (15):8565–8578, August 2014.

[220] R Murr, T Vaissière, C Sawan, V Shukla, and Z Herceg. Orchestration of chromatin-based processes: mind the TRRAP. *Oncogene*, 26(37):5358–5372, August 2007.

[221] George-Lucian Moldovan, Boris Pfander, and Stefan Jentsch. PCNA, the maestro of the replication fork. *Cell*, 129(4):665–679, May 2007.

[222] Fei Ye, Joshua A Bauer, Jennifer A Pietenpol, and Yu Shyr. Analysis of high-throughput RNAi screening data in identifying genes mediating sensitivity to chemotherapeutic drugs: statistical approaches and perspectives. *BMC genomics*, 13 Suppl 8:S3, 2012.

[223] Brenda C O'Connell, Britt Adamson, John R Lydeard, Mathew E Sowa, Alberto Ciccia, Andrea L Bredemeyer, Michael Schlabach, Steven P Gygi, Stephen J Elledge, and J Wade Harper. A genome-wide camptothecin sensitivity screen identifies a mammalian MMS22L-NFKBIL2 complex required for genomic stability. *Molecular cell*, 40(4):645–657, November 2010.

[224] Vincent Guacci, Jeremiah Stricklin, Michelle S Bloom, Xuánzōng Guō, Meghna Bhatter, and Douglas Koshland. A novel mechanism for the establishment of sister chromatid cohesion by the ECO1 acetyltransferase. *Molecular biology of the cell*, 26(1):117–133, January 2015.

[225] Akari Yoshimura, Masayuki Seki, Tomoko Hayashi, Yumiko Kusa, Shusuke Tada, Yutaka Ishii, and Takemi Enomoto. Functional relationships between Rad18 and WRNIP1 in vertebrate cells. *Biological & pharmaceutical bulletin*, 29(11):2192–2196, November 2006.

[226] Fumitoshi Onoda, Masahiro Takeda, Masayuki Seki, Daisuke Maeda, Jun-ichi Tajima, Ayako Ui, Hideki Yagi, and Takemi Enomoto. SMC6 is required for MMS-induced interchromosomal and sister chromatid recombinations in Saccharomyces cerevisiae. *DNA repair*, 3(4):429–439, April 2004.

[227] Ryan Kelley and Trey Ideker. Systematic interpretation of genetic interactions using protein networks. *Nature biotechnology*, 23(5):561–566, May 2005.

[228] Michael Costanzo, Anastasia Baryshnikova, Chad L Myers, Brenda Andrews, and Charles Boone. Charting the genetic interaction map of a cell. *Current opinion in biotechnology*, 22(1):66–74, February 2011.

[229] Andrei Zinovyev, Inna Kuperstein, Emmanuel Barillot, and Wolf-Dietrich Heyer. Synthetic Lethality between Gene Defects Affecting a Single Non-essential Molecular Pathway with Reversible Steps. *PLoS computational biology*, 9(4):e1003016, April 2013.

[230] Joanna R Morris, Nicholas H Keep, and Ellen Solomon. Identification of residues required for the interaction of BARD1 with BRCA1. *The Journal of biological chemistry*, 277(11):9382–9386, March 2002.

[231] Sandra G Durkin and Thomas W Glover. Chromosome Fragile Sites. *dx.doi.org*, 2007.

[232] Andrew N Blackford, Rebekka A Schwab, Jadwiga Nieminuszczy, Andrew J Deans, Stephen C West, and Wojciech Niedzwiedz. The DNA translocase activity of FANCM protects stalled replication forks. *Human molecular genetics*, 21(9):2005–2016, May 2012.

[233] J R Savage. Classification and relationships of induced chromosomal structual changes. *Journal of medical genetics*, 13(2):103–122, April 1976.

[234] Frank B Couch, Carol E Bansbach, Robert Driscoll, Jessica W Luzwick, Gloria G Glick, Rémy Bétous, Clinton M Carroll, Sung Yun Jung, Jun Qin, Karlene A Cimprich, and David Cortez. ATR phosphorylates SMARCAL1 to prevent replication fork collapse. *Genes & development*, 27(14):1610–1623, July 2013.

[235] Martin Steger, Olga Murina, Daniela Hühn, Lorenza P Ferretti, Reto Walser, Kay Hänggi, Lorenzo Lafranchi, Christine Neugebauer, Shreya Paliwal, Pavel Janscak, Bertran Gerrits, Giannino Del Sal, Oliver Zerbe, and Alessandro A Sartori. Prolyl isomerase PIN1 regulates DNA double-strand break repair by counteracting DNA end resection. *Molecular cell*, 50(3):333–343, May 2013.

[236] E Raderschall, E I Golub, and T Haaf. Nuclear foci of mammalian recombination proteins are located at single-stranded DNA regions formed after DNA damage. *Proceedings of the National Academy of Sciences of the United States of America*, 96(5):1921–1926, March 1999.

[237] Josep V Forment, Rachael V Walker, and Stephen P Jackson. A high-throughput, flow cytometry-based method to quantify DNA-end resection in mammalian cells. *Cytometry. Part A : the journal of the International Society for Analytical Cytology*, 81(10):922–928, October 2012.

[238] Kenneth K Karanja, Eu Han Lee, Eric A Hendrickson, and Judith L Campbell. Preventing over-resection by DNA2 helicase/nuclease suppresses repair defects in Fanconi anemia cells. *Cell cycle (Georgetown, Tex.)*, 13(10):1540–1550, 2014.

[239] Raphael Ceccaldi, Jessica C Liu, Ravindra Amunugama, Ildiko Hajdu, Benjamin Primack, Mark I R Petalcorin, Kevin W O'Connor, Panagiotis A Konstantinopoulos, Stephen J Elledge, Simon J Boulton, Timur Yusufzai, and Alan D D'Andrea. Homologous-recombination-deficient tumours are dependent on Polθ-mediated repair. *Nature*, 518(7538):258–262, February 2015.

[240] Ellen E McCarthy, Julide T Celebi, Richard Baer, and Thomas Ludwig. Loss of Bard1, the heterodimeric partner of the Brca1 tumor suppressor, results in early embryonic lethality and chromosomal instability. *Molecular and cellular biology*, 23(14):5056–5063, July 2003.

[241] Valeria Naim and Filippo Rosselli. The FANC pathway and BLM collaborate during mitosis to prevent micro-nucleation and chromosome abnormalities. *Nature cell biology*, 11(6):761–768, June 2009.

[242] V Ashutosh Rao, Chiara Conti, Josee Guirouilh-Barbat, Asako Nakamura, Ze-Hong Miao, Sally L Davies, Barbara Saccá, Ian D Hickson, Aaron Bensimon, and Yves Pommier. Endogenous gamma-H2AX-ATM-Chk2 checkpoint activation in Bloom's syndrome helicase deficient cells is related to DNA replication arrested forks. *Molecular cancer research : MCR*, 5(7):713–724, July 2007.

[243] Anne Bothmer, Davide F Robbiani, Niklas Feldhahn, Anna Gazumyan, André Nussenzweig, and Michel C Nussenzweig. 53BP1 regulates DNA resection and the choice between classical and alternative end joining during class switch recombination. *The Journal of experimental medicine*, 207 (4):855–865, April 2010.

[244] Diane R Hoffelder, Li Luo, Nancy A Burke, Simon C Watkins, Susanne M Gollin, and William S Saunders. Resolution of anaphase bridges in cancer cells. *Chromosoma*, 112(8):389–397, June 2004.

[245] Jiri J Bartek, Jiri J Lukas, and Jirina J Bartkova. DNA damage response as an anti-cancer barrier: damage threshold and the concept of 'conditional haploinsufficiency'. *Audio, Transactions of the IRE Professional Group on*, 6(19):2344–2347, September 2007.

Acknowledgments

First, I would like to express my gratitude to Prof. Alessandro A. Sartori for giving me the opportunity to do my PhD in his laboratory, for providing me with exciting possibilities and the chance to develop as a scientist and for the support throughout my PhD as well as for my future plans.
Furthermore, I want to thank all present and past members of the Sartori laboratory for their scientific input but also for their readiness to cooperate and help out, for the great working atmosphere and for their friendship. I am particularly grateful to Sara, Christina, Kay, Adrian and Chrigi who contributed significantly to my work.

I would like to acknowledge Reihaneh Zarizzi and Prof. Claus Sørensen for the PFGE experiments, Dr. Simon Nørrelykke for image analysis, Dr. Antonio Porro for assistance with analysing chromosomal aberrations and Jonas Schmid for technical assistance with the DNA fiber assay. Moreover, I would like to express my gratitude to Prof. Richard Baer and Prof. Xiaochun Yun as well as to all PIs of the research groups in the IMCR for sharing reagents.
In addition, I want to acknowledge the support of the present and past members of the RNAi Screening and Image Analysis facility (ScopeM) at ETH Zürich who contributed to my project, particularly in developing, conducting and analysing the RNAi screens. Most of all, I would like to thank Dr. Roger Meier for his efforts during the screen data analysis.
I would also like to sincerely thank my thesis committee members Prof. Anne Müller, Prof. Orlando Schärer and Dr. Thomas Marti for critical discussions and insightful comments and for their thoughtful advice.
I consider myself very fortunate having had the opportunity to work at the IMCR during

my PhD. I want to thank everyone for creating a great and welcoming atmosphere and for their willingness to help and collaborate. Particularly, I am grateful to Farah, Odete, the technicians and Danielle for providing the infrastructure that has allowed me to focus almost exclusively on my work. I also want to thank Prof. Josef Jiricny for running the IMCR and for all his efforts to make it a wonderful place to work at.

Furthermore, I want to thank my friends, particularly Melanie, Anja, Maria, Sabine and Emilia who have shared many good moments with me during the PhD. The biggest thank you for an enormous amount of encouragement and help goes to Mike. It made the PhD a really great time spending it with you.

I am most thankful to my wonderful family, who have at no moment ever ceased to support, encourage and impress me.

Appendix

Curriculum Vitae

Hella Anna Bolck

Date of birth: 18.09.1985
Place of origin: Berlin (Germany)
Nationality: German

Education and Research Experience

Since Sept. 2011 **Ph.D. in Cancer Biology**

Cancer Biology PhD Program, Life Science Zürich Graduate School, University of Zürich; Switzerland

PhD thesis reseach in the laboratory of Prof. A. A. Sartori, Institute of Molecular Cancer Research

PhD thesis title: A Novel Connection between CtIP and BRCA1/BARD1 Emerges through Functional RNAi Screening.

Oct. 2005 - Aug. 2011 **Diplom in Biochemistry and Molecular Biology.**

Friedrich-Schiller-University Jena; Germany

Diplom thesis research in the laboratory of Prof. T. Heinzel, Center for Molecular Biomedicine

Diplom thesis title: The combinatorial treatment with the HDACi LBH589 and TKis induces apoptosis in acute myeloid leukemia.

Aug. 2008 – Jun. 2009 **Visiting graduate student**

Biochemistry and Molecular Biology PhD program, Michigan State University; USA

Graduate Research Assistant in the laboratory of Prof. R. W. Henry, Department of Biochemistry and Molecular Biology

Project title: The interaction of the pRB tumorsuppressor protein with apoptotic-, cell cycle- and small nuclear RNA genes.

Jun. 2005 **Abitur (Matura)**

Rosa-Luxemburg-Oberschule (Gymnasium), Berlin; Germany

Related Professional Experience

Feb. 2014 - Dec. 2015	**PhD student representative** Cancer Biology PhD program Zürich; Switzerland
Oct. 2014 - Jun. 2015	**Supervision of a master student** Laboratory of Prof. A. A. Sartori
Sept. 2013 – Dec. 2013	**Supervision of a semester student** Laboratory of Prof. A. A. Sartori
Apr. 2011 and May 2012	**Teaching assistant** Practical block course "Genome Instability and Molecular Cancer Research" for Master students, University of Zurich
Dec. 2011	**Teaching assistant** Laboratory course "Classical and Molecular Genetics" for Bachelor students, University of Zurich

Presentations at Scientific Conferences

Sep. 2015	**3rd Swiss Image-Based Screening conference** Novartis, Basel; Switzerland, (Poster presentation)
Mar. 2015	**Keystone Symposia meeting on Genomic Instability and DNA Repair** Whistler; Canada, (Poster presentation)
Jan. 2015	**12th Charles Rodolphe Brupbacher Symposium** Breakthroughs in Cancer Research and Therapy, Zürich; Switzerland (Poster presentation)
Oct. 2013	**2nd Swiss Image-Based Screening conference** EPFL, Lausanne; Switzerland (Poster presentation)
Mar. 2013	**EMBO Practical Course: High-throughput RNAi and data analysis** EMBL, Heidelberg; Germany (Poster presentation)
May 2012	**1st Swiss Meeting on Genome Stability and Chromatin Dynamics** Weggis; Switzerland (Poster presentation)

Awards, Scholarships and Research Grants

Jan. 2015	**Young Investigators Award** – Charles Rodolphe Brupbacher Foundation for Cancer Research, Zürich; Switzerland
Jan. 2015	**Translational Cancer Research Grant** – University Research Priority Programs (URPP) of the University of Zürich; Switzerland
Jan. 2015	**Cancer Network Zürich Travel Grant** – for Keystone Symposium
Mar. 2015	**Travel Grant** – Hartmann Müller-Stiftung für medizinische Forschung for Keystone Symposium
Feb. 2014	**Best Talk Award** – Cancer Biology PhD Student Retreat

Publications

in preparation	**Bolck HA**, Przetocka S, Meier R, Walker C, Hänggi K, von Aesch C, Zarrizi R, Horvath P, F. Nørrelykke S, Stebler M, Thalmann A, Porro A, S. Sørensen C, Sartori AA. *CtIP and BRCA1/BARD1 cooperate to promote faithful DNA replication.*
May 2014 Cell Reports	Murina O, von Aesch C, Karakus U, Ferretti LP, **Bolck HA**, Hänggi K, Sartori AA. *FANCD2 and CtIP cooperate to repair DNA interstrand crosslinks.*
Jul. 2013 Swiss Med Wkly	Hühn D*, **Bolck HA*** (*both authors contributed equally to this work), Sartori AA. *Targeting DNA double-strand break signalling and repair: recent advances in cancer therapy. (Review)*
Aug. 2012 Mol. Cancer Ther.	Pietschmann K*, **Bolck HA*** (*both authors contributed equally to this work), Buchwald M, Spielberg S, Polzer H, Spiekermann K, Bug G, Heinzel T, Böhmer FD, Kraemer OH. *Breakdown of the FLT3-ITD/STAT5 axis and synergistic apoptosis induction by the histone deacetylase inhibitor Panobinostat and FLT3-specific inhibitors.*
Apr. 2009 Biochim. Biophys. Acta	Kuo M-H, Xu X-J, **Bolck HA**, Guo D. *Functional connection between histone acetyltransferase Gcn5p and methyltransferase Hmt1p.*

Targeting DNA double-strand break signalling and repair: recent advances in cancer therapy

Daniela Hühn, **Hella A. Bolck**, Alessandro A. Sartori

Review article published in Swiss Medical Weekly, 2013.

Together with Daniela Hühn and Alessandro A. Sartori I conceived and wrote the article. I generated the figures for this Review.

Established in 1871
Swiss Medical Weekly
Formerly: Schweizerische Medizinische Wochenschrift
The European Journal of Medical Sciences

Review article: Medical intelligence | Published 29 July 2013, doi:10.4414/smw.2013.13837
Cite this as: Swiss Med Wkly. 2013;143:w13837

Targeting DNA double-strand break signalling and repair: recent advances in cancer therapy

Daniela Hühn, Hella A. Bolck, Alessandro A. Sartori

Institute of Molecular Cancer Research, University of Zurich, Switzerland

Abstract

Genomic instability, a hallmark of almost all human cancers, drives both carcinogenesis and resistance to therapeutic interventions. Pivotal to the ability of a cell to maintain genome integrity are mechanisms that signal and repair deoxyribonucleic acid (DNA) double-strand breaks (DSBs), one of the most deleterious lesions induced by ionising radiation and various DNA-damaging chemicals. On the other hand, many current therapeutic regimens that effectively kill cancer cells are based on the induction of excessive DSBs. However, these drugs often lack selectivity for tumour cells, which results in severe side effects for the patients, thus compromising their therapeutic potential. Therefore, the development of novel tumour-specific treatment strategies is required.

Unlike normal cells, however, cancer cells are often characterised by abnormalities in the DNA damage response including defects in cell cycle checkpoints and/or DNA repair, rendering them particularly sensitive to the induction of DSBs. Therefore, new anticancer agents designed to exploit these vulnerabilities are becoming promising drugs for enhancing the specificity and efficacy of future cancer therapies. Here, we summarise the latest preclinical and clinical developments in cancer therapy based on the current knowledge of DSB signalling and repair, with a special focus on the combination of small molecule inhibitors with synthetic lethality approaches.

Key words: *genomic instability; DNA damage response; DNA repair; cancer therapy; small molecule inhibitors; synthetic lethality*

Introduction

Cancer is the major cause of death in Switzerland among people aged 45–84 years [1]. The latest Swiss cancer statistics indicate that prostate cancer in men and breast cancer in women are the most common types, with 6,000 and 5,500 incidences per year, respectively. Notably, lung cancer is still the leading cause of cancer-related death in the Swiss population, accounting for approximately 3,000 deaths each year [2].

Almost all human cancers are characterised by genomic instability, which is considered to play a key role in the conversion of a normal cell into a premalignant cell [3]. Mechanisms contributing to genomic instability include aberrant repair of deoxyribonucleic acid (DNA) lesions as well as defective signalling to cell-cycle checkpoints and induction of apoptosis. Damaging agents, emanating from endogenous and environmental sources such as oxidative stress and ultraviolet (UV) radiation, constantly challenge the integrity of DNA. Remarkably, spontaneous DNA damage, mostly hydrolytic cytosine deamination and oxidative DNA base damage, occurs at a rate of up to 10^5 lesions per cell per day [4, 5].

In order to counteract these insults and preserve genome stability, cells activate a coordinated signal-transduction network, which is collectively known as the DNA damage response (DDR). Generally, this response consists of a series of events such as detection of the DNA damage by sensors, accumulation of repair factors by mediators and repair of the lesion by effectors [6]. Cells are equipped with a variety of distinct, but partially compensatory, DNA repair mechanisms, each addressing a specific type of lesion [5]. DNA double-strand breaks (DSBs) are considered to be the most hazardous lesions, since a single unrepaired DSB may trigger cell death whereas a misrepaired DSB potentially results in mutations such as chromosomal rearrangements, which can promote carcinogenesis. Therefore, activation of cell-cycle checkpoints and faithful repair in response to DSBs are a primary barrier to malignant transformation.

The fact that DSBs are highly cytotoxic is exploited in conventional cancer treatment with radiation therapy and certain chemotherapeutic drugs such as DNA crosslinkers and topoisomerase inhibitors. Although those agents induce DSBs in all cells, hyperproliferating cancer cells are much more susceptible to killing than normal cells. However, most of these well-established treatments cause a number of adverse effects, mainly by affecting the fast-dividing cells of the patient, such as haematopoietic stem cells, hair follicles and cells lining the stomach and intestines. Therefore, novel strategies to treat cancer are eagerly anticipated and the subject of extensive research.

In this review, we summarise how DSB repair and its genetic interactions have emerged as targets for improved cancer treatment strategies in the recent past. We also highlight the current knowledge of small molecule inhibitors

(SMIs) of DSB signalling and repair factors, which are promising candidates for clinical use. For a comprehensive overview of targeting DDR pathways for cancer therapy, we direct the reader to recently published reviews [7–9].

DNA damage response

The DDR is a multifaceted signalling network, which is elicited upon detection of DNA lesions in order to coordinate the cell cycle, DNA repair and possibly senescence or apoptosis (fig. 1). Three members of the phosphatidylinositol-3-kinase (PI3K) related kinases (PIKKs) – ATM (ataxia telangiectasia mutated), ATR (ATM- and Rad3-related) and DNA-PKcs (DNA-dependent protein kinase catalytic subunit) – become activated upon DNA damage to trigger the DDR [10]. Through a cascade of phosphorylation events, ATM and ATR activate multiple proteins, most notably p53 and the downstream checkpoint kinases CHK1 and CHK2, which in turn phosphorylate WEE1 kinase and CDC25 phosphatases. Consequently, through regulating the activity of cyclin-dependent kinases (CDKs), the progression from one cell cycle phase to another is delayed [11]. Depending on which CDK is inhibited; the cell cycle is arrested either at the G1/S or the G2/M transition. The resulting cell-cycle arrest allows time for repair, thereby preventing genome duplication or cell division in the presence of damaged DNA. Thus, cells with an abrogated DDR generally display an increased sensitivity towards DNA-damaging agents.

DNA repair pathways

Depending on the type of DNA damage, cells invoke specific DNA repair pathways in order to restore the genetic information (see fig. 1). Briefly, minor changes to DNA such as oxidised or alkylated bases, small base adducts and single-strand breaks (SSBs) are restored by the base excision repair (BER) pathway [4]. A key player in this process is poly-adenosine-diphosphate-ribose (PAR) polymerase (PARP). Upon detection of SSBs, PARP covalently transfers PAR chains to itself and to acceptor proteins in the vicinity of the lesion, thereby facilitating the repair of SSBs. More complex, DNA helix-distorting base lesions, such as those induced by UV light, are repaired by nucleotide excision repair (NER) [5]. Another kind of damage disturbing the helical structure of DNA is represented by base mismatches. Mismatch repair factors recognise and process misincorporated nucleotides as well as insertion or deletion loops that arise during recombination or from errors of DNA polymerases [12]. Covalent links between the two strands of the double helix represent a type of DNA damage referred to as interstrand crosslinks (ICLs). ICLs represent the most deleterious lesions produced by chemotherapeutic agents such as mitomycin C (MMC), cisplatin and cyclophosphamide. ICL repair is complex and involves the collaboration of several repair pathways, namely Fanconi anaemia, NER, translesion synthesis and homologous recombination (HR) [13].

DNA double-strand break repair

Thus far, four mechanistically distinct DSB repair mechanisms in mammalian cells have been described: nonhomologous end joining (NHEJ), alternative-NHEJ, single-strand annealing and HR [14]. NHEJ and HR represent the two major DSB repair pathways, with NHEJ operating throughout the cell cycle and HR being most active during S-phase (fig. 2) [15]. NHEJ starts with the binding of the Ku70/80 heterodimer to both ends of the break, followed by the recruitment of the catalytic subunit of DNA-dependent protein kinase (DNA-PKcs). Subsequent phosphorylation events mediated by the DNA-PK holoenzyme lead to appropriate DNA end processing by the Artemis nuclease. DSB repair by NHEJ is completed by rejoining of the ends

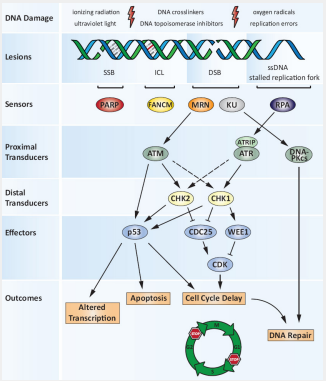

Figure 1

The DNA damage response.

Exogenous and endogenous DNA damaging agents generate various types of lesions including DNA single- and double-strand breaks (SSBs and DSBs). The multifunctional MRN complex detects DSBs, while FANCM is required for the DNA interstrand crosslink (ICL)-induced checkpoint response. PARP predominantly acts as a SSB sensor protein. RPA binds to regions of single-stranded DNA (ssDNA) that are exposed at stalled replication forks or after DSB resection. MRN and RPA mediate the recruitment of ATM and ATR-ATRIP, respectively, and the subsequent activation of the respective pathways, coordinating cell-cycle checkpoints, DNA repair and apoptotic responses to DNA damage. The Ku70/Ku80 heterodimer (KU) competes with MRN for binding to DSBs. KU recruits DNA-PKcs to form the catalytically active DNA-PK holoenzyme which is a major component of the canonical NHEJ machinery during DSB repair. MRN on the other hand initiates HR (see also fig. 2). Once activated, the DNA damage signalling cascade extends through multiple phosphorylation events primarily via the cell-cycle checkpoint kinases CHK1 and CHK2. Their signals converge on downstream effectors such as the tumour suppressor protein p53 or the CDC25 protein phosphatase and WEE1 tyrosine kinase. As a result, CDK activity is inhibited, delaying cell cycle progression from G1 to S (the G1/S checkpoint) or from G2 to M phase (the G2/M checkpoint). The DNA damage response (DDR) thus orchestrates a variety of cellular outcomes: the transcriptional programme of the damaged cell is altered and the cell cycle is transiently arrested, thereby facilitating repair of the DNA lesions. In situations where DNA damage is too severe and cannot be repaired, the DDR triggers apoptosis or senescence.

ADP = adenosine diphosphate; ATM = ataxia telangiectasia mutated protein; ATR = ATM- and Rad3-related; ATRIP = ATR-interacting protein; CDK = cyclin-dependeant kinase; DNA = deoxyribonucleic acid; DNA-PK = DNA-dependeant protein kinase; DNA-PKcs = DNA-PK catalytic subunit; FANCM = Fanconi anaemia complementation group M; HR = homologous recombination; ICL = interstrand crosslink; MRN = MRE11-RAD50-NBS1 complex; NEHJ = nonhomologous end joining; PARP = poly(ADP-ribose) polymerase; RPA = replication protein A

catalysed by a complex consisting of X-ray repair cross-complementing protein 4 (XRCC4), XRCC4-like factor (XLF) and DNA ligase IV. HR takes over if NHEJ is unsuccessful in ligating the broken DNA ends or when the DSB is first recognised by the MRE11-RAD50-NBS1 (MRN) complex rather than by Ku70/80 [16]. Together with CtBP-interacting protein (CtIP; CtBP = C-terminal binding protein), MRN resects DSBs to generate short 3'-single-stranded-DNA (ssDNA) tails that get immediately coated with replication protein A (RPA) [17]. The BRCA2-PALB2 complex promotes RAD51 nucleation onto ssDNA, thereby replacing RPA. The RAD51 nucleoprotein filament then invades the homologous, intact DNA template forming a displacement loop. The second end of the broken chromosome is captured and anneals to the complementary strand of the donor DNA molecule, resulting in the formation of two Holliday junctions (HJs). After DNA synthesis and ligation of both strands, the double HJ is either dissolved or is dismantled by the catalytic action of resolvases in order to complete repair [18]. Thus, repair by HR is error-free since it copies the missing genetic information from the undamaged sister chromatid, whereas NHEJ is error-prone since DNA ends without sequence homology are religated with the risk of causing mutations [19]. Given that a single unrepaired DSB has the potential to kill a cell, inhibition of repair by compounds that target factors involved in NHEJ or HR will increase the sensitivity of cancer cells to DSB-inducing anticancer agents.

Harnessing DNA damage signalling and repair for cancer therapy

The fact that cells with a compromised DDR are hypersensitive to DNA damage-inducing agents is currently under vigorous investigation for use in targeted cancer therapy. More precisely, during their pathogenesis, many cancer cells acquire defects in a certain DNA repair pathway and become dependent on a compensatory mechanism in order to survive. Hence, pharmacological inhibition of the "backup" pathway in combination with DNA damage will selectively kill cancer cells but spare their normal counterparts. Furthermore, highly proliferative cancer cells are inherently hypersensitive to DNA damage because S-phase, in which DNA replication takes place, is the most vulnerable period of the cell cycle.

Targeting DSB signalling pathways

As previously mentioned, cell-cycle checkpoint activation in response to DSBs gives a cell time for DNA repair before entry into S-phase or mitosis. Consequently, cell-cycle checkpoints reduce the efficacy of DNA-damaging agents used in cancer therapy. Therefore, selective abrogation of checkpoint signalling sensitises cancer cells to chemo- and radio-therapy, potentiating cancer treatment [20]. Importantly, more than 50% of human tumours are defective in p53 tumour suppressor function and cell-cycle checkpoint inhibitors have been demonstrated particularly to sensitise p53-deficient cancer cells to various anticancer agents in clinical use [21].

In the late 1960s, long before the discovery of cell-cycle checkpoints, the first attempts to sensitise cancer cells to standard cytotoxic therapy were made using ordinary compounds such as caffeine [22]. Later it was found that caffeine directly binds to and inhibits ATM and ATR *in vitro* and thus interferes with initiation of the DDR [23, 24]. However, since caffeine is a relatively nonselective agent, efforts have been made to develop more potent and selective inhibitors of the PIKK family members ATM, ATR and DNA-PKcs (table 1). In 2004, KuDOS Pharmaceuticals (now AstraZeneca) reported the identification of KU-55933, a specific SMI of ATM [25]. On the molecular level, KU-55933, like most kinase inhibitors, competes with the ATP-binding site of the enzyme, thereby inhibiting the catalytic activity of ATM [26]. Based on the promising preclinical results, KU-60019, a KU-55933 analogue with

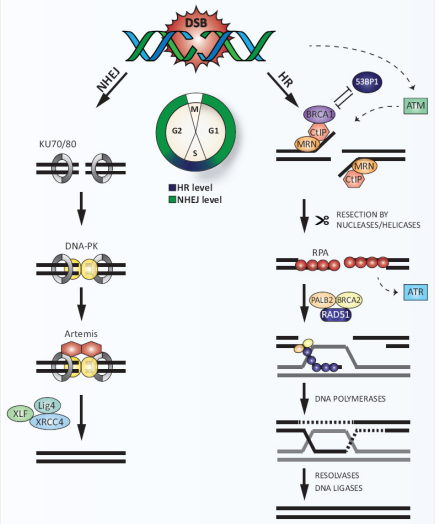

Figure 2

DNA double-strand break (DSB) repair.

DSBs are predominantly repaired by two distinct pathways: NHEJ or HR. NHEJ operates throughout the cell cycle, but mainly during the G1 and G2 phases, whereas HR peaks in S phase. Rapid association of the Ku70/80 heterodimer to DSBs promotes NHEJ by recruiting DNA-PKcs. DNA ends are processed by the nucleolytic activity of Artemis, followed by religation catalysed by a complex of XLF, Ligase IV (Lig4) and XRCC4. Alternatively, MRN, which is initially recruited to DSBs in competition with Ku70/80, initiates DSB resection together with CtIP thereby promoting HR. 53BP1 antagonises BRCA1 in DSB resection. Extensive DSB resection by other nucleases and formation of RPA-coated ssDNA stimulates the activation of ATR. Displacement of RPA by RAD51 is mediated by BRCA2 and PALB2, resulting in the formation of RAD51 nucleoprotein filaments. Subsequent strand invasion into the homologous DNA template and capturing of the second DNA end leads to the formation of a double Holliday junction, which is processed by resolvases. Finally, the DNA is sealed by ligases to accomplish error-free repair of the DSB.

53BP = p53 binding protein; ATM = ataxia telangiectasia mutated protein; CtBP = C-terminal binding protein; CtIP = CtBP-interacting protein; DNA = deoxyribonucleic acid; DNA-PK = DNA-dependent protein kinase; DNA-PKcs = DNA-PK catalytic subunit; HR = homologous recombination; MRN = MRE11-RAD50-NBS1 complex; NHEJ = nonhomologous end joining; PALB1/2 = partner and localiser of BRCA1/2; RPA = replication protein A; ssDNA = single-stranded DNA; XLF = XRCC4-like factor; XRCC4 = X-ray repair cross-complementing protein 4

improved pharmacokinetics and bioavailability, was synthesised and shown to radiosensitise glioma cells approximately 10 times more efficiently than KU-55933 [27]. Compounds selectively targeting ATR have long been awaited, particularly when inhibitors of CHK1, a direct downstream target of ATR, had proven to be clinically effective [28]. Finally, in 2011, three ATR inhibitors, NU-6027, VE-821 and ETP-46464 were described. NU-6027 is a pyrimidine analogue originally discovered as an adenosine triphosphate (ATP) competitive inhibitor of CDKs, but recently reported also to inhibit ATR at low micromolar concentrations and to confer cisplatin cytotoxicity independently of CDK inhibition [29, 30]. The ATR inhibitor VE-821 (Vertex Pharmaceuticals) was identified using a high-throughput screen against full-length recombinant ATR [31]. Preclinical testing of VE-821 using pancreatic cancer cells demonstrated its chemo- and radiosensitisation properties [32]. ETP-46464 was discovered by screening compounds with a previously reported activity against the related PI3Ks using a cell-based system assaying for ATR activity [33]. In the same study, NVP-BEZ235, a recognised dual PI3K/mTOR inhibitor (mTOR = mammalian target of rapamycin), was also reported to block efficiently ATM, ATR and DNA-PK activity. Furthermore, NVP-BEZ235 was found to act as a radio- and chemo-sensitiser in various cancer cell lines and is currently being tested as a single agent in various Phase I/II clinical trials [34, 35]. Importantly, most, if not all, of the aforementioned compounds are likely to inhibit additional protein kinases, especially when used at concentrations in the high micromolar range, thus potentially exhibiting "off-target" effects.

Downstream of ATM and ATR act the two transducer kinases CHK1 and CHK2, against which several inhibitors have emerged during recent years. One of the first SMIs, UCN-01, a derivative of staurosporine, was originally isolated from a *Streptomyces* strain as a protein kinase antagonist with cytotoxic effects [36]. UCN-01 was later shown to be a potent inhibitor of CHK1 and to block its kinase activity by interacting with the ATP-binding pocket [37, 38]. Six Phase II clinical trials of UCN-01, either as a single agent or in combination with other drugs, in patients with different types of advanced cancer have already been completed. Recently, three novel CHK1 inhibitors, GDC-0425 (Genentech Inc.), SCH900776 (now renamed MK-8776, Merck) and LY-2606368 (Eli Lilly), have entered Phase I clinical trials either as single agents or in combination with gemcitabine, a nucleoside analogue [39]. Another promising drug that interferes with checkpoint activation is the WEE1 tyrosine kinase inhibitor MK-1775 (Merck), which was discovered by screening a chemical library [40]. MK-1775 is already under investigation in a Phase II trial combined with carboplatin in order to assess the benefit for patients with p53-mutated epithelial ovarian cancer. Last but not least, efforts to target CDC25 phosphatases, which also represent key molecules in checkpoint regulation, led to the discovery of several CDC25 inhibitors, amongst which the most potent are quinonoid-based derivatives such as the bis-quinone compound IRC-08386 [41, 42].

In summary, several SMIs that interfere with checkpoint activation show great promise of advancing in clinical studies and eventually being used as chemo- or radio-sensitisers as well as monotherapeutic agents in cancer treatment. Nevertheless, since many of the SMIs have only very recently been discovered, their safety, tolerability and efficacy when used alone or in combination has to be further investigated.

Targeting DSB repair

Impairing the repair of DSBs using drugs that either inhibit the enzymatic activity or interfere with protein-protein interactions of repair factors provides another approach to sensitising cancer cells for chemo- and radio-therapy. A key player in DSB repair by NHEJ is DNA-PK (see fig. 1), which, like ATM and ATR, belongs to the PIKK family of protein kinases. In 2003, two DNA-PKcs-specific inhibitors, NU-7026 and NU-7441, were reported, both of which are practically inactive against ATM and ATR [43, 44]. Unfortunately, neither of them has progressed into clinical development. However, Celgene Corporation is currently recruiting patients with advanced tumours unresponsive to standard therapies in order to test the pharmacokinetics and preliminary efficacy of the dual DNA-PK/mTOR inhibitor, CC-115, in a Phase I trial. Moreover, a very recent preclinical study reported that KU-60648 (AstraZeneca), a dual inhibitor of DNA-PK and PI3K, acts as a chemosensitiser in cell-based assays and in mice xenografts [45]. More recent attempts to find novel DSB repair inhibitors led to the identification of mirin, the first inhibitor of the MRN complex that acts by blocking the nuclease activity of MRE11 [46]. Interestingly, mirin was shown to kill BRCA2-deficient cells, an effect that was even more pronounced when combined with a PARP inhibitor [47]. However, since mirin has to be applied at high micromolar concentrations to inhibit MRN, such treatment is prone to increase the risks of undesired "off-target" effects and the generation of more selective derivatives is eagerly anticipated.

During the course of DSB repair by HR, ssDNA is generated and immediately coated by RPA, which later on is replaced by the RAD51 recombinase (see fig. 2). Inhibiting the DNA-binding activity of RPA by the SMI MCI13E yielded encouraging preclinical results in combination with cisplatin [48]. Moreover, several means to prevent RAD51 action have been reported, including SMIs (B02, RI-1) as well as inhibitory peptides that interfere with the binding of BRCA2 to RAD51 [49–52]. Although peptides blocking protein-protein interactions represent an interesting concept for inhibiting DSB repair, their potential application in the clinics has yet to be established.

In summary, safety, tolerability, pharmacokinetics and efficacy of most of the aforementioned SMIs have still to be carefully validated before they may enter clinical trials to examine their benefit for cancer therapy.

Synthetic lethality approaches to target DSB repair-deficient cancers

Mutations in DSB repair genes render cancer cells dependent on alternative DNA repair pathways. Thus, comprom-

ised abilities to repair DSBs confer a weakness that can be therapeutically exploited on the basis of the concept of synthetic lethality, whereby inhibition of the "back-up" pathway induces greater toxicity in DSB repair-deficient cancer cells as compared with normal cells (fig. 3).

PARP inhibitors

The first "proof-of-principle" study verifying synthetic lethality as a suitable approach for targeted cancer therapy was published in 2005, after it had been demonstrated that HR-defective BRCA1- or BRCA2-deficient cell lines display dramatically increased sensitivity to inhibition of the SSB repair enzyme PARP [53, 54]. Subsequently, clinical development of potent small molecule PARP inhibitors (PARPis) rapidly advanced, and the first Phase II results in 2009 showed that monotherapy with the PARPi olaparib (AZD-2281; AstraZeneca) achieved encouraging response rates of 41% and 33% in patients with BRCA1- or BRCA2-mutated advanced breast and ovarian cancers, respectively [55, 56]. Furthermore, preclinical studies suggested the potential use of PARPi also in sporadic cancers that share phenotypical features with cancers arising from hereditary *BRCA* mutations, a phenomenon that is referred to as "BRCAness" [57]. Reasons for "BRCAness" can be the inactivation of BRCA1 or BRCA2 function caused by aberrant epigenetic or posttranslational modifications, or a wider range of mutations in other genes resulting in defective DSB signalling and HR. For example, it was reported that depletion of factors such as ATR, ATM, CHK1, CHK2, NBS1, CtIP and RAD51 in cultured cells synergistically increases PARPi cytotoxicity to an extent similar to mutations in *BRCA1/2*. This indicates that BRCA-deficient cells are, at least in part, sensitive to PARP inhibition because of a defect in HR [58, 59]. The current understanding suggests that inhibition of PARP leads to the accumulation of SSBs which are converted into DSBs upon encountering DNA replication forks during S-phase when HR is most active [60]. Consequently, in the absence of functional HR, such as in cancer cells lacking BRCA1 or BRCA2, PARP inhibition results in the accumulation of DSBs and, ultimately, in apoptosis or mitotic catastrophe. Importantly, normal cells survive the treatment owing to functional HR, providing the kind of selectivity that is considered the ultimate goal of cancer therapy. Nowadays, most PARPi in preclinical and clinical trials belong to the third generation of SMIs designed to compete with the substrate nicotine adenine dinucleotide (NAD^+) resulting in reversible inhibition of PARP. Recent reports indicate that in addition to catalytic inhibition, some PARPi induce cytotoxic PARP–DNA complexes, trapping PARP proteins on damaged DNA. Currently, PARPi are divided into two classes: catalytic inhibitors and dual inhibitors that not only block the enzymatic activity but also act as so-called PARP "poisons" [61, 62].

Today, 7 years after PARPi were first established for cancer therapy and despite some quite promising clinical studies, none of them has gained official approval for the treatment of cancer patients. In 2011, encouraging results from a

Table 1: Small molecule inhibitors of DNA damage response factors in preclinical or clinical development for cancer therapy.

Target	Inhibitor	Mono- or combination therapy / clinical study stage	Clinical trial identifier/ reference
ATM	KU-55933	IR, etoposide, doxorubicin, camptothecin, in preclinical testing	[25, 95]
	KU-60019	IR in preclinical testing using glioma cells	[27]
ATR	NU-6027	Hydroxyurea, cisplatin, temozolomide, rucaparib in preclinical testing	[29]
	VE-821	Cisplatin in breast and ovarian cell lines IR, gemcitabine in pancreatic cancer cells in preclinical testing	[31, 96] [32]
	ETP-46464	Single agent in p53-deficient cancer cells in preclinical testing	[33]
DNA-PKcs	NU-7441	IR, etoposide in preclinical testing of cancer cell lines and tumour xenografts	[44, 97]
	NU-7026	IR and combined with AG14361 (PARPi) in preclinical testing Anthracyclines, mitoxantrone, etoposide in preclinical testing using leukaemia cells	[43] [98]
DNA-PKcs/PI3K	KU-60648	Etoposide, doxorubicin in preclinical testing	[45]
DNA-PKcs/mTOR	CC-115	Single agent in Phase I safety and tolerability study (recruiting)	NCT01353625
PI3K/mTOR/PIKK	NVP-BEZ235	Single agent in several clinical trials IR, cisplatin in preclinical testing	www.clinicaltrials.gov [34, 35]
CHK1/(CHK2)	UCN-01	Single agent in Phase II for relapsed T-cell lymphoma (completed) Single agent in Phase II for metastatic melanoma (completed) Five-fluorouracil in Phase II for metastatic pancreatic cancer (completed) Topotecan in Phase II for various forms of ovarian cancer (completed) Topotecan in Phase II for small cell lung cancer (completed) Olaparib in pre-clinical testing for multiple mammary tumour types	NCT00082017 NCT00072189 NCT00045747 NCT00072267 NCT00098956 [99]
	GDC-0425	Single agent or with gemcitabine in Phase I dose-escalation study (recruiting)	NCT01359696
	MK-8776	Single agent or with gemcitabine in Phase I dose-escalation study (completed)	NCT00779584
	LY-2606368	Single agent in Phase I study in patients with advanced cancer (recruiting)	NCT01115790
WEE1	MK-1775	Carboplatin in Phase II for epithelial ovarian cancer	NCT01164995
CDC25	IRC-083864	Single agent in preclinical testing using pancreatic and prostate cancer cells	[42]
MRE11	mirin	Single agent or with olaparib (PARPi) in preclinical testing using BRCA2-deficient cells	[47]
RPA	MCI13E	Single agent or with cisplatin in preclinical testing	[48]
RAD51	B02	IR, mitomycin C, cisplatin in preclinical testing	[100]
	RI-1	Mitomyin C in preclinical testing	[50]

ADP = adenosine diphosphate; ATM = ataxia telangiectasia mutated protein; ATR = ATM- and Rad3-related; CHK = checkpoint kinase; DNA = deoxyribonucleic acid; DNA-PK = DNA-dependent protein kinase; DNA-PKcs = DNA-PK catalytic subunit; IR = ionising radiation; mTOR = mammalian target of rapamycin; PAR = poly(ADP-ribose); PARP = PAR polymerase; PARPi = PARP inhibitor; PI3K = phosphatidylinositol-3-kinase; PIKK = PI3K-related kinase; RPA = replication protein A

Phase II trial with iniparib (BSI-201, Sanofi-Aventis) in patients with triple negative breast cancer, which shares many features with BRCA-associated breast cancer, failed to translate into overall patient survival in a Phase III trial [63]. Later that year, AstraZeneca announced that olaparib would not progress into Phase III for hereditary *BRCA* mutation-associated breast cancer. This decision was possibly driven by economic concerns rather than by clinical issues [64]. Notwithstanding all setbacks, clinical development and research on the mechanism of action of PARPi is still ongoing (table 2). Despite controversies about its effectiveness as a PARPi, Sanofi's iniparib is under clinical investigation as a single agent and in combination with chemotherapeutic regimens in patients with recurrent solid tumours (NCT01455532), nonsmall-cell lung cancer (NCT01082549) and ovarian cancer (NCT01033292) [65, 66]. Likewise, AstraZeneca is continuing Phase II trials with olaparib to treat serous ovarian cancer, since it shares many features with BRCA1/2-mutated cancers. Indeed, activity of olaparib as a monotherapy was evident in women with pretreated high-grade serous ovarian cancer without germline *BRCA1/2* mutations [67]. This finding clearly demonstrates positive responses of a subpopulation of sporadic cancers to PARPi therapy and also underlines the importance of classifying patients according to biomarkers in order to predict the efficacy of PARPi. Such potential biomarkers also include deficiency of the phosphatase and tensin homologue (PTEN) tumour suppressor. Interestingly, due to its role in the regulation of RAD51 transcription, loss of PTEN is associated with defective HR [68, 69]. In general, detection of compromised HR provides a rationale to stratify patients for PARPi treatment. Several ways of identifying HR defects are under investigation, including gene expression profiling and gene copy number analysis of DNA repair factors [70, 71]. Further approaches assess the DSB repair capacity of tumours by measuring expression of the MRN complex, monitoring RAD51 foci formation and poly(ADP-ribosyl)ation as surrogate markers for DSB repair proficiency [72]. As for most cancer therapies, a major challenge of using PARPis is the acquired resistance of initially PARPi-sensitive cancer cells due, for example, to the loss of 53BP1 (a p53 binding protein) or to overexpression of multidrug-resistance efflux transporters [72, 73]. In addition, secondary *BRCA2* mutations have been identified, which restore the full-length protein thereby re-establishing BRCA2 functions and conferring PARPi resistance [74].

Thus, despite considerable efforts to develop PARPi for clinical use, conventional DNA-damaging chemo- and radio-therapy largely remains the mainstay of cancer treatment. However, several onging preclinical and clinical studies employ PARPi both as monotherapy and as chemo- or radio-sensitisers, because an improvement of current anti-cancer regimes is long-awaited.

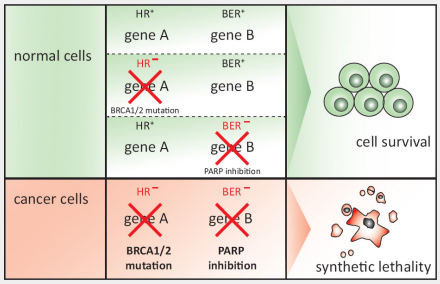

Figure 3

Synthetic lethality.

Synthetic lethality is defined as a combination of mutations or perturbations in two or more genes that leads to cell death, whereas inactivation of any one of the genes alone does not. Perturbation of genes can occur through genetic mutation or silencing, depletion by RNAi or inhibition by SMIs and is depicted by a red cross. If genes that are essential for a certain DNA repair pathway (e.g. gene A) are inactivated in normal cells, alternative pathways with functional genes (e.g. gene B) are utilised to respond to DNA damage. Conversely, cancer cells mutated or silenced for a component of a DDR pathway are compromised in their ability to process DSBs. These cells then rely on alternative DNA repair pathways to repair the breaks. Therefore, inhibition of the alternative pathway will cause cell death due to persisting DSBs. Please refer to main text for details about the example given for synthetic lethality between *BRCA1/2* mutation and PARP inhibition.

ADP = adenosine diphosphate; BER = base excision repair; DDR = DNA damage response; DNA = deoxyribonucleic acid; DSB = double-strand break; HR = homologous recombination; PARP = poly(ADP-ribose) polymerase; RNA = ribonucleic acid; RNAi = RNA interference; SMI = small molecule inhibitor

Synthetic lethal strategies emerging from preclinical research

As intensive basic research is leading towards a better understanding of cellular functions and their underlying genetic networks, more and more genetic interactions become apparent as potential targets for synthetic lethality in cancer therapy. Beyond BRCA1 and BRCA2, their joint interaction partner PALB2 is emerging as a breast cancer susceptibility gene, thus providing another opportunity for PARPi-based therapies [75].

PARP inhibition is not the only approach that takes advantage of synthetic lethal interactions between two DNA repair pathways, as inhibition of apurinic/apyrimidinic (AP) endonuclease 1, an essential component of BER, was recently shown to eliminate cancer cells with HR defects [76]. Moreover, synthetic lethality with components of the cell-cycle checkpoint machinery could be exploited in cancers harbouring activated oncogenes, since oncogene-induced replication stress activates the ATR-CHK1 signalling pathway. For example, exacerbated toxicity was reported upon inhibition of CHK1 in lymphoma cells with upregulated c-Myc expression [77]. This finding underscores the concept that cancers with elevated levels of replication stress rely on intact checkpoint signalling for cell survival. Replicative stress induces pan-nuclear distribution of phosphorylated histone variant H2AX (γ-H2AX), which is a useful biomarker for classification of tumour biopsies in order to stratify patients [78].

Finally, disruption of the FA repair pathway was shown to be synthetically lethal with abrogated checkpoint signalling. More precisely, inactivation of ATM or CHK1 resulted in reduced viability of FA-deficient cells, illustrating the concept that checkpoint signalling and FA are mutually compensatory pathways in the maintenance of genome integrity [79, 80]. These observations highlight the

usefulness of SMIs, as currently tested for CHK1, to treat tumours bearing a specific genetic background. Although many of the strategies that are based on the concept of synthetic lethality have so far only been investigated in preclinical settings, some hold great promise of entering clinical trials soon.

Haploinsufficiency of DDR factors

There is increasing evidence that haploinsufficiency of DDR components promotes genome instability and drives tumourigenesis. Dosage insufficiencies of DNA repair genes might, however, only be unmasked once a cell is challenged with an increased load of DNA damage such as oncogene-induced replicative stress [81, 82]. Synthetic lethal approaches might therefore be applicable not only in cancer cells with deficiencies, but also in those bearing haploinsufficiencies for DDR factors. Evidence from gene targeting studies in mice revealed that, for example, the loss of one allele of ATR or CtIP is sufficient to cause increased chromosomal aberrations, genomic instability and tumour susceptibility [83, 84]. This indicates that heterozygous carriers of DDR defects are more prone to develop tumours once the threshold of endogenous DNA damage is increased as, for example, in precancerous lesions [85]. However, scientists are just beginning to unravel how haploinsufficiency of DDR genes contributes to carcinogenesis and how these may be exploited for novel synthetic lethal approaches in cancer therapy.

Table 2: PARP inhibitors in preclinical or clinical development for cancer therapy*.

Inhibitor	Mono- or combination therapy	Preclinical and clinical study stage	Clinical trial identifier/ reference
Olaparib (AZD-2281, KU-59436) AstraZeneca	Single agent	Phase II trials showing with promising response rates in patients with BRCA1/ or BRCA2 mutated advanced breast and ovarian cancers	NCT01078662, NCT00494234 [55, 56]
	Single agent	Phase II trial demonstrating efficacy for advanced high-grade serous ovarian cancer without germline BRCA1/2 mutations, but not with TNBC	NCT00679783 [67]
	Cediranib	Phase I/II study for treatment of recurrent serous ovarian cancer and TNBC	NCT01116648
	Single agent and combinations with other drugs	Several ongoing Phase I/II trials for various cancers, dose-limiting adverse effects for combination of olaparib and topotecan	NCT00516438, NCT00819221, NCT01296763, NCT00912743, [101]
	Cisplatin, radiation	Phase I trial to test olaparib as a radio- and/or chemo-sensitiser in combination with high-dose radiotherapy with or without a daily cisplatin dose in locally advanced NSCLC	NCT01562210
Iniparib** (BSI-201) Sanofi-Aventis	Single agent and combinations with other drugs	Ongoing Phase I/II trials in solid tumours such as sarcomas as well as breast, uterine and ovarian cancers	NCT01455532, NCT01033292, NCT00687687
	Gemcitabine/ carboplatin	Promising results from a Phase II trial failed to translate into survival benefit for TNBC patients with unselected BRCA1/2 status in Phase III	NCT00938652, NCT01130259, [63]
	Radiotherapy	Ongoing Phase I trial of iniparib as radiosensitiser in nonoperable brain metastases	NCT01551680
	Temozolomide and radiotherapy	Ongoing Phase I/II trials for newly diagnosed malignant glioblastoma	NCT00687765
	Gemcitabine/ carboplatin	Ongoing Phase III trial in advanced squamous NSCLC	NCT01082549
Veliparib (ABT-888) Abbott Laboratories	Temozolomide, carboplatin/paclitaxel	International randomised Phase II trial of veliparib combined with chemotherapy in BRCA1/2-mutated, metastatic breast cancer	NCT01506609
	Single agent	Phase I trial for refractory BRCA 1/2-mutated solid cancers; platinum-refractory ovarian, fallopian tube, or primary peritoneal cancer or basal-like breast cancer Additional evaluation of BRCA1/2 expression and changes in PAR and γ-H2AX in peripheral blood mononuclear cells as diagnostic biomarkers	NCT00892736
	Single agent and combinations with chemo- and radio-therapy	Phase I and II trials to identify efficient combinatorial regimens in various solid and lymphoid tumours, promising results in combination with topotecan and cyclophosphamide	NCT01154426, NCT01282333, NCT01386385 and more, [102-104]
Rucaparib (AG-014699, PF-01367338, CO-338) Cancer Research UK Clovis Oncology Pfizer	Single agent	Phase I/II trials for BRCA1/2-mutated breast or ovarian cancer	NCT01482715
	Temozolomide	Initial Phase I trial as enhancer for chemotherapy in unselected solid tumours; severe myelosuppression of the combination in Phase II study for previously untreated metastatic melanoma	[105]
	Single agent and with carboplatin	Phase I/II testing in advanced solid tumors with and without BRCA mutations Several biomarkers for therapeutic response are being evaluated concurrently.	NCT01009190, NCT00664781
Niraparib (MK-4827) Merck Tesaro Inc.	Single agent	Phase I trial in advanced solid tumours showing that MK-4827 is well tolerated, blocks PARP and has promising antitumour activity in both BRCA-deficient and sporadic cancer	[106]
	Single agent and with temozolomide	Phase I dose-escalation study for solid tumours and haematological malignancies	NCT00749502, NCT01294735

* For a complete overview of PARPi currently used in clinical trials, we direct the reader to [61, 107].
** Since the primary mechanism of action for iniparib is likely not via inhibition of PARP activity, it is no longer considered to be a *bona fide* PARPi [65].
ADP = adenosine diphosphate; γ-H2AX = phosphorylated histone variant H2AX; NSCLC = nonsmall cell lung cancer; PARP = poly(ADP-ribose) polymerase; PARPi = PARP inhibitor; TNBC = triple negative breast cancer

Conclusions and future perspectives

To date, DSB-inducing agents have been the core components of conventional cancer therapy, confirming the rationale of inflicting excessive DNA damage in order to kill cancer cells. However, most chemotherapeutic regimens cause severe side effects that limit their therapeutic potential. As summarised in this review, SMIs and synthetic lethal approaches targeting the individual genetic profile of the tumours are under clinical development, with the aim to improve the patients' benefit by increasing the efficacy while lowering the toxicity of cancer treatments. A prerequisite for personalised therapy is the molecular characterisation of tumours with reliable biomarkers to assign patients the appropriate treatment. In order to stratify cancer patients according to their DNA repair status, tumour biopsies can be analysed with immunohistochemistry, fluorescence *in-situ* hybridisation (FISH), gene sequencing, expression profiling and other methods [86]. Relevant biomarker assays should ideally predict the functionality of DNA repair pathways, rather than just providing information about mutations or expression levels of proteins involved in the DDR. Certainly, such a detailed molecular profiling of cancer versus normal tissue from a given patient is critical to maximise the potential of personalised cancer drugs in terms of both therapeutic success and cost-effectiveness.

Recent *in-vitro* and *in-vivo* research has deepened our knowledge about synthetic genetic interactions and put forward alternative ways to treat cancer. Furthermore, by utilising ribonucleic acid (RNA) interference technologies, screens for synthetic lethal interactions of cancer-specific defects in DNA repair pathways have augmented the discovery of targets for cancer therapy. For example, studies using MMR-deficient cells lacking human muts homologue 2 (MSH2) revealed synthetic sickness with POLB, a DNA polymerase acting in BER [87]. Since MSH2 is mutated in 40% of patients with hereditary nonpolyposis colorectal cancer, targeted inhibition of POLB potentially opens new therapeutic applications. Moreover, gaining further insights into the structure and mechanism of action of DNA repair factors such as CtIP will aid the design of new and more efficient SMIs of the DDR. Recently discovered inhibitors of RPA and RAD51 are promising candidates, which are in preclinical testing in order to be approved for the use in clinical trials soon [48, 50].

Interestingly, the latest scientific progress in the field of microRNAs (miRNAs) has demonstrated an intensive interplay of these small regulatory RNAs with the DDR, including DSB repair. Recent studies revealed that DNA damage globally induces miRNA biogenesis and, *vice versa*, that numerous miRNAs modulate the expression of DDR factors [88–90]. Notably, BRCA1 expression was shown to be downregulated by miR-182, conferring hypersensitivity to PARPi [91]. Conversely, BRCA1 was demonstrated to suppress expression of miR-155, an oncogenic miRNA that is overexpressed in many cancers [92, 93]. These observations highlight the therapeutic potential of miRNA mimics or inhibitors in future approaches for cancer therapy [94].

In summary, as the concept of personalised medicine emerges, tumour-specific defects of DSB repair pathways represent a promising therapeutic target to be exploited for the selective elimination of cancer cells. Thus, there is an air of optimism for targeted cancer therapy through exploiting the DDR of tumour cells in the clinics.

Acknowledgement: We wish to thank D. Nadal (University Children's Hospital of Zurich) and J. Peña-Diaz for critical reading of the manuscript and helpful discussions. We also would like to apologize to all authors whose significant contributions could not be cited due to space limitations.

Funding / potential competing interests: AAS is supported by the Vontobel-Stiftung. DH and HAB are supported by grants of the Krebsliga Zürich and of the Krebsliga Schweiz (KFS-3025-08-2012).

Authors' contribution: DH and HAB: The two authors contributed equally.

Correspondence: *Professor Alessandro A. Sartori, Ph D, Institute of Molecular Cancer Research, University of Zurich, Winterthurerstrasse 190, CH-8057 Zürich, Switzerland, Sartori[at]imcr.uzh.ch*

References

1 Bundesamt für Statistik – Todesfälle: Anzahl, Entwicklung und Ursachen. www.bfs.admin.ch.

2 Krebsliga Schweiz – Krebs in der Schweiz: wichtige Zahlen (Stand: Juni 2012). www.krebsliga.ch.

3 Hanahan D, Weinberg RA. Hallmarks of cancer: the next generation. Cell. 2011;144(5):646–74.

4 Barnes DE, Lindahl T. Repair and genetic consequences of endogenous DNA base damage in mammalian cells. Annu Rev Genet. 2004;38:445–76.

5 Hoeijmakers JHJ. DNA damage, aging, and cancer. N Engl J Med. 2009;361(15):1475–85.

6 Jackson SP, Bartek J. The DNA-damage response in human biology and disease. Nature. 2009;461(7267):1071–8.

7 Bouwman P, Jonkers J. The effects of deregulated DNA damage signalling on cancer chemotherapy response and resistance. Nat Rev Cancer. 2012;12(9):587–98.

8 Lord CJ, Ashworth A. The DNA damage response and cancer therapy. Nature. 2012;481(7381):287–94.

9 Curtin NJ. DNA repair dysregulation from cancer driver to therapeutic target. Nat Rev Cancer. 2012;12(12):801–17.

10 Falck J, Coates J, Jackson SP. Conserved modes of recruitment of ATM, ATR and DNA-PKcs to sites of DNA damage. Nature. 2005;434(7033):605–11.

11 Derheimer FA, Kastan MB. Multiple roles of ATM in monitoring and maintaining DNA integrity. FEBS Lett. 2010;584(17):3675–81.

12 Jiricny J. The multifaceted mismatch-repair system. Nat Rev Mol Cell Biol. 2006;7(5):335–46.

13 Schärer OD. DNA interstrand crosslinks: natural and drug-induced DNA adducts that induce unique cellular responses. Chembiochem. 2005;6(1):27–32.

14 Ciccia A, Elledge SJ. The DNA damage response: making it safe to play with knives. Mol Cell. 2010;40(2):179–204.

15 Chapman JR, Taylor MRG, Boulton SJ. Playing the end game: DNA double-strand break repair pathway choice. Mol Cell. 2012;47(4):497–510.

16 Symington LS, Gautier J. Double-strand break end resection and repair pathway choice. Annu Rev Genet. 2011;45:247–71.

17 Sartori AA, Lukas C, Coates J, Mistrik M, Fu S, Bartek J, et al. Human CtIP promotes DNA end resection. Nature. 2007;450(7169):509–14.

18 Moynahan ME, Jasin M. Mitotic homologous recombination maintains genomic stability and suppresses tumorigenesis. Nat Rev Mol Cell Biol. 2010;11(3):196–207.

19 Jackson SP. Sensing and repairing DNA double-strand breaks. Carcinogenesis. 2002;23(5):687–96.

20 Bao S, Wu Q, McLendon RE, Hao Y, Shi Q, Hjelmeland AB, et al. Glioma stem cells promote radioresistance by preferential activation of the DNA damage response. Nature. 2006;444(7120):756–60.

21 Ma CX, Cai S, Li S, Ryan CE, Guo Z, Schaiff WT, et al. Targeting Chk1 in p53-deficient triple-negative breast cancer is therapeutically beneficial in human-in-mouse tumor models. J Clin Invest. 2012;122(4):1541–52.

22 Gaudin D, Yielding KL. Response of a "resistant" plasmacytoma to alkylating agents and x-ray in combination with the 'excision' repair inhibitors caffeine and chloroquine. Proc Soc Exp Biol Med. 1969;131(4):1413–6.

23 Sarkaria JN, Busby EC, Tibbetts RS, Roos P, Taya Y, Karnitz LM, et al. Inhibition of ATM and ATR kinase activities by the radiosensitizing agent, caffeine. Cancer Res. 1999;59(17):4375–82.

24 Blasina A, Price BD, Turenne GA, McGowan CH. Caffeine inhibits the checkpoint kinase ATM. Curr Biol. 1999;9(19):1135–8.

25 Hickson I, Zhao Y, Richardson CJ, Green SJ, Martin NMB, Orr AI, et al. Identification and characterization of a novel and specific inhibitor of the ataxia-telangiectasia mutated kinase ATM. Cancer Res. 2004;64(24):9152–9.

26 Knight ZA. Small molecule inhibitors of the PI3-kinase family. Curr Top Microbiol Immunol. 2010;347:263–78.

27 Golding SE, Rosenberg E, Valerie N, Hussaini I, Frigerio M, Cockcroft XF, et al. Improved ATM kinase inhibitor KU-60019 radiosensitizes glioma cells, compromises insulin, AKT and ERK prosurvival signaling, and inhibits migration and invasion. Mol Cancer Ther. 2009;8(10):2894–902.

28 Wagner JM, Kaufmann SH. Prospects for the Use of ATR Inhibitors to Treat Cancer. Pharmaceuticals. 2010;3(5):1311–34.

29 Peasland A, Wang L-Z, Rowling E, Kyle S, Chen T, Hopkins A, et al. Identification and evaluation of a potent novel ATR inhibitor, NU6027, in breast and ovarian cancer cell lines. Br J Cancer. 2011;105(3):372–81.

30 Arris CE, Boyle FT, Calvert AH, Curtin NJ, Endicott JA, Garman EF, et al. Identification of novel purine and pyrimidine cyclin-dependent kinase inhibitors with distinct molecular interactions and tumor cell growth inhibition profiles. J Med Chem. 2000;43(15):2797–804.

31 Reaper PM, Griffiths MR, Long JM, Charrier J-D, MacCormick S, Charlton PA, et al. Selective killing of ATM- or p53-deficient cancer cells through inhibition of ATR. Nat Chem Biol. 2011;7(7):428–30.

32 Prevo R, Fokas E, Reaper PM, Charlton PA, Pollard JR, McKenna WG, et al. The novel ATR inhibitor VE-821 increases sensitivity of pancreatic cancer cells to radiation and chemotherapy. Cancer Biol Ther. 2012;13(11):1072–81.

33 Toledo LI, Murga M, Zur R, Soria R, Rodriguez A, Martinez S, et al. A cell-based screen identifies ATR inhibitors with synthetic lethal properties for cancer-associated mutations. Nat Struct Mol Biol. 2011;18(6):721–7.

34 Yang F, Qian X-J, Qin W, Deng R, Wu X-Q, Qin J, et al. Dual Phosphoinositide 3-Kinase/Mammalian Target of Rapamycin Inhibitor NVP-BEZ235 Has a Therapeutic Potential and Sensitizes Cisplatin in Nasopharyngeal Carcinoma. PLoS ONE. 2013;8(3):e59879.

35 Mukherjee B, Tomimatsu N, Amancherla K, Camacho CV, Pichamoorthy N, Burma S. The dual PI3K/mTOR inhibitor NVP-BEZ235 is a potent inhibitor of ATM- and DNA-PKCs-mediated DNA damage responses. Neoplasia. 2012;14(1):34–43.

36 Takahashi I, Saitoh Y, Yoshida M, Sano H, Nakano H, Morimoto M, et al. UCN-01 and UCN-02, new selective inhibitors of protein kinase C. II. Purification, physico-chemical properties, structural determination and biological activities. J Antibiot. 1989;42(4):571–6.

37 Graves PR, Yu L, Schwarz JK, Gales J, Sausville EA, O'Connor PM, et al. The Chk1 protein kinase and the Cdc25C regulatory pathways are targets of the anticancer agent UCN-01. J Biol Chem. 2000;275(8):5600–5.

38 Zhao B, Bower MJ, McDevitt PJ, Zhao H, Davis ST, Johanson KO, et al. Structural basis for Chk1 inhibition by UCN-01. J Biol Chem. 2002;277(48):46609–15.

39 Guzi TJ, Paruch K, Dwyer MP, Labroli M, Shanahan F, Davis N, et al. Targeting the replication checkpoint using SCH 900776, a potent and functionally selective CHK1 inhibitor identified via high content screening. Mol Cancer Ther. 2011;10(4):591–602.

40 De Witt Hamer PC, Mir SE, Noske D, Van Noorden CJF, Würdinger T. WEE1 kinase targeting combined with DNA-damaging cancer therapy catalyzes mitotic catastrophe. Clin Cancer Res. 2011;17(13):4200–7.

41 Lavecchia A, Di Giovanni C, Novellino E. CDC25 phosphatase inhibitors: an update. Mini Rev Med Chem. 2012;12(1):62–73.

42 Brezak M-C, Valette A, Quaranta M, Contour-Galcera M-O, Jullien D, Lavergne O, et al. IRC-083864, a novel bis quinone inhibitor of CDC25 phosphatases active against human cancer cells. Int J Cancer. 2009;124(6):1449–56.

43 Veuger SJ, Curtin NJ, Richardson CJ, Smith GCM, Durkacz BW. Radiosensitization and DNA repair inhibition by the combined use of novel inhibitors of DNA-dependent protein kinase and poly(ADP-ribose) polymerase-1. Cancer Res. 2003;63(18):6008–15.

44 Leahy JJJ, Golding BT, Griffin RJ, Hardcastle IR, Richardson C, Rigoreau L, et al. Identification of a highly potent and selective DNA-dependent protein kinase (DNA-PK) inhibitor (NU7441) by screening of chromenone libraries. Bioorg Med Chem Lett. 2004;14(24):6083–7.

45 Munck JM, Batey MA, Zhao Y, Jenkins H, Richardson CJ, Cano C, et al. Chemosensitization of cancer cells by KU-0060648, a dual inhibitor of DNA-PK and PI-3K. Mol Cancer Ther. 2012;11(8):1789–98.

46 Dupré A, Boyer-Chatenet L, Sattler RM, Modi AP, Lee J-H, Nicolette ML, et al. A forward chemical genetic screen reveals an inhibitor of the Mre11-Rad50-Nbs1 complex. Nat Chem Biol. 2008;4(2):119–25.

47 Ying S, Hamdy FC, Helleday T. Mre11-dependent degradation of stalled DNA replication forks is prevented by BRCA2 and PARP1. Cancer Res. 2012;72(11):2814–21.

48 Neher TM, Bodenmiller D, Fitch RW, Jalal SI, Turchi JJ. Novel irreversible small molecule inhibitors of replication protein A display single-agent activity and synergize with cisplatin. Mol Cancer Ther. 2011;10(10):1796–806.

49 Huang F, Motlekar NA, Burgwin CM, Napper AD, Diamond SL, Mazin AV. Identification of specific inhibitors of human RAD51 recombinase using high-throughput screening. ACS Chem Biol. 2011;6(6):628–35.

50 Budke B, Logan HL, Kalin JH, Zelivianskaia AS, Cameron McGuire W, Miller LL, et al. RI-1: a chemical inhibitor of RAD51 that disrupts homologous recombination in human cells. Nucleic Acids Res. 2012;40(15):7347–57.

51 Nomme J, Renodon-Cornière A, Asanomi Y, Sakaguchi K, Stasiak AZ, Stasiak A, et al. Design of potent inhibitors of human RAD51 recombinase based on BRC motifs of BRCA2 protein: modeling and experimental validation of a chimera peptide. J Med Chem. 2010;53(15):5782–91.

52 Pessetto ZY, Yan Y, Bessho T, Natarajan A. Inhibition of BRCT(BRCA1)-phosphoprotein interaction enhances the cytotoxic effect of olaparib in breast cancer cells: a proof of concept study for synthetic lethal therapeutic option. Breast Cancer Res Treat. 2012;134(2):511–7.

53 Farmer H, McCabe N, Lord CJ, Tutt ANJ, Johnson DA, Richardson TB, et al. Targeting the DNA repair defect in BRCA mutant cells as a therapeutic strategy. Nature. 2005;434(7035):917–21.

54 Bryant HE, Schultz N, Thomas HD, Parker KM, Flower D, Lopez E, et al. Specific killing of BRCA2-deficient tumours with inhibitors of poly(ADP-ribose) polymerase. Nature. 2005;434(7035):913–7.

55 Tutt A, Robson M, Garber JE, Domchek SM, Audeh MW, Weitzel JN, et al. Oral poly(ADP-ribose) polymerase inhibitor olaparib in patients with BRCA1 or BRCA2 mutations and advanced breast cancer: a proof-of-concept trial. Lancet. 2010;376(9737):235–44.

56 Audeh MW, Carmichael J, Penson RT, Friedlander M, Powell B, Bell-McGuinn KM, et al. Oral poly(ADP-ribose) polymerase inhibitor olaparib in patients with BRCA1 or BRCA2 mutations and recurrent ovarian cancer: a proof-of-concept trial. Lancet. 2010;376(9737):245–51.

57 Turner N, Tutt A, Ashworth A. Hallmarks of 'BRCAness' in sporadic cancers. Nat Rev Cancer. 2004;4(10):814–9.

58 McCabe N, Turner NC, Lord CJ, Kluzek K, Bialkowska A, Swift S, et al. Deficiency in the repair of DNA damage by homologous recombination and sensitivity to poly(ADP-ribose) polymerase inhibition. Cancer Res. 2006;66(16):8109–15.

59 Huehls AM, Wagner JM, Huntoon CJ, Karnitz LM. Identification of DNA repair pathways that affect the survival of ovarian cancer cells treated with a poly(ADP-ribose) polymerase inhibitor in a novel drug combination. Mol Pharmacol. 2012;82(4):767–76.

60 Karanam K, Kafri R, Loewer A, Lahav G. Quantitative live cell imaging reveals a gradual shift between DNA repair mechanisms and a maximal use of HR in mid S phase. Mol Cell. 2012;47(2):320–9.

61 Park SR, Chen A. Poly(Adenosine diphosphate-ribose) polymerase inhibitors in cancer treatment. Hematol Oncol Clin North Am. 2012;26(3):649–70–ix.

62 Murai J, Huang S-YN, Das BB, Renaud A, Zhang Y, Doroshow JH, et al. Trapping of PARP1 and PARP2 by Clinical PARP Inhibitors. Cancer Res. 2012;72(21):5588–99.

63 O'Shaughnessy J, Osborne C, Pippen JE, Yoffe M, Patt D, Rocha C, et al. Iniparib plus chemotherapy in metastatic triple-negative breast cancer. N Engl J Med. 2011;364(3):205–14.

64 Guha M. PARP inhibitors stumble in breast cancer. Nat Biotechnol. 2011;29(5):373–4.

65 Liu X, Shi Y, Maag DX, Palma JP, Patterson MJ, Ellis PA, et al. Iniparib nonselectively modifies cysteine-containing proteins in tumor cells and is not a bona fide PARP inhibitor. Clin Cancer Res. 2012;18(2):510–23.

66 Patel AG, De Lorenzo SB, Flatten KS, Poirier GG, Kaufmann SH. Failure of iniparib to inhibit poly(ADP-Ribose) polymerase in vitro. Clin Cancer Res. 2012;18(6):1655–62.

67 Gelmon KA, Tischkowitz M, Mackay H, Swenerton K, Robidoux A, Tonkin K, et al. Olaparib in patients with recurrent high-grade serous or poorly differentiated ovarian carcinoma or triple-negative breast cancer: a phase 2, multicentre, open-label, non-randomised study. Lancet Oncol. 2011;12(9):852–61.

68 Mendes-Pereira AM, Martin SA, Brough R, McCarthy A, Taylor JR, Kim J-S, et al. Synthetic lethal targeting of PTEN mutant cells with PARP inhibitors. EMBO Mol Med. 2009;1(6-7):315–22.

69 Dedes KJ, Wetterskog D, Mendes-Pereira AM, Natrajan R, Lambros MB, Geyer FC, et al. PTEN deficiency in endometrioid endometrial adenocarcinomas predicts sensitivity to PARP inhibitors. Sci Transl Med. 2010;2(53):53ra75.

70 Konstantinopoulos PA, Spentzos D, Karlan BY, Taniguchi T, Fountzilas E, Francoeur N, et al. Gene expression profile of BRCAness that correlates with responsiveness to chemotherapy and with outcome in patients with epithelial ovarian cancer. J Clin Oncol. 2010;28(22):3555–61.

71 Tung N, Wang Y, Collins LC, Kaplan J, Li H, Gelman R, et al. Estrogen receptor positive breast cancers in BRCA1 mutation carriers: clinical risk factors and pathologic features. Breast Cancer Res. 2010;12(1):R12.

72 Oplustilova L, Wolanin K, Mistrik M, Korinkova G, Simkova D, Bouchal J, et al. Evaluation of candidate biomarkers to predict cancer cell sensitivity or resistance to PARP-1 inhibitor treatment. Cell Cycle. 2012;11(20):3837–50.

73 Jaspers JE, Kersbergen A, Boon U, Sol W, van Deemter L, Zander SA, et al. Loss of 53BP1 causes PARP inhibitor resistance in Brca1-mutated mouse mammary tumors. Cancer Discov. 2013;3(1):68–81.

74 Barber LJ, Sandhu S, Chen L, Campbell J, Kozarewa I, Fenwick K, et al. Secondary mutations in BRCA2 associated with clinical resistance to a PARP inhibitor. J Pathol. 2013;229(3):422–9.

75 Poumpouridou N, Kroupis C. Hereditary breast cancer: beyond BRCA genetic analysis; PALB2 emerges. Clin Chem Lab Med. 2012;50(3):423–34.

76 Sultana R, McNeill DR, Abbotts R, Mohammed MZ, Zdzienicka MZ, Qutob H, et al. Synthetic lethal targeting of DNA double-strand break repair deficient cells by human apurinic/apyrimidinic endonuclease inhibitors. Int J Cancer. 2012;131(10):2433–44.

77 Ferrao PT, Bukczynska EP, Johnstone RW, McArthur GA. Efficacy of CHK inhibitors as single agents in MYC-driven lymphoma cells. Oncogene. 2012;31(13):1661–72.

78 Ivashkevich A, Redon CE, Nakamura AJ, Martin RF, Martin OA. Use of the γ-H2AX assay to monitor DNA damage and repair in translational cancer research. Cancer Lett. 2012;327(1-2):123–33.

79 Kennedy RD, Chen CC, Stuckert P, Archila EM, la Vega De MA, Moreau LA, et al. Fanconi anemia pathway-deficient tumor cells are hypersensitive to inhibition of ataxia telangiectasia mutated. J Clin Invest. 2007;117(5):1440–9.

80 Chen CC, Kennedy RD, Sidi S, Look AT, D'Andrea A. CHK1 inhibition as a strategy for targeting Fanconi Anemia (FA) DNA repair pathway deficient tumors. Mol Cancer. 2009;8:24.

81 Bartek J, Lukas J, Bartkova J. DNA damage response as an anti-cancer barrier: damage threshold and the concept of 'conditional haploinsufficiency'. Cell Cycle. 2007;6(19):2344–7.

82 Kerzendorfer C, O'Driscoll M. Human DNA damage response and repair deficiency syndromes: linking genomic instability and cell cycle checkpoint proficiency. DNA Repair (Amst.). 2009;8(9):1139–52.

83 Chen P-L, Liu F, Cai S, Lin X, Li A, Chen Y, et al. Inactivation of CtIP leads to early embryonic lethality mediated by G1 restraint and to tumorigenesis by haploid insufficiency. Mol Cell Biol. 2005;25(9):3535–42.

84 Brown EJ, Baltimore D. ATR disruption leads to chromosomal fragmentation and early embryonic lethality. Genes Dev. 2000;14(4):397–402.

85 Halazonetis TD, Gorgoulis VG, Bartek J. An oncogene-induced DNA damage model for cancer development. Science. 2008;319(5868):1352–5.

86 Vollebergh MA, Jonkers J, Linn SC. Genomic instability in breast and ovarian cancers: translation into clinical predictive biomarkers. Cell Mol Life Sci. 2012;69(2):223–45.

87 Martin SA, McCabe N, Mullarkey M, Cummins R, Burgess DJ, Nakabeppu Y, et al. DNA polymerases as potential therapeutic targets for cancers deficient in the DNA mismatch repair proteins MSH2 or MLH1. Cancer Cell. 2010;17(3):235–48.

88 Zhang X, Wan G, Berger FG, He X, Lu X. The ATM kinase induces microRNA biogenesis in the DNA damage response. Mol Cell. 2011;41(4):371–83.

89 Wang Y, Huang J-W, Li M, Cavenee WK, Mitchell PS, Zhou X, et al. MicroRNA-138 modulates DNA damage response by repressing histone H2AX expression. Mol Cancer Res. 2011;9(8):1100–11.

90 Landau D-A, Slack FJ. MicroRNAs in mutagenesis, genomic instability, and DNA repair. Semin Oncol. 2011;38(6):743–51.

91 Moskwa P, Buffa FM, Pan Y, Panchakshari R, Gottipati P, Muschel RJ, et al. miR-182-mediated downregulation of BRCA1 impacts DNA repair and sensitivity to PARP inhibitors. Mol Cell. 2011;41(2):210–20.

92 Chang S, Wang R-H, Akagi K, Kim K-A, Martin BK, Cavallone L, et al. Tumor suppressor BRCA1 epigenetically controls oncogenic microRNA-155. Nat Med. 2011;17(10):1275–82.

93 Jiang S, Zhang H-W, Lu M-H, He X-H, Li Y, Gu H, et al. MicroRNA-155 functions as an OncomiR in breast cancer by targeting the suppressor of cytokine signaling 1 gene. Cancer Res. 2010;70(8):3119–27.

94 Broderick JA, Zamore PD. MicroRNA therapeutics. Gene Ther. 2011;18(12):1104–10.

95 Li Y, Yang D-Q. The ATM inhibitor KU-55933 suppresses cell proliferation and induces apoptosis by blocking Akt in cancer cells with overactivated Akt. Mol Cancer Ther. 2010;9(1):113–25.

96 Charrier J-D, Durrant SJ, Golec JMC, Kay DP, Knegtel RMA, MacCormick S, et al. Discovery of potent and selective inhibitors of ataxia telangiectasia mutated and Rad3 related (ATR) protein kinase as potential anticancer agents. J Med Chem. 2011;54(7):2320–30.

97 Zhao Y, Thomas HD, Batey MA, Cowell IG, Richardson CJ, Griffin RJ, et al. Preclinical evaluation of a potent novel DNA-dependent protein kinase inhibitor NU7441. Cancer Res. 2006;66(10):5354–62.

98 Willmore E, de Caux S, Sunter NJ, Tilby MJ, Jackson GH, Austin CA, et al. A novel DNA-dependent protein kinase inhibitor, NU7026, poten-

tiates the cytotoxicity of topoisomerase II poisons used in the treatment of leukemia. Blood. 2004;103(12):4659–65.

99 Tang Y, Hamed HA, Poklepovic A, Dai Y, Grant S, Dent P. Poly(ADP-ribose) polymerase 1 modulates the lethality of CHK1 inhibitors in mammary tumors. Mol Pharmacol. 2012;82(2):322–32.

100 Huang F, Mazina OM, Zentner IJ, Cocklin S, Mazin AV. Inhibition of homologous recombination in human cells by targeting RAD51 recombinase. J Med Chem. 2012;55(7):3011–20.

101 Samol J, Ranson M, Scott E, Macpherson E, Carmichael J, Thomas A, et al. Safety and tolerability of the poly(ADP-ribose) polymerase (PARP) inhibitor, olaparib (AZD2281) in combination with topotecan for the treatment of patients with advanced solid tumors: a phase I study. Invest New Drugs. 2012;30(4):1493–500.

102 Kummar S, Ji J, Morgan R, Lenz H-J, Puhalla SL, Belani CP, et al. A phase I study of veliparib in combination with metronomic cyclophosphamide in adults with refractory solid tumors and lymphomas. Clin Cancer Res. 2012;18(6):1726–34.

103 Kummar S, Chen A, Ji J, Zhang Y, Reid JM, Ames M, et al. Phase I study of PARP inhibitor ABT-888 in combination with topotecan in adults with refractory solid tumors and lymphomas. Cancer Res. 2011;71(17):5626–34.

104 Patel AG, Flatten KS, Schneider PA, Dai NT, McDonald JS, Poirier GG, et al. Enhanced killing of cancer cells by poly(ADP-ribose) polymerase inhibitors and topoisomerase I inhibitors reflects poisoning of both enzymes. J Biol Chem. 2012;287(6):4198–210.

105 Plummer R, Lorigan P, Steven N, Scott L, Middleton MR, Wilson RH, et al. A phase II study of the potent PARP inhibitor, Rucaparib (PF-01367338, AG014699), with temozolomide in patients with metastatic melanoma demonstrating evidence of chemopotentiation. Cancer Chemother Pharmacol. 2013;71(5):1191–9.

106 Sandhu SK, Wenham RM, Wilding G, McFadden M, Sun L, Toniatti C, et al. First-in-human trial of a poly (ADP-ribose) polymerase (PARP) inhibitor MK-4827 in advanced cancer patients (pts) with antitumor activity in BRCA-deficient and sporadic ovarian cancers. J Clin Oncol. (Meeting Abstracts). 2010;28(15_suppl):3001.

107 Javle M, Curtin NJ. The role of PARP in DNA repair and its therapeutic exploitation. Br J Cancer. 2011;105(8):1114–22.

Figures (large format)

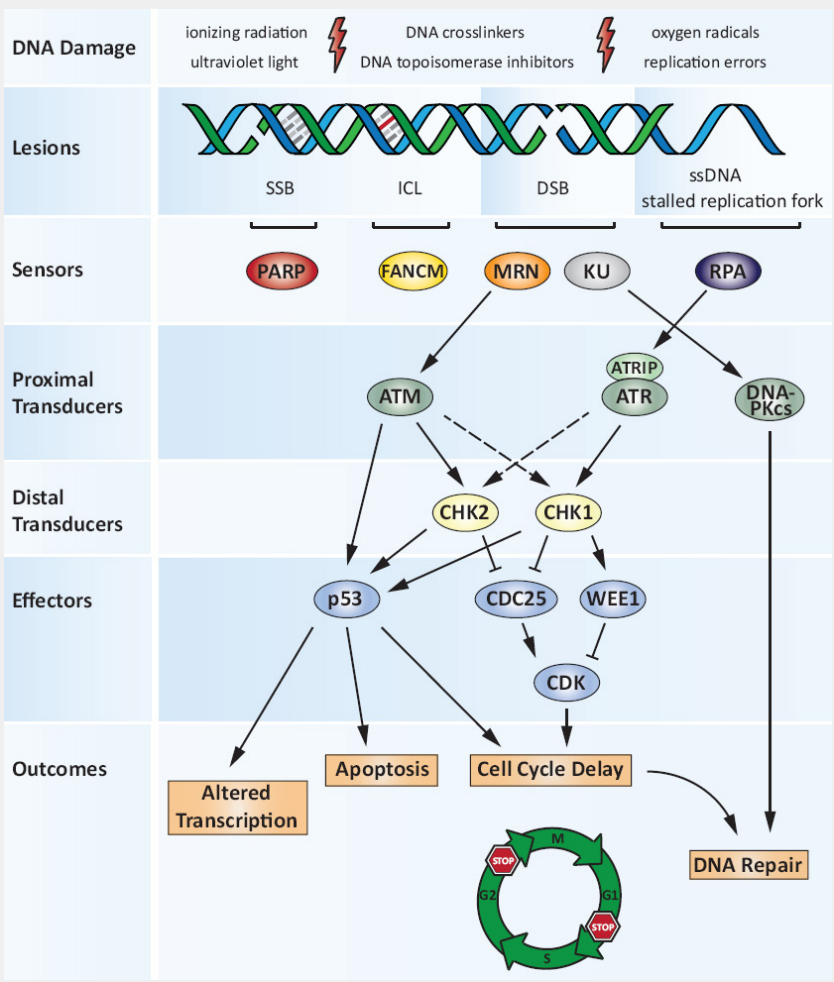

Figure 1

The DNA damage response.

Exogenous and endogenous DNA damaging agents generate various types of lesions including DNA single- and double-strand breaks (SSBs and DSBs). The multifunctional MRN complex detects DSBs, while FANCM is required for the DNA interstrand crosslink (ICL)-induced checkpoint response. PARP predominantly acts as a SSB sensor protein. RPA binds to regions of single-stranded DNA (ssDNA) that are exposed at stalled replication forks or after DSB resection. MRN and RPA mediate the recruitment of ATM and ATR-ATRIP, respectively, and the subsequent activation of the respective pathways, coordinating cell-cycle checkpoints, DNA repair and apoptotic responses to DNA damage. The Ku70/Ku80 heterodimer (KU) competes with MRN for binding to DSBs. KU recruits DNA-PKcs to form the catalytically active DNA-PK holoenzyme which is a major component of the canonical NHEJ machinery during DSB repair. MRN on the other hand initiates HR (see also fig. 2). Once activated, the DNA damage signalling cascade extends through multiple phosphorylation events primarily via the cell-cycle checkpoint kinases CHK1 and CHK2. Their signals converge on downstream effectors such as the tumour suppressor protein p53 or the CDC25 protein phosphatase and WEE1 tyrosine kinase. As a result, CDK activity is inhibited, delaying cell cycle progression from G1 to S (the G1/S checkpoint) or from G2 to M phase (the G2/M checkpoint). The DNA damage response (DDR) thus orchestrates a variety of cellular outcomes: the transcriptional programme of the damaged cell is altered and the cell cycle is transiently arrested, thereby facilitating repair of the DNA lesions. In situations where DNA damage is too severe and cannot be repaired, the DDR triggers apoptosis or senescence.

ADP = adenosine diphosphate; ATM = ataxia telangiectasia mutated protein; ATR = ATM- and Rad3-related; ATRIP = ATR-interacting protein; CDK = cyclin-dependant kinase; DNA = deoxyribonucleic acid; DNA-PK = DNA-dependant protein kinase; DNA-PKcs = DNA-PK catalytic subunit; FANCM = Fanconi anaemia complementation group M; HR = homologous recombination; ICL = interstrand crosslink; MRN = MRE11-RAD50-NBS1 complex; NEHJ = nonhomologous end joining; PARP = poly(ADP-ribose) polymerase; RPA = replication protein A

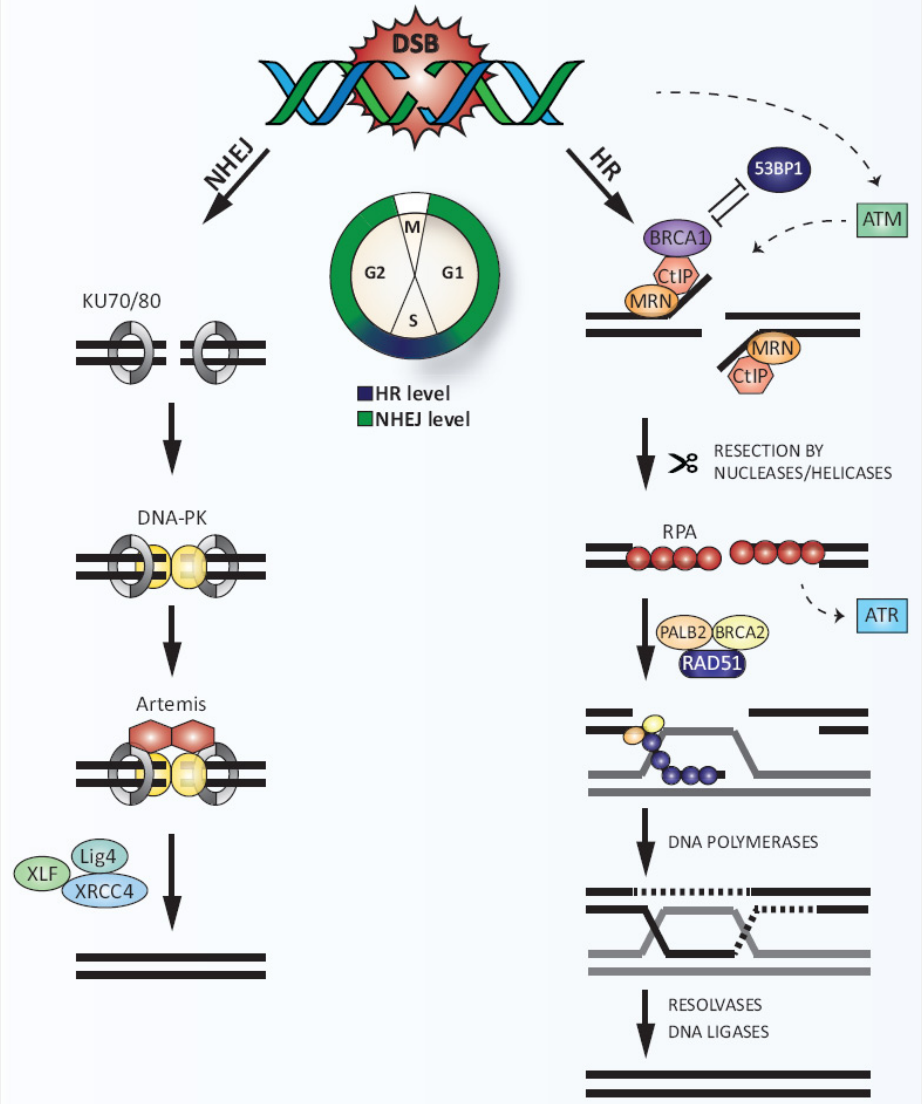

Figure 2

DNA double-strand break (DSB) repair.

DSBs are predominantly repaired by two distinct pathways: NHEJ or HR. NHEJ operates throughout the cell cycle, but mainly during the G1 and G2 phases, whereas HR peaks in S phase. Rapid association of the Ku70/80 heterodimer to DSBs promotes NHEJ by recruiting DNA-PKcs. DNA ends are processed by the nucleolytic activity of Artemis, followed by religation catalysed by a complex of XLF, Ligase IV (Lig4) and XRCC4. Alternatively, MRN, which is initially recruited to DSBs in competition with Ku70/80, initiates DSB resection together with CtIP thereby promoting HR. 53BP1 antagonises BRCA1 in DSB resection. Extensive DSB resection by other nucleases and formation of RPA-coated ssDNA stimulates the activation of ATR. Displacement of RPA by RAD51 is mediated by BRCA2 and PALB2, resulting in the formation of RAD51 nucleoprotein filaments. Subsequent strand invasion into the homologous DNA template and capturing of the second DNA end leads to the formation of a double Holliday junction, which is processed by resolvases. Finally, the DNA is sealed by ligases to accomplish error-free repair of the DSB.

53BP = p53 binding protein; ATM = ataxia telangiectasia mutated protein; CtBP = C-terminal binding protein; CtIP = CtBP-interacting protein; DNA = deoxyribonucleic acid; DNA-PK = DNA-dependant protein kinase; DNA-PKcs = DNA-PK catalytic subunit; HR = homologous recombination; MRN = MRE11-RAD50-NBS1 complex; NEHJ = nonhomologous end joining; PALB1/2 = partner and localiser of BRCA1/2; RPA = replication protein A; ssDNA = single-stranded DNA; XLF = XRCC4-like factor; XRCC4 = X-ray repair cross-complementing protein 4

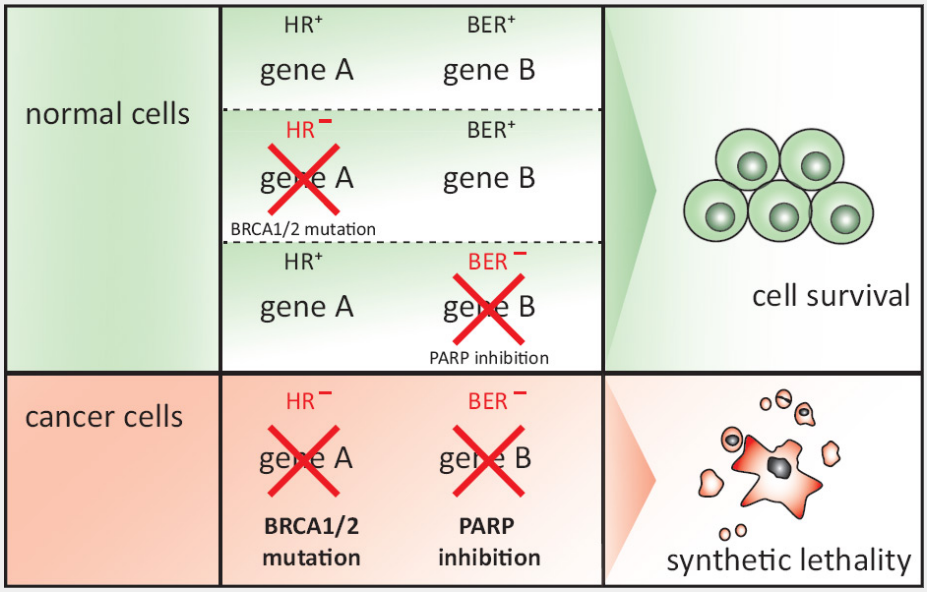

Figure 3

Synthetic lethality.

Synthetic lethality is defined as a combination of mutations or perturbations in two or more genes that leads to cell death, whereas inactivation of any one of the genes alone does not. Perturbation of genes can occur through genetic mutation or silencing, depletion by RNAi or inhibition by SMIs and is depicted by a red cross. If genes that are essential for a certain DNA repair pathway (e.g. gene A) are inactivated in normal cells, alternative pathways with functional genes (e.g. gene B) are utilised to respond to DNA damage. Conversely, cancer cells mutated or silenced for a component of a DDR pathway are compromised in their ability to process DSBs. These cells then rely on alternative DNA repair pathways to repair the breaks. Therefore, inhibition of the alternative pathway will cause cell death due to persisting DSBs. Please refer to main text for details about the example given for synthetic lethality between *BRCA1/2* mutation and PARP inhibition.

ADP = adenosine diphosphate; BER = base excision repair; DDR = DNA damage response; DNA = deoxyribonucleic acid; DSB = double-strand break; HR = homologous recombination; PARP = poly(ADP-ribose) polymerase; RNA = ribonucleic acid; RNAi = RNA interference; SMI = small molecule inhibitor

FANCD2 and CtIP cooperate to repair DNA interstrand crosslinks

Olga Murina,Christine von Aesch, Ufuk Karakus, Lorenza P. Ferretti, **Hella A. Bolck**, Kay Hänggi and Alessandro A. Sartori

Article published in Cell Reports, 2014.

I examined whether CtIP can bind to ubiquitin. Specifically, I established and performed pull-down assays using nitrilotriacetic acid (Ni-NTA) agarose beads, which were coupled to recombinant His-tagged ubiquitin (rHis-Ub) as shown in Figure 3E.

Please cite this article in press as: Murina et al., FANCD2 and CtIP Cooperate to Repair DNA Interstrand Crosslinks, Cell Reports (2014), http://dx.doi.org/10.1016/j.celrep.2014.03.069

Cell Reports
Report

OPEN ACCESS
CellPress

FANCD2 and CtIP Cooperate to Repair DNA Interstrand Crosslinks

Olga Murina,[1] Christine von Aesch,[1] Ufuk Karakus,[1] Lorenza P. Ferretti,[1] Hella A. Bolck,[1] Kay Hänggi,[1,2] and Alessandro A. Sartori[1,*]
[1]Institute of Molecular Cancer Research, University of Zurich, Winterthurerstrasse 190, 8057 Zürich, Switzerland
[2]Institute of Experimental Immunology, University of Zurich, Winterthurerstrasse 190, 8057 Zürich, Switzerland
*Correspondence: sartori@imcr.uzh.ch
http://dx.doi.org/10.1016/j.celrep.2014.03.069

SUMMARY

The resolution of DNA interstrand crosslinks (ICLs) requires a complex interplay between several processes of DNA metabolism, including the Fanconi anemia (FA) pathway and homologous recombination (HR). FANCD2 monoubiquitination and CtIP-dependent DNA-end resection represent key events in FA and HR activation, respectively, but very little is known about their functional relationship. Here, we show that CtIP physically interacts with both FANCD2 and ubiquitin and that monoubiquitinated FANCD2 tethers CtIP to damaged chromatin, which helps channel DNA double-strand breaks generated during ICL processing into the HR pathway. Consequently, CtIP mutants defective in FANCD2 binding fail to associate with damaged chromatin, which leads to increased levels of nonhomologous end-joining activity and ICL hypersensitivity. Interestingly, we also observe that CtIP depletion aggravates the genomic instability in FANCD2-deficient cells. Thus, our data indicate that FANCD2 primes CtIP-dependent resection during HR after ICL induction but that CtIP helps prevent illegitimate recombination in FA cells.

INTRODUCTION

Fanconi anemia (FA) is a rare hereditary disorder characterized by bone marrow failure, developmental abnormalities, and cancer predisposition (Moldovan and D'Andrea, 2009). Cells isolated from FA patients display chromosomal instability and hypersensitivity to DNA interstrand crosslink (ICL)-inducing agents such as mitomycin C (MMC) and cisplatin. The high cytotoxicity of MMC, a property exploited in cancer therapy, is primarily based on the strong inhibitory effect of unrepaired ICLs on DNA replication (Deans and West, 2011). Recent studies indicate that the FA pathway orchestrates replication-coupled ICL repair—involving nucleolytic incision, translesion DNA synthesis (TLS), and homologous recombination (HR)—to maintain genomic stability (Knipscheer et al., 2009). In response to ICL damage, the FA core complex, consisting of eight proteins (FANCA, B, C, E, F, G, L, and M), promotes monoubiquitination of FANCD2 and FANCI (Garcia-Higuera et al., 2001; Smogorzewska et al., 2007). The ubiquitinated FANCD2/I complex relocalizes to damaged chromatin, where it coordinates downstream repair events (Kim and D'Andrea, 2012). ICL repair is initiated by nucleolytic incisions on either side of the crosslink and carried out by SLX4-associated XPF-ERCC1 and MUS81-EME1 nucleases and FAN1 (Kottemann and Smogorzewska, 2013). ICL incision converts the stalled replication fork into a one-ended DNA double-strand break (DSB), which is repaired by HR. Interestingly, FA phenotypes can be partially rescued by inhibition of nonhomologous end-joining (NHEJ), suggesting that the FA pathway not only promotes error-free HR but also actively suppresses inappropriate repair of DSB intermediates by NHEJ in order to prevent chromosomal instability (Adamo et al., 2010; Pace et al., 2010).

Although FANCD2 is critically important for ICL repair, its contribution to HR remains largely elusive (Nakanishi et al., 2011; Smogorzewska et al., 2007). HR is initiated by DNA-end resection, which occurs in human cells through the combined action of CtIP and the MRE11-RAD50-NBS1 (MRN) complex, together with DNA2 or EXO1 nucleases (Nimonkar et al., 2011; Sartori et al., 2007). Importantly, DNA-end resection is a key determinant of DSB repair pathway choice, as it commits cells to HR, while, at the same time, suppresses NHEJ (Chapman et al., 2012). A putative connection between the resection machinery and the FA pathway was recently proposed, based on data showing that DNA2 and EXO1 depletion leads to cisplatin hypersensitivity (Karanja et al., 2012). Additionally, CtIP was shown to accumulate at sites of locally induced ICLs (Duquette et al., 2012). However, the contribution of DNA-end resection to ICL repair and the regulation of CtIP by the FA pathway have not yet been thoroughly investigated.

RESULTS

FANCD2 Is Required for CtIP Localization to ICL Damage

Similar to FA cells, we observed that CtIP depletion results in hypersensitivity and increased chromosomal aberrations following MMC treatment, implicating a key role for CtIP in ICL repair (Figures 1A, S1A, and S1B). Because FANCD2 monoubiquitination constitutes a key step of the FA pathway, we investigated

OPEN ACCESS
CellPress

Please cite this article in press as: Murina et al., FANCD2 and CtIP Cooperate to Repair DNA Interstrand Crosslinks, Cell Reports (2014), http://dx.doi.org/10.1016/j.celrep.2014.03.069

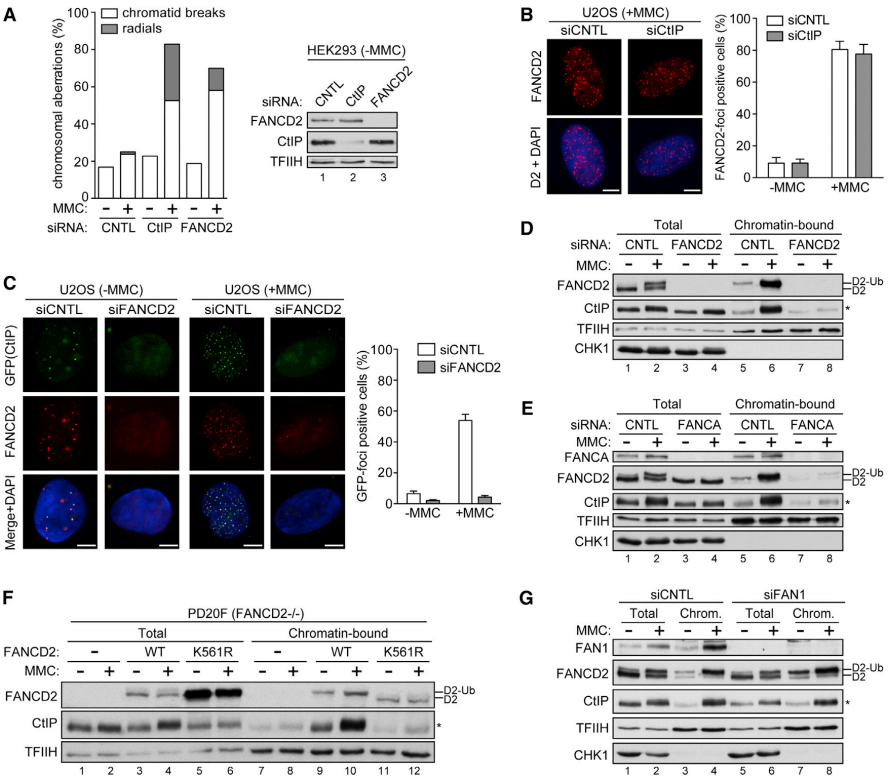

Figure 1. FANCD2 Is Required for the Accumulation of CtIP at Sites of ICL Damage

(A) Metaphase spreads from HEK293 cells transfected with the indicated small interfering RNAs (siRNAs) and treated for 20 hr with MMC (25 ng/ml) were analyzed for chromosomal aberrations. A total of 100 metaphase spreads from three independent experiments were analyzed for each condition. The percentages of cells displaying chromatid breaks or radial chromosomes are shown (see also Figure S1B).

(B) After 48 hr of transfection with indicated siRNAs, U2OS cells grown on coverslips were treated for 24 hr with MMC (120 ng/ml), pre-extracted, fixed, and immunostained for FANCD2. Nuclei were visualized by DAPI-staining. Graph shows the percentage of cells displaying more than ten FANCD2 foci/nuclei.

(C) U2OS cells stably expressing GFP-tagged CtIP were transfected with indicated siRNAs, and 48 hr later, cells grown on coverslips were treated as in (B) and immunostained for FANCD2. Graph shows the percentage of cells displaying more than ten GFP-CtIP foci/nuclei.

(D and E) U2OS cells were transfected with indicated siRNAs, and 48 hr later, cells were treated as in (B) and extracts were analyzed by immunoblotting.

(F) FANCD2 mutant human fibroblasts (PD20F) and PD20F stably expressing wild-type FANCD2 (WT) or K561R mutant FANCD2 were treated as in (B) and harvested for immunoblot analysis (see also Figure S1H).

(G) U2OS cells were transfected with FAN1 siRNA and processed as in (D).

In (B) and (C), for each condition, at least 100 cells were scored and the data are presented as the mean ± SD (n = 3). The scale bar represents 5 μm.

whether CtIP affects FANCD2 foci formation. However, silencing of CtIP did not significantly change the assembly of FANCD2 foci after MMC treatment (Figure 1B). Moreover, FANCD2 monoubiquitination and chromatin assembly still efficiently occurred in CtIP-depleted cells (Figures S1C and S1D). Recently, it was shown that the knockdown of CtIP leads to a 2-fold reduction in FANCD2 accumulation at ICLs induced by 8-methoxypsoralen plus UVA laser microirradiation (PUVA) (Duquette et al., 2012). Therefore, we subjected CtIP-depleted cells to PUVA treatment and noticed partially reduced levels of monoubiquitinated FANCD2 on chromatin (Figures S1E and S1F). Taken together, our data indicate that CtIP is not strictly required for FANCD2 monoubiquitination in response to ICL-inducing agents but that its loss may lead to a negative feedback loop limiting FA pathway activation during ICL repair.

We also noticed that CtIP was highly enriched on chromatin upon MMC or PUVA treatment (Figures S1C and S1F). Consistent with this, ICL damage caused a strong increase in CtIP foci that colocalized with FANCD2 (Figure 1C). Remarkably, both spontaneous and damage-induced CtIP foci were abrogated in FANCD2-depleted cells (Figure 1C). Accordingly, FANCD2 depletion impaired CtIP chromatin association in

Please cite this article in press as: Murina et al., FANCD2 and CtIP Cooperate to Repair DNA Interstrand Crosslinks, Cell Reports (2014), http://dx.doi.org/10.1016/j.celrep.2014.03.069

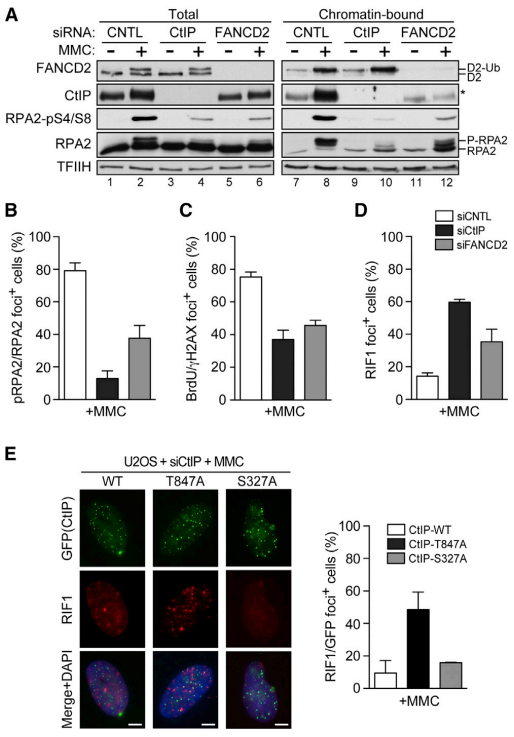

Figure 2. FANCD2 and CtIP Promote DNA-End Resection during ICL Repair

(A) U2OS cells were transfected with indicated small interfering RNAs (siRNAs), and 48 hr after siRNA transfection, cells were either mock-treated or treated for 24 hr with MMC (120 ng/ml) and extracts were analyzed by immunoblotting. RPA2 and P-RPA2 represent nonmodified and hyperphosphorylated forms of RPA2, respectively.

(B) Same cells as in (A) were grown on coverslips, pre-extracted, fixed, and coimmunostained for RPA2-pS4/S8 (pRPA2) and RPA2 (see also Figure S2C). Graph shows the percentage of RPA2-foci-positive cells displaying more than ten pRPA2 foci.

(C) Same cells as in (A) were coimmunostained for γH2AX and BrdU to visualize single-stranded DNA under nondenaturing conditions (see also Figure S2D). Graph shows the percentage of γH2AX-foci-positive cells displaying more than ten BrdU foci.

(D) Same cells as in (A) were immunostained for RIF1 (see also Figure S2E). Graph shows the percentage of nuclei displaying more than ten RIF1 foci.

(E) U2OS cells were transfected with CtIP siRNA, and 24 hr post-siRNA transfection, cells were transfected with siRNA-resistant GFP-tagged CtIP wild-type (WT), T847A, or S327A mutant CtIP (see also Figure S2F). After 48 hr of siRNA transfection, cells were treated as in (A) and immunostained for RIF1. Graph shows the percentage of GFP-foci positive cells displaying more than 10 RIF1 foci. The scale bar represents 5 μm.

In (B)–(E), for each condition, at least 100 cells were scored and data are presented as the mean ± SEM (n = 3).

MMC- and PUVA-treated cells (Figures 1D and S1G). In response to ICL damage, FANCD2 becomes monoubiquitinated at K561 by the FA core complex (Garcia-Higuera et al., 2001; Meetei et al., 2003). Depletion of FANCA, a subunit of the FA core complex, abolished both FANCD2 and CtIP association with damaged chromatin (Figure 1E). Importantly, impaired CtIP accumulation at ICLs in FANCD2-deficient fibroblasts (PD20F) was restored by complementation with wild-type (WT) FANCD2, but not with the K561R mutant (Figures 1F and S1H). In addition, CtIP failed to form MMC-induced foci in cells pretreated with the proteasome inhibitor MG-132, which leads to the sequestration of ubiquitin in the cytoplasm, further indicating that FANCD2 monoubiquitination is a prerequisite for CtIP localization to ICLs (Figure S1I).

During the initial processing of DSBs, CtIP acts together with the MRE11-RAD50-NBS1 (MRN) complex. We therefore explored whether efficient localization of CtIP to ICLs may require the MRN complex. However, while NBS1 downregulation resulted in defective chromatin association of MRE11, the levels of chromatin-bound FANCD2 and CtIP remained unaltered (Figure S1J). On the other hand, monoubiquitinated FANCD2 was reported to directly interact with and recruit FAN1 and SLX4 to coordinate ICL incision (Kottemann and Smogorzewska, 2013; Yamamoto et al., 2011). However, depletion of FAN1 or SLX4 did not significantly affect the binding of CtIP to damaged chromatin (Figures 1G and S1K). Collectively, our results suggest that proper localization of CtIP to ICLs is controlled by FANCD2 but occurs independently of both MRN and structure-specific nucleases involved in ICL incision.

FANCD2 Facilitates CtIP-Mediated DNA-End Resection during ICL Repair

We observed that both MMC and PUVA treatment resulted in robust RPA2-S4/S8 phosphorylation (Figures S2A and S1E). RPA2 phosphorylation, particularly at S4 and S8, has been widely used as a surrogate marker for single-stranded DNA (ssDNA) that is generated by DNA-end resection (Kousholt et al., 2012). Remarkably, knockdown of CtIP or FANCD2 strongly impaired RPA2 hyperphosphorylation in response to ICL-inducing agents, which was particularly evident in the chromatin-bound fractions (Figures 2A and S2B). Likewise, the percentage of cells with RPA2-pS4/S8 foci was significantly reduced in CtIP- or FANCD2-depleted cells (Figures 2B and S2C). Moreover, by immunostaining of cells with anti-bromodeoxyuridine (anti-BrdU), we found that MMC triggered substantial ssDNA formation, which was reduced upon depletion of CtIP or FANCD2 (Figures 2C and S2D). Impaired DNA-end resection commits cells to error-prone repair of DSBs by NHEJ. Recently, RIF1 was characterized as a key NHEJ-promoting factor by virtue of its role in counteracting resection (Chapman et al., 2013; Di Virgilio et al., 2013; Escribano-Díaz et al., 2013; Zimmermann et al., 2013). Indeed, MMC-induced RIF1 foci were elevated in CtIP- or FANCD2-depleted cells, further supporting the idea that both factors promote DNA-end resection and, thus, suppress NHEJ during ICL repair (Figures 2D and S2E).

To further substantiate the role of CtIP-dependent resection in ICL repair, we monitored RIF1 foci in cells expressing GFP-tagged CtIP-WT, CtIP-T847A, or CtIP-S327A (Figure S2F). The mutated residues in CtIP represent CDK phosphorylation sites required for resection (T847A) or for interaction with BRCA1 (S327A) (Figure S2G) (Huertas and Jackson, 2009; Yu and

OPEN ACCESS
CellPress

Please cite this article in press as: Murina et al., FANCD2 and CtIP Cooperate to Repair DNA Interstrand Crosslinks, Cell Reports (2014), http://dx.doi.org/10.1016/j.celrep.2014.03.069

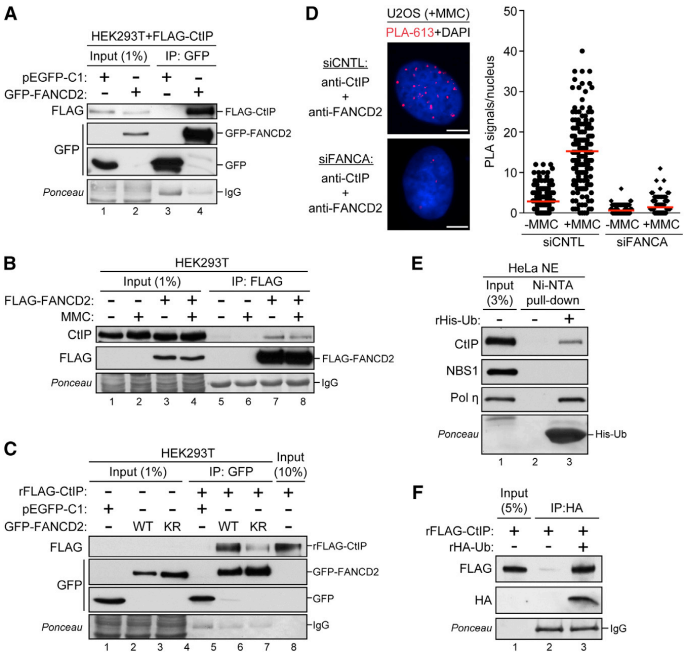

Figure 3. CtIP Physically Interacts with FANCD2 and Ubiquitin

(A) HEK293T cells were cotransfected with FLAG-CtIP along with either empty vector or GFP-FANCD2, and 48 hr after transfection, cells were lysed in NP-40 buffer and whole cell extracts were analyzed before (input) or after immunoprecipitation (IP) with anti-GFP (see also Figure S3A).

(B) HEK293T cells were transfected with either empty vector or FLAG-FANCD2, and 48 hr post-transfection, cells were either mock-treated or treated for 24 hr with MMC (120 ng/ml). Cells were lysed in Triton-X buffer, and whole-cell extracts were analyzed before (input) or after IP using anti-FLAG M2 affinity resin.

(C) HEK293T cells were transfected with empty vector, GFP-FANCD2 (WT), or GFP-FANCD2 K561R (KR). Then 48 hr after transfection, cells were lysed in NP-40 buffer and whole-cell extracts were subjected to IP with anti-GFP. After stringent washings, immunoprecipitated GFP-tagged proteins were incubated with 0.5 μg of recombinant FLAG-tagged CtIP (rFLAG-CtIP; see also Figure S3B). Inputs and recovered protein complexes were analyzed by immunoblotting.

(D) U2OS cells transfected with the indicated siRNAs were left untreated or treated as in (B). After pre-extraction, cells were fixed on coverslips and incubated with antibodies against CtIP and FANCD2 before the detection of protein-protein interactions using a fluorescently labeled probe (PLA-613). Nuclei were visualized by DAPI staining. Graph shows the quantification of the PLA signals/nucleus. PLA signals from at least 100 cells were analyzed (n = 3) (see also Figures S3C and S3D). The scale bar represents 5 μm.

(E) His alone (–) or recombinant His-tagged ubiquitin (rHis-Ub) coupled to nickel nitrilotriacetic acid (Ni-NTA) agarose beads were incubated with HeLa nuclear extracts (NE). Input and precipitated bead fractions from the pull-downs were subjected to immunoblotting. Ponceau staining is shown to indicate the amounts of rHis-Ub used in the pull-down assay.

(F) Recombinant FLAG-tagged CtIP was incubated either alone or together with recombinant hemagglutinin (HA)-tagged ubiquitin and the samples were subjected to IP with anti-HA. Inputs and recovered protein complexes were analyzed by immunoblotting.

Chen, 2004). Our analysis revealed a strong increase in RIF1 foci in MMC-treated T847A mutant cells, whereas the S327A mutation had no significant impact on RIF1 foci formation (Figure 2E). In agreement with this result, T847A mutant cells were hypersensitive to MMC, whereas the viability of cells expressing CtIP-S327A was similar to CtIP-WT cells, further supporting the idea that BRCA1-CtIP interaction is not required for resection during ICL repair (Figures S2H and S2I) (Reczek et al., 2013). Thus far, our findings suggest a pivotal regulatory role for FANCD2 in priming CtIP-mediated DNA-end resection to prevent aberrant NHEJ activity following ICL damage.

CtIP Physically Interacts with FANCD2 and Ubiquitin

Given that CtIP localization to sites of ICL damage is facilitated by FANCD2, we next addressed whether they exist in a complex and found that FLAG-CtIP efficiently coimmunoprecipitated with GFP-FANCD2, and vice versa (Figures 3A and S3A). Moreover, we were able to specifically detect endogenous CtIP coimmunoprecipitating with FLAG-FANCD2 but did not observe significant changes in complex formation upon MMC treatment, suggesting that monoubiquitination of FANCD2 may not be essential for CtIP binding (Figure 3B). In order to further address this issue, we mixed recombinant CtIP purified from insect cells with GFP-FANCD2 immunoprecipitated from human embryonic kidney 293T (HEK293T) cells. While CtIP efficiently bound to FANCD2-WT, it only weakly interacted with the FANCD2-K561R mutant, indicating that FANCD2 and CtIP physically interact and that complex formation might be reinforced by FANCD2 monoubiquitination (Figures 3C and S3B).

To verify the existence of endogenous CtIP-FANCD2 complexes, we performed proximity ligation assays (in situ PLA). As shown in Figure 3D, we could readily detect nuclear PLA signals in undamaged cells, which significantly increased in numbers upon MMC treatment, indicating that the FANCD2-CtIP interaction is enhanced following ICL damage. Moreover, we observed a strong reduction in CtIP-FANCD2 complex formation in FANCA-depleted, but not SLX4- or FAN1-depleted, cells (Figures 3D, S3C, and S3D). These findings further support the importance of FANCD2 monoubiquitination for the accumulation of CtIP at damaged chromatin, presumably by facilitating FANCD2-CtIP interaction. Although sequence analysis revealed that CtIP does not contain any known ubiquitin-binding motifs (Hofmann,

Please cite this article in press as: Murina et al., FANCD2 and CtIP Cooperate to Repair DNA Interstrand Crosslinks, Cell Reports (2014), http://dx.doi.org/10.1016/j.celrep.2014.03.069

2009), our results prompted us to examine whether CtIP can bind to ubiquitin. As shown in Figure 3E, we discovered that CtIP is able to interact with ubiquitin, although less efficiently compared to Polη that contains a ubiquitin-binding domain (UBD) (Bienko et al., 2005; Plosky et al., 2006). Furthermore, we observed comparable ubiquitin binding abilities of GFP-CtIP and UBZ-domain containing GFP-SLX4 (Figure S3E) (Yamamoto et al., 2011). However, while the ubiquitin I44A mutant completely abolished UBZ-mediated interactions of SLX4 and Polη with ubiquitin, it did not affect the binding of CtIP, implicating a distinct type of ubiquitin recognition (Figure S3F). We were also able to detect an interaction between purified, recombinant proteins, implying that CtIP can directly recognize ubiquitin (Figure 3F). Collectively, these data demonstrate that CtIP interacts with FANCD2 and that FANCD2 monoubiquitination enhances FANCD2-CtIP complex formation, perhaps owing to the ability of CtIP to bind ubiquitin.

FANCD2-CtIP Interaction Promotes Crosslink Resistance

To establish the functional significance of the FANCD2-CtIP interaction for ICL repair, we sought to identify the FANCD2-binding motif in CtIP. Whereas FANCD2 did not bind to a region of CtIP containing putative coiled-coil motifs (45–160), it bound efficiently to fragments of CtIP comprising amino acid (aa) residues 45–298 or 45–371 (Figure 4A), highlighting the region between aa residues 160–298 of CtIP to be important for FANCD2 binding. Detailed protein sequence analysis of this region revealed four motifs with high sequence conservation between vertebrates (Figure S4A). Remarkably, cells expressing RRK/AAA or RYIE/AAIA mutant variants of CtIP were impaired in MMC-induced GFP-CtIP foci formation and showed increased RIF1 foci (Figures S4B and S4C). Consistent with a defect in CtIP foci formation, RRK/AAA and RYIE/AAIA mutants exhibited reduced FANCD2 binding in glutathione S-transferase (GST) pull-down experiments (Figures 4B and 4C). Moreover, PLA signals were reduced in both CtIP mutants after MMC treatment, further supporting the role of RRK and RYIE motifs in CtIP-FANCD2 interaction (Figures 4D and 4E). MMC-induced CtIP foci were also abrogated in U2OS cells stably expressing GFP-tagged CtIP-RRK/AAA and -RYIE/AAIA mutants, whereas RIF1 foci were significantly increased in those cells (Figure 4F). However, both CtIP mutants were efficiently recruited to DSB-containing tracks generated by laser microirradiation (Figure S4D). Underscoring a differential regulation of CtIP in response to ICL damage, CtIP recruitment to laser-induced DNA lesions was FANCD2-independent (Figure S4E). Of note, a truncated CtIP mutant lacking residues 153–322 was still proficient in ubiquitin binding, indicating that neither RRK (aa 177–179) nor RYIE (aa 185-188) sequence motifs are required for the interaction between CtIP and ubiquitin (Figures S4F and S4G). Finally, both RRK/AAA and RYIE/AAIA mutant cells were hypersensitive to MMC, further supporting the idea that FANCD2 regulates CtIP functionality during ICL repair (Figure 4G).

CtIP Counteracts ICL-Induced DNA Damage in the Absence of FANCD2 Activation

To genetically determine the epistatic relationship between CtIP and FANCD2 in ICL repair, we generated an MRC5 cell line stably expressing doxycycline (DOX)-inducible small hairpin RNA (shRNA) against CtIP (Figure 5A). Interestingly, depletion of FANCD2 in DOX-treated MRC5 cells led to a further increase in MMC hypersensitivity (Figures 5A and 5B). In agreement with this, survival of PD20 cells upon MMC treatment was further reduced after silencing of CtIP (Figure S5A). CtIP/FANCD2-deficient MRC5 cells also showed elevated levels of MMC-induced RIF1 foci and radial chromosomes compared to cells depleted for either factor alone, indicative of potent, illegitimate repair of DSBs by NHEJ (Figures 5C, 5D, S5B, and S5C). Previously, BRCA1 has been reported to regulate the accumulation of FANCD2 into repair foci and CtIP recruitment to PUVA-induced ICLs (Garcia-Higuera et al., 2001; Duquette et al., 2012). Further supporting a dual, nonredundant role for CtIP in ICL repair, knockdown of BRCA1 in DOX-treated MRC5^{shCtIP} cells resulted in increased MMC sensitivity (Figure S5D). Thus, our data suggest that CtIP-dependent DNA-end resection is essential to counteract the toxic effects of ICL damage when the FA/BRCA signaling pathway is compromised.

ATR kinase is a major regulator of the FA pathway and promotes FANCD2/I monoubiquitination (Andreassen et al., 2004; Smogorzewska et al., 2007). Recently, both ATM and ATR kinases have been implicated in DNA-damage-induced CtIP phosphorylation (Peterson et al., 2013; Wang et al., 2013). In order to gain further mechanistic insight into the regulation of CtIP during ICL repair, we applied selective ATR and/or ATM inhibitors prior to MMC treatment (Reaper et al., 2011). CtIP and RPA2 phosphorylation was strongly elevated after ATR inhibition; meanwhile, FANCD2 monoubiquitination and CHK1 phosphorylation were reduced as expected (Figure 5E, lane 2). Interestingly, MMC-induced hyperphosphorylation of CtIP and, to a lesser extent, of RPA2 was reversed when both inhibitors were combined (Figure 5E, lane 4). These data suggest that ATM gets hyperactivated when ATR kinase is blocked, probably as a result of prevalent cleavage of collapsed replication forks into DSBs. The structure-specific endonuclease MUS81-EME1 has been implicated in the conversion of stalled replication forks into DSBs, particularly in checkpoint-deficient cells (Hanada et al., 2006; Murfuni et al., 2013). Indeed, inhibition of ATR combined with MUS81 depletion significantly reduced the phosphorylation of H2AX and KAP1, both established ATM targets, indicating that MUS81 is at least partially required for the processing of ICL-stalled forks into DSBs (Figure 5F). Remarkably, phosphorylation levels of CtIP were also decreased, further implying CtIP in promoting DNA-end resection and HR of replication-associated DSBs in the absence of a fully functional FA pathway. Taken together, our results demonstrate that during conventional ICL repair, CtIP-mediated DNA-end resection is regulated by FANCD2 but that CtIP also helps prevent illegitimate repair of stalled forks in FA-pathway-defective cells.

DISCUSSION

CtIP is an essential factor required for the initiation of DNA-end resection during HR and, thus, for the suppression of DSB repair by NHEJ. Given that FA-pathway-deficient cells exhibit increased chromosomal instability in response to ICL damage, FA proteins have also been implicated in NHEJ inhibition. Indeed, we

OPEN ACCESS CellPress

Please cite this article in press as: Murina et al., FANCD2 and CtIP Cooperate to Repair DNA Interstrand Crosslinks, Cell Reports (2014), http://dx.doi.org/10.1016/j.celrep.2014.03.069

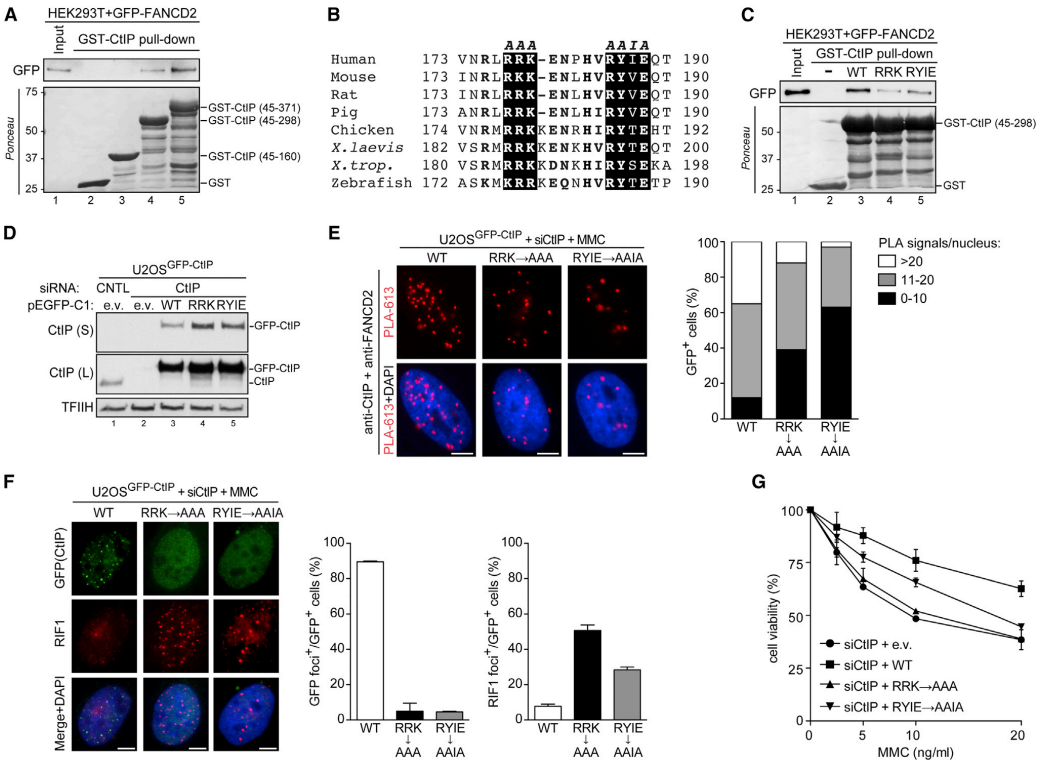

Figure 4. Functional Characterization of CtIP Mutants Impaired in FANCD2 Binding

(A) GST or GST-CtIP proteins were coupled to glutathione Sepharose beads and incubated with HEK293T cell lysates transiently overexpressing GFP-FANCD2. The recovered materials were analyzed by immunoblotting.

(B) Alignment of the putative FANCD2-interacting region in CtIP orthologs. RRK and RYxE motifs are highlighted in black boxes. Other, highly conserved amino acid residues are marked in bold typeface (see also Figure S4A).

(C) GST or indicated GST-CtIP (45–298) proteins were coupled to glutathione Sepharose beads and incubated with HEK293T cell lysates transiently overexpressing GFP-FANCD2. The recovered materials were analyzed by immunoblotting.

(D) U2OS cells stably expressing siRNA-resistant GFP-tagged wild-type (WT) and mutant (RRK/AAA and RYIE/AAIA) CtIP were transfected with CtIP siRNA for 72 hr, and whole-cell extracts were analyzed by immunoblotting. (S) and (L) indicate short and long exposures of the same immunoblot, respectively.

(E) Same cells as in (D) were transfected with CtIP siRNA. After 48 hr of siRNA transfection, cells grown on coverslips were treated for 24 hr with MMC (120 ng/ml), fixed, and incubated with antibodies against CtIP and FANCD2 before the detection of protein-protein interactions using a fluorescently labeled probe (PLA-613). Graph shows the quantification of the PLA signals/nucleus in GFP-positive cells. PLA signals from at least 100 cells were analyzed (n = 2).

(F) Same cells as in (E) were fixed and immunostained for RIF1. Graphs show the percentage of GFP-positive cells displaying more than ten GFP-CtIP foci or more than ten RIF1 foci, respectively. For each condition, at least 100 cells were scored. Data are presented as the mean ± SEM (n = 2).

(G) Same cells as in (D) were either mock-treated or continuously treated with the indicated doses of MMC, and the survival was determined after 5 days using the CellTiter-Blue cell viability assay. Data are presented as the mean ± SD (n = 3).

In (E) and (F), the scale bar represents 5 μm.

observed that depletion of CtIP or FANCD2 leads to an increase in radial chromosome formation and RIF1 foci after MMC treatment, indicative of enhanced NHEJ activity. Accordingly, DNA-end resection, as measured by phosphorylated RPA2 and BrdU focus formation, was reduced in CtIP- or FANCD2-depleted cells. Several mechanisms have been proposed how FA proteins prevent NHEJ, including the restriction of NHEJ factors to access DNA termini, cryptic exonuclease, or nucleosome-assembly activity of FANCD2 (Adamo et al., 2010; Pace et al., 2010; Sato et al., 2012). Based on our data, we propose that FANCD2 suppresses error-prone NHEJ through promoting CtIP-dependent resection (Figure S6).

We observed that monoubiquitinated FANCD2 tethers CtIP to damaged chromatin and identified two short, highly conserved motifs within CtIP responsible for CtIP-FANCD2 interaction. Consequently, CtIP mutants defective in FANCD2 binding are

Please cite this article in press as: Murina et al., FANCD2 and CtIP Cooperate to Repair DNA Interstrand Crosslinks, Cell Reports (2014), http://dx.doi.org/10.1016/j.celrep.2014.03.069

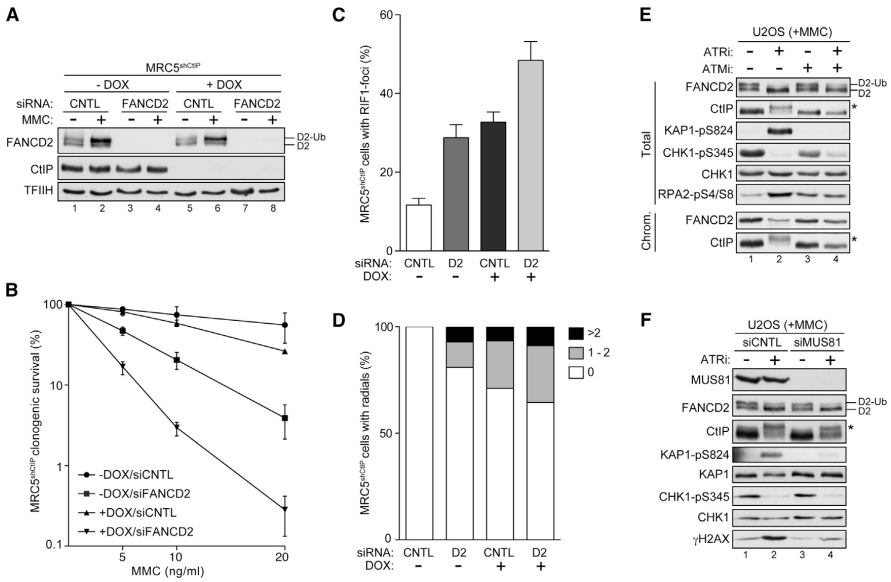

Figure 5. CtIP Contributes to Genome Stability in FA-Pathway-Deficient Cells

(A) MRC5 cells stably expressing doxycycline (DOX)-inducible shRNA against CtIP (MRC5^{shCtIP}) were transfected with indicated siRNAs. Then 24 hr after siRNA transfection, cells were cultivated in the absence or presence of DOX (1 μg/ml) for 48 hr. Cells were treated with MMC (120 ng/ml) for 24 hr and subjected to immunoblotting.

(B) Same cells as in (A) were treated for 24 hr with indicated doses of MMC, and survival was determined after 10 days by colony-formation assay. Data are presented as the mean ± SD (n = 3).

(C) Same cells as in (A) were immunostained for RIF1. Graph shows the percentage of RIF1-foci-positive cells displaying more than ten RIF1 foci. For each condition, at least 100 cells were scored. Data are presented as the mean ± SD (n = 3) (see also Figure S5B).

(D) Metaphase spreads from the same cells as in (A) treated for 20 hr with MMC (20 ng/ml) were analyzed for chromosomal aberrations. A total of 45 metaphase spreads from three independent experiments were analyzed for each condition. The percentages of cells displaying radial chromosomes are shown (see also Figure S5C).

(E) U2OS cells were pretreated for 15 min with DMSO, ATR inhibitor (VE-821, 1 μM), ATM inhibitor (KU-55933, 10 μM), or both inhibitors together. Cells were then treated for 20 hr with MMC (120 ng/ml), and extracts were analyzed by immunoblotting.

(F) U2OS cells were transfected with MUS81 siRNA, and 48 hr after siRNA transfection, cells were pretreated for 15 min with DMSO or ATR inhibitor (VE-821, 1 μM). Cells were then treated as in (E) and harvested for immunoblot analysis.

impaired in the formation of MMC-induced foci. Whereas FANCD2 monoubiquitination may not be essential for the physical interaction with CtIP, it is required to retain CtIP on damaged chromatin. Remarkably, we show that CtIP directly interacts with ubiquitin in vitro. Although bioinformatic analysis failed to predict any motifs resembling known UBDs in CtIP, it is plausible that the FANCD2-CtIP interaction is reinforced by the ability of CtIP to recognize ubiquitin. However, a CtIP mutant lacking both FANCD2-interacting motifs was proficient in ubiquitin binding. Furthermore, a mutant form of ubiquitin (I44A) defective in most UBD-mediated interactions was still able to interact with CtIP. Therefore, one could hypothesize that CtIP may employ a dual mode of recognizing monoubiquitinated FANCD2, but, if so, binds ubiquitin by a unique mechanism that involves a new type of UBD (Bomar et al., 2007). Clearly, further investigations are needed to establish the role of CtIP-ubiquitin interaction in the DNA damage response. On the other hand, it was proposed that monoubiquitination of FANCD2 could alter FANCD2 conformation (Joo et al., 2011). Thus, it is tempting to speculate that such structural changes in FANCD2 stimulate CtIP-FANCD2 interaction. Finally, the FANCD2/I complex may also facilitate CtIP recruitment to damaged chromatin via its histone chaperone activity (Sato et al., 2012). Increased MMC-induced sensitivity and RIF1 foci formation in cells expressing CtIP mutants (RRK/AAA and RYIE/AAIA) further strengthen the significance of CtIP-FANCD2 interaction in ICL repair. Notably, R177Q and Y186C, two cancer-associated missense mutations in human CtIP, map exactly to the region implicated in FANCD2 interaction (Figure S4A). Given that RRK and RYIE motifs reside in a highly conserved stretch of 12 amino acids, it is also reasonable to think that they constitute a single FANCD2 interaction "domain." These data are similar to those described in the accompanying paper by Unno et al. (2014) published in this issue of *Cell Reports*.

Depletion of CtIP in FANCD2-deficient cells aggravates the phenotypes of cells lacking either factor alone, indicating that CtIP contributes to genome stability in FA-pathway-defective

OPEN ACCESS CellPress

Please cite this article in press as: Murina et al., FANCD2 and CtIP Cooperate to Repair DNA Interstrand Crosslinks, Cell Reports (2014), http://dx.doi.org/10.1016/j.celrep.2014.03.069

cells. Likewise, inactivation of FAN1 or SLX4 enhanced crosslink sensitivity of cells compromised in FANCD2 activation, suggesting that these proteins, though being recruited to ICLs by FANCD2, can promote MMC resistance in a FA-pathway-independent manner (Yamamoto et al., 2011; Zhou et al., 2012). Furthermore, only partial epistasis of FANCD2 over CtIP could be explained by an additional role of CtIP upstream of FANCD2 or by the proposed role of FANCD2 in protecting stalled forks from degradation (Duquette et al., 2012; Schlacher et al., 2012). There is increasing evidence that arrested and unprotected replication forks frequently collapse and give rise to DSBs, which can then undergo resection and repair by HR (Couch et al., 2013). Accordingly, we observed enhanced ATM-dependent phosphorylation of CtIP and RPA2 in cells co-treated with MMC and ATR inhibitor, indicative of ongoing DSB resection (Fugger et al., 2013). In line with this, CtIP phosphorylation was reduced upon depletion of MUS81, an endonuclease implicated in the cleavage of stalled forks and DSB formation (Ciccia et al., 2008). Furthermore, CtIP-dependent processing of collapsed forks upon hydroxyurea treatment was recently reported to be beneficial for genome integrity in the absence of FANCM (Blackford et al., 2012). Therefore, we conclude that CtIP can partially suppress genomic instability in the absence of FANCD2, whereas, in FA-pathway-proficient cells, monoubiquitinated FANCD2 coordinates CtIP-mediated DNA-end resection during ICL repair.

EXPERIMENTAL PROCEDURES

Cell Culture and Transfection

U2OS, HEK293T, and HEK293 cells were grown in Dulbecco's modified Eagle's medium (DMEM) supplemented with 10% fetal calf serum (FCS), 100 U/ml penicillin, and 100 μg/ml streptomycin. U2OS clones stably expressing siRNA-resistant forms of GFP-CtIP were described previously (Sartori et al., 2007). FANCD2-deficient cells (PD20F) were obtained from Fanconi Anemia Research Foundation (FARF) and cultured in DMEM supplemented with 10% FCS and standard antibiotics. PD20F cells complemented with FANCD2 wild-type (FARF) or K561R (kindly provided by Josef Jiricny) were grown in standard medium supplemented with 1 μg/ml Puromycin. MRC5^{shCtIP} cells were grown in DMEM supplemented with 10% Tet system approved FCS, 100 U/ml penicillin, 100 μg/ml streptomycin, Blasticidin (5 μg/ml), and Zeocin (250 μg/ml). Plasmids were transfected either by using the standard calcium phosphate method or FuGENE 6 (Roche) according to manufacturer's instructions. Transfection of all siRNA oligos was done with 40 nM final concentration using Lipofectamine RNAiMAX (Invitrogen). Data for survival curves were generated by colony-formation assays as described previously (Sartori et al., 2007).

Triton Extraction

Isolation of Triton-insoluble (chromatin-enriched) fraction was performed as previously described (Peña-Diaz et al., 2012). In brief, cells were rinsed twice in cold PBS and incubated for 5 min on ice in preextraction buffer (25 mM HEPES [pH 7.4], 50 mM NaCl, 1 mM EDTA, 3 mM $MgCl_2$, 300 mM sucrose, 0.5% Triton X-100, and protease inhibitors). After buffer removal, adherent cellular material was harvested by scraping the cells into Laemmli buffer. The chromatin-enriched fraction was then heat denatured, sonicated, and analyzed by immunoblotting.

SUPPLEMENTAL INFORMATION

Supplemental Information includes Supplemental Experimental Procedures and six figures and can be found with this article online at http://dx.doi.org/10.1016/j.celrep.2014.03.069.

AUTHOR CONTRIBUTIONS

O.M. and A.A.S. designed the research. L.P.F. performed the laser microirradiation experiments, and H.A.B. helped with the ubiquitin binding assay. K.H. generated the inducible MRC5^{shCtIP} cell line. All other experiments were performed by O.M. with the help of C.A. and U.K. O.M. and A.A.S. analyzed the data and wrote the paper.

ACKNOWLEDGMENTS

We are very grateful to Minoru Takata and Junya Unno for providing reagents and for communicating results prior to publication. We thank Pavel Janscak for providing purified recombinant human CtIP protein and experimental advice. We are grateful to Agata Smogorzewska, Johan de Winter, Josef Jiricny, Matthias Peter, the Fanconi Anemia Research Fund, and Vertex Pharmaceuticals for providing reagents. We thank Josef Jiricny and Orlando Schärer for critical reading of the manuscript. This work was supported by grants from the Swiss National Science Foundation (31003A_135507 and PDFMP3-127523), the Promedica Stiftung, the Olga Mayenfisch Stiftung, and the Vontobel Foundation (to A.A.S.).

Received: August 30, 2013
Revised: March 4, 2014
Accepted: March 27, 2014
Published: May 1, 2014

REFERENCES

Adamo, A., Collis, S.J., Adelman, C.A., Silva, N., Horejsi, Z., Ward, J.D., Martinez-Perez, E., Boulton, S.J., and La Volpe, A. (2010). Preventing nonhomologous end joining suppresses DNA repair defects of Fanconi anemia. Mol. Cell *39*, 25–35.

Andreassen, P.R., D'Andrea, A.D., and Taniguchi, T. (2004). ATR couples FANCD2 monoubiquitination to the DNA-damage response. Genes Dev. *18*, 1958–1963.

Bienko, M., Green, C.M., Crosetto, N., Rudolf, F., Zapart, G., Coull, B., Kannouche, P., Wider, G., Peter, M., Lehmann, A.R., et al. (2005). Ubiquitin-binding domains in Y-family polymerases regulate translesion synthesis. Science *310*, 1821–1824.

Blackford, A.N., Schwab, R.A., Nieminuszczy, J., Deans, A.J., West, S.C., and Niedzwiedz, W. (2012). The DNA translocase activity of FANCM protects stalled replication forks. Hum. Mol. Genet. *21*, 2005–2016.

Bomar, M.G., Pai, M.-T., Tzeng, S.-R., Li, S.S.-C., and Zhou, P. (2007). Structure of the ubiquitin-binding zinc finger domain of human DNA Y-polymerase eta. EMBO Rep. *8*, 247–251.

Chapman, J.R., Taylor, M.R.G., and Boulton, S.J. (2012). Playing the end game: DNA double-strand break repair pathway choice. Mol. Cell *47*, 497–510.

Chapman, J.R., Barral, P., Vannier, J.-B., Borel, V., Steger, M., Tomas-Loba, A., Sartori, A.A., Adams, I.R., Batista, F.D., and Boulton, S.J. (2013). RIF1 is essential for 53BP1-dependent nonhomologous end joining and suppression of DNA double-strand break resection. Mol. Cell *49*, 858–871.

Ciccia, A., McDonald, N., and West, S.C. (2008). Structural and functional relationships of the XPF/MUS81 family of proteins. Annu. Rev. Biochem. *77*, 259–287.

Couch, F.B., Bansbach, C.E., Driscoll, R., Luzwick, J.W., Glick, G.G., Bétous, R., Carroll, C.M., Jung, S.Y., Qin, J., Cimprich, K.A., and Cortez, D. (2013). ATR phosphorylates SMARCAL1 to prevent replication fork collapse. Genes Dev. *27*, 1610–1623.

Deans, A.J., and West, S.C. (2011). DNA interstrand crosslink repair and cancer. Nat. Rev. Cancer *11*, 467–480.

Di Virgilio, M., Callen, E., Yamane, A., Zhang, W., Jankovic, M., Gitlin, A.D., Feldhahn, N., Resch, W., Oliveira, T.Y., Chait, B.T., et al. (2013). Rif1 prevents resection of DNA breaks and promotes immunoglobulin class switching. Science *339*, 711–715.

Please cite this article in press as: Murina et al., FANCD2 and CtIP Cooperate to Repair DNA Interstrand Crosslinks, Cell Reports (2014), http://dx.doi.org/10.1016/j.celrep.2014.03.069

Duquette, M.L., Zhu, Q., Taylor, E.R., Tsay, A.J., Shi, L.Z., Berns, M.W., and McGowan, C.H. (2012). CtIP is required to initiate replication-dependent interstrand crosslink repair. PLoS Genet. *8*, e1003050.

Escribano-Díaz, C., Orthwein, A., Fradet-Turcotte, A., Xing, M., Young, J.T.F., Tkáč, J., Cook, M.A., Rosebrock, A.P., Munro, M., Canny, M.D., et al. (2013). A cell cycle-dependent regulatory circuit composed of 53BP1-RIF1 and BRCA1-CtIP controls DNA repair pathway choice. Mol. Cell *49*, 872–883.

Fugger, K., Chu, W.K., Haahr, P., Kousholt, A.N., Beck, H., Payne, M.J., Hanada, K., Hickson, I.D., and Sørensen, C.S. (2013). FBH1 co-operates with MUS81 in inducing DNA double-strand breaks and cell death following replication stress. Nat Commun *4*, 1423.

Garcia-Higuera, I., Taniguchi, T., Ganesan, S., Meyn, M.S., Timmers, C., Hejna, J., Grompe, M., and D'Andrea, A.D. (2001). Interaction of the Fanconi anemia proteins and BRCA1 in a common pathway. Mol. Cell *7*, 249–262.

Hanada, K., Budzowska, M., Modesti, M., Maas, A., Wyman, C., Essers, J., and Kanaar, R. (2006). The structure-specific endonuclease Mus81-Eme1 promotes conversion of interstrand DNA crosslinks into double-strands breaks. EMBO J. *25*, 4921–4932.

Hofmann, K. (2009). Ubiquitin-binding domains and their role in the DNA damage response. DNA Repair (Amst.) *8*, 544–556.

Huertas, P., and Jackson, S.P. (2009). Human CtIP mediates cell cycle control of DNA end resection and double strand break repair. J. Biol. Chem. *284*, 9558–9565.

Joo, W., Xu, G., Persky, N.S., Smogorzewska, A., Rudge, D.G., Buzovetsky, O., Elledge, S.J., and Pavletich, N.P. (2011). Structure of the FANCI-FANCD2 complex: insights into the Fanconi anemia DNA repair pathway. Science *333*, 312–316.

Karanja, K.K., Cox, S.W., Duxin, J.P., Stewart, S.A., and Campbell, J.L. (2012). DNA2 and EXO1 in replication-coupled, homology-directed repair and in the interplay between HDR and the FA/BRCA network. Cell Cycle *11*, 3983–3996.

Kim, H., and D'Andrea, A.D. (2012). Regulation of DNA cross-link repair by the Fanconi anemia/BRCA pathway. Genes Dev. *26*, 1393–1408.

Knipscheer, P., Räschle, M., Smogorzewska, A., Enoiu, M., Ho, T.V., Schärer, O.D., Elledge, S.J., and Walter, J.C. (2009). The Fanconi anemia pathway promotes replication-dependent DNA interstrand cross-link repair. Science *326*, 1698–1701.

Kottemann, M.C., and Smogorzewska, A. (2013). Fanconi anaemia and the repair of Watson and Crick DNA crosslinks. Nature *493*, 356–363.

Kousholt, A.N., Fugger, K., Hoffmann, S., Larsen, B.D., Menzel, T., Sartori, A.A., and Sørensen, C.S. (2012). CtIP-dependent DNA resection is required for DNA damage checkpoint maintenance but not initiation. J. Cell Biol. *197*, 869–876.

Meetei, A.R., de Winter, J.P., Medhurst, A.L., Wallisch, M., Waisfisz, Q., van de Vrugt, H.J., Oostra, A.B., Yan, Z., Ling, C., Bishop, C.E., et al. (2003). A novel ubiquitin ligase is deficient in Fanconi anemia. Nat. Genet. *35*, 165–170.

Moldovan, G.L., and D'Andrea, A.D. (2009). How the fanconi anemia pathway guards the genome. Annu. Rev. Genet. *43*, 223–249.

Murfuni, I., Basile, G., Subramanyam, S., Malacaria, E., Bignami, M., Spies, M., Franchitto, A., and Pichierri, P. (2013). Survival of the replication checkpoint deficient cells requires MUS81-RAD52 function. PLoS Genet. *9*, e1003910.

Nakanishi, K., Cavallo, F., Perrouault, L., Giovannangeli, C., Moynahan, M.E., Barchi, M., Brunet, E., and Jasin, M. (2011). Homology-directed Fanconi anemia pathway cross-link repair is dependent on DNA replication. Nat. Struct. Mol. Biol. *18*, 500–503.

Nimonkar, A.V., Genschel, J., Kinoshita, E., Polaczek, P., Campbell, J.L., Wyman, C., Modrich, P., and Kowalczykowski, S.C. (2011). BLM-DNA2-RPA-MRN and EXO1-BLM-RPA-MRN constitute two DNA end resection machineries for human DNA break repair. Genes Dev. *25*, 350–362.

Pace, P., Mosedale, G., Hodskinson, M.R., Rosado, I.V., Sivasubramaniam, M., and Patel, K.J. (2010). Ku70 corrupts DNA repair in the absence of the Fanconi anemia pathway. Science *329*, 219–223.

Peña-Diaz, J., Bregenhorn, S., Ghodgaonkar, M., Follonier, C., Artola-Borán, M., Castor, D., Lopes, M., Sartori, A.A., and Jiricny, J. (2012). Noncanonical mismatch repair as a source of genomic instability in human cells. Mol. Cell *47*, 669–680.

Peterson, S.E., Li, Y., Wu-Baer, F., Chait, B.T., Baer, R., Yan, H., Gottesman, M.E., and Gautier, J. (2013). Activation of DSB processing requires phosphorylation of CtIP by ATR. Mol. Cell *49*, 657–667.

Plosky, B.S., Vidal, A.E., Fernández de Henestrosa, A.R., McLenigan, M.P., McDonald, J.P., Mead, S., and Woodgate, R. (2006). Controlling the subcellular localization of DNA polymerases iota and eta via interactions with ubiquitin. EMBO J. *25*, 2847–2855.

Reaper, P.M., Griffiths, M.R., Long, J.M., Charrier, J.-D., Maccormick, S., Charlton, P.A., Golec, J.M.C., and Pollard, J.R. (2011). Selective killing of ATM- or p53-deficient cancer cells through inhibition of ATR. Nat. Chem. Biol. *7*, 428–430.

Reczek, C.R., Szabolcs, M., Stark, J.M., Ludwig, T., and Baer, R. (2013). The interaction between CtIP and BRCA1 is not essential for resection-mediated DNA repair or tumor suppression. J. Cell Biol. *201*, 693–707.

Sartori, A.A., Lukas, C., Coates, J., Mistrik, M., Fu, S., Bartek, J., Baer, R., Lukas, J., and Jackson, S.P. (2007). Human CtIP promotes DNA end resection. Nature *450*, 509–514.

Sato, K., Ishiai, M., Toda, K., Furukoshi, S., Osakabe, A., Tachiwana, H., Takizawa, Y., Kagawa, W., Kitao, H., Dohmae, N., et al. (2012). Histone chaperone activity of Fanconi anemia proteins, FANCD2 and FANCI, is required for DNA crosslink repair. EMBO J. *31*, 3524–3536.

Schlacher, K., Wu, H., and Jasin, M. (2012). A distinct replication fork protection pathway connects Fanconi anemia tumor suppressors to RAD51-BRCA1/2. Cancer Cell *22*, 106–116.

Smogorzewska, A., Matsuoka, S., Vinciguerra, P., McDonald, E.R., 3rd, Hurov, K.E., Luo, J., Ballif, B.A., Gygi, S.P., Hofmann, K., D'Andrea, A.D., and Elledge, S.J. (2007). Identification of the FANCI protein, a monoubiquitinated FANCD2 paralog required for DNA repair. Cell *129*, 289–301.

Unno, J., Itaya, A., Taoka, M., Sato, K., Tomida, J., Sakai, W., Sugasawa, K., Ishiai, M., Ikura, T., Toshiaki, I., et al. (2014). FANCD2 binds CTIP and regulates DNA-end resection during DNA interstrand crosslink repair. Cell Rep. *7*, Published online May 1, 2014. http://dx.doi.org/10.1016/j.celrep.2014.04.005.

Wang, H., Shi, L.Z., Wong, C.C.L., Han, X., Hwang, P.Y.-H., Truong, L.N., Zhu, Q., Shao, Z., Chen, D.J., Berns, M.W., et al. (2013). The interaction of CtIP and Nbs1 connects CDK and ATM to regulate HR-mediated double-strand break repair. PLoS Genet. *9*, e1003277.

Yamamoto, K.N., Kobayashi, S., Tsuda, M., Kurumizaka, H., Takata, M., Kono, K., Jiricny, J., Takeda, S., and Hirota, K. (2011). Involvement of SLX4 in interstrand cross-link repair is regulated by the Fanconi anemia pathway. Proc. Natl. Acad. Sci. USA *108*, 6492–6496.

Yu, X., and Chen, J. (2004). DNA damage-induced cell cycle checkpoint control requires CtIP, a phosphorylation-dependent binding partner of BRCA1 C-terminal domains. Mol. Cell. Biol. *24*, 9478–9486.

Zhou, W., Otto, E.A., Cluckey, A., Airik, R., Hurd, T.W., Chaki, M., Diaz, K., Lach, F.P., Bennett, G.R., Gee, H.Y., et al. (2012). FAN1 mutations cause karyomegalic interstitial nephritis, linking chronic kidney failure to defective DNA damage repair. Nat. Genet. *44*, 910–915.

Zimmermann, M., Lottersberger, F., Buonomo, S.B., Sfeir, A., and de Lange, T. (2013). 53BP1 regulates DSB repair using Rif1 to control 5′ end resection. Science *339*, 700–704.

Cell □eports□□olume *7*

□upplemental Information

FANCD2 and CtIP Cooperate in the Repair of DNA Interstrand Crosslinks

□lga Murina□Christine □on Aesch□□fuk □arakus□□oren□a P□Ferretti□□ella A□ □olck□□ay □□nggi□and Alessandro A□□artori

Supplemental Experimental Procedures

Plasmids.

The pcDNA3.1-based expression vectors for FLAG-FANCD2, GFP-FANCD2 and GFP-FANCD2 K561R were kindly provided by Minoru Takata (Kyoto University, Japan). Expression constructs for epitope-tagged CtIP were described previously (Steger et al., 2013). The pGEX-4T1 plasmids for bacterial expression of CtIP fragments were described previously (Sartori et al., 2007). CtIP 45-298 fragment was generated by introducing two stop codons in pGEX-4T1 CtIP 45-371. The pcDNA5-based GFP-SLX4 expression vector was a kind gift from Johan P. de Winter (VU University Medical Center, The Netherlands) (Stoepker et al., 2011). The pET23-based 6xHis-ubiquitin vector for bacterial expression was kindly provided by Matthias Peter (ETH Zurich, Switzerland). All CtIP and ubiquitin mutations were introduced by site-directed mutagenesis using Expand Long Template PCR System (Roche) and confirmed by sequencing. To generate an entry vector harboring shCtIP (target sequence: CGTCAGCCTTACAACGCAA (You et al., 2009)), annealed double-stranded DNA oligos were ligated into pENTR/HI/TO (Invitrogen). The lentiviral destination construct encoding shCtIP (pLenti4-shCtIP) was generated in an *in vitro* recombination reaction after transformation of bacteria with pENTR-shCtIP and pLenti4/DEST (Invitrogen).

siRNA sequences.

All siRNA duplexes were purchased from Microsynth AG, the sequences were as follows: Luciferase (CNTL; CGUACGCGGAAUACUUCGA), CtIP (CtIP-1; GCUAAAACAGGAACGAAUC) and CtIP-2 (UCCACAACAUAAUCCUAAU) (Sartori et al., 2007), FANCD2 (CAGAGUUUGCUUCACUCUCUA) (Kratz et al.,

2010), FANCA (CAGCGTTGAGATATCAAAGAT) (Kim et al., 2008), FAN1 (GUAAGGCUCUUUCAACGUA) (Kratz et al., 2010), NBS1 (GGAGGAAGAUGUCAAUGUUUU) (Yoo et al., 2009), SLX4 (AAACGUGAAUGAAGCAGAAUU) (Svendsen et al., 2009), MUS81 (CAGCCCUGGUGGAUCGAUA) (Neelsen et al., 2013), BRCA1 (GGAACCUGUCUCCACAAAG) (Bruun et al., 2003).

Lentivirus production.

Lentiviruses encoding either the Tet-Repressor protein (TetR) or shCtIP were generated in human 293FT cell line as previously described (Tiscornia et al., 2006). Briefly, 293FT cells were transfected with a lentiviral vector (pLenti6/TR or pLenti4-shCtIP) in combination with ViraPowerTM Packaging Mix using LipofectamineTM 2000 according to the manufacturers protocol (Invitrogen). Virus-containing supernatant was collected 72 h post-transfection and filtered through a sterile 0.45 μm low protein-binding filter (Millex-HV 0.45 μm PVDF, Millipore). The filtrated viral supernatant was aliquoted into 1.5 ml cryovials and stored at -80°C.

Generation of a stable MRC5 cell line with inducible shCtIP expression.

SV40-immortalized MRC5 cells were first transduced with viral supernatant harbouring pLenti6/TR and, 24 h later, infected with viral supernatant containing pLenti4/shCtIP. 48 h after the second transduction, cells were split at low confluency and grown in selection medium containing Blasticidin (5 μg/ml) and ZeocinTM (500 μg/ml) for 11 days. Antibiotic-resistant colonies were isolated, expanded and individual clones screened for doxycycline (DOX) -inducible expression of shCtIP by immunoblotting.

Generation of the stable U2OS cell lines expressing GFP-CtIP-S327A, -RRK/AAA or -RYIE/AAIA.

U2OS cells (40% confluent) were transfected with the pEGFP-C1 plasmid containing siRNA-resistant CtIP cDNA, harbouring corresponding mutations in the coding sequence, using FuGENE 6 (Roche). 24 h after transfection, standard medium was replaced with selection medium containing Genetecin® (G418, GIBCO, 500 μg/ml). The medium was replaced every 2-3 days and antibiotic-resistant colonies were isolated and screened for GFP-CtIP expression by both immunofluorescence microscopy and western blotting.

Immunofluorescence Microscopy

U2OS or MRC5^{shCtIP} cells grown on coverslips were either fixed directly in formaldehyde and permeabilized or pre-extracted for 5 min on ice before fixation in 4% formaldehyde (w/v) in PBS for 12 min as described previously (Sartori et al., 2007). After incubation with indicated primary and appropriate Alexa Fluor-488, -594 and -647 conjugated secondary antibodies (1:1'000) (Life Technologies), coverslips were mounted with Vectrashield® (Vector Laboratories) containing DAPI and sealed. Images were acquired on a Leica DMRB fluorescence microscope. Laser micro-irradiation was performed as described previously (Eid et al., 2010).

Metaphase spread analysis.

HEK293 cells were transfected with indicated siRNAs at a final concentration of 40 nM using Lipofectamine RNAiMax transfection reagent (Invitrogen). 48 hours later cells were either mock-treated or treated with MMC (25 ng/ml) for 20 hours. Prior to harvesting, cells were treated with Colcemid (Gibco) at a final concentration of 0.1

μg/ml for 1 hour. Then, cells were collected in a 15 ml Falcon tube and centrifuged at 200 g for 5 minutes. Cells were resuspended in 5 ml of a hypotonic KCl solution (0.075 M) and incubated for 10 minutes at 37°C. To fix the cells, 1 ml of fixing solution containing Methanol:Acetic acid (3:1) was added to the suspension, mixed and centrifuged at 200 g for 5 minutes. Then, cells were resuspended directly in fixing solution containing Methanol:Acetic acid (3:1), which was added dropwise, while gently vortexing, and spun down. This step was repeated twice. Finally, the cell pellet was resuspended in 0.5-1 ml Methanol:Acetic acid fixing solution depending on the density of the cell suspension. 20 μl (2 drops) of the cell suspension was dropped on a pre-wetted glass slide (45° tilted) from 30 cm distance. Slide was air-dried and DNA was stained with DAPI. Immunofluorescent images were acquired in the DAPI-channel using the Leica DMRB microscope with Leica DFC 360 FX camera and the Leica objective HCX PL AP0 100x.

To prepare metaphase spreads from MRC5^{shCtIP} cells, they were transfected with nontargeting or FANCD2 siRNA. 6 h after siRNA transfection, cells were cultivated in absence or presence of DOX (1 μg/ml) for 48 h. Cells were treated with MMC (20 ng/ml) for 20 h and with Colcemid at a final concentration of 0.1 μg/ml in the last 3 hours. Cells were harvested as described above.

Antibodies.

The primary antibodies used in this study are listed in a separate table below. Secondary HRP-conjugated anti-mouse and anti-rabbit antibodies were form GE-Healthcare and the HRP-conjugated anti-goat was from Santa Cruz Biotech. Alexa Fluor-488, -594, and -647-conjugated secondary antibodies were from Invitrogen.

Chemicals.

Mitomycin C (MMC), 8-Methoxypsoralen (8-MOP) and MG132 were purchased from Sigma. ATM inhibitor (KU-55933) was purchased from Tocris Bioscience. ATR inhibitor (VE-821) was provided by Vertex Pharmaceuticals (Abingdon, UK).

Immunoblotting, Immunoprecipitation, GST pulldown and Far-Western.

If not specified otherwise, cell extracts were prepared in Laemmli buffer (4% SDS, 20% glycerol, 120 mM Tris-HCl pH 6.8). Proteins were resolved by SDS–PAGE and transferred to nitrocellulose. Immunoblots were performed by using the appropriate antibodies and proteins visualized using the ECL detection system (Amersham).

For GST pulldown assays and immunoprecipitation assays, cells were lysed in either NP-40 extraction buffer (50 mM Tris-HCl, pH 7.5, 120 mM NaCl, 1 mM EDTA, 15 mM sodium pyrophosphate and 1 % NP-40 supplemented with phosphatase inhibitors (20 mM NaF, 1 mM sodium orthovanadate), protease inhibitors (1 mM benzamidine and 0.1 mM PMSF), deubiquitinase inhibitor (10 mM N-ethylmaleimide) and 10U Benzonase® (Roche)) or Triton X-100 buffer (50 mM Tris-HCl, pH 7.5, 200 mM NaCl, 1 mM EDTA, 0.2 % Triton X-100 supplemented with phosphatase, protease and deubiquitinase inhibitors) and clarified by centrifugation at 14000 rpm. GST pull-downs and immunoprecipitations were performed as described previously (Sartori et al., 2007). Far-western blot analysis was performed as described (Wu et al., 2007). Anti-GFP immunoprecipitates from HEK293T cells transfected with GFP-CtIP-wt or GFP-CtIP-ΔN were subjected to far-western analysis using recombinant HA-Ubiquitin (10 µg, Boston Biochem) as a probe followed by anti-HA immunoblotting.

Purification of recombinant human CtIP.

Insect Sf9 cells infected with FLAG-GST-CtIP-6H recombinant baculovirus were harvested 50 h after infection. The cell pellet was resuspended in lysis buffer (50 mM Tris-HCl, pH 7.5, 0.5 M NaCl, 0.1% NP-40, 10 % glycerol, 10 mM imidazole) supplemented with protease inhibitors (Roche). Cells were disrupted by douncer homogenization and cell debris was removed by centrifugation at 45K for 45 min at 4°C. Supernatant was filtered and loaded to Ni-NTA beads (Qiagen) overnight at 4°C. Beads were washed extensively with lysis buffer and lysis buffer supplemented with 60 mM imidazole and then protein was eluted using lysis buffer supplemented with 400 mM imidazole. Elution fractions were pooled, NaCl concentration was adjusted to 150 mM and loaded to heparin beads (GE Healthcare) for 90 min at 4°C. Heparin beads were washed with wash buffer (50 mM Tris-HCl, pH 7.5, 0.15 M NaCl, 0.1 % NP-40, 10 % glycerol) and proteins were eluted with elution buffer (50 mM Tris-HCl pH 7.5, 1 M NaCl, 0.1% NP-40, 10% glycerol). Elution fractions were pooled and dialyzed against dialysis buffer (50 mM Tris-HCl, pH 7.5, 0.15 M NaCl, 20% glycerol), aliquoted and stored at -80°C.

***In vitro* protein interaction.**

To analyze *in vitro* protein interaction between CtIP and FANCD2, GFP-FANCD2 wild-type or K561R mutant transiently expressed in HEK293T cells were immunoprecipitated with the anti-GFP antibody, coupled to Protein-A Sepharose beads (GE Healthcare) for 2 h at 4°C and immunocomplexes were stringently washed four times with NTEN buffer (0.5% NP- 40, 0.1 mM EDTA, 20 mM Tris-HCl, pH 7.4, 1 M NaCl). 0.5 µg of recombinant human FLAG-GST-CtIP-6His purified from Sf9 insect cells were incubated either alone or with GFP-fusion FANCD2 immunocomplexes bound to Protein-A Sepharose beads for 2 h at 4°C in 1 ml

TEN100 buffer (0.1 mM EDTA, 20 mM Tris-HCl, pH 7.4, 100 mM NaCl, 200 µg/ml BSA). Immunocomplexes were washed four times with NTEN350 buffer (0.5% NP-40, 0.1 mM EDTA, 20 mM Tris-HCl, pH 7.4, 350 mM NaCl), boiled in SDS-sample buffer and analyzed by SDS-PAGE followed by immunoblotting.

To analyze *in vitro* protein interaction between CtIP and ubiquitin, recombinant human FLAG-GST-CtIP-6His (0.2 µg) was incubated either alone or together with recombinant HA-Ubiquitin (5 µg, Boston Biochem) for 2 h at 4 C in the following buffer (20 mM HEPES, pH 7.5, 150 mM NaCl, 1 mM EDTA, 1 mM EGTA, 25 nM NaF, 1% Triton-X-100, 10% glycerol, 10 µM ZnCl2, 200 µg/ml BSA supplemented with EDTA-free protease inhibitor cocktail). The samples were subjected to immunoprecipitation using anti-HA antibody. Immunocomplexes were washed four times with NTEN250 buffer (0.5% NP-40, 0.1 mM EDTA, 20 mM Tris-HCl, pH 7.4, 250 mM NaCl), boiled in SDS-sample buffer and analyzed by immunoblotting.

***In vitro* Ubiquitin-binding assay.**

pET23-6xHis-ubiquitin wt vector (His-Ub wt, kind gift from Matthias Peter), I44A mutant or empty vector were grown in BL21-CodonPlus(DE3)-RIL Escherichia coli (Invitrogen) and protein expression was induced upon addition of 1 mM IPTG for 4 h at 37 °C. Proteins were solubilized in the lysis buffer containing 50 mM Tris-HCl, pH 7.5, 300 mM NaCl, 1 mM EDTA, 10 % glycerol, 1 % Triton X-100 and 20 mM imidazole supplemented with 1 mM DTT, 1 mM PMSF and EDTA-free protease inhibitor cocktail (Roche). His-Ub proteins were coupled to Ni-NTA Agarose (Qiagen), washed three times with lysis buffer supplemented with 500 mM NaCl and additional 20 mM imidazole, once with TEN100 buffer (20 mM Tris-HCl, pH 7.4, 0.1 mM EDTA and 100 mM NaCl) and incubated in TEN100 buffer supplemented with 1

mg/ml BSA for 30 min at 4 °C. Next, His-Ub proteins bound to Ni-NTA Agarose were incubated either with 1 mg of HeLa nuclear extract or with 1 mg of HEK293T lysates transiently expressing GFP-CtIP or GFP-CtIP-ΔN for 2 h at 4 °C in 1 ml of cell lysis buffer (20 mM HEPES, pH 7.5, 150 mM NaCl, 1 mM EDTA, 1 mM EGTA, 25 nM NaF, 1% Triton-X-100, 10% glycerol, 10 μM ZnCl2, supplemented with phosphatase inhibitors (20 mM NaF) and EDTA-free protease inhibitor cocktail). Beads were then washed once with NTEN300 buffer (0.5% NP-40, 0.1 mM EDTA, 20 mM Tris-HCl, pH 7.4, 300 mM NaCl), transferred to a new tube, washed another three times with NTEN300 and once with TEN100 buffer. Complexes were boiled in SDS sample buffer and analyzed by SDS–PAGE followed by immunoblotting.

***In Situ* Proximity Ligation Assay.**

In situ proximity ligation assay (PLA) in combination with immunofluorescence confocal microscopy was performed using Duolink II Detection Kit with anti-Mouse PLUS and anti-Rabbit MINUS PLA Probes, according to the manufacturer's instructions (Olink Bioscience) (Söderberg et al., 2006).

CellTiter-Blue® Cell Viability assay.

U2OS clones stably expressing siRNA-resistant forms of GFP-CtIP or MRC5^{shCtIP} cells were transfected with indicated siRNA. 48 hours post-transfection cells were seeded in triplicates at a density of 500 cells/well in 96 well plate. 24 h later cells were continuously treated with indicated doses of MMC and grown for 5 days at 37°C. To measure cell viability, CellTiter-Blue® reagent (Promega) was added on the last day, cells were incubated at 37°C for 4 h, and then fluorescence was measured at 560/590 nm.

PUVA treatment.

U2OS cells were incubated in PBS containing 10 μg/ml 8-MOP (Sigma) for 30 min. After incubation, cells were exposed to 10 kJ/m2 UV-A (365 nM, Vilber Lourmat Bio-Link BLX Crosslinker) in the presence of 8-MOP. Post-treatment PBS was removed and fresh media was added. At the indicated timepoints cells were harvested and proteins were analyzed by immunoblotting.

Supporting Table: Primary antibodies

Antibody target	Species	Supplier/Reference	Application*
pATM S1981	rabbit	2152-1 (Epitomics)	IB
ATR (N-19)	goat	sc-1887 (Santa Cruz)	IB
BRCA1 (D-9)	mouse	sc-6954 (Santa Cruz)	IB
BrdU	mouse	RPN202 (GE Healthcare)	IF
CHK1 (G-4)	mouse	sc-8408 (Santa Cruz)	IB
pCHK1 S345	rabbit	2341(Cell Signaling)	IB
CtIP (14-1)	mouse	gift from Richard Baer	IF
CtIP	rabbit	A300-488A (Bethyl)	IF (in situ PLA)
CtIP (D-4)	mouse	sc-271339 (Santa Cruz)	IB
ERCC1 (FL-297)	rabbit	sc-10785 (Santa Cruz)	IB
FAN1	sheep	gift from John Rouse	IB
FANCA	rabbit	A301-980A (Bethyl)	IB
FANCD2 (FI17)	mouse	sc-20022 (Santa Cruz)	IB and IF (in situ PLA)
FANCD2	rabbit	ab2187 (Abcam)	IF
FLAG	mouse	F3165 (Sigma)	IB
GFP	rabbit	ab290 (Abcam)	IP
GFP	mouse	sc-9996 (Santa Cruz)	IB
HA	mouse	sc-7392 (Santa Cruz)	IB and IP
γH2AX (20E3)	rabbit	9718 (Cell Signaling)	IB and IF
KAP1 pS824	rabbit	A300-767A (Bethyl)	IB
MRE11 (12D7)	mouse	GTX70212 (GeneTex)	IB
MUS81	mouse	M1445 (Sigma)	IB
NBS1 (1D7)	mouse	GTX70224 (GeneTex)	IB
Pol η	rabbit	ab17725 (Abcam)	IB
RIF1	rabbit	A300-569A (Bethyl)	IF
RPA2 (Ab-3)	mouse	NA19L (Calbiochem)	IB and IF
pRPA S4/S8	rabbit	A300-245A (Bethyl)	IB and IF
SLX4	rabbit	A302-270A (Bethyl)	IB
β-Tubulin (D-10)	mouse	sc-5274 (Santa Cruz)	IB
TFIIH p89 (S-19)	rabbit	sc-293 (Santa Cruz)	IB

*IB: Immunoblot, IF: Immunofluorescence, IP: Immunoprecipitation

SUPPLEMENTARY FIGURE LEGENDS

Figure S1 (related to Figure 1). CtIP localizes to ICL lesions in a FANCD2-dependent but NBS1- and SLX4-independent manner.

(**A**) U2OS cells were transfected with non-targeting (CNTL), CtIP or FANCD2 siRNA. 48 h after transfection, cells were treated for 24 h with mitomycin C (MMC) and survival was determined after eight days by colony formation. Data are presented as the mean ± SD (N=3). (**B**) Representative images of metaphase spreads from cells described in (C) after treatment with MMC (25 ng/ml) for 20 h. Selected chromosomal aberrations are displayed in higher magnifications. (**C**) U2OS cells were transfected with indicated siRNAs. 48 h after transfection, cells were treated for 24 h with MMC (120 ng/ml) and total and chromatin-bound proteins were analyzed by immunoblotting. (**D**) U2OS cells were transfected with different CtIP siRNAs. 48 h after transfection, cells were treated as in (C) and total proteins were analyzed by immunoblotting. Signal intensities of FANCD2 isoforms were quantified using Image J software and L/S indicates the ratio of monoubiquitinated (L) to non-monoubiquitinated (S) FANCD2. (**E**) U2OS cells were grown in absence (-) or presence (+) of 10 μg/ml 8-MOP for 30 min prior to UVA exposure and harvested at the indicated time points after PUVA treatment. RPA2 and P-RPA2 represent non-modified and hyperphosphorylated forms of RPA2, respectively. (**F,G**) U2OS cells were transfected with the indicated siRNAs. 48 h after transfection, cells were either mock-treated (-) or treated with PUVA and released for 4 h. Total and chromatin-bound proteins were analyzed by immunoblotting using the indicated antibodies. (**H**) FANCD2-mutant human fibroblasts (PD20F) and PD20F cells stably expressing either wild-type FANCD2 (wt) or the K561R mutant were grown on coverslips, mock-treated or treated as in (C), pre-extracted, fixed and co-immunostained for CtIP and γH2AX. (**I**) U2OS cells grown on coverslips were pre-treated for 2 h with DMSO or MG-132 (20 μM) and then treated with MMC (500 ng/ml) for 4 h.

Cells were pre-extracted, fixed and co-immunostained for CtIP and γH2AX. (**J,K**) U2OS cells were transfected with indicated siRNAs. 48 h after transfection, cells were treated as in (C) and total and chromatin-bound proteins were analyzed by immunoblotting. The arrow indicates a non-specific band detected by the anti-SLX4 antibody. In (C, D, F, G, J and K), the asterisks indicate hyperphosphorylated CtIP. In (C, F, G and J), D2 and D2-Ub represent non-ubiquitinated and monoubiquitinated forms of FANCD2, respectively. In (C, F, G, J, and K), TFIIH and CHK1 were used as loading controls for chromatin-enriched and soluble proteins, respectively. In (H and I), graphs show the percentage of γH2AX-foci positive cells displaying more than 10 CtIP foci. For each condition at least 100 cells were scored. Data are presented as the mean ± SD (N=2). In (H and I) scale bar, 10 μm.

Figure S2 (related to Figure 2). FANCD2 and CtIP promote resection during ICL repair.

(**A**) U2OS cells were treated with MMC (120 ng/ml) for the indicated time points and whole cell lysates were analyzed by immunoblotting. (**B**) U2OS cells were transfected with the indicated siRNAs. 48 h after siRNA transfection, cells were either mock-treated (-) or treated with PUVA, released for 2 and 4 h and harvested for immunoblot analysis. (**C-E**) U2OS cells were transfected with indicated siRNAs. 48 h after siRNA transfection, cells grown on coverslips were treated for 24 h with MMC (120 ng/ml), pre-extracted, fixed and either co-immunostained for RPA2 and RPA2-pS4/S8 (C), γH2AX and BrdU (D), or immunostained for RIF1 (E). Scale bar, 10 μm. (**F**) U2OS cells transfected with CtIP siRNA, were co-transfected with siRNA-resistant GFP-tagged CtIP wild-type (wt), T847A or S327A mutant CtIP 24 h post-siRNA transfection. 48 h post-siRNA transfection, cells were analyzed by immunoblotting prior to MMC treatment. (**G**) HEK293T cells were transfected with the indicated pEGFP-C1 expression vectors. After 48 h, cells were lysed in NP-40 buffer and

whole cell extracts (4 mg) were analyzed by immunoblotting before (Input) and after immunoprecipitation (IP) using anti-GFP antibody. Ponceau staining is shown to indicate the amounts of immunoglobulins (IgG) used in the IPs. (**H**) U2OS cells stably expressing empty vector (e.v.) or siRNA-resistant GFP-tagged wild-type CtIP (wt), T847A, or S327A mutant CtIP were transfected with CtIP siRNA for 72 h and whole cell extracts were analyzed by western blotting. (**I**) Same cells as in (H) were either mock-treated or continuously treated with MMC and the survival was determined after 5 days using the CellTiter-Blue® Cell Viability assay. Data are presented as the mean ± SD (N≥3).

Figure S3 (related to Figure 3). FANCD2-CtIP interaction requires FANCA but not SLX4 or FAN1.

(**A**) HEK293T cells were co-transfected with GFP-FANCD2 together with either empty vector or FLAG-CtIP. 48 h after transfection, cells were lysed in NP40 buffer and whole cell extracts were analyzed by immunoblotting before (Input) and after immunoprecipitation (IP) using anti-FLAG M2 affinity resin. Ponceau staining is shown to indicate the amounts of immunoglobulins (IgG) used in the IPs. (**B**) Coomassie-stained gel of recombinant FLAG-GST-CtIP-6His (0.5 µg) purified from Sf9 insect cells. (**C**) U2OS cells were transfected with indicated siRNAs. 48 h after siRNA transfection, cells were lysed and whole cell extracts were analyzed by immunoblotting. (**D**) Detection of endogenous CtIP-FANCD2 complexes by *in* situ PLA. Same cells as in (C) grown on coverslips were treated for 24 h with MMC (120 ng/ml) and pre-extracted prior to fixation. After incubation with antibodies against CtIP alone or against both CtIP and FANCD2, protein-protein interactions were detected using a fluorescently labeled probe (PLA-613). Scale bar, 20 µm. (**E**) Recombinant His-tagged ubiquitin (rHis-Ub) was immobilized on Ni-NTA agarose beads and incubated with whole cell extracts from HEK293T cells expressing GFP-SLX4 (*left*) or GFP-CtIP (*right*). Inputs

and precipitated bead fractions from the pull-downs were subjected to immunoblotting with anti-GFP antibody. Ponceau staining is shown to indicate the amounts of His-Ubiquitin used in the pull-down assays. (**F**) His alone (-) or recombinant wt and I44A mutant ubiquitin (rHis-Ub) coupled to Ni-NTA agarose beads were incubated with HeLa nuclear extracts (NE). Input and precipitated bead fractions from the pull-downs were subjected to immunoblotting. Ponceau staining is shown to indicate the amounts of rHis-Ub used in the pull-down assay.

Figure S4 (related to Figure 4). Identification and functional characterization of CtIP mutants impaired in FANCD2 interaction.

(**A**) Multiple sequence alignment of the putative FANCD2-interacting region in CtIP orthologs (amino acids 160-298) was performed using Clustal W (www.ebi.ac.uk/Tools/msa). PDSP, RRK, RYxE and ILV motifs are highlighted in black boxes. Other, highly conserved amino acid residues are marked in bold typeface. R177Q and Y186C represent two cancer-associated CtIP mutations recorded in the Catalogue of Somatic Mutations in Cancer (COSMIC*)* database (www.cancer.sanger.ac.uk). (**B**) U2OS cells were transfected with CtIP siRNA and after 24 h co-transfected with the indicated siRNA-resistant GFP-tagged CtIP constructs. 48 h post-siRNA transfection, cells grown on coverslips were treated for 24 h with MMC (120 ng/ml), fixed and immunostained for RIF1. Graphs show the percentage of GFP-positive cells displaying more than 10 GFP-CtIP foci and the percentage of GFP-positive cells displaying more than 10 RIF1 foci, respectively. For each condition at least 100 cells were scored. Data are presented as the mean ± SEM (N=2). (**C**) Same cells as in (B) were analyzed by immunoblotting. (**D**) U2OS cells stably expressing siRNA-resistant GFP-CtIP-wt, GFP-CtIP-RRK/AAA, or GFP-CtIP-RYIE/AAIA were transfected with CtIP siRNA and treated as in (D). 15 min after irradiation, cells were fixed, immunostained for γH2AX and analyzed by fluorescence microscopy. (**E**) U2OS cells stably expressing siRNA-resistant GFP-CtIP-wt

were transfected with indicated siRNAs. 24 h after siRNA transfection, cells grown on coverslips were sensitized with BrdU (10 μM) for 24 h prior to laser microirradiation. 30 min after irradiation, cells were fixed, co-immunostained for FANCD2 and γ-H2AX and analyzed by fluorescence microscopy. (**F**) Recombinant His-tagged ubiquitin (rHis-Ub) was immobilized on Ni-NTA agarose beads and incubated with whole cell extracts from HEK293T cells depleted of endogenous CtIP and expressing GFP-CtIP-wt or GFP-CtIP-ΔN (deleted of CtIP amino acids 153-322). Inputs and precipitated bead fractions from the pull-downs were subjected to immunoblotting with anti-GFP antibody. Ponceau staining is shown to indicate the amounts of rHis-Ub used in the pull-down assays. (**G**) Anti-GFP immunoprecipitates from HEK293T cells transfected with GFP-CtIP-wt or GFP-CtIP-ΔN were subjected to far-western analysis using recombinant HA-Ubiquitin as a probe followed by anti-HA immunoblotting. Ponceau staining is shown to indicate the amounts of proteins transferred onto the nitrocellulose membrane. In (B, D and E) scale bar, 5 μm.

Figure S5 (related to Figure 5). Analysis of CtIP/FANCD2 and CtIP/BRCA1 double-deficient cells in response to MMC treatment.

(**A**) FANCD2-deficient cells (PD20F) and PD20F stably expressing wild-type FANCD2 (D2) transfected with indicated siRNAs. 48 h post-siRNA transfection, cells were treated with the indicated doses of MMC for 24 h and survival was determined after eight days by colony formation. Data are presented as the mean ± SEM (N=3) (*left*). The same cells were analyzed by immunoblotting (*right*). (**B**) MRC5^{shCtIP} cells were transfected with indicated siRNAs. 6 h post-siRNA transfection, cells were cultivated in the absence or presence of doxycycline (DOX, 1 μg/ml) for 48 h. Cells grown on coverslips were treated for 24 h with MMC (120 ng/ml), pre-extracted, fixed and immunostained for RIF1. Scale bar, 10 μm. (**C**) Representative images of metaphase spreads from cells described in (B) after treatment with

MMC (20 ng/ml) for 20 h. Selected radial chromosomes are displayed in higher magnifications. (**D**) MRC5^{shCtIP} cells were transfected with indicated siRNAs. 6 h post-siRNA transfection, cells were cultivated in the absence or presence of doxycycline (DOX, 1 µg/ml) for 48 h. Cells were continuously treated with the indicated doses of MMC and the survival was determined after 5 days using the CellTiter-Blue® Cell Viability assay. Data are presented as the mean ± SD (N=3) (*left*). The same cells were analyzed by immunoblotting (*right*).

Figure S6. CtIP-mediated resection counteracts ICL-induced DNA damage in a FANCD2-dependent and -independent manner.

Replication fork stalling at ICLs triggers activation of the ATR kinase resulting in monoubiquitination and stable association of the FANCD2-FANCI complex on chromatin. Monoubiquitinated FANCD2 recruits FAN1 and SLX4-associated nucleases to coordinate ICL incision giving rise to DSB intermediates. Translesion synthesis (TLS) polymerases bypass the unhooked crosslink and nucleotide excision repair (NER) removes the remaining adducts. Monoubiquitinated FANCD2 interacts with CtIP, thereby tethering it to damaged chromatin to ensure proper coordination of ICL processing and DNA-end resection. Once the DSB is formed, CtIP is phosphorylated by ATM kinase and promotes resection, thus initiating homologous recombination (HR), and, concomitantly antagonizing non-homologous end joining (NHEJ). In the absence of FANCD2, or in case of impaired activation of the FA-pathway, persistent ICLs trigger the conversion of stalled replication forks into DSBs, a process that is at least partially dependent on the endonucleolytic activity of MUS81. Also in this case, CtIP-dependent resection commits cells to error-free repair of DSBs, thus preserving genome stability in response to ICL damage.

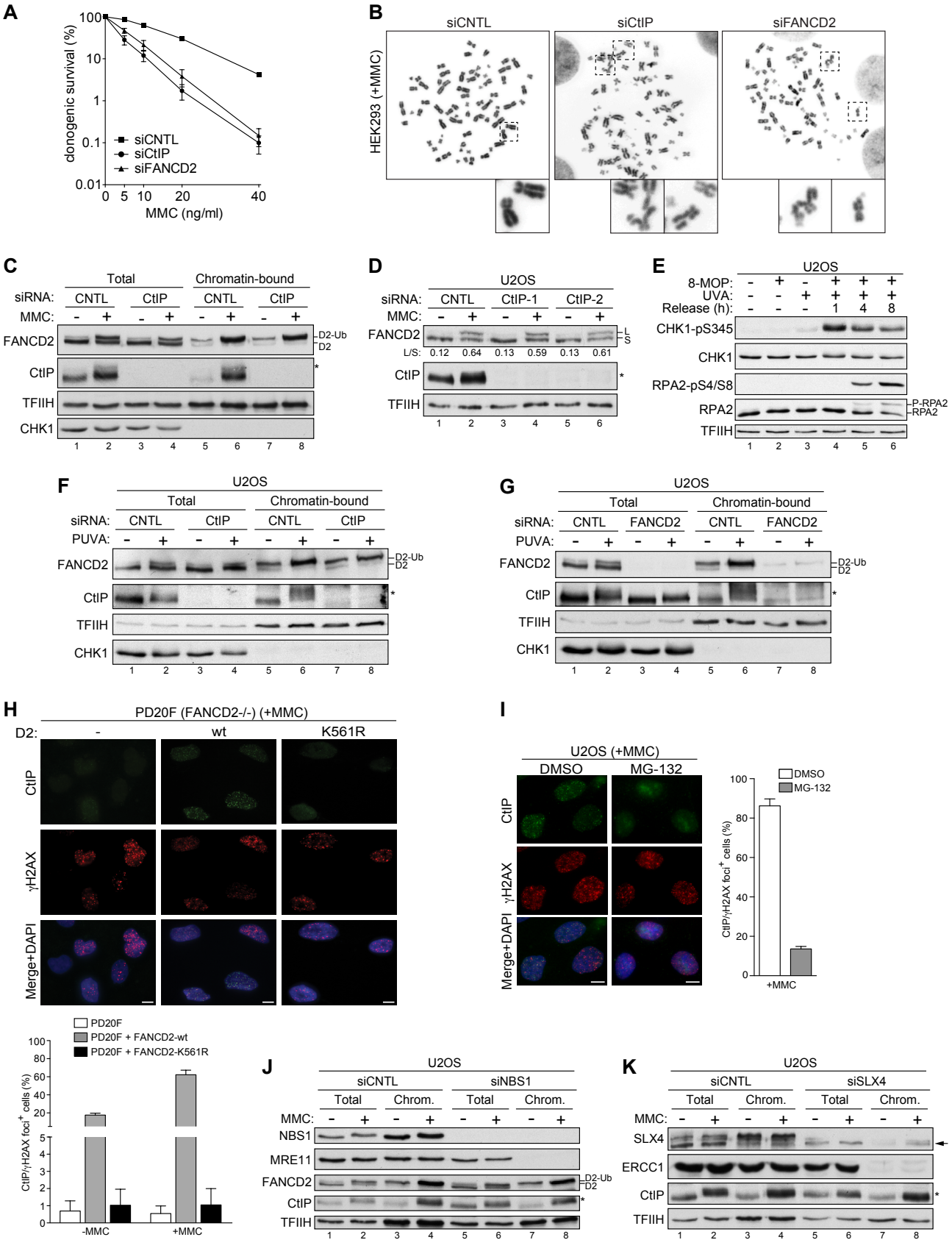
A
clonogenic survival (%)
MMC (ng/ml)
siCNTL
siCtIP
siFANCD2
B
siCNTL
siCtIP
siFANCD2
HEK293 (+MMC)
C
Total
Chromatin-bound
siRNA:
CNTL
CtIP
MMC:
FANCD2
D2-Ub
D2
CtIP
TFIIH
CHK1
D
U2OS
siRNA:
CNTL
CtIP-1
CtIP-2
MMC:
FANCD2
L
S
L/S:
0.12
0.64
0.13
0.59
0.13
0.61
CtIP
TFIIH
E
U2OS
8-MOP:
UVA:
Release (h):
CHK1-pS345
CHK1
RPA2-pS4/S8
RPA2
P-RPA2
RPA2
TFIIH
F
U2OS
Total
Chromatin-bound
siRNA:
CNTL
CtIP
PUVA:
FANCD2
D2-Ub
D2
CtIP
TFIIH
CHK1
G
U2OS
Total
Chromatin-bound
siRNA:
CNTL
FANCD2
PUVA:
FANCD2
D2-Ub
D2
CtIP
TFIIH
CHK1
H
PD20F (FANCD2-/-) (+MMC)
D2:
-
wt
K561R
CtIP
γH2AX
Merge+DAPI
PD20F
PD20F + FANCD2-wt
PD20F + FANCD2-K561R
CtIP/γH2AX foci+ cells (%)
-MMC
+MMC
I
U2OS (+MMC)
DMSO
MG-132
CtIP
γH2AX
Merge+DAPI
DMSO
MG-132
CtIP/γH2AX foci+ cells (%)
+MMC
J
U2OS
siCNTL
siNBS1
Total
Chrom.
MMC:
NBS1
MRE11
FANCD2
D2-Ub
D2
CtIP
TFIIH
K
U2OS
siCNTL
siSLX4
Total
Chrom.
MMC:
SLX4
ERCC1
CtIP
TFIIH

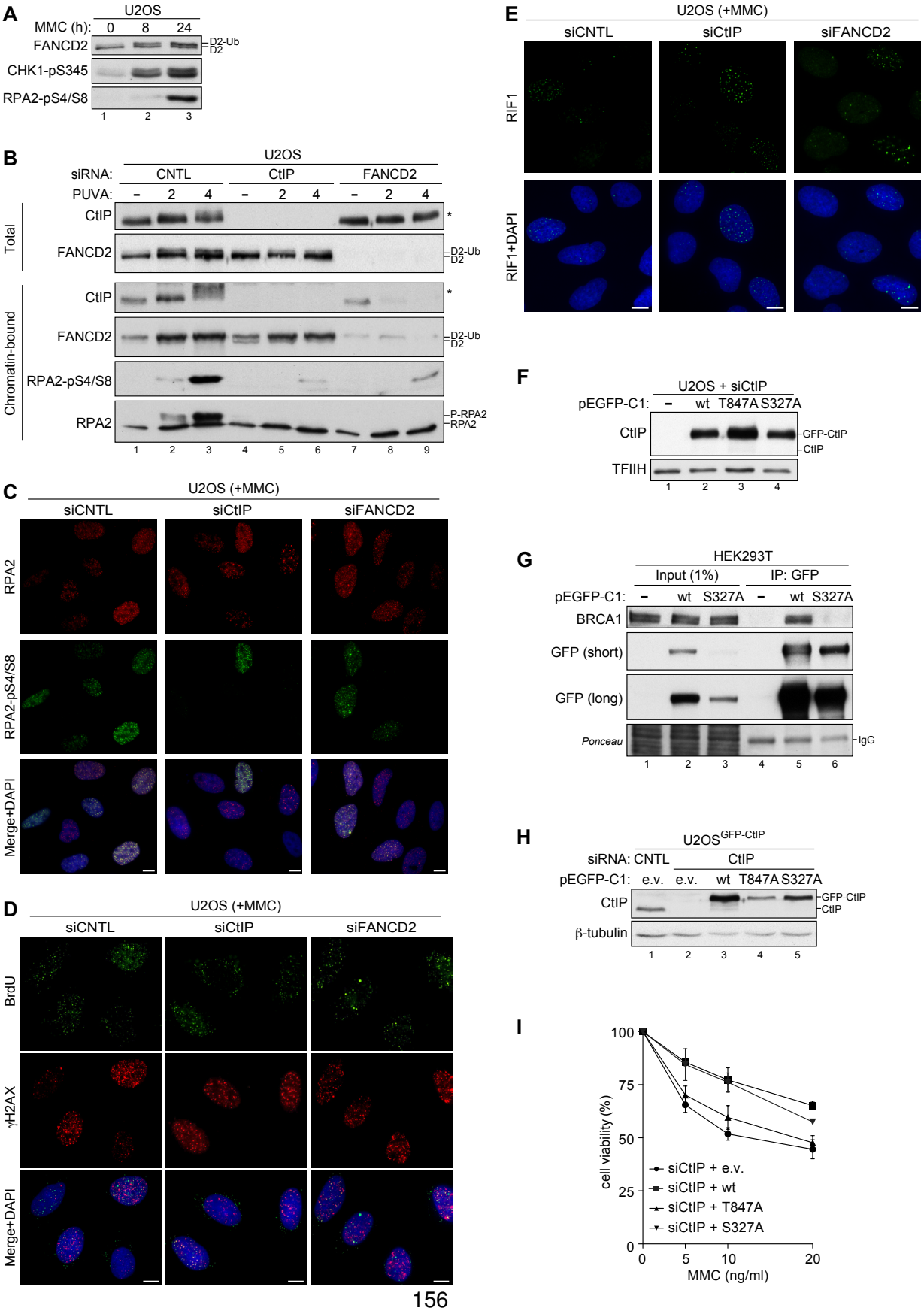
A
U2OS
MMC (h): 0 8 24
FANCD2
D2-Ub
D2
CHK1-pS345
RPA2-pS4/S8
1 2 3
B
U2OS
siRNA: CNTL CtIP FANCD2
PUVA: – 2 4 – 2 4 – 2 4
Total
Chromatin-bound
CtIP
FANCD2
RPA2-pS4/S8
RPA2
P-RPA2
RPA2
1 2 3 4 5 6 7 8 9
C
U2OS (+MMC)
siCNTL siCtIP siFANCD2
RPA2
RPA2-pS4/S8
Merge+DAPI
D
U2OS (+MMC)
siCNTL siCtIP siFANCD2
BrdU
γH2AX
Merge+DAPI
E
U2OS (+MMC)
siCNTL siCtIP siFANCD2
RIF1
RIF1+DAPI
F
U2OS + siCtIP
pEGFP-C1: – wt T847A S327A
CtIP
GFP-CtIP
CtIP
TFIIH
1 2 3 4
G
HEK293T
Input (1%) IP: GFP
pEGFP-C1: – wt S327A – wt S327A
BRCA1
GFP (short)
GFP (long)
Ponceau
IgG
1 2 3 4 5 6
H
U2OS GFP-CtIP
siRNA: CNTL CtIP
pEGFP-C1: e.v. e.v. wt T847A S327A
CtIP
GFP-CtIP
CtIP
β-tubulin
1 2 3 4 5
I
cell viability (%)
100
75
50
25
0
0 5 10 20
MMC (ng/ml)
siCtIP + e.v.
siCtIP + wt
siCtIP + T847A
siCtIP + S327A

Murina. Figure S3

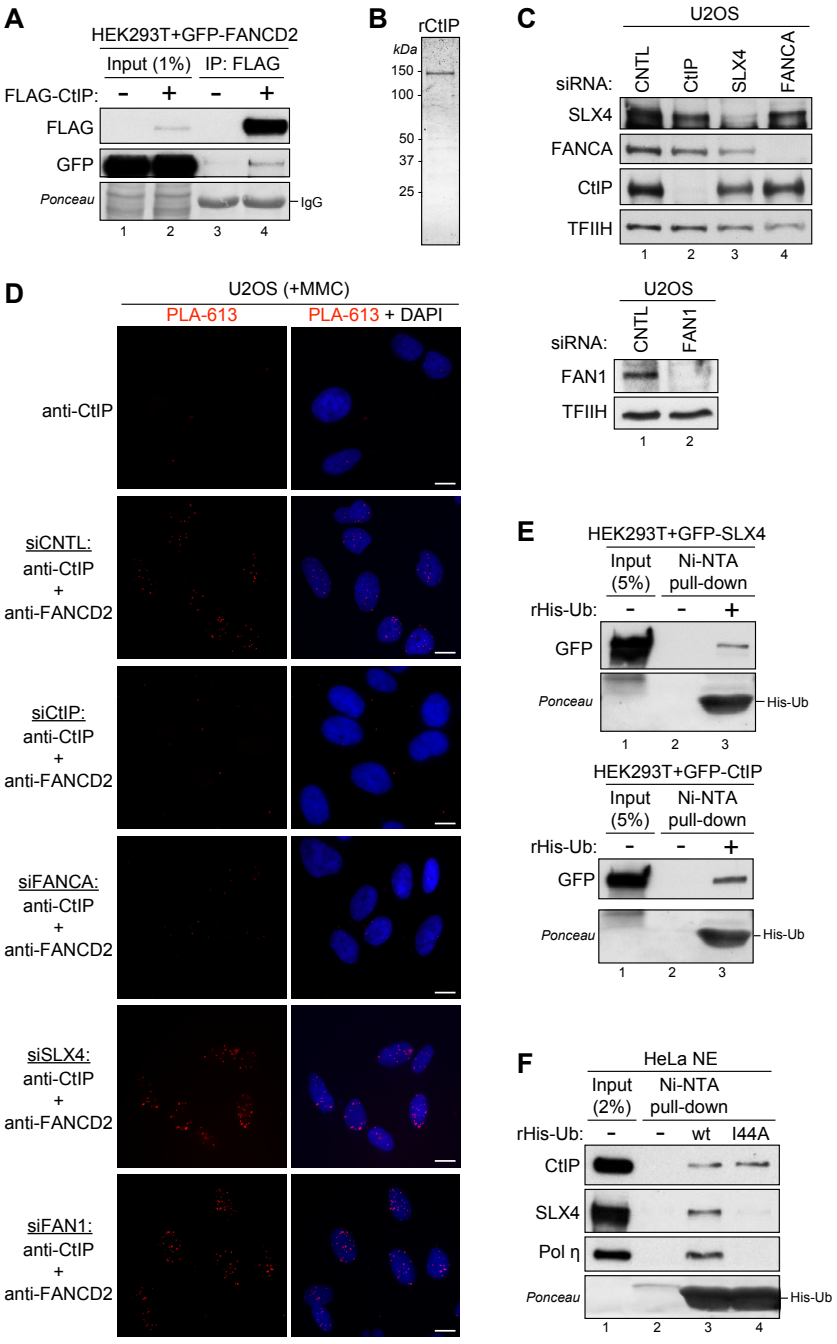

Murina. Figure S4

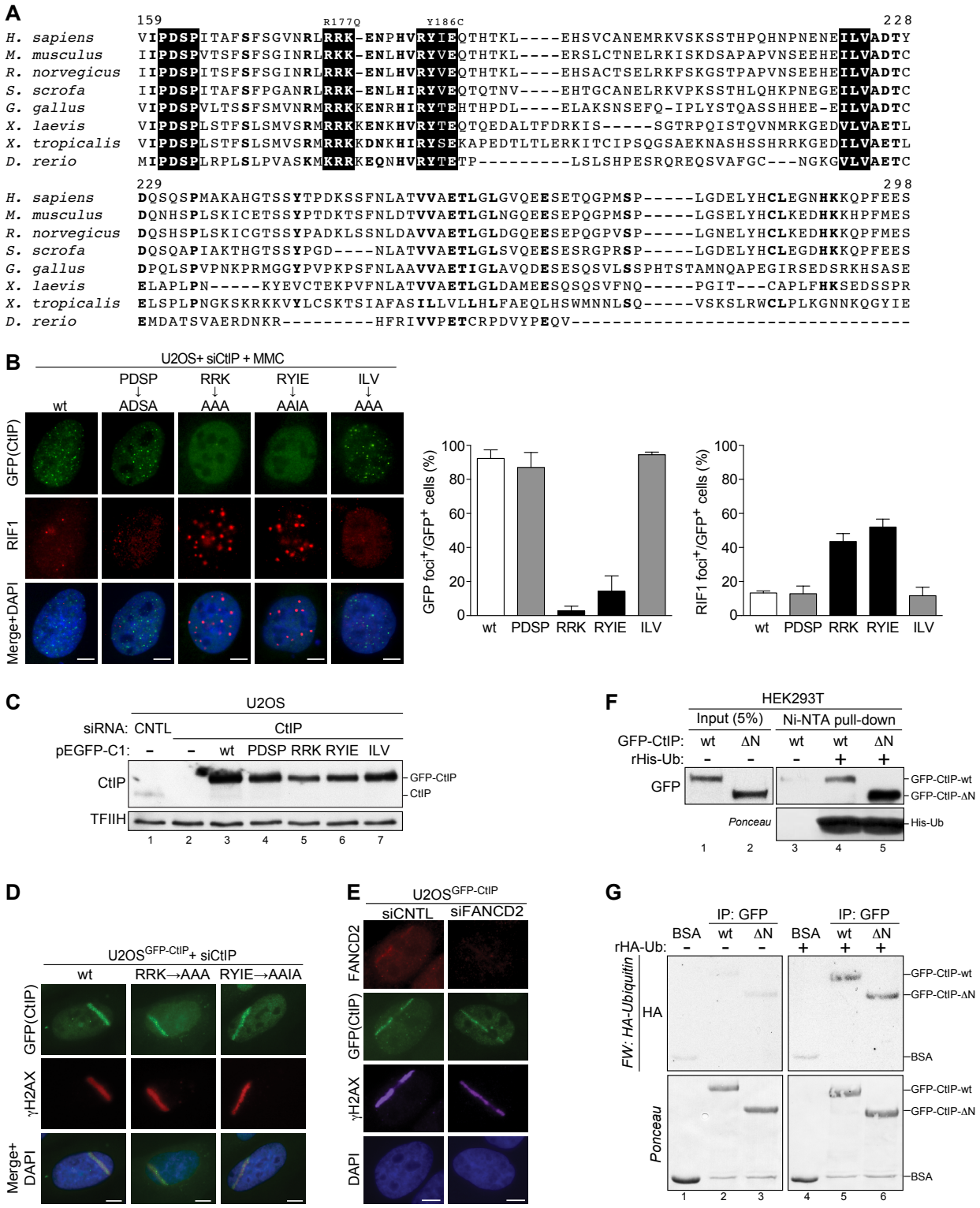

Murina. Figure S5

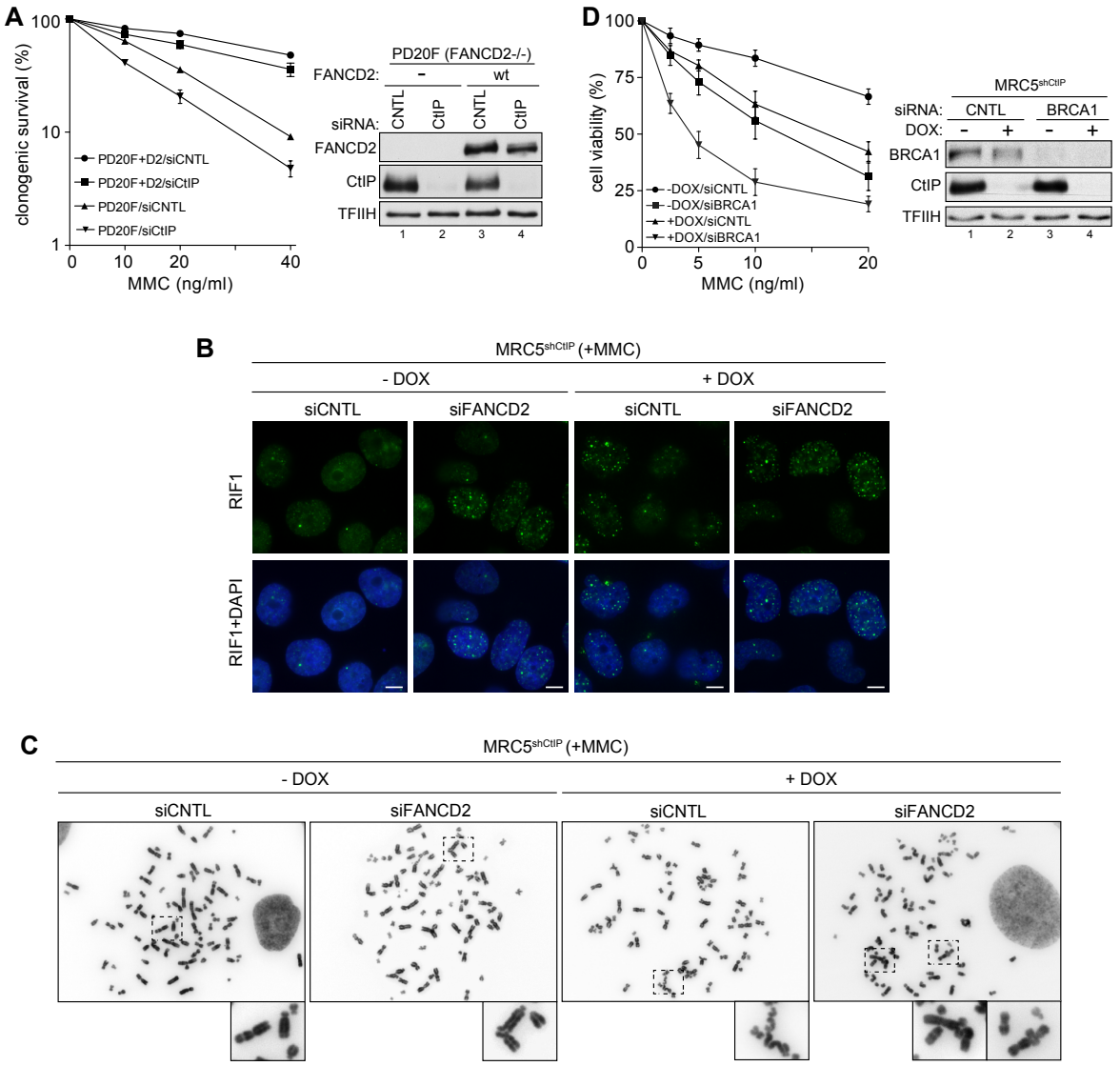

Murina. Figure S6

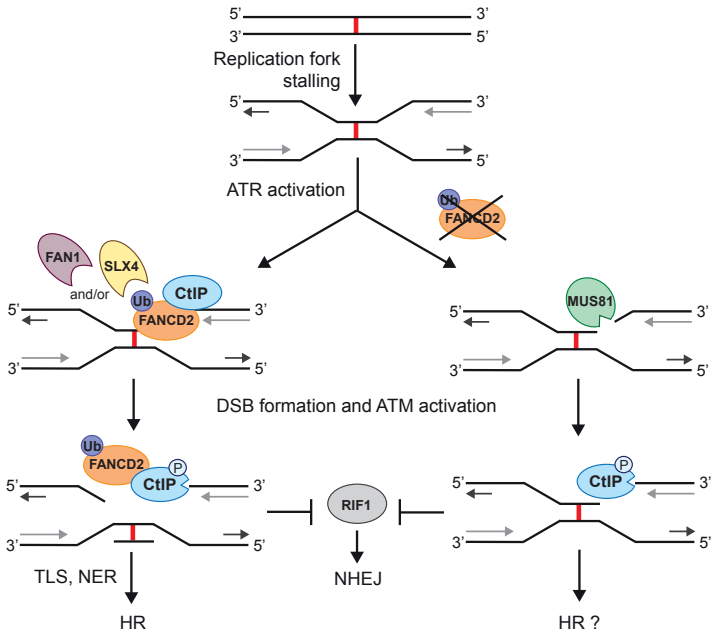

Supplemental References

Bruun, D., Folias, A., Akkari, Y., Cox, Y., Olson, S., and Moses, R. (2003). siRNA depletion of BRCA1, but not BRCA2, causes increased genome instability in Fanconi anemia cells. DNA Repair (Amst.) *2*, 1007–1013.

Eid, W., Steger, Martin, El-Shemerly, M., Ferretti, L.P., Peña-Diaz, J., König, C., Valtorta, E., Sartori, A.A., and Ferrari, S. (2010). DNA end resection by CtIP and exonuclease 1 prevents genomic instability. EMBO Rep. *11*, 962–968.

Kim, J.M., Kee, Y., Gurtan, A., and D'Andrea, A.D. (2008). FA core complex moves to chromatin. *111*, 4837–4838.

Kratz, K., Schöpf, B., Kaden, S., Sendoel, A., Eberhard, R., Lademann, C., Cannavo, E., Sartori, A.A., Hengartner, M.O., and Jiricny, J. (2010). Deficiency of FANCD2-associated nuclease KIAA1018/FAN1 sensitizes cells to interstrand crosslinking agents. Cell *142*, 77–88.

Neelsen, K.J., Zanini, I.M.Y., Herrador, R., and Lopes, M. (2013). Oncogenes induce genotoxic stress by mitotic processing of unusual replication intermediates. The Journal of Cell Biology *200*, 699–708.

Sartori, A.A., Lukas, C., Coates, J., Mistrik, M., Fu, S., Bartek, J., Baer, R., Lukas, J., and Jackson, S.P. (2007). Human CtIP promotes DNA end resection. Nature *450*, 509–514.

Söderberg, O., Gullberg, M., Jarvius, M., Ridderstråle, K., Leuchowius, K.-J., Jarvius, J., Wester, K., Hydbring, P., Bahram, F., Larsson, L.-G., et al. (2006). Direct observation of individual endogenous protein complexes in situ by proximity ligation. Nat. Methods *3*, 995–1000.

Steger, Martin, Murina, O., Hühn, D., Ferretti, L.P., Walser, R., Hänggi, K., Lafranchi, L., Neugebauer, C., Paliwal, S., Janscak, P., et al. (2013). Prolyl Isomerase PIN1 Regulates DNA Double-Strand Break Repair by Counteracting DNA End Resection. Mol Cell *50*, 333–343.

Stoepker, C., Hain, K., Schuster, B., Hilhorst-Hofstee, Y., Rooimans, M.A., Steltenpool, J., Oostra, A.B., Eirich, K., Korthof, E.T., Nieuwint, A.W.M., et al. (2011). SLX4, a coordinator of structure-specific endonucleases, is mutated in a new Fanconi anemia subtype. Nat Genet *43*, 138–141.

Svendsen, J.M., Smogorzewska, A., Sowa, M.E., O'Connell, B.C., Gygi, S.P., Elledge, S.J., and Harper, J.W. (2009). Mammalian BTBD12/SLX4 assembles a Holliday junction resolvase and is required for DNA repair. Cell *138*, 63–77.

Tiscornia, G., Singer, O., and Verma, I.M. (2006). Production and purification of lentiviral vectors. Nat Protoc *1*, 241–245.

Wu, Y., Li, Q., and Chen, X.-Z. (2007). Detecting protein-protein interactions by Far western blotting. Nat Protoc *2*, 3278–3284.

Yoo, H.Y., Kumagai, A., Shevchenko, A., Shevchenko, A., and Dunphy, W.G.

(2009). The Mre11-Rad50-Nbs1 complex mediates activation of TopBP1 by ATM. Mol. Biol. Cell *20*, 2351–2360.

You, Z., Shi, L.Z., Zhu, Q., Wu, P., Zhang, Y.-W., Basilio, A., Tonnu, N., Verma, I.M., Berns, M.W., and Hunter, T. (2009). CtIP Links DNA Double-Strand Break Sensing to Resection. Mol Cell *36*, 954–969.